Universidade do Minho
Escola de Engenharia

Nuno Filipe Antunes Oliveira Ferreira Alves

Biped locomotion control through a biologically-inspired closed-loop controller

Outubro de 2012

Biped locomotion control through a biologically-inspired closed-loop controller
Nuno Filipe Antunes Oliveira Ferreira Alves
UMinho | 2012

Universidade do Minho
Escola de Engenharia

Nuno Filipe Antunes Oliveira Ferreira Alves

Biped locomotion control through a biologically-inspired closed-loop controller

Dissertação de Mestrado
Ciclo de Estudos Integrados Conducentes ao
Grau de Mestre em Engenharia Biomédica

Trabalho realizado sob a orientação da
Professora Doutora Cristina P. Santos
Universidade do Minho
e coorientação do
Doutor Juan C. Moreno
CSIC – Madrid

Outubro de 2012

Acknowledgements

I would like to express all my gratefulness to my advisor Cristina Santos, for her continuous and opportune supervising, always paying attention to the detail and giving me important advices to work out this dissertation.

A special word goes to my other advisor Juan C. Moreno. His knowledge and experience in the area were fundamental to this work. He guided me along the training period and it was a real pleasure to work with him.

I also want to show gratitude to Jose Luis Pons, for the opportunity they gave me to work in such an important Research Center as CSIC (*Consejo Superior de Investigaciones Cientificas* - Madrid - Spain), as well as their support all through the internship term, which was greatly appreciated.

Sincere gratitude to my colleagues from the Bioengineering Group of CSIC and from the ASB (*Adaptive System Behavior* - Braga - Portugal) group should be noted with whom exchange of views on various issues have proven vitally important in promoting gradual development of this work as well as in highlighting and clarifying priority steps for the improvement of the study.

Finally, I want to thank to my family and friends all the support they have given me all year round, especially because they always believe in my work.

Abstract

Currently motor disability in industrialized countries due to neural and physical impairments is an increasingly worrying phenomenon and the percentage of patients is expected to be increasing continuously over the coming decades due to a process of ageing the world is undergoing. Additionally, rising retirement ages, higher demand of elderly people for an independent, dignified life and mobility, huge cost in the provision of health care are some other determinants that motivate the restoration of motor function as one of the main goals of rehabilitation. Modern concepts of motor learning favor a task-specific training in which all movements in daily life should be trained/assisted repetitively in a physically correct fashion.

Considering the functional activity of the neuronal circuits within the spinal cord, namely the central pattern generator (CPG), as the foundation to human locomotion, motor relearning should be based on intensive training strategies directed to the stimulation and reorganization of such neural pathways through mechanisms addressed by neural plasticity. To this end, neuromodelings are required to simulate the human locomotion control to overcome the current technological challenges such as developing smaller, intelligent and cost-effective devices for home and work rehabilitation scenarios which can enable a continuous therapy/assistance to guide the impaired limbs in a gentle manner, avoiding abrupt perturbations and providing as little assistance as necessary. Biomimetic models, taking neurological and biomechanical inspiration from biological animals, have been embracing these challenges and developing effective solutions on refining the locomotion models in terms of energy efficiency, simplicity in the structure and robust adaptability to environment changes and unexpected perturbations.

Thus, the aim target of this work is to study the applicability of the CPG model for gait rehabilitation, either for assistance and/or therapy purposes. Focus is developed on the locomotion control to increase the knowledge of the underlying principles useful for gait restoration, exploring the brainstem-spinal-biomechanics interaction more fully. This study has great application in the project of autonomous robots and in the rehabilitation technology, not only in the project of prostheses and orthoses, but also in the searching of procedures that help to recuperate motor functions of human beings.

Encouraging results were obtained which pave the way towards the simulation of more complex behaviors and principles of human locomotion, consequently contributing for improved automated motor rehabilitation adapted to the rehabilitation emerging needs.

Resumo

Actualmente a debilidade motora em países industrializados devido a deficiências neurais e físicas é um fenómeno crescente de apreensão sendo expectável um contínuo aumento do rácio de pacientes nas próximas décadas devido ao processo de envelhecimento. Inclusivé, o aumento da idade de reforma, a maior procura por parte dos idosos para uma mobilidade e vida autónoma e condigna, o elevado custo nos cuidados de saúde são incentivos para a restauração da função motora como um dos objectivos principais da reabilitação. Conceitos recentes de aprendizagem motora apoiam um treino de tarefas específicas no qual movimentos no quotidiano devem ser treinados/assistidos de forma repetitiva e fisicamente correcta.

Considerando a actividade funcional dos circuitos neurais na medula, nomeadamente o gerador de padrão central (CPG), como a base da locomoção, a reaprendizagem motora deve-se basear em estratégias intensivas de treino visando a estimulação e reorganização desses vias neurais através de mecanismos abordados pela plasticidade neural. Assim, são necessários modelos neurais para simular o controlo da locomoção humana de modo a superar desafios tecnológicos actuais tais como o desenvolvimento de dispositivos mais compactos, inteligentes e económicos para os cenários de reabilitação domiciliar e laboral que podem permitir uma terapia/assistência contínua na guia dos membros debilitados de uma forma suave, evitando perturbações abruptas e fornecendo assistência na medida do necessário. Modelos biomiméticos, inspirando-se nos princípios neurológicos e biomecânicos dos animais, têm vindo a abraçar esses desafios e a desenvolver soluções eficazes na refinação de modelos de locomoção em termos da eficiência de energia, da simplicidade na estrutura e da adaptibilidade robusta face a alterações ambientais e perturbações inesperadas.

Então, o objectivo principal do trabalho é estudar a aplicabilidade do modelo de CPG para a reabilitação da marcha, para efeitos de assistência e/ou terapia. É desenvolvido um foco no controlo da locomoção para maior entendimento dos princípios subjacentes úteis para a recuperação da marcha, explorando a interacção tronco cerebral-espinal medula-biomecânica de forma mais detalhada. Este estudo tem potencial aplicação no projecto de robôs autónomos e na tecnologia de reabilitação, não só no desenvolvimento de ortóteses e próteses, mas também na procura de procedimentos úteis para a recuperação da função motora.

Foram obtidos resultados promissores susceptíveis de abrir caminho à simulação de comportamentos e princípios mais complexos da marcha, contribuindo consequentemente para uma aprimorada reabilitação motora automatizada adaptada às necessidades emergentes.

Contents

List of Figures

List of Tables

Chapter 1

Introduction

1.1 Motivation

In this chapter it is outlined the development framework of the current Master's Dissertation. The chapter concerns the problematics of gait restoration of motor function for disabled patients with lower-limb impairments of the central nervous system (CNS), such as e.g. stroke, spinal cord injury (SCI), traumatic brain injury (TBI), cerebral palsy (CP) among other diseases through robot-assisted gait rehabilitation. In this regard, gait restoration is a fundamental part of rehabilitation with a major influence on people's daily life and community living.

Particularly, CP is the most leading motor disability in childhood, affecting approximately 1 in 303 8-years-old children in the U.S.A. It is a group of disorders resulted from a brain injury or malformations which potentially affects such a person's ability to move and maintain muscle control, balance, posture and coordination that may not be able to walk independently [30]. SCI consists of an interruption on the neurological connection paths from the brain to the rest of the body causing musculature paralysis, lost of sensibility and autonomous nervous system alteration. The severity of consequences arising from spinal lesion depends basically on the lesion level and extension, discriminating therefore different degrees of injury known as complete injury (total interruption of connection paths) and incomplete injury by which there remain still some operating functions, e.g., reflexes, voluntary movement capability, sensibility... [31]. The annual incidence of SCI in the U.S.A. is estimated to be around 40 cases per million population or approximately 12000 new appearances each year [32]. Stroke is pointed to be the most common cause of disability in industrialized countries due to both the debilitating initial symptoms and in many cases the

severe long-term impairment in activities such as walking and speech with an incidence estimated approximately to 200 patients per 100 000 inhabitants in the EU5 nations (France, Spain, Germany, UK and Italy) each year and with a prevalence around 200-300 cases . The main cause of stroke is the interruption of the cerebral blood flow which leads to neurologic deficits. Whilst unclear decreases in incidence or prevalence have been reported during the last decade, an increase in burden due to aging populations of the EU5 countries and other demographic changes is a growing possibility [33].

In addition to physical disabilities, the detrimental effects also extend to significant emotional burden. Apart from people requiring the ability to perform their work further into old age due to rising retirement ages, the elderly are increasingly expecting for a continuous or at least higher as possible independent life and mobility so that they can encourage themselves a feeling of belonging to a normal community without requiring external care for daily life. Thus, an improved restoration of motor function constitutes an unceasing growth in demand.

1.2 Problem formulation

During the preceding decades rehabilitation, particularly gait rehabilitation, has been attempting to find solutions to tackle the issue of quality of live improvement of disabled people with lower extremities impairment. Gait rehabilitation has implied not only the retraining but also assistance or replacement of a certain motor function depending if there is some or none motor function remaining, respectively. Thus, the former application of rehabilitation is focused on demonstrating therapeutic benefits for people with paralysis, whilst the latter one is intended to permanently substitute lost neuromuscular function of people with muscle weakness. Upon the rehabilitation strategy relying on the development of motor learning which is believed of favoring a task-specific training (i.e., walking relearning in gait rehabilitation), conventional therapy methods such as treadmill therapy have demonstrated interesting results on the repetitive and physiologically correct fashion training of walking movements important for daily life. Nonetheless, main drawbacks or limitations emerge from this conventional training: not all walking movements needed for daily life can be trained such as walking on uneven floor or stair climbing due to physiotherapists' overstrain; great physically effort from at least two therapist is required; an intensive hand-to-hand therapy programme is restricted to economic constraints; the therapy can promote lack of motivation for both patient and therapist to exercise the affected limb(s), and there-

fore, the reduction of the training session.

Conversely, robotic devices for gait rehabilitation emerged since the 1990s can offer new possibilities and perspectives for the improvement of neurorehabilitation after neurological injuries in order to compensate the shortcomings deriving from conventional therapy. Intensive and varied trainings in terms of frequency and session time are no longer a problem as well as therapists can be more relieved from exhausting manual labor taking more of a supervisory role. Current studies are specially focused on developing devices which can be able to guide the impaired limbs in a gentle manner, avoiding abrupt perturbations and providing as little assistance as necessary. Considering the human nervous system itself as an adaptive controller susceptible of being re-programmed, robots are thought to teach in a such more effective way the nervous system that they can help it to control the movement and/or possibly regain the function once already lost. This accomplishments might be achieved through effective repetitive and active effort by the patients in addition to human-machine interaction to promote their motivation and participation.

1.3 Solution

Within this context, this Master's Dissertation is focused on understanding the principles underlying human motor control, more particularly, human locomotion. A major knowledge of human walking principles can play a major role on neurorehabilitation: the contribution to further potential advantages of robotic devices such as therapy documentation within quality programmes; better comprehension of human intention and adaptation to it; importantly, maximization of motor skills learning and neural recovery through the combination of robotic devices and neurocomputational modelings so that safe, lightweight and flexible human-robot interaction for hands-off assistive robotics can be provided. The more fully acknowledgment of gait principles will offer improvements on finding, tracking and following the patient's activity, on providing more suitable and precise feedback, on enhancing patients's motivation and engagement. The more the neuromodelings can simulate the human locomotion control, the more quickly are some technological challenges overcome, i.e., the more feasible will be the development of combined therapeutic/assistive rehabilitation robotic systems sufficiently lightweighted, compliant, safe and back-driveable that can be generally worn during the activities of daily living by the majority of impaired persons regardless of the type of injury.

In order to simulate human locomotion substantial neurophysiologic and biomechanical modeling has been developed with the goal of describing correctly the body segment movements and their dynamics and kinematics involved. Particularly biped models have been increasingly used to seek greater knowledge about the human locomotion principles by simulating body physics and the environment. Examples of several works relating biped models are included in [34–40], ranging from pendulum models to multi-link planar/spatial models. All these recent works have shared a common broad issue concerning the complexity of generating and controlling stable locomotion due to high dimensional nonlinear dynamics, higher number of degrees of freedom (DOFs) involved, environment interaction, among other aspects [41, 42]. It is broadly recognized that not only even extremely simple unactuated systems (e.g. with no feet structures or upper limbs included) can generate ambulatory motion, but also dynamic simulators do not share several constraints and difficulties emerged from the use of robots for neuroscience research [42, 43]. In this work, a biped robot simulation tool was used, analyzed and studied which enables the simulation of the exact dynamics of a two-dimensional biped robot model on a walking surface [41, 44]. The choice for the referred biped model can be justified by its simplicity and simultaneously by describing the human gait quite well. In addition, the model can be slightly altered according to other purposes or needs [45].

With regard to motor function relearning aforementioned discussed, functional activity of the neuronal circuits within the spinal cord, namely the central pattern generator (CPG), has been demonstrating to play an important role in this context since its function constitutes the foundation to human locomotion [46]. From this viewpoint, considering that motor learning has involved the reorganization of neural pathways or CPGs through mechanisms addressed by neural plasticity (ability of the brain based on new experiences), there is strong awareness that strategies for recovering gait ability should be based on intensive training strategies directed to the stimulation of CPGs [43, 46, 47]. Within the same line of thought, it is also suggested that CPGs and the brainstem share a hierarchical relationship for controlling and modulating the walking patterns, i.e., voluntary commands from the brainstem (high-level control) assumed to reflect the person's intention are descended to CPGs (low-level control) to change the gait patterns, for instance, modify direction, speed, amplitude of trajectories, circumvent obstacles or walking on uneven ground, ... Therefore, the implementation of biological-inspired models to control the locomotion of a biped robot has become increasingly appealing, taking neurological and biomechanical inspiration from biological animals

and pursuing in refining the locomotion models in terms of energy efficiency, simplicity in the structure and robust adaptability to environment changes as main important features [48–50]. One of the recent biomimetic control architectures readily applied for biped locomotion reproduction and control and simultaneously developed as a priority in the Dissertation is the CPG model architecture based on nonlinear oscillators, due to its interesting properties such as: limit cycle behavior exhibition (i.e. isolated and stable rhythmic patterns) returning to its normal rhythmic behavior after transient perturbations of the state variables; few control parameters to enable, for instance, modulation of speed, direction or even the type of gait; fast control loops; allowance of gait modulation by simple control signals [43].

Relating the potential use of CPG models for locomotion control on rehabilitation, its application can be two-fold. From the function recovery perspective, the effective synchronization of artificial oscillators with the biological ones and the production of correct rhythmic patterns can be a precursor on compensating the deficits of the biological CPGs after neural injury, for instance, by providing the required torque to the controlled joints such that the therapeutic device and patient may together contribute for a successful motion generation [51]. Furthermore, better recovery expectancies of persons with locomotion abnormalities (e.g. stroke, Parkinson's disease and spinal cord injured patients) are well known related to intensive (longer and more frequent training sessions) rehabilitation programs as their aim target is the improvement of function by taking advantage of the plasticity of neuronal centers [52]. Therefore, the parallel intervention of artificial and injured biological CPGs can have an important role on stimulating plasticity in the affected nervous system and enhancing functional recovery. From the function substitution viewpoint, robustness in dynamic conditions is a major requirement and therefore CPG controllers are proposed as possible novel controllers with the ability of adaptiveness to unknown environments and perturbations. More detailed information about the importance of biomimetic approaches for both the two targets of rehabilitation is highlighted in chapter 2.

Several studies have already conducted CPG controllers within the rehabilitation field for several applications, including the production of rhythmic oscillations of a forearm about the elbow for robot-assisted/therapy during a locomotory task [51], the robustness and sensitivity evaluation of the controller for rhythmic movement assistance [53, 54], simulation studies of balance recovery and robustness to perturbations during walking for walking assist systems [28, 55, 56], the integration of CPGs with brain-computer interfaces [57], the use of CPGs to control prosthetic devices [58–61].

Thus, the aim target of this work is to study, analyze and discuss the applicability of CPG models for rehabilitation, either for assistance and/or therapy purposes. Focus is developed on the control of biped locomotion to increase the knowledge of the underlying principles useful for human assistance and therapy, exploring the brainstem-spinal-biomechanics interaction more fully that is still under-exploited. Currently, as the present walking orthotic/prosthetic systems are not sufficiently prepared to successfully react to unexpected real-world environment changes (such as uneven ground, slopes, obstacles, pushes, ...), the ultimate goal is to include a CPG model provided of the principles underlying the robust control of locomotion, the rules and the degree of pre-programmed behavior that may offer the flexibility to adapt to changes in the environment. To this effect, two main theoretical foundations are here explored. The first concern is the validation study of the synchronization and stability attained by nonlinear oscillators in relation to mechanical systems and to spinal oscillators: a minor part of the study is focused on performing hardware experiments (with an orthosis) for the control of a swinging task to verify synchronization of the CPGs with the natural dynamics of the mechanical system; subsequently, biomechanical simulations representing the major contribution of the work are developed for biped locomotion control, namely the learning of the correct design of joint nominal trajectories and interlimb coordination, the reproduction of those walking patterns on the biped model, the control of stable and steady-state walking gaits in open-loop (with no feedback pathways) and in closed-loop (external longitudinal feedback from biomechanical system is provided to modulate the spinal CPG reference outputs). Another theoretical assumption aforementioned discussed important for validation is that the spinal (automatic) and brain (voluntary) control are superposed or interact in a fashion way, by verifying the system's recovery to stable walking after the introduction of perturbations: to this purpose simulations are implemented likewise in closed-loop, this time, however, including also internal feedback pathways from the brainstem in addition to external feedback in order to represent voluntary modulation. The endorsement of this principle can enable the simulation of more complex behaviors (reaction to perturbations) and the coordination of automated and voluntary modulations which can be relevant for therapy and/or assistance.

Concerning the innovation this research can provide, it is designed a closed-loop CPG controller which may offer important improvements on stability and gait features such as higher mean walking velocity, step length and adaptation to environment changes by using sensory feedback, in contrast to other recent works that have implemented an open-loop con-

trol excluding therefore any longitudinal sensory feedback from the biomechanical system [28, 55, 62]. Moreover, stable gaits are produced not only on flat ground but also on a higher set of floor slopes compared to that achieved in [55, 62–64], apart from that stable gaits are attained switching between zero, positive and negative ground slopes within the same simulation. In order to create and maintain the entrainment of the controller with the body dynamics, it is proposed that the phase modulation of the oscillators using sensory feedback [65] such that the controller may be strongly coupled with the mechanical system it controls, rather than implementing the *phase resetting* adopted in recent works [28, 55, 66]. Another contribution from this research is based on the control of the postural balance of the biped system to ensure its stability and thus promoting an adaptive walking of the biped system against environmental variations.

1.4 Thesis structure

This study is organized as follows: a state-of-the-art of rehabilitation and assistive devices is developed in chapter 2; in chapter 3 a theoretical background of CPGs and their properties is introduced; the overall system design for biped locomotion control is explained in chapter 4; simulation setup, simulation procedures and stability criteria are described in chapter 5; chapter 6 presents results and discussion and chapter 7 includes the conclusion and future developments.

Chapter 2

State of the art of rehabilitation and assistive devices

Locomotion improvement can be attained through key factors such as neural plasticity, muscular tone and coordination reinforcement among others [67]. The functional activity of neuronal circuits within the spinal cord in humans, the central pattern generator, are thought to be the foundation of locomotion [46]. Moreover, neural plasticity underlies memory and learning processes being involved in the refinement and reorganization of neuronal circuits during nervous system development [68]. Many plasticity-related changes are induced during motor learning or after a neurotrama at both cortical and spinal level [69]. Thus, gait recovery strategies are currently based on intensive and repetitive task-specific strategies directed to the stimulation of neuronal circuits [46, 47] and to the improvement of muscular strength and movement coordination [67]. For instance, in stoke patients intensive and repetitive task-related practice promotes enhanced motor function associated to neuronal plasticity and brain functional changes [70, 71].

With regards to these aforementioned key factors, the manual-assisted training demonstrates several limitations that constraint the motor learning: low intensive training; training duration dependent on the physiotherapist commitment; execution of an irreproducible or suboptimal gait pattern; evidence of physical strain injuries in addition to ergonomically bad positions and extreme fatigue; possible requirement of multiple physiotherapists when assisting highly impaired patients; financial constraints.

Conversely, the assistive training devices offer a solution to these shortcomings. Some potentials of robot rehabilitation are highlighted as follows: they can control important variables (force, position, ...) through precise instrumentation making the task more or less

challenging according to the patient function ability; they can be useful for the accurate assessment of motor impairment and diagnosis (spasticity, tone, strength) minimizing the problems related to subjective clinical scales (e.g. FIM^{TM}[1] [72], Asworth [73]) and to poor interrater reliability [74]; they can reproduce repetitive (passive ranging, active reaching, gait training) and extremely physically demanding activities (e.g. reach-to-grasp tasks) for unlimited time; they can avoid the necessity of using more than one therapist when leading with severely impaired patients reducing therefore health care costs [75]; they can bring not only a better understanding of motor control principles but also broaden the therapy documentation within quality programmes. However, these technologies bring with them implicit and noticed handicaps to the rehabilitation scenario such as safety, clinician and patient fears, excessively high up-front costs for small centers in developed and developing countries, lack of smaller and cost-effective devices for home therapy and tele-rehabilitation scenarios [75].

Within the rehabilitation programme, significant relevance of gait function restoration has become clear in recent works, in which one has defined the rehabilitation programme priorities from a viewpoint of rehabilitation and life quality [76–81]. These work examples have all defined the gait ability restoration as a primary target of any rehabilitation programme, i.e., the gait function restoration is a high priority objective regardless of the neurological injury level, the time after lesion or even age [81]. Depending on the type and level of the patient's neural injury, either the rehabilitation program interventions or main goals can be different. However, the performance of a repetitive gait movement constitutes a common part of all programs in order to re-educate that specific movement. The presence of paretic musculature due to neural impairment implies the use of different systems which may provide a mechanical compensation to lower limbs, along with the exploitation of technical aids to enhance the balance preservation of the subject. Gait restoration is a two-sided process, characterized by compensating or rehabilitating a function.

Gait compensation consists of supplementing or completely replacing the motor function and protecting human joints, providing continuous support through extra power or movement accuracy enhancement. It is frequently conducted in the chronic stage of movement disorders or neural lesions in which it is not expected any improvements on gait function. Conversely, gait rehabilitation is focused on engineering a re-education of the referred function. It is generally developed in the acute stage of an injury aimed at retraining the nervous system and/or the musculoskeletal system and recovering the normal movement capacity. The tech-

[1] FIM^{TM} is a trademark of the Uniform Data System for Medical Rehabilitation, a divison of UB Foundation Activities, Inc.

nical means conducted in both stages may be coincident, since it may be possible to use gait compensation systems to conduct gait rehabilitation exercises. Within these rehabilitation scenarios, robotic exoskeletons have been mainly developed to allow a large number of task-specific repetitions in order to reinforce the effect of the basis for rehabilitation, the neural feedback [82]. Unlike conventional training, robot-assisted therapy on patients following a stroke or other neurological disorders is suggested to promote more effective short-term plasticity of locomotor circuits, to provide a framework on the achievement of more functional gait patterns, to restore or more accurately and effectively substitute muscle coordination patterns [83].

This thesis is focused on the lower limb rehabilitation to promote gait restoration of neurological injured or disabled subjects with gait abnormalities. It is necessary therefore to describe the main technological alternatives normally exploited in the clinical practice to provide compensation and/or rehabilitation of the gait function: (1) passive exoskeletons, (2) active exoskeletons, (3) functional electrical stimulation and (4) hybrid exoskeletons. An outlook into future developments as well as open research questions and challenges is also included.

2.1 Passive exoskeletons

In general, the term *exoskeleton* is used to describe a device that augments the performance of an able-bodied wearer, whereas the term *orthosis* is typically used to describe a device that is used to assist a person with a limb pathology. Passive exoskeletons were the first system introduced in the clinical practice for gait compensation through the knee-ankle-foot orthoses which could also include the hip joint, officially called as *(hip-) knee-ankle-foot orthoses, (H)KAFO*, figures 2.1(a) and 2.1(b), whose first design was developed in the fifties to achieve gait compensation on sick patients from poliomyelitis after an epidemic [84]. *HKAFO* orthosis is a mechanical structure whose main function is to stabilize the leg joints during the gait stance phase, allowing a swinging gait with the combined use of gait walkers or walking sticks. The mobility thus produced was slower, had low functionality requiring a great energetic consumption, which was estimated to be at least 43% higher than that required for the use of a wheelchair [85]. This fact helps to explain the low impact of the mentioned gait orthoses compared to the wheelchairs.

A few years later, efforts for accomplishing a gait compensation energetically less de-

Figure 2.1: Gait passive orthoses: 1(a) knee-ankle-foot orthosis (KAFO) [1]; 1(b) hip-knee-ankle-foot orthosis (HKAFO) [2]; 1(c) HKAFO orthosis with reciprocating mechanism on the hip joint [2].

manding were made through the development of dynamical orthoses enabling a passive motion of the hip joint, known as gait reciprocating orthoses [86–90] (figure 2.1(c)). Nevertheless, both low gait velocity and still higher energetic cost were recognized as the main reasons for disregarding these orthoses [91–93].

2.2 Active exoskeletons

The first active exoskeleton was undertaken in the seventies by Vukobratovic, comprising actuators on the hip, knee and ankles in order to assist the movement on the sagittal plane [94]. That system was tested on 100 subjects with several leg paralysis degrees through the use of walking sticks. Since then, many exoskeletons for gait compensation were built with a great variety of actuation technologies and sensorization as well as control strategies. The main systems found in the literature are summarized in tables 2.1 and 2.2.

Table 2.1: Active exoskeletons presented in the literature.

System	Actuation	Control strategy	Features	Evaluation	Year
PAGO [9]	Pneumatic cylinders on hip and knee.	Position-based.	Compact energy source.	Paraplegic T3 SCI patient.	2001
Roboknee [95]	Elastic actuators on knee.	Force-based.	3 kg. Low impedance. Battery autonomy: <1 h.	None.	2004
AAFO [96]	Elastic actuator on ankle-foot.	Force-based. Position-based.	2.6 kg. Low impedance and power consumption.	Drop-foot patients.	2004
AFOUD [11]	D.C. motor on the ankle.	Position-based.	2.6 kg.	None.	2005
AFOUM [12]	Pneumatic actuators on the ankle-foot.	EMG-based.	1.7 kg. "Noisy" actuator.	Chronic incomplete SCI patients.	2005
TUPLEE [4, 97]	D.C. motors on the knee.	EMG-based	5 kg.	None.	2006
RGT [13, 98]	Pneumatic actuators on the ankle-foot.	Position-based.	Tripod mechanism. Broad ROM.	Chronic stroke patient.	2006
AAFOUY [14, 99]	Elastic actuator on ankle-foot.	Position-based.	Broad ROM.	Hemiplegic patient.	2006
Anklebot [15, 100]	D.C. on the ankle.	Position-based.	3.6 kg. Low impedance.	Chronic stroke patients.	2007
PPAFO [16, 101]	Pneumatic actuator on the ankle-foot.	Force-based.	3.1 kg. Compact and portable energy source.	Plantarflexor, dorsiflexor and SCI impaired patients.	2011

2.2.1 H.A.L.

The *Hybrid Assistive Leg* (H.A.L., in the early 2000s) is a full exoskeleton commercially available since 2011 to help healthy people for performance-augmenting purposes with a cost between $14,000 and $19,000 (figure 2.2) [107]. It is considered to be a complex fitting system (great efforts and time-consuming on donning and doffing). Up to now, there has been a lack of evidence of H.A.L. effectiveness on gait restoration of impaired people for ADLs enhancing.

The control of joints motor relies on two monitor systems responsible for detecting the

Table 2.2: Active exoskeletons presented in the literature (continuation).

System	Actuation	Control strategy	Features	Evaluation	Year
HAL [102–104]	D.C. motors on hip, knee and ankle.	EMG-based. Position-based.	23 kg. Complex fitting system.	Paraplegic, hemiplegic patients.	2009
eLegs [6, 105]	Not available.	Not available.	20 kg. Battery autonomy: 6 h. Scalability.	Patients with incomplete and complete paralysis	2010
SCKAFO [17]	Knee: brake and D.C. motor. Ankle: brake.	Force-based. Position-based.	1.9 kg. Portable energy source. Modularity.	None.	2011
PIGRO [5, 106]	Pneumatic cylinders on hip, knee and ankle.	Position-based.	Scalability. Modularity.	None.	2011
ASOD [18]	Pneumatic actuators on the anterior lower leg.	Position-based. Force-based.	0,95 kg. Battery autonomy: 2h. Low consumption.	None.	2011
REX [7]	Not available.	Not available.	39 kg. Battery autonomy: 2 h. Scalability.	Not available.	2011
VPO [8]	D.C. motors on hip, knee	Position-based.	12 kg. Battery autonomy: 1 h. Modularity.	Paraplegic T10-complete SCI patient.	2011

Figure 2.2: H.A.L. exoskeleton [3].

user's intention, namely an electromyography (EMG)-based system and a walking pattern-based system [102, 103]. Regarding the estimation of joint torques from EMG signals, the optimal calibration of the exoskeleton for a corresponding user has lasted approximately 2 months according to a report [3]. An algorithm for gravity compensation is later included in order to support the wearer's weight so as to lower the error from the reference angles, if a constant large force such as gravity affects the joints of the H.A.L. [104]. In addition, the wearer's intention during sit-to-stand and stand-to-sit transfers is estimated based on a preliminary motion of their upper body and posture positions [104].

2.2.2 T.U.P.L.E.E.

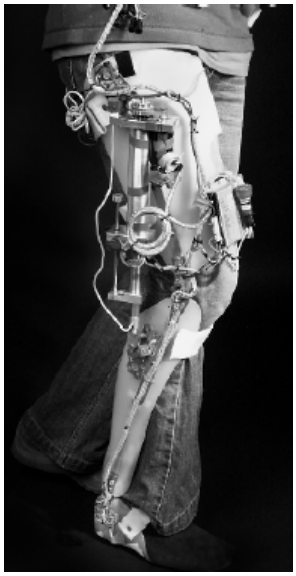

Figure 2.3: T.U.P.L.E.E. prototype [4].

The *Technische Universität Berlin Powered Lower Extremity Exoskeleton* (T.U.P.L.E.E., 2006) system is used to support the thigh muscles during flexion and extension of the knee (figure 2.3)[4]. Till today, no experiments were performed on impaired subjects due to safety issues. Before experiments with patients can be performed, motions should be made smoother and the EMG input safer by adding control layers to cope with undesired bursts [4, 97].

The EMG-based control system is adopted to evaluate EMG signals from thigh muscles to determine the intended motion of the subject, allowing thus a continuous control of the exoskeleton. Within the control structure, a torque control loop is implemented where the knee torque resulting from the muscle activations in the human thigh is estimated based on

EMG signals and on muscle model. For the whole system, only a few sensors are required which makes easier the calibration performance. In contrast to H.A.L. [104] which implements a physical model algorithm with dynamic equations, no knowledge about masses or velocities of the body parts is needed. In spite of the level of support being changed by the orthosis depending on the activation of the different muscles, it will however never hinder any motion [97]. However, it is not possible to integrate algorithms for maintaining postural stability of the human, due to the absence of a dynamic body model so as information about masses, accelerations, and angles is available [4].

2.2.3 P.I.G.R.O.

Figure 2.4: P.I.G.R.O. prototype [5].

The Department of Mechanics of Politecnico di Torino has designed a 6-DOF machine called *Pneumatic Interactive Gait Rehabilitation Orthosis* (P.I.G.R.O., 2001) (figure 2.4) [9]. Unlike the previous exoskeletons, it is also characterized by being scalable or while allowing anthropometric regulations from 10% percentile female to 95% percentile male. As a modular exoskeleton, it is possible to activate one or more legs independently. Clinical trials on impaired subjects are yet to be performed [5].

In terms of control and actuation system, pneumatic actuation systems provide more comfortable interaction between machine and patient, safety, transparency in relation to electric actuation systems adopted by H.A.L. and T.U.P.L.E.E. exoskeletons. The control system is based on closed-loop position control for each joint independently, incorporating a PID controller whose gains are adjusted according to the wearer [5, 106].

2.2.4 eLegs

Figure 2.5: eLegs exoskeleton [6].

An exoskeleton recently designed and developed at Berkeley Bionics is the so-called eLegs (2010) whose architecture is kinematically similar to the counterpart of the human [108]. It is readily available for commercialization as a market version of the MIT mobile medical robots, enabling the capability of walking, stair climbing and standing up (figure 2.5). The system can provide a maximal gait speed around 3 Km/h. Two handicaps of this system are pointed out: some portions must be worn, what constitute points of interface between the wearer and the exoskeleton, more specifically, torso brace and straps, an upper strap and a knee brace; crutches are required for providing support and stability. Currently, the machine is only available for clinical rehabilitations and hospital and it is expected to be available for personal use by the end of 2013. More information about control strategy are not accessible.

Comparing to P.I.G.R.O., its scalability is lower, since it is only suitable for those who can self-transfer from a wheelchair to a chair, who are between 1,58 - 1,95 m tall and have a maximal weight of 100 Kg [108]. Unlike P.I.G.R.O. and T.U.P.L.E.E. systems, the presence of an autonomous battery is an advantage in terms of portability.

2.2.5 REX

The Rex Bionic, Lda. company has also designed and manufactured a device called REX (2011) to enable wheelchair users and other mobility impaired subjects to stand up from a

Figure 2.6: REX device [7].

chair, to walk, to shift sideways and to climb stairs, enhancing therefore their independent upright position and mobility (figure 2.6) [7]. In contrast to eLegs and Rewalk, REX does not require crutches or other supports. Moreover, a joystick is adopted as a means of the user controlling the exoskeleton, rather than employing sensors to detect intent of the user. Like eLegs, REX can provide a maximal gait speed around 3 Km/h and is commercially available since 2011. More information about the control strategy and clinical outcomes are not accessible.

Regarding the scalability of the orthosis, REX is suitable for those with weakened muscles and by some people with disabilities due to stroke, SCI and/or multiple sclerosis. Furthermore, the subjects must be between 1,58 - 1,95 m tall and with a maximal weight of 100 Kg [108].

2.2.6 V.P.O.

Figure 2.7: V.P.O. prototype [8].

Towards the aid locomotion in paraplegic subjects, a powered lower limb exoskeleton called *Vanderbilt Powered Orthosis* (V.P.O., 2011) was developed to assist SCI patients actuating on the hip and knee joints, while the orthosis control is attained by the incorporation of a user interface and control structure through upper-body influence (figure 2.7) [8].

Both actuators and transmission units are assumed to be backdriveable[2], what is an improvement in relation to previous exoskeletons. However, the battery has lower autonomy than that of the previous exoskeletons and the average speed provided is also lower (0.8 Km/h). This orthosis presents several enhanced features in portability and wearability terms: (1) strong focus on ergonomics and user acceptance; (2) the device is extended below mid-abdomen without requiring any other portions to be worn, enhancing thus transparency; (3) the compactness of the device is promoted; (4) the modularity of the orthosis enhances ease of donning and doffing; (5) can ensure safety in case of power failure event [8, 110].

In contrast to HAL, Rewalk and eLegs systems, V.P.O. does not require to include some portions to be worn either over the shoulders or under the shoes. Inclusively, V.P.O. has apparently also lower weight [8, 110]. Priority challenges to be addressed in the near future are still the promotion of more scalability, transparency, wearability and longer battery autonomy. Inclusively, its total weight should be further decreased [110].

2.2.7 Ankle and/or knee orthoses

Several devices have been designed with the aim target of powering or restoring the knee and ankle movements. In this context, complex bone structures of the ankle and its several DOFs promote the difficulty of controlling its movements. Unlike wearable passive orthoses, these actuated exoskeletons are capable of controlling joints kinematics and dynamics, compensating joint weaknesses and motion deformities [26]. For instance, drop-foot gait is a common handicap resulted from neurological diseases such as stroke, multiple sclerosis, cerebral palsy, among others. Below, just a few examples among many are highlighted which have been mainly conducted or are very close to be conducted on clinical trials in addition to enable overground assistance for ADLs and quality of life improvement.

2.2.7.1 P.A.G.O.

Another system was developed aimed at addressing functional gait restoration in paraplegic persons, namely the *Pneumatic Active Gait Orthosis* (P.A.G.O., 2001) [9]and has the ad-

[2]Backdrivability is related to actuators containing high force sensitivity and high impact resistance [109].

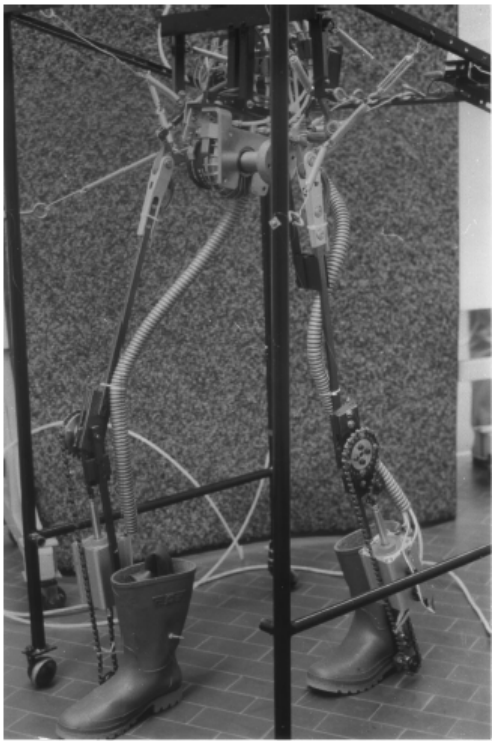

Figure 2.8: P.A.G.O. prototype [9].

vantage over other exoskeletons of its energy source being more compact and lightweight, critical features for wearability [9]. P.A.G.O. exoskeleton was not commercialized up to now [26].

2.2.7.2 Roboknee

Figure 2.9: Roboknee exoskeleton [10].

Roboknee (2004) is developed with the purpose of assisting the knee joint by powering the thigh muscles (quadriceps and hamstrings) to enable knee flexion/extension during

several daily activities like stair climbing, standing and so forth (figure 2.9) [95]. This exoskeleton provides better low-impedance interaction with the user becoming therefore very transparent to the wearer in relation to other systems which use electric and pneumatic actuators. The low impedance is achieved by the use of a linear series elastic actuator (SEA), consisting of a brushless DC motor in series with a spring. It is composed of compliant elastic elements conferring significant compliance between the actuator's output and the load in addition to allowing for greater control gains [95]. .

Concerning the portability and wearability features, Roboknee exhibits lower weight and comfort comparing the counterpart exoskeletons (Table 2.1), although it presents yet low compact actuators, short lifetime and some complexity on donning and doffing. It provides a maximal gait speed around 2,5 Km/h. Moreover, Roboknee cannot support paraplegic patients due to its inability of supporting simultaneously multiple joints in lower limbs and of controlling the posture of the patient [102]. Consecutively, new advancements on Roboknee are expected in order to evaluate its performance on clinical trials.

2.2.7.3 A.A.F.O.

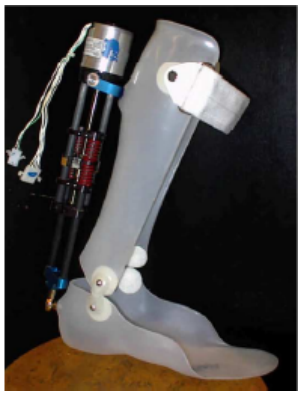

Figure 2.10: A.A.F.O. prototype [10].

A powered ankle-foot orthosis was developed by Massachusetts Institute of Technology (MIT) group, the so-called *Active Ankle-Foot Orthosis* (A.A.F.O., 2004), to enable drop-foot gait assistance (figure 2.10) [96]. The orthosis seems to share the same mechanical brace of previous constant-impedance ankle-foot orthoses (AFOs) in addition to a force-controlled (ground force and angle position data) SEA capable of controlling orthotic joint stiffness and damping through impedance variation according to walking phase and step-to-step gait variations, which is believed to provide better clinical outcomes over both unassisted gait and conventional AFOs. Moreover, SEA can be protected from shock loads and the spring

can also prevent undesired phenomena such as backlash effects, torque ripple and friction. The device presents compactness, is more lightweighted than Roboknee, although it is not yet energetically autonomous and therefore not portable.

Clinical tests were conducted on two drop-foot patients experimenting a unilateral drop-foot condition without any other disability on the affected leg. Comparing with the conventional AFO orthoses, the frequency of foot slaps was considerably decreased at faster gait speeds as well as drop foot or toe drag events could be reduced as function of sufficiently increased swing dorsiflexion amount by using the variance-impedance control. Consequently, not only swing phase ankle kinematics were more natural but also spatial and temporal gait symmetry could be improved although not significantly, while providing effective assistance during powered plantar flexion. Moreover, positive feedbacks from users were characterized by a good transparency of the device, better portability features in relation to those of conventional AFOs already weared by them and their manifested interest for the possibility of A.A.F.O. purchase. These orthoses have shown better outcomes over conventional AFOs with constant impedance and to be significantly less complex as a permanent assistance device in relation to functional electrical stimulation [96].

Nonetheless, the application of A.A.F.O. on ADLs requires improvements on the actuation system regarding the achievement of lighter and less power-intensive actuator and improvements on adaptability and versatility to many activities of the users' daily living (e.g. walking on stairs, ramps).

2.2.7.4 A.F.O.U.D.

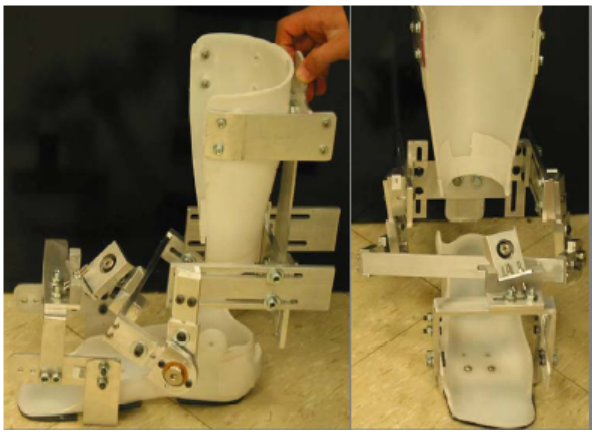

Figure 2.11: A.F.O.U.D. system [11].

Another active ankle orthosis was developed, the *Ankle Foot Orthosis at University of*

Delaware (A.F.O.U.D., 2005), enabling motion and providing power in both the flexion-extension and inversion-eversion movements in order to assist subjects with weakness of ankle dorsiflexor muscles (figure 2.11) [11].The weight of the orthosis is about 2.6 Kg, although the authors are expecting to reduce the weight involved. A new version of the system has been developed with a total weight of 3.7 Kg, incorporating also the measurement of joint forces and moments applied by the human at both joints through the use of force-torque sensors and encoders [111].

This system must still be redesigned to reduce its weight and must also include an actuator to consider the possibility of regarding the orthosis as a training device to restore a normal walking pattern. Experiments of the exoskeleton with impaired humans have yet not been reported up to now [111].

2.2.7.5 A.F.O.U.M.

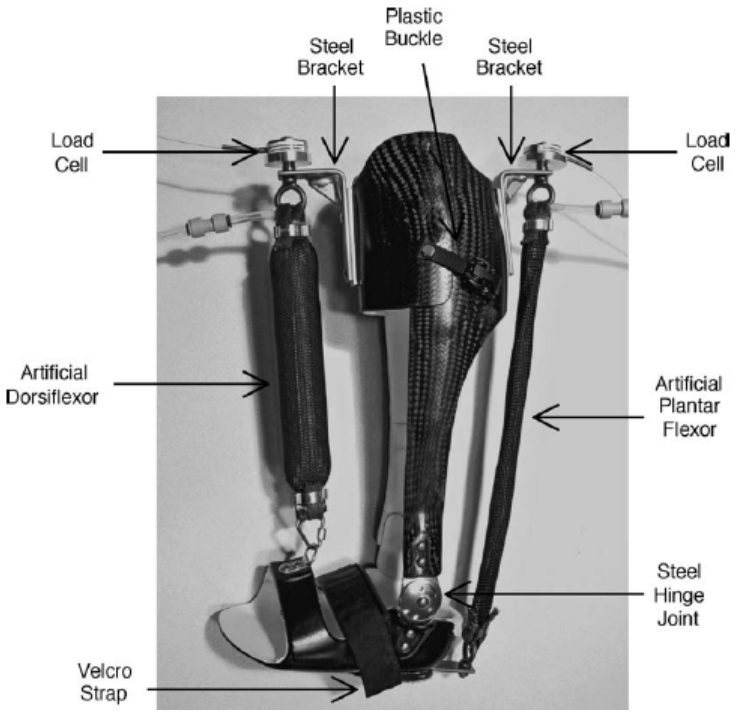

Figure 2.12: A.F.O.U.M. device [12].

The *Ankle-Foot-Orthosis at University of Michigan* (A.F.O.U.M., 2006) is an active exoskeleton mostly pneumatically-actuated, including two artificial pneumatic muscles (figure 2.12) [12]. The device can be relatively lightweight, provide artificial high-power outputs and offer safety through the use of those low-impedance artificial muscles, which can power

and control the dorsiflexor and plantar flexor torques about the ankle and and knee extension/flexion.

An easier donning and doffing was met by using a bivalve carbon fiber design with plastic buckles. Of all the counteract AFOs, A.F.O.U.M. is the most lightweighted. However, there is reported an ineffective energy transmission from the artificial muscles in addition to limitations on the knee torque production due to the actuators. Moreover, the actuator is considered noisy and lacked of a compressor [112]. Since A.F.O.U.M. is not provided of a portable energy supply, the device is not considered fully portable, what is a crucial limitation comparing to other exoskeletons.

Concerning the control strategy, a proportional myoelectric controller is implemented to adjust air pressure in the artificial pneumatic muscles proportional to the processed biological muscle activation pattern measured by EMG. This is, the timing and magnitude of artificial muscle forces can be determined by the presence of the user's own surface EMG, taking inspiration from biology [12]. On the other hand, the controller is relied on an error-amplification strategy in the sense that kinematics errors produced by muscles are enhanced to facilitate their detection by the nervous system which can therefore correct the subsequent electrical commands to the muscles [112].

2.2.7.6 R.G.T.

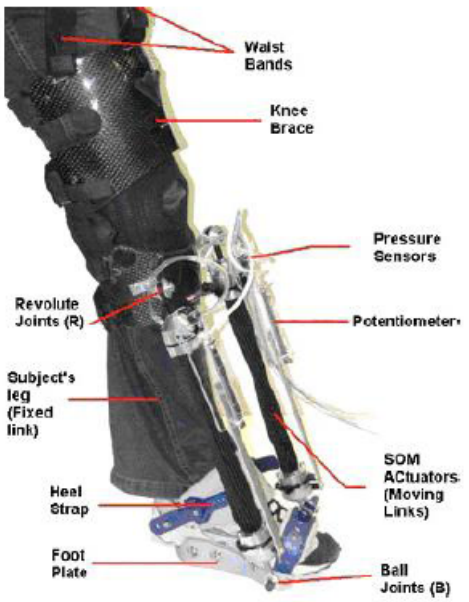

Figure 2.13: R.G.T. orthosis [13].

Some researchers at the Arizona State University have designed an active AFO, the

Robotic Gait Trainer (R.G.T., 2006), comprising two compliant, safe spring-in-muscle actuators linked at both sides of the foot under the toes, providing a tripod structure with the heel (figure 2.13) [98].

The actuators are based on pneumatic muscles including an internal compression spring which enables the force to be applied in both plantar and dorsiflexion directions, the so-called *Spring Over Muscle* actuators. In order to increase achieve a better ankle rehabilitation, it is developed a tripod mechanism consisting of a flat plate and three bi-directional links. More precisely, two links are bi-directional actuators and the third link is the leg of the user (fixed link) [98].

Comparing with other previous technologies such as those employing pneumatic muscles (e.g. P.A.G.O., A.F.O.U.M.) or motor-actuated systems (e.g. A.A.F.O.), R.G.T. includes preferably springs over conventional pneumatic muscles which are more compliant, lightweight, enable the reduction of the actuators amount and hence the control simplicity. Moreover, in contrast to the comparative exoskeletons which cannot fully rehabilitate the ankle joint through the entire range of movement (ROM), the tripod structure can generate a ROM correspondent to the safe anatomical range of the ankle joint. Consecutively, the system is considered naturally compliant allowing a more natural gait by achieving positional accuracy . In contrast to other AFOs, in R.G.T. (so as in A.F.O.U.D.) movement of the foot about the ankle joint in dorsiflexion and plantarflexion as well as inversion and eversion is possible, a feature unique to the lightweight, compact and easily portable device [98].

However, R.G.T. includes also some limitations: it is yet not scalable; it demonstrates excessive bulkiness and weight; the response time of the pneumatic system is not preferably shortened. Clinical tests in order to produce concrete, statistically evidence of RGT therapy benefits for stroke patients is yet to be carried out [13].

2.2.7.7 A.A.F.O.U.Y.

The *Active Ankle-Foot Orthosis at the University of Yonsei* (A.A.F.O.U.Y., 2006) was also developed to prevent foot drop and toe drag during walking by actively controlling the ankle joint dorsiflexion/plantarflexion (figure 2.14) [14]. The main goal is to mitigate forefoot collision with the floor at the heel strike, to provide the toe clearance and to help the push-off through the ankle joint control. Although ankle dorsiflexion/plantarflexion motion is enabled, motions in other directions are not restricted though.

In relation to control and actuation systems, proper ankle moments are provided based

Figure 2.14: A.A.F.O.U.Y. prototype [14].

on an accurate detection of the gait phase similar to a finite-state machine, by means of a gait phase detection algorithm. In relation to the R.G.T. device, A.A.F.O.U.Y. provides lower dorsiflexion ROM and similar plantarflexion ROM and does not share some portability properties of the former system.

Results of clinical trial have shown the prevention not only of the foot drop by the proper plantarflexion during loading response but also of the toe drag by sufficient amount of plantarflexion in pre-swing and reasonable dorsiflexion during swing phase, enhancing almost all temporal gait parameters. [99].

2.2.7.8 Anklebot

Figure 2.15: Anklebot exoskeleton [15].

The MIT group (2007) has designed an ankle robot aimed at stroke rehabilitation due to the prevalence of foot-drop, the Anklebot (figure 2.15) [15]. This device is innovative in

relation to counterpart AOFs such as A.A.F.O.U.Y. and R.G.T., since it can not only provide higher ankle DOFs (dorsiflexion-plantarflexion, inversion-eversion and external rotation), but also enables higher ROM in all DOFs. However, it is less lightweighted than the comparative AFOs (e.g., A.AF.O., A.F.O.U.D.). It is low-friction and is backdriveable, presents low mechanical impedance, does not apparently interfere with natural or impaired gait and provides comfort to the wearers. Up to now, it is the only available ankle robot for commercialization [100].

In a clinical study developed on chronic stroke patients, it was found that Anklebot can be safely weared by most hemiparetic patients and with minimum disruption of their unloaded gait pattern [100].

2.2.7.9 P.P.A.F.O.

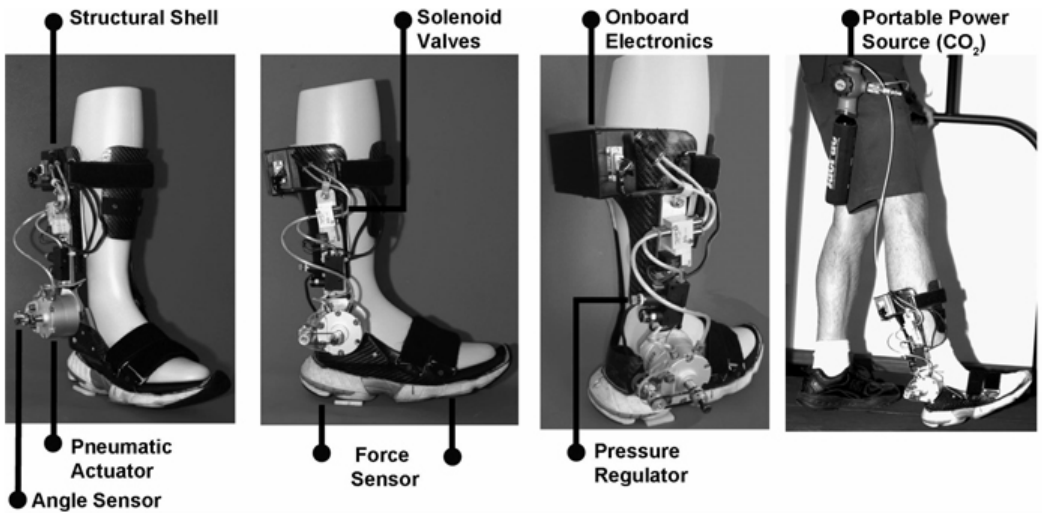

Figure 2.16: P.P.A.F.O. system [16].

A more recent orthosis was developed, namely the *Portable Powered Ankle-Foot Orthosis* (P.P.A.F.O., 2011), to enhance the capability of the assistive torque application for daily use both to increase walking function through training and/or to improve strength and ROM by means of prescribed external power-assist modalities (figure 2.16) [16].

P.P.A.F.O. demonstrates a higher weight than previous AFOs (e.g., A.F.O.U.M., A.F.O.U.D.), it includes a more adequate energy source which is more compact like that of P.A.G.O. Additionally, the pneumatic power source is portable (bottle of compressed CO_2) and electronics is embedded, two facts enabling the P.P.A.F.O. to provide untethered powered assistance, what is a great advantage in terms of portability. Nonetheless, it can only provide

plantarflexor-dorsiflexor torque assistance, in contrast to its counterparts (e.g., A.A.F.O.U.Y., R.G.T., Anklebot) [16].

P.P.A.F.O. actuation is controlled both in timing and magnitude according to four discernible gait events through the use of force sensors. Furthermore, for each subject it is incorporated a heuristic tuning scheme to determine the timing and magnitude of the P.P.A.F.O. assistance [16].

A first clinical evaluation was performed on a patient with cauda equina syndrome caused by spinal disk rupture, who could walk without walking aids although an orthosis was required for community ambulation. The outcomes have shown introduction of minimal perturbations on the ankle joint kinematics by the assistance device and on the effective assistive capabilities. Nevertheless, device control issues derived from the walking strategy of the hell of the patient and the device fitting to the user prevented a full demonstration of untethered functional assistance. Moreover, sensors could not reliably detect all gait events. Further recruitment and testing of multiple impaired subjects are thus expected to access the device as a viable rehabilitation tool. Logical issues such as the refill of power sources are yet not addressed. Other features including more compact and lightweight actuators and enhanced control schemes are under development for the weight reduction of the orthosis and augmentation of performance and efficiency [16].

A second clinical trial was developed on two disabled patients, one with severe plantarflexor impairment and the other with severe dorsiflexor impairment [101]. P.P.A.F.O. has demonstrated appropriately timed functional assistance in both patients with a good assistance performance according to the feedback of patients. However, a higher sample size is needed to evaluate the effectiveness of the functional assistance as well as further improvements already reported in the previous study are yet to be met. Improved P.P.A.F.O. control algorithms for different locomotion modes (standing, ramp walking, stairs) are yet to be addressed. Nevertheless, P.P.A.F.O. is on the right track to expand rehabilitation and daily-wear assistance opportunities for gait restoration enhancement.

2.2.7.10 S.C.K.A.F.O.

The active *Stance-Control Knee-Ankle-Foot Orthosis* (S.C.K.A.F.O., 2011) is the recent proposed prototype aimed at providing assistance to SCI patients with partially denervated knee and ankle muscles (figure 2.17) [17]. The device comprises a passive compliant joint for ankle plantar flexion restriction in addition to a powered knee unit (composed of a controllable

Figure 2.17: S.C.K.A.F.O. prototype [17].

mechanical locking system and an electrical DC motor that actuate independently) for the prevention of knee flexion during stance phase and for the swing flexion-extension control. Moreover, the ankle unit consists of a passive joint responsible for avoiding drop-foot gait and limiting ankle dorsiflexion.

The exoskeleton is one of the most lightweighted devices, although heavier than A.F.O.U.M. More interesting features of portability are as follows: (1) both knee and ankle units are modular which enable the device to support a large segment of potential users, due to its scalability to different subjects and different levels of dysfunction; (2) it is energetically efficient; (3) the energy source consists of an external supply unit [17].

The actuation system is comprised of an electrical DC motor and a commercial electronically controllable locking mechanism. The locking of the knee flexion during stance does not require energy consumption. Currently, the control system can only control the walking motion without detecting other states such as standing or sitting down. The control is based on identifying the main events which define the gait phases through feedback measurements, although more information is not provided [17].

Although the S.C.K.A.F.O. presents already some important features in terms of wearability, this device is still at a very early stage of research.

2.2.7.11 A.S.O.D.

An exoskeleton inspired by the biological musculoskeletal system of a human foot and lower leg is proposed, the so-called *Active Soft Orthotic Device* (A.S.O.D., 2011), which can mimic the muscle-tendon-ligament architecture in a biological musculoskeletal system of a human foot and a lower leg (figure 2.18) [18].

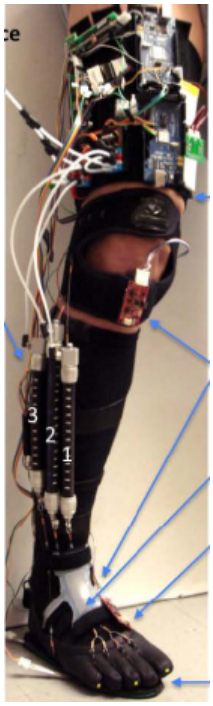

Figure 2.18: A.S.O.D. prototype [18].

The term *soft* is derived from the incorporation of soft plastics and composite materials (providing low weight, flexibility, robustness to the structure) which tend to mitigate the ankle DOFs restriction while providing assistance. These soft material respond to the shortcomings in the enhancement of the DOFs number in prior exoskeletons containing rigid frame structures and mechanical joints. The actuators consist of pneumatic artificial muscle actuators powering and controlling plantar-dorsiflexion as well as inversion-eversion motions, in contrast to prior orthotic designs that either constrain or actuate the ankle joint only in a sagittal plane [18].

The exoskeleton can provide active assistance without limiting 3D motion of the foot, is compact, may conform to the human leg due to the flexibility of the actuators and other components, it is the most lightweighted in the literature and it constitutes an almost untethered system while it is disposed of multiple physical layers to be worn (modularity). The power consumption relating the pneumatic actuation is relatively small associated to pneumatic actuation, by which three rechargeable batteries can promote enough power for more than two hours. Conversely, the battery autonomy of previous exoskeletons cannot exceed two hours [18].

Further improvements should include the design refinement for wearability improvement and for significant reduction of the electronics, the increasing of artificial muscles to incor-

porate posterior muscles for a complete gait cycle by actively assisting plantarflexion, the incorporation of portable air compressors and compressed air canisters to substitute the actual air source connection on which the system is dependent, the development of relevant clinical requirements and potential control strategies that would work seamlessly with the motion of the user. Once these requirements are met, one may achieve a fully untethered wearable system to enhance new and improved rehabilitation techniques both inside and outside of the clinic [18].

2.2.8 Revision of active systems

The inherent limitations of passive exoskeletons can be addressed by the development of active powered systems by providing net power to the joints for motion control and torque assistance. They can have great impact either as clinical rehabilitation tools or as daily-wear applications means, being also used in locomotion studies for gait perturbations. Till date, the problem of scarce powered systems available on the market has been related to the size and power features of the devices which have confined them to clinical settings. However, there are a few portable systems which may achieve a fully untethered wearable system which may open a rich space for future rehabilitation techniques both inside and outside of the clinic and thus provide a new level of mobility and active assistance (e.g., Roboknee, P.P.A.F.O., V.P.O., A.S.O.D., ...).

The main actuator types adopted by the aforementioned active orthoses can be review as follows:

1. Hydraulic actuators:
    - Power to joints is transmitted through pressured fluid;
    - Great potential force and torque production;
    - Higher power-to-weight and power-to-volume;
    - Noisy;
    - Frequent maintenance;
    - Other units are required such as compressors, cooling systems, ..., with high power consumption;
2. Pneumatic actuators:

- Power to joints is attained through pressured gas;
- Lower weight and cheaper in relation to hydraulic actuators;
- Better power-to-weight ratio than electrical actuation;
- Safety provided by low impedance;
- Provide for non-flammable, clean actuation system;
- Potentially noisy;
- Frequent maintenance;
- Other units are required such as compressors, accumulators with high power consumption;

3. Electric motors:

    - Mostly used;
    - Simple installation;
    - Low weight;
    - Noiseless;
    - Higher control bandwidth;
    - Provide for clean actuation system;
    - Maintenance not required;

Within the group of electric motors, SEA is considered to be crucial for the powered systems intended for daily wear due to several additional advantages such as low impedance, isolation from shock loads, filtration of undesired events (effects of backlash, torque ripple, friction) by the spring, stable behavior independently of the environment involved. On the other hand, pneumatic actuators seem to be a preferable solution over the electrical actuation in terms of rehabilitation inside clinical settings where untethered power source is not required, since they are very reliable and easily maintained, with high availability on compressed air sources and with more interesting power-weight ratio [113].

However, many authors argue that powered exoskeletons alone may not comprise an effective alternative for gait compensation though, due to the many limitations which must still be overcome [3, 10, 114–116]:

- The torque/load ratio of actuators should be incremented;

- More portable and lighter energy storage systems should be developed: powered devices are often heavy and bulky with limited torque and power, making the movements of the wearer difficult to augment;

- Design and construction of exoskeleton devices at a lower cost, complexity and lower time-consuming should be encouraged to facilitate large-scale manufacturing;

- There are required developments on bio-inspired actuation systems, compatible with the forces produced by the user, implementing muscular-tendinous functions and producing enhanced biomimetic limb dynamics;

- Development of exoskeletons which can promote a significant decrease in the metabolic demands of walking;

- The kinematics compatibility between the body and the exoskeletons should be higher in order to enhance comfort and safety;

- The interfaces between the tissues and the exoskeleton which determine the interaction efforts should be optimized to provide an efficient support to the user joints;

- The exchange systems of physical and cognitive information between the user and the exoskeleton should be more transparent and friendly: there is still a lack of direct information exchange between the human wearer's nervous system and the wearable device;

- Aspects related to exoskeleton usability should be deeper explored: more natural and noiseless devices for cosmetic purposes; actuators with high levels of performance, lifetime, advanced efficient and compact driving electronics, compact and lightweight energy source; more scalable and compliant devices;

- Adaptability and versatility of exoskeletons should be improved: various gait trainers are usually unable to fully adapt their movements to the activity of the patient; mostly, the system requires clinical settings to operate and thus cannot be used by the patient for therapy at home;

- There should be performed technical, clinical and rigorous evaluations which could provide sufficient evidence about the aforementioned aspects.

Although the active exoskeletons for rehabilitation provide several advantages over conventional therapies, there is yet a lack of evidence concerning the use of robotic assistive devices for ADLs improvement. The reinforcement of the effect of the basis for rehabilitation (i.e. neural feedback) is still far from straightforward, by which exoskeletons in physical therapy can be attractive but yet not fully explored. For instance, regarding stroke robotic rehabilitation therapy, there is till far not yet a consensus with respect to effectiveness at chronic or acute stages after stroke [10], although it has demonstrated to be at least as effective as conventional therapy with regard to ADLs improvement [117].

2.3 Functional electrical stimulation

In parallel with the previous alternatives, the muscular electrical stimulation has been broadly exploited for gait compensation, where the muscles are stimulated through electric impulses previously configured to generate an articulated motion of functional tasks [118], then called functional electrical stimulation (FES). The use of FES was undertaken in the 1960s, in which the first FES implementations on paraplegic patients used percutaneous electrodes to stimulate the muscular groups of quadriceps and gluteus to induce gait patterns [119] and to compensate the foot plantar drop during the swing phase [120]. During the last two decades there has been developed FES systems based on designs from Kantrowitz and Liberson [121–128], having achieved recent technological advances in the FES technology which enabled a more complete and efficient stimulation such as multichannel stimulation, implantable electrodes, advanced sensors and automatic control systems [129]. Some of the main advantages from FES can be reported: the possibility of long use autonomy due to the movement generation taking place from the force produced by the stimulated muscle [130], walking improvement with the stimulator when not in use as a result of regular use of FES in gait training or ADLs [131].

However, FES also includes technological difficulties. Firstly, one drawback is related to the premature onset of the muscular fatigue which reduces the duration of FES employment. On the other hand, the complexity regarding the joint trajectory control generated by the stimulation is still high, therefore not yet satisfactorily addressed [129, 132]. Furthermore, a considerable portion of the general disabled subjects may not undertake FES according to their specific condition which severely limits its effectiveness as a rehabilitation technique. For instance, in a study relating rehabilitation paraplegic subjects, FES-assisted paraplegic

gait was characterized by its slowness, awkwardness, high energetic demand and unnatural walking [133]. Overall, FES is considered effective in reducing both upper and lower motor impairment by the literature, especially those approaches incorporating task-specific strategies [134–137].

2.4 Hybrid exoskeletons

As already discussed before, the technologies previously described present drawbacks which avoid the development of effective strategies for gait compensation. Since the main limitation of FES is the control of the joint trajectory, some research groups have combined reciprocating orthoses with FES as a combined source of movement production. However, the literature shows that FES inclusion on reciprocating orthoses can only provide small improvements in terms of metabolic cost and gait velocity, wherefore they do not constitute an attractively efficient alternative for gait compensation [138–141].

Conversely, the combination of the active exoskeleton technologies and FES can achieve an interesting performance in which is possible to combine advantages and principles of actuation and rehabilitation of both technologies in addition to mitigate their individual limitations in the context of either gait compensation or rehabilitation. Importantly, hybrid exoskeletons are based on FES employment to produce movement using an exoskeleton to correct or to compensate the trajectories generated by FES and therefore to minimize the appearance of muscular fatigue. This rehabilitation technique has demonstrated several benefits and very promising results over standard or convention techniques [131, 135, 142, 143]:

1. Reduction of the exoskeleton power demand through FES muscle power generation:
    - Less powerful joint actuators.
    - Lighter and power-demanding overall system.
2. Muscle fatigue due to FES can be counterbalanced by exoskeleton's design and hybrid control:
    - FES employment during training sessions for longer periods of time is possible.
    - Benefits from FES actuation can be also increased (muscle strength, cardio-respiratory fitness).
3. It is an intensive, community-based gait therapy:

- ADLs can be promoted.
- Neural plasticity can be better stimulated.
- Gait compensation and/or rehabilitation in real environments can be preferably targeted.

In this section it is presented the detailed analysis of hybrid exoskeletons for gait compensation on disabled patients existing in the literature. The main differences among the varied hybrid exoskeletons are basically related to the control architecture of joint trajectories and actuation principles. To that effect, there are two clearly differentiated trends: one corresponding to the incorporation of actuators with energy dissipation through brakes or clutches [20, 22, 23, 144] in order to perform the trajectory control; the other consisting of the use of actuators with the capability of providing power to the joints [24, 145, 146].

The first hybrid control architectures have included muscular models to control the muscular stimulation and the generated motion dynamics, which enabled uncoupling the control of FES from the exoskeleton. Obinata et al. has suggested a control architecture based on the concept above, although it has not been implemented in practice beyond numerical simulations [147]. Later performed work *in vivo* has demonstrated that the control of muscular torque generated by FES includes several difficulties due the non-linearity character of muscles whose dynamic characteristics vary over time [148]. Several studies have proposed control architectures to hybrid exoskeleton control, including also the identification of muscle dynamic characteristics [149–151]. However, the deterioration induced from the muscular response, fundamentally related to time, caused the lack of effectiveness on the pre-alimentation technique of the muscular model for hybrid exoskeleton control.

2.4.1 Control through joint brakes (semi-active exoskeletons)

A possible way to overcome the main issue related to the dynamic characteristics of the muscular system under FES is to employ actuators capable of dissipating joint power: by generating movement through FES and controlling the trajectory through the aforementioned actuators, FES can be regarded as an intermittent source of power source. This control principle has demonstrated its effectiveness in real conditions comparing to control architectures with the pre-alimentation of the muscular model. This approach provides a fundamental advantage over controllers with pre-alimentation of the muscular model, since while FES is capable to generate a sufficient joint trajectory, the exoskeleton actuators can modulate it.

One of the most extended solutions on the hybrid exoskeleton design is based on FES employment to produce joint trajectories during the swing phase, using articulated brakes both for modulating the trajectory during the swing phase and for stabilizing the joints during the stance phase, thus considerably reducing the demand over the musculature during the gait cycle [20, 22, 23, 144].

2.4.1.1 V.H.C.M. exoskeleton

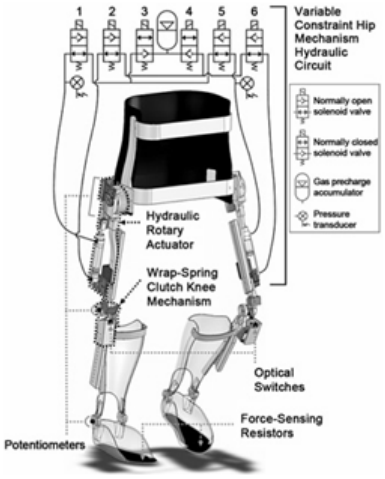

Figure 2.19: V.H.C.M. exoskeleton [19].

The reciprocating mechanisms are one of the most prescribed devices for gait function restoration promoting flexibility, step length, and walking velocity [144]. In relation to an orthosis locking the knee and ankle joints, a reciprocating mechanism may mechanically couple the ipsilateral hip extension with the contralateral hip flexion and vice versa, wherefore one cannot take a step forward by maintaining the postural balance and by enabling an upright gait [152]. However, the reciprocating mechanism tends to limit step length and gait speed, due to the degree of ipsilateral hip extension restricting the contralateral hip flexion (i.e. a fixed 1:1 hip flexion:extension coupling ratio) [144]. Moreover, these orthoses are very limited in generating foot ground clearance with minimal upper body effort [21]. A solution for this problem has been suggested through the *Variable Hip Constraint Mechanism* (V.H.C.M.) exoskeleton development (figure 2.19), in which a hydraulic system replaces the mechanical reciprocator whose transmission rate can be modified by operating on the electrovalves of the hydraulic circuit [153]. Hip actuators are constituted of hydraulic cylinders which activate a gear linked to the exoskeleton hip joint. The system friction is not negligible, thus 7% of the torque produced by the hip flexor musculature is still required to

overcome the actuator passive resistance [146, 153]. V.H.C.M. control may avoid the hip bilateral flexion, providing trunk and hip stability when coupled, allowing free movement of the hip and its increased flexion when uncoupled during the swing phase, by which the user is allowed to change and improve the step length in addition to the stance hip stability maintenance without the system interference on the movement [19, 146].

V.H.C.M. takes part of a hybrid exoskeleton made up of an orthosis whose knee and ankle joints have clutches coupled to a torsion spring [154]. The activation of the device through a solenoid is capable of locking the knee during the flexion motion allowing a certain extension degree, while the deactivation enables the knee free movement. The FES-hybrid system consists of a 16-channel intramuscular stimulation system, acting over the flexor and extensor muscles of the hip, knee and ankle, as also the spinal erector muscle and the gluteus medius. V.H.C.M. is therefore a semi-active hybrid exoskeleton as it combines the use of a passive gait orthosis with the use of FES as power source. FES is programmed by a set of stimulation rules previously adjusted to the user, working in open-loop in synchronism with the exoskeleton. The hybrid system control is based on a state machine, whose operation conditions are based on event detection which identify the monopodal and bipodal support of the stance phase and the swing phase [146]. According to the states detected by the controller, the system will lock or unlock the hip, knee and ankle joints, in addiction to provide the muscular stimulation sequence suitable for the actual gait phase within the subject is found.

An evaluation with healthy participants shows that the V.H.C.M. could provide a joint kinematics of the hip and knee similar to normal gait, while the ankle joint trajectory during the swing phase presents a great deviation from normal values. The weight of the system (22 Kg) represents an inconvenience by affecting the gait velocity which is slightly lower comparing to the gait solely performed with FES or with the reciprocating mechanism [155]. Moreover, weight and cosmesis requirements for clinical use are yet far from being fully complied [19]. Conversely, the muscles involved in the leg control during the swing phase (*tibialis anterior*, quadriceps and hamstring) exhibit higher activation on the gait with the V.H.C.M., what is also attributed to the system's weight [155]. However, the knee joint blocking during the monopodal support or standing position eliminates the necessity of stimulating quadriceps, reducing thus the muscular stimulation cycle [20]. Nevertheless, no studies of the effect on musculature fatigue were performed. It was developed a system evaluation on a subject with a complete T7-spinal cord injury, although the published results

were restricted to the hip and knee joint kinematics, without discussion of the results obtained [19]. The use effectiveness and applicability of the system in patients are questioned due to its excessive weight which leads to a decreased walking velocity and an increased muscle activation.

2.4.1.2 C.B.O. exoskeleton

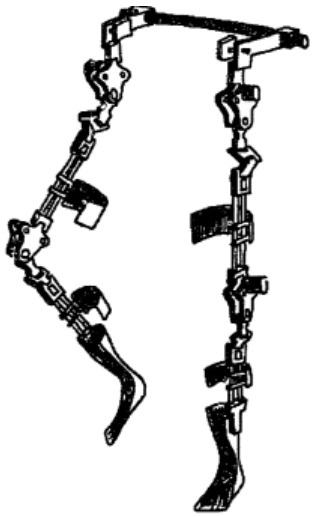

Figure 2.20: C.B.O. exoskeleton [20].

Other hybrid exoskeleton proposed in the literature is the so-called *Controlled Brake Orthosis* (C.B.O., 1996) (figure 2.20) with 8 DOFs [20], including the hip, knee and ankle flexion-extension, along with the hip adduction-abduction of both legs. The exoskeleton hip and knee joints possess brakes composed of magnetic particles which can control the hip and knee joints flexion-extension movement. The hip adduction-abduction is free although restricted in its ROM by the orthosis in order to avoid the legs crossing during the swing phase [156]. The ankle has an elastic actuator to control the foot dorsal flexion, whose stiffness is adequate for avoiding the foot drop during the swing phase and consecutive stumble [23]. With this configuration, joint actuators of the C.B.O. due to magnetic brakes can be highly back-driveable (the resulting friction and damping of the device is small when compared to the passive compliance and damping of the natural joints) and the exoskeleton is appreciable lighter (6 Kg) than that proposed by Kobetic. The brakes of magnetic particles are considered compact, low-weight and energy efficient passive devices well suited for applications involving human interaction while causing no human injury resulting from unstable behavior [20]. Other difference is found in the FES system in which C.B.O. has four channels, stimulating the quadriceps of both legs to cause the knee extension, while the knee and hip flexion

is conducted through the peroneal nerve stimulation, triggering thus the flexion withdrawal reflex [157]. The effect of muscle fatigue is therefore reduced by means of controllable rigid brakes during stance supporting a wide stability region with no muscle stimulation [20]. In opposition to orthoses with their joints locking in all gait phases, C.B.O. controllable joints can thus enable more natural knee and hip trajectories [158]. Another contribution of this exoskeleton is the establishment of the re-alimentation of joint torques produced by FES (closed-loop FES) obtained through strain gauge bridges disposed on the exoskeleton structure, since the present control scheme allows manipulation on the stimulation intensity as a function of the trajectory and torque error, averaged in a step-by-step basis in order to stimulate the muscles with the amplitude necessary to achieve joint movement [20]. Subsequently, muscle fatigue can be controlled. The suggested control strategy is straightforward: if the stimulation intensity is excessive, the control system will act modulating the trajectory through brake actuation, dissipating then the energy in excess which might be ordered in excess through FES to muscles; conversely, if the stimulation intensity is not sufficient, the muscle will not produce the minimal joint torque to achieve the intended trajectory, by which it shall increase the error on the trajectory.

The preliminary evaluation of this exoskeleton was performed through a comparative analysis of the gait on a subject with complete T6 spinal lesion confronting the hybrid orthosis and the FES alone without braces [20]. Interesting results were found on the diminishing of the quadriceps stimulation cycle, passing from stimulating quadriceps around 85% of the gait cycle when employing only FES to solely 10% when using the hybrid system. This considerable decreasing of the load cycle is due to the support function that joint brakes allow achieving during the stance phase, wherefore it is not required to stimulate the stabilizing musculature of the knee (in this case the quadriceps) to avoid the joint collapse, although the stimulation is only necessary during the swing phase, where, in addition, the contribution of the knee torque is slightly lower. On the other hand, in spite of achieving better knee trajectory control in qualitative terms reducing then the trajectory variability between steps, the hip trajectory control is not appropriate, due to the movement being produced by the peroneal nerve stimulation. Although the flexion withdrawal reflex stimulation is an efficient fashion to synchronously achieve the combined flexion of the hip, knee and ankle, the effectiveness loss of this mechanism shortly after its employment onset for eliciting full hip flexion restricts its implementation [145, 158].

A later publication by the same group was focused on the clinical evaluation of the hybrid

system [158]. In this respect, several experiments were performed regarding the comparison of time-space and physiological characteristics of the gait through FES confronted with a gait attained through the hybrid system in four patients with spinal injury. The characteristics of the patients were all homogeneous. The spinal injury consisted of complete T6-T7, except for a patient whose lesion was the incomplete T8, what could let him have a certain capacity for autonomous wandering. The gait speed attained through the use of C.B.O. confronted to that developed with FES augmented on a single patient, while the walking distance covered was only longer for some subjects. The evaluation of the variables related to the physiological effort (cardiac rhythm, oxygen consuming and arterial pressure) did not show any differences between using C.B.O. or FES. Measurements concerning the relation of FES intensity and joint torque produced revealed a lower muscular fatigue generation using the hybrid system. Although this was a major finding, an important drawback in the referred study has emerged from the performing of different gait protocols for each patient both on the route covered and different used technical aids. According to the authors, theses facts were motivated by the presence of patients with different physical and functional abilities. The lack of normalization of the patient sample in addition to the low number of subjects does not enable the possibility of extrapolating the results beyond the effects of pure chance, although it is unquestionable that the outcomes demonstrate some indications which should be taken into account when designing hybrid exoskeletons.

In terms of design, acceptance and use on daily basis, this system comprises some important limitations that can be highlighted [158]: in contrast to reciprocating gait orthoses which have demonstrated to be appropriated for donning and doffing without assistance [159], in the case of C.B.O. the leg brace covering both hip and knee joints is too long bringing thus complexity and heavy load when donning and doffing independently; controllable brakes with high power requirements tend to undermine the use of a single battery charge for longer time which contradicts the principle that viable gait assist system should be self-contained and battery powered; C.B.O. cannot compensate for insufficient power joint derived by inconsistencies of the flexion withdrawal reflex; C.B.O. employment in rehabilitation is not suitable for general patients in the sense that it can be harmful and dangerous within specific contexts.

2.4.2 Energy storage-based hybrid exoskeletons

The previous hybrid exoskeletons have shown through the use of joint brakes interesting improvements on the joint trajectory control and muscle fatigue decline, limitations characteristic of FES-aided gait. Another approach has been suggested with the purpose of emphasizing the emergence of major improvements on hybrid system's portability and on the management of muscle fatigue, namely by means of an optimization of the stimulation strategy and a means of storing energy. Bearing in mind the reduction of muscle stimulation necessity as aim target, it is proposed the employment of energy storage from the quadriceps during the swing phase in addition to joint brakes use within the stance phase, since the underlying strategy is to release the energy stored during the swing phase to other phase or joint. Energy storage can be mediated by an elastic element and a joint brake. Another benefit of using energy storage is the possibility to prevent the withdrawal reflex stimulation closely related to the lack of joint power issues, as discussed above [82].

2.4.2.1 S.B.O. exoskeleton

The *Spring Brake Orthosis* (S.B.O., 2000) (figure 2.21) has been developed in order to achieve a more natural swing phase trajectory for gait in SCI patients than that produced by withdrawal reflex [21, 160]. In this regard, it is proposed a spring knee orthosis with hip and knee on-off brakes, a spring at the knee joint brake which releases energy to enable knee flexion after toe-off and two-channel FES of quadriceps for knee extension. Hip flexion is also automatically attained due to energy releasing with no need of withdrawal reflex or other mechanism. Consequently, ground clearance may be improved by a simultaneous hip and knee flexion as compared to reciprocating orthoses, as mentioned earlier. The energy is stored in the spring provided at the knee extension which can be ensured by a brake without further quadriceps contraction. Thus, when the brake is off, soon the spring is contracted. A low muscle fatigue can be therefore achieved [160].

A fuzzy logic controller (FLC) was introduced in the FES-drive control scheme for the control of knee joint kinematics according to knee joint position and velocity error, avoiding then the complexity involved in accurate modeling for muscle stimulation. Since the aim target is the mitigation of muscle fatigue and impact force in extreme knee extension, FLC is responsible for the prediction of the duration of muscle torque required for full extension, so that shank full extension can be achieved without any impact force (no muscle activity) by the end in a safe and humanly tolerable fashion [21].

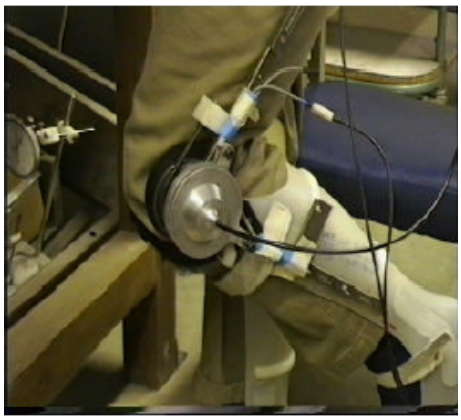

Figure 2.21: S.B.O. gait system [21].

In addition to the previous advantages already mentioned over C.B.O. and reciprocating systems, it is worth noting that there is no need for heavy and bulky battery and DC motor, unlike the powered orthoses. In contrast to DC motor actuators, there is no danger of threatening the patient safety. In opposition to C.B.O. characterized by an excessive power dissipation, little power is dissipated in the S.B.O. [21]. However, it is assumed by the authors the lack of suitability of the present brake design to employ the gait machine outside the clinical facility as a consequence of excessive size, weight and high power consumption of the actuator [160]. Thus far, no trials with disabled subjects have been performed.

2.4.2.2 J.C.O. exoskeleton

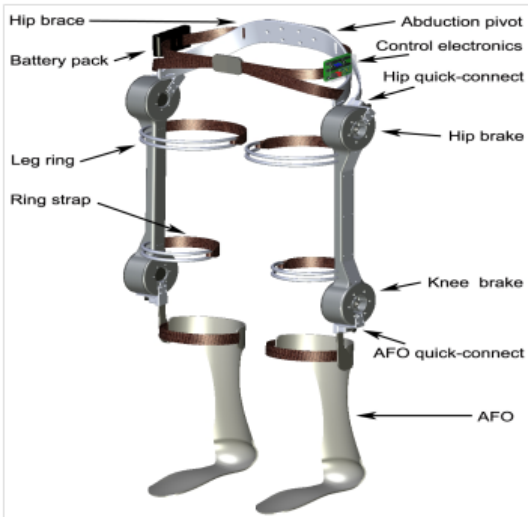

Figure 2.22: J.C.O. exoskeleton [22].

To recap, the stimulation management is of a great importance when developing hybrid systems which can be used for a long period of time. There have been developed other

hybrid exoskeletons endorsing the same elastic-energy storage concept [22, 23, 161, 162]. Farris *et al.* has presented the so-called *Joint Coupled Orthosis* (J.C.O., 2009) depicted in figure 2.22 [22], a hybrid exoskeleton incorporating controllable brakes on hip and knee joints mechanically and unidirectionally coupled through an elastic actuator which are active during early swing, so that the knee flexion promotes the hip flexion [22]. Like in the S.B.O., this configuration enables the use of a single channel of FES over each quadriceps at maximal hip flexion. The equilibrium position of the elastic actuator may flex the knee and also the hip due to the elastic coupling. Depending on the stimulation of the quadriceps during the swing phase, the knee extension is produced without causing the hip flexion and also extending the elastic coupling, keeping then the energy for the following step. The control of the knee and hip trajectories during stance phase is achieved through friction brakes placed at hip and knee joints, as in the above systems, which release after toe-off. Nevertheless, unlike the S.B.O., the stimulation time is not controlled as well as the FES pulse parameters are not tunable. To compensate those features, muscle fatigue can be managed by monitoring the knee ROM. In opposition to the C.B.O. and the S.B.O., the design of the brake provides a significantly greater torque-to-weight ratio than the brake composed on magnetic particles [161].

A preliminary implementation on ten healthy subjects with a hybrid exoskeleton on a leg consisted of the performance of three gait cycles of 5 minutes with a one minute rest period between them, where it is shown the knee ROM declining on the first two gait cycles, while on the third it has stabilized at around 85% of the maximum value achieved at the beginning of the experiments [22]. While this outcome is promising in the sense of the J.C.O. possibly providing long periods of continuous locomotion without significant degradation of performance unimpeded by quadriceps muscle fatigue, particular muscular conditions of disabled patients prevent its extrapolation to a general impaired population. Till date, clinical trials of J.C.O. system have not be performed.

2.4.2.3 E.S.O. exoskeleton

According to the concept of energetic storage and employment of a single FES channel to produce movement, Durfee has submitted the preliminary steps for the development of the *Energy Storing Orthosis* (E.S.O., 2005) exoskeleton (figure 2.23) [23]. E.S.O. exoskeleton can extract at knee extension within the swing phase the excess of energy from quadriceps stimulation which is stored in three different devices: two gas springs whose equilibrium positions correspond to knee flexion and hip extension; during the stance phase, the stored

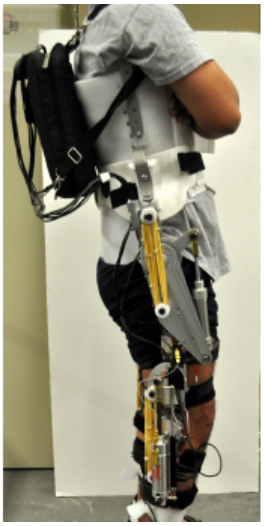

Figure 2.23: E.S.O. exoskeleton [23].

energy is transmitted to the hip actuator to drive the hip motion, enabling hip extension and forward progression in addition to store the energy in the hip elastic storage element.

Unlike in the S.B.O. system proposed by Gharooni *et al.* [21], E.S.O. is intended to provide decoupled hip extension and flexion that may increase gait-assist performance in relation to that obtained with S.B.O. Opposed to C.B.O., this system requires only a single channel FES for the surface stimulation of each quadriceps. Not only stimulated muscle power is exploited to move the limb but also to push forward the orthosis, while the energy is sufficiently high to be transferred to another joint and enable joint motion drive without the additional necessity of muscle stimulation [23]. However, like the other comparative gait systems, E.S.O. exoskeleton includes hip and knee joint brakes to lock the joints during stance phase and control motion during swing phase [162]. Their function is to hold knee in extended position while the hip extension starts, to provide control of the stance phase to prevent collapse and to control the knee and hip trajectories during extension/flexion.

In relation to elastic storage elements, while gas springs work as elastic storage elements on the knee and hip joints, pneumatic cylinders together with other components form the energy storage system. It is advantageous incorporating a pneumatic system characterized by low-weight, compactness and simplicity [162]. Gas springs are preferably adopted by Durfee *et al.* over mechanical springs due to their higher force-to-weight and stored energy-to-weight ratios and constant force production throughout their entire stroke [23]. However, Kangude *et al.* have opted to employ elastic bands made from natural rubber instead of gas springs, since they are interestingly more lightweight [162]. The pneumatic fluid power

system is another energy storage and transfer capable of storing large amounts of energy from the quadriceps in a compact volume and also lightweight.

Regarding energy efficiency, the main concern is to avoid energy dissipation during the energy storing, channeling and discharging from the quadriceps which leads to higher amount of energy required, causing thus faster fatigue and minor total covered distance. The system proposed by Durfee was not yet optimized in energetic terms, due to excessive energy losses.

With regard to the exoskeleton design, total system size, weight and time to don and doff determinant for a successful assistive technology product have not still met. No experiments or device evaluations have been performed on impaired subjects thus far [23].

2.4.3 Compensation through torque supply (active exoskeletons)

The joint trajectory control of the systems previously presented is based on energy dissipation from the joints through the use of brakes in cases where the joint trajectory exceeds that established as reference for a standard gait. The generation of the joint trajectory of those hybrid systems is achieved through FES system. The muscular fatigue management for delaying muscle fatigue onset is based on the limitation of stimulation time mainly during the stance phases in which is necessary to stabilize joints for support and stability delivering. However, although these approaches have demonstrated their effectiveness on reducing the muscular demanding, the system loses its effectiveness with the muscular fatigue appearance due to the motion generation being the sole responsibility of the FES, since joint brakes are not capable of providing positive torque, and inclusively and consequently, systems cannot provide full control of the joint. For those systems performing an open-loop FES control, they can only contribute to a low movement quality regarding joint trajectory and speed. Systems with a closed-loop FES control like C.B.O. tend to be ineffective on counterbalancing the muscle stimulation intensity adjustment in terms of muscle fatigue and on obtaining sufficient joint power [145, 158].

On the other hand, the hybrid exoskeletons comprising active actuators on joints with the capability of providing torque can actuate in parallel with FES system, actively controlling the joint trajectory through the contribution or dissipation of energy. Furthermore, the ability of delivering torque allows the performing of a more effective management of the muscle fatigue and of the close-loop FES control, increasing therefore the FES time employment.

2.4.3.1 H.A.S. exoskeleton

Tomovic *et al.* have suggested for the first time the concept of assisted hybrid system, under which the FES employment and joint torque delivering were proposed [163], even though the first physical development was only undertaken in 1989 [145] for gait restoration of severely handicapped. The orthosis named *Hybrid Assistive Orthosis* (H.A.S.) is modular (lightweight knee-ankle brace equipped with a DC servomotor and a motor-actuated drum brake coupled to the knee joint with a ball screw) allowing the replacement of hip, knee or ankle joints by actuators or brakes. The present hybrid configuration includes actuators on knee joints attached through cable transmission, placing the motors at the proximal side. These actuators enable the locking and unlocking of the joint during the stance phase, enabling torque addiction during the swing phase. On the ankle joint is incorporated an elastic actuator (spring mechanism) which controls the dorsal flexion and prevents the plantar flexion during the swing phase. FES system comprises six stimulation channels: the *gluteus medius* muscles for balance; quadriceps for hip flexion and knee extension; peroneal nerve stimulation used to cause knee and hip flexion withdrawal reflex and ankle dorsal flexion. This latter stimulation may enable a simpler step forward rather than synchronously stimulating the flexor muscles of the joints. The stimulation parameters are previously calibrated according to the specific subject. Concerning the control strategy adopted, a finite-state machine is responsible for event detection controlling thus FES and the activation/deactivation of the actuators.

The hybrid orthosis evaluation was performed through the analysis of a single case, more specifically related to a patient with incomplete C5-C6 SCI and without voluntary control over the lower extremities. That study consisted of performing the gait with free speed in three different situations: with the orthosis in passive mode and without FES; with FES and without orthosis; with the hybrid system. The results have shown that the patient has reached greater gait speed with the hybrid system than with other configurations, although the speed difference compared with the gait through FES is only 10% higher and always significantly lower than the non-pathologic gait speed. Popovic *et al.* (1989) analyzed the physiologic cost of attaining gait with the three configurations through the acquisition of normalized O2 consuming and founded that the physiologic cost was considerably lower when using the hybrid system [145]. However, the main inconvenience comes from the use of flexion withdrawal reflex, because its effectiveness after 10 minutes of employment on experiments developed by Popovic has started to decline.

2.4.3.2 Hy.P.O. exoskeleton

Figure 2.24: Hy.P.O. exoskeleton [24].

The hybrid system so-called *Hybrid Powered Orthosis* (Hy.P.O., 2007) (figure 2.24) incorporates two DC motors, whose maximal power and torque are respectively 70W and 0,14 N.m and gear reduction ratio is of 156:1 for hip and knee joints control [24]. The motors are placed in the front of the exoskeleton in order to facilitate its clothing and have a suitable dimension to enable the gait generation regardless of FES what may be beneficial in terms of preventing the muscle fatigue of hindering the use of FES while walking. FES actuates on the quadriceps musculature. Hy.P.O. hybrid control assumes open-loop FES and provides a joint trajectory control through the delivering or dissipation of torque by motor actuators.

In relation to the exoskeleton design, Hy.P.O. weight is of 9.2 Kg including the actuators, although this weight is supported by the structure of the orthosis resting on the ground and the user does not feel therefore the weight. The design limits the ranges of joint rotations such that the excess of joints extension and flexion can be prevented. Unlike the most comparative orthoses, the user can wear Hy.P.O. from the front of the body while staying seated in a wheelchair. These all features are fundamental for ADLs.

Regarding the control strategy, the control of the actuator feedback can counterbalance uncertainty in generated joint torques provided by FES through the feedback information of joint angle and joint angle velocity. The tracking at each joint to pre-assigned angular trajectory is possible whether each actuator power is enough for the compensation implying thus the manual tuning of gain parameters. In a study, feedback control via the actuators on the joint angles has achieved robust and precise tracing of the reference trajectories of joints against uncertainty of the generated torques from FES [24].

There was also made a comparison of the evolution of hip and knee joints along the gait using three different configurations: without FES actuation; with FES system though without a suited stimulation pattern for joint trajectories; with an optimized FES system. In the three cases, the hybrid system could reproduce the joint trajectories, even though it was noticed a considerable reduction on the torque provided by motors when using the optimized FES. The system demonstrated effectiveness on compensating the trajectories for the cases of either insufficient or excessive stimulation. However, the muscular fatigue effect is not taken into account, but instead its management is indirectly attained through joint trajectory control [24].

Research regarding the effectiveness and practicality of Hy.P.O. with experiments of impaired patients are yet to be performed.

2.4.3.3 WalkTrainer exoskeleton

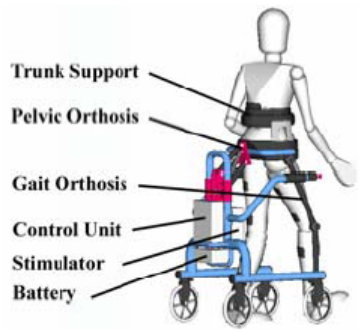

Figure 2.25: WalkTrainer exoskeleton [25].

The closing the FES control loop has been suggested by Stauffer using the system called WalkTrainer (2009) (figure 2.25) [25]. WalkTrainer is a hybrid system whose exoskeleton incorporates hip, knee and ankle joint control as well as pelvis segment control in six DOFs including a moving structure through which it is performed the exoskeleton joint control. Moreover, this structure includes a partial bodyweight support system of the patient like other systems of gait training which supports the exoskeleton and the user [164]. The closed-loop FES is possible through the monitoring of interaction forces between the user body segments and the exoskeleton implemented with strain gauges. This configuration enables both the conduct of joint position control and impedance control. WalkTrainer is characterized as a rehabilitation system for ambulatory gait, whose rehabilitation strategy consists of the imposition of joint trajectories corresponding to a standard gait and of closely mimicking natural movements. Depending on the partial bodyweight support system and by

using the feedback of interaction forces with the exoskeleton to control FES, the system is intended to minimize the interaction forces through the modulation of muscle stimulation.

The closed-loop FES controller has the following features: joint trajectories are controlled by DC motors; the torque error is compensated by a classic PID controller; a feedforward model of the torque-intensity characteristics of the muscle involved in the movement is also incorporated. The aim of this control strategy is of tuning the stimulation to provide the difference between the force required and the force by the patient delivered. Therefore, problems related to jerky motions and rapid fatigue that can emerge from inappropriate muscle control characteristic of open-loop FES may be overcome by closing the loop. This strategy is intended to follow the principle of promoting the active participation of muscles in the sense that muscles should be controlled either by the patient or promoted by FES.

In the same work it is also presented evaluation results by using WalkTrainer on six patients with paraplegia whose lesion characteristics are heterogeneous. The trials consist of one hour employment of the system per week over twelve weeks. In spite of the feasibility of getting paraplegic patients to walk again with WalkTrainer and the observation of reduction on Asworth spasticity index, there is no evidence of enhancing changes on driving force or coordination though [25]. Further trials with higher training load and more strict inclusion criteria are expected to discover other potential benefits.

2.4.3.4 Rewalk orthosis

Figure 2.26: Rewalk orthosis [26].

The ultimate hybrid active orthosis, the Rewalk system (2006), has been developed aimed at providing an alternative mobility solution to the wheelchaired people characterized by se-

vere locomotion impairments, offering to them several mobility events such as standing, self-directed and independent walking, sitting, stair climbing, slope ascending/descending and upright mobility. The safety and stability of the user can be ensured by the use of crutches, railing and software. Rewalk is constituted of lightweight wearable brace support suit integrating DC motors at hip and knee joints only at the sagittal plane, rechargeable batteries, sensors and a on-board computer-based control system. The control of locomotion processes is achieved with the detection of upper-body movements. The device is considered untethered, intuitive and generator of natural joint trajectories for ADLs, it is currently available on the market for institutional use only, such as rehabilitation facilities and hospitals. It is expected to be commercialized for personal use in the second half of 2012. The weight of the system is around 18 Kg, it can provide a maximal gait speed about 3 Km/h and the autonomy of the battery is less than 3 h [165].

In terms of scalability, Rewalk is suitable for those who have healthy control of the upper-body joints to use both hands and shoulders, healthy cardiovascular system in addition to bone density and ability to stand, who are between 1,60 - 1,90 m tall and weigh less or equal to 100 Kg [108].

A first clinical trial has been recently developed at the Sheba Medical Center (Israel) and published in the beginning of 2012 to evaluate the safety and tolerance of the use of Rewalk exoskeleton ambulation system in subjects with complete SCI [166]. The outcomes after an average of 13-14 training sessions were promising translated by no adverse safety events, general positive feedback from the volunteers, while there was reported a moderate level of fatigue after the experiment. A more efficient walking performance was achieved by individuals with lower-level SCI. Nonetheless, more information is still not available.

Rewalk is on the right track of restoring the mobility functions of an impaired person, thus improving both quality of life and physical health.

2.4.3.5 Other hybrid gait trainers

The FES system has been also combined to other bodyweight support systems in some studies, in which interesting outcomes were obtained regarding gait endurance and speed [134, 167, 168]. Nonetheless, these few studies do not demonstrate a higher effectiveness of these hybrid systems over conventional therapy. In a recent randomized control trial developed by Nooijen *et al.* (2009), a comparison of gait quality improvement was developed using four different configurations of body weight supported locomotor training: treadmill with

manual assistance, treadmill with electrical stimulation, overground with electrical stimulation and treadmill with the locomotor robot. None of training approaches has taken a leader role in improving gait quality [169].

2.4.4 Revision of hybrid control technologies

The control of gait movement through FES-exoskeleton hybrid actuation is an approach which enables the combination of the advantages of both techniques and the mitigation of their individual limitations. On the one hand, FES generates joint motion with a low energy consumption and, on the other hand, the exoskeleton not only provides a structural support to the lower limbs but also allows the joint trajectory modulation. This structural support enables the joint stabilization during the stance phases, what may considerably reduce the demanding over the musculature to avoid the joint collapse.

The approaches used to produce joint movement vary among the addressed different systems: stimulation of the agonist and antagonist muscles, energy storage or generation of flexion withdrawal reflex. The latter case allows generating the ankle, knee and hip flexion through the use of a single stimulation channel [118]. Furthermore, it avoids the necessity of stimulating the hip flexor musculature, hardly accessible through surface electrodes. However, that physiologic mechanism triggered by the peroneal nerve stimulation deteriorates within some minutes [145, 157]. This fact caused the dismissing of the present mechanism on later hybrid systems, replacing the knee flexion and hip extension either by direct stimulation of the involved muscles [19, 25, 144] or by passive [22, 23] or active actuators [24]. However, among the advantages of using this reflex mechanism, the production of more natural movements and the use of a single stimulation channel to generate coordinated movement of three joints are highlighted. The advance in knowledge of the physiologic mechanisms which restrict the muscular stimulation through the peroneal nerve excitation might enable the use of the reflex mechanism during a longer period.

Intensive research over the last decades was focused on hybrid systems development for compensation of gait capability on impaired subjects, especially SCI patients. Indeed, relating this neurological disease, one should be aware of various differentiating functional particularities: the affected musculature location, the muscle atrophy arising in the lesion chronic phase, the alteration of sensitivity, the reducing of physical capacity among others are all differentiating factors which require the performing of a specific clinical evaluation on patients with spinal injury. Therefore, it is important to validate the proposed gait com-

pensation strategies, both the hardware component and the control architecture [164, 170].

One should be focused in the near future on improving transmitted motor actions to human joints optimizing interaction control strategies, developing efficient compact and autonomous solutions in order to encourage both assistance and therapy in stroke and SCI patients during the daily activities of the wearer [10, 171].

2.5 Open research questions

Here it is reviewed a list of questions which remain yet to be addressed. These questions concern the main challenges that must be overcome or at least to be improved or optimized from several perspectives, namely technological, engineering, physiologic, aesthetic among others. A review of these questions has the aim of promoting future discussions of new research strategies that may address them. These challenges are fundamental for the manufacturing and testing of any new prototype system directed towards the gait restoration of handicapped subjects for their daily living. From all the classes of orthoses presented, the hybrid orthoses may apparently be able to better meet the crucial underlying requirements effectively. Firstly, the orthosis should be designed to provide postural stability and trajectory control without excessively hindering movements during forward progression and bearing in mind the minimization of interaction forces between the exoskeleton and the wearer. Secondly, FES should offer more effective and efficient power for forward progression in order to reduce muscle fatigue by taking into consideration changes on the muscle dynamic properties and environment when performing gait.

2.5.1 Future guidelines

An important question which remains to be further analyzed is the practicality of the system on the restoration of motor functions during the quotidian. One should bear in mind that the contribution of locomotion restoration of impaired subjects's daily life can be yet somewhat controversial from the point of view of the patients. They can be brought to a feeling of disappointment and discouragement if the robotic device cannot effectively cope with the patient's psychological, physiological problems and locomotion difficulties, leading consecutively the patients to disregard the orthosis during therapy. Conversely, wheelchair can provide the covering of considerable distances while expending comparable energy to normal gait which can induce on patients a reluctance and lack of motivation in adopting the

upright position with the aid of exoskeletons [9]. Thus, in order to prevent or minimize these problems, the following items should be attained, endorsing the line of thought proposed by Kobetic (2009) [19]: (1) Be cosmetic. (2) Be easy to don and doff in low time without assistance while sitting on a chair. (3) Be easy and intuitive to operate. (4) Provide the capability to stand up and sit down with minimal effort. (5) Provide postural support without power or stimulation for standing. (6) Provide the capability to go up and down stairs. (7) Carry its own weight. (8) Provide up to an hour of continuous walking. (9) Provide safety features in case of power failure. (10) Require less than 50 percent of individual's maximal aerobic capacity to walk. (10) Enable higher walking speeds.

From the engineering point of view the next issues are recommended to be considered [19, 82]: (1) Mechanical components of the hybrid orthosis could complement the functional movements generated by FES. (2) The exoskeleton could minimize and automatically adjust muscle stimulation. (3) The system should seamlessly combine bracing and FES system components. (4) Be reliable. (5) Produce minimum increase of energy rate and cost with respect to able-bodied subjects performing the same task. (6) Be compact and autonomous. (7) Systems should be designed with more knowledge of the neural mechanisms involved during recovery (e.g. reflex activation, proprioceptive feedback) and taking into account the activity of the intact and affected neural circuits.

From a viewpoint of clinical outcomes, several works found in the literature seem to lack from evaluation of disabled patients [22, 155] or to use small sample size of patients to obtain effective results when using the hybrid system [19, 23, 25, 144, 145, 158], although preliminary evaluations on healthy subjects through the hybrid exoskeleton have been developed. In the same way, in order to facilitate comparison of technologies and the drawing of conclusions about the effectiveness of each technology for gait compensation, several procedures can be recommended: (1) Treatment protocols and therapy regimes should be homogeneous. (2) Longer training periods should be performed to better compare results. (3) Well-designed randomized multicentre clinical trials with large, but strictly selected samples (e.g. with restrictions in AIS impairment score, lesion level, age, diagnosis ...) and relevant control groups who received more conventional gait training should be encouraged. (4) There is a need for clinical trials with extended follow-up periods, outcome measurements on the level of participation, including quality of life and social participation [172].

2.5.2 Control strategy

There are two main goals of the robotic control approaches as already discussed in the beginning of this section: rehabilitate a function or compensate a function.

2.5.2.1 Rehabilitation function

With regards to the therapy goal, the control algorithms are targeted at promoting neural plasticity through intensive training for motor recovery, by which every effort is undertaken on seeking a full comprehension of the mechanisms involved on the neuronal circuits reorganization underlying the motor learning. The main control strategies for gait restoration reviewed here are two-fold, namely assistive control and challenge-based control. The challenge-based controllers tend to make a task more difficult or challenging, for instance, for the amplification of movement errors. Following the line of thought that kinematic errors during a movement performance are a fundamental neural signal to promote motor adaptation, the strategy is to enhance kinematics errors produced by muscles to facilitate their detection by the nervous system which can therefore correct the subsequent electrical commands to the muscles. This error-amplification strategy has already been employed in some lower-limb rehabilitation such as in [12, 173, 174].

However, since evidence of differential clinical benefits of training with challenge-based controllers is still sparse, one will only focus on assistive control.

2.5.2.1.1 Assistive control The majority of work has been focused on developing assistive controllers, which give assistance to the weakened muscles to attain the desired limb trajectories. There are several points endorsing this strategy: (1) muscles stretching can be promoted for the prevention of soft tissue stiffening and for spasticity reduction to some extent; (2) new proprioceptive feedback can be stimulated by assisting the limbs to reproduce some trajectories that would not otherwise to achieve if unassisted, what may be important for brain plasticity induction; (3) patients might eventually learn to achieve the desired patterns by the demonstration of those patterns; (4) the improving of motor performance may be reinforced by intensive repetition of normative walking patterns; (5) increasingly intensive and difficult tasks can be performed preventing thus bad performance, and consecutively, injuries [175]. However, there are downsides regarding this strategy. Assisting a movement may lead to a diminishing of the physical effort of patients or of their own force output and/or attention while they tend to consume less energy than in case of manual therapy. Moreover,

the motor system may not be effectively encouraged to learn how to perform the task successfully, in addition to the fact that the learned task may not be the targeted task due to the induction of changes on the dynamics of the task. These negative impacts may be very probably related to excessive assistance given which cannot effectively promote voluntary movements [175]. In order to counter the apparent limitations pointed above, a different assistance approach has emerged to promote active and self-initiated motions and effort of the patient, where the patient is only assisted as much as necessary to accomplish the task. Under the concept of "assistance-as-needed", the robotic device should either correct or assist movements with a degree of assistance dependent on the deviation magnitude of the desired trajectory. Therefore, patients are encouraged to move along a gait trajectory with some error variability, while making the robot compliant within a deadband extent in which no assistance is provided [82].

Impedance-based assistance is currently the most commonly adopted control approach, based on the incorporation of PD feedback position controllers aimed at regulating the mechanical impedance according to user's intent and environmental changes. Thus, the larger is the deviation from the desired trajectory, the higher are the assistance forces applied.

Other assistive controllers rely on surface EMG signals recorded from selected muscles, i.e. EMG-based controllers, wherefore assistance can be then triggered according to the measured effort magnitude. Some orthoses have followed this approach for gait rehabilitation such as H.A.L., T.U.P.L.E.E., K.A.F.O. [4, 12, 176]. EMG signals are believed to enhance motor relearning by promoting proprioceptive feedback associated to residual myoelectric activity detected and fed back to the controller, which may amplify then the residual intention through the induction of desired muscle activation pattern for the targeted muscle forces [82]. In other words, while the patient assumes the control of the movement to perform, the orthosis should compensate with a force magnitude proportional to the EMG amplitude after predicting the intent of the user. By using an adaptive bio-inspired controller, more specifically the proportional myoelectric control [12, 176], advantages regarding the control of lower-limb robotic orthoses are highlighted comparing other control approaches: (1) the magnitude of the orthosis mechanical assistance can be scaled by mimicking the physiological muscles; (2) a greater reduction in biological muscle recruitment can be apparently induced; (3) the nervous system is enabled to adapt the orthosis control for novel motor tasks. However there are several limitations which should be yet addressed: (1) the surface electrode interface can introduce complexity in the attainment of a reliable and consistent

EMG signal; (2) the tuning of the proportional myoelectric controller gains and thresholds for each artificial muscle is required; (3) surface EMG cannot easily access many musculoskeletal system synergistic muscles; (4) the robot may not move in a desired way in case of the patient creating an abnormal, uncoordinated muscle activation pattern; (5) poor accuracy and potential invasiveness of sensing may be achieved [112, 175].

Like the EMG-based approach, a novel group of controllers are intended to adapt their control parameters according to the performance measurement of the user, so that assistance can be automatically and timely tuned to the patient's specific needs in terms of direction and amplitude, both along the movement and throughout the rehabilitation stroke. These adaptive controllers take thus the intended motion (e.g. direction, velocity, amplitude) into account in order to being synchronized with it, instead of following an inflexible control strategy [175]. One can thus argue that adaptive control may overcome a main challenge of the assistance-as-need approach regarding the suitable definition of the desired limb trajectories to be imposed. On the other hand, when offering a mechanically compliant assistance for movement is the focus, the controller should be robust to undesired events that are variable among individuals (such as increased tone, weakness, or lack of coordinated control effects), by canceling them through an adequate amount of power [175]. Instead of forcing the wearer to follow pre-specified trajectories, the desired trajectories are rather adapted and adjusted to the intention of the user. Adaptive control has already been implemented for gait rehabilitation [96, 177].

The new trends of rehabilitation is focused on developing outdoor-mobile overground robots which can overcome some financial and logistical issues related to both assistance and prolonged training intensive therapy for the every day life of the wearer. Therefore, automate locomotor training is the key to reduce health care costs and resources. To that purpose, a full comprehension of muscle and tendon function, of the mechanisms involved on the neuronal circuits reorganization during human recovery, of the musculoskeletal morphology and neural control must be pursued in order to capture the major principles underlying human locomotion, to reach a significant decrease in the metabolic demands and increase in the speed of walking and to improve the design of economical, efficient, stable and low-mass exoskeletons. Seen in these terms, bio-inspired adaptive controllers such as central pattern generators (CPGs), internal models (model-based feed-forward control) or reflexes (e.g. neuromuscular models with feedback reflex schemes [178, 179]) can play a major impact for the conquest of these challenges as they may demonstrate considerable improvements on robustness in the model parameters, simplicity, non expensive sensing, adaptivity, gait symmetry, intuitive in-

teraction for the participants, efficiency and velocity comparable to the human's capabilities and naturalness of motion.

2.5.2.2 Compensation function

One could observe that the majority of the active and hybrid technologies have implemented a precise kinematics or impedance control. In any case, these approaches are typically adequate for training and recovery of motor function, based on reference joint trajectories collected from healthy subjects at specific speeds and known environments. Nevertheless, for those cases which restoring a function has merely implicit the complete replacement of that function, important emphasis should be placed on requirements such as practicability, naturalness of movement and adaptiveness to dynamic conditions [82]. The current controllers are not able to fully solve the non-natural gait issues, since the specificities of gait and inherent walking dynamics variations at constant/varying velocities in addition to other environmental disturbances (e.g. terrain variation) are not effectively adapted, which contribute for non-energetic efficient systems and, consequently, for enhancing the user's energy expenditure as he is trying to compensate the resulted imperfections during walking.

In this way, adaptive controllers shall take up a lot of focus in near future relied upon biomimetic control architectures [82]. Popovic (1989) has begun promoting the idea that mobility control could be strongly improved by greater insights of neurophysiological mechanisms and learning processes understanding [145].

In conclusion, the thesis will therefore be focused on developing a biomimetic control architecture, namely the CPGs for locomotion control.

Table 2.3: Hybrid Exoskeletons presented in the literature.

System	Actuation	FES	Hybrid Strategy	Evaluation	Year
V.H.C.M. [144]	Hip: hydraulic. Knee: brake. Ankle: brake.	16-channel: Hip, knee and ankle flexors and extensors. Spinal erector.	Dissipation of joint power.	Only complete T7 SCI evaluated. Joint kinematics.	2006
C.B.O. [20, 23, 158]	8 DOFs. Hip: brake. Knee: brake. Ankle: elastic.	4-channel: Quadriceps. Peroneal nerve.	Dissipation of joint power.	5 subjects (T6 to T8). Joint kinematics. Gait velocity. Physiologic cost: cardiac rhythm, O2 consuming, arterial pressure.	1996
J.C.O. [23, 162]	Hip: brake/ elastic. Knee: brake/ elastic. Mechanical coupling knee-hip.	2-channel: Quadriceps.	Dissipation of joint power.	Spinal injured not evaluated. Joint kinematics.	2009
H.A.S. [145]	Knee: D.C. motor. Ankle: elastic.	6-channel: gluteus medius, quadriceps, peroneal nerve.	Joint torque supply.	Incomplete C5. Gait speed. O2 consuming. Muscular fatigue (quadriceps).	1989
Hy.P.O. [24]	Hip: D.C. motor. Knee: D.C. motor.	2-channel: quadriceps.	Joint torque supply.	Spinal injured not evaluated. Joint kinematics. Efforts over the exoskeleton.	2007
WalkTrainer [25]	Pelvis: 6 DOFs, D.C. motors. Hip: D.C. motor. Knee: D.C. motor. Ankle: D.C. motor.	20-channel.	Joint torque supply.	2 complete and 4 incomplete spinal injured. Joint kinematics. Efforts over the exoskeleton. Spasticity.	2009

Chapter 3

Central Pattern Generators (CPGs)

3.1 CPG-based locomotion modeling

CPGs constitute a biologically inspired approach characterized by neural oscillators coupling that can be able to synchronize their frequencies and/or phases to control biped locomotion which implies multidimensional coordinated periodic patterns required to satisfy multiple constraints in terms of efficient locomotion, energy and adaptation to complex terrain. A mathematical model can open up the possibility of constructing structures similar to neural oscillators found in animals. The term *central* suggests that sensory feedback (from the peripheral nervous system) is not required for producing the rhythms. CPG neural networks, controllers of each individual locomotor organ, have the property of interacting to each other for coordination in a distributed fashion in addition to modify their operability depending on the external environment and higher level commands from CNS [43]. As indicated in chapter 1, the CPG model used in this work is coupled to a biomechanical simulation of a body and its interaction with the environment, so that the effect of sensory feedback on the CPG activity and its entrainment by the mechanical body can be studied.

Concerning the mathematical model aforementioned mentioned, it is based on nonlinear oscillators, i.e. systems of differential equations that exhibit limit cycle behavior and whose parameters offer the opportunity of smoothly and rapidly modify the gait pattern. Limit cycles are closed loop trajectories in state space $x - y$ which indicate the system is periodic in time and the state variables oscillate rhythmically over time during stable, steady-state locomotion [180]. These nonlinear oscillators belonging to a specified CPG are assumed to control the stepping movements of a single limb, while interlimb coordination can be achieved through a CPG network synchronization [181]. High demand for knowledge is

developed towards how inter-oscillator couplings and differences of intrinsic frequencies affect the synchronization and the phase lags within a population of oscillatory centers, rather than studying local mechanisms of rhythm generation [43]. An oscillator produces therefore a closed cycle asymptotically stable (i.e., the system returns back to the limit cycle in case of being perturbed) with an intrinsic period (and hence frequency) with which the system repeats the pattern of activity. A few important oscillator models applied in the field of robotics are listed and characterized in [182].

3.2 Movement primitives learning

The majority of oscillators overviewed in [182] for controlling several DOFs of a robot are still difficult to design, because insufficient methodologies to calculate different parameters responsible for the generation of the correct oscillations pattern have been still developed [28]. So, a great problem related to CPG model structure and parameterization based on tuning by trial and error methods has been persisting over time, which has been addressed through supervised and unsupervised learning. Whenever the desired rhythmic pattern that the CPG should produce is known or can be measured supervised learning techniques can be applied. In this sense, it is endorsed in this work the concept of imitation learning as an efficient method for motor learning to accomplish desired locomotion movements, inspired by human's capability of learning and imitating demonstrated movements. Many researches have followed this approach [27, 28, 66, 183]. One of the supervised techniques most explored are the statistical learning algorithms based on locally weighted regression through which demonstrated trajectories are learned and the output of dynamical movement primitives (DMPs) constitute the desired trajectories [66, 183]. Nonetheless, according to Righetti (2006), the previous method requires preprocessing of the teaching signal to extract its main period [28].

Conversely, in this work it was implemented another methodology following the line of thought of Righetti (2006) who has proposed the use of adaptive frequency oscillators (AFOs) with the capability of learning arbitrary rhythmic signals in a supervised learning framework not requiring any external regression or optimization algorithms nor any preprocessing of the teaching signal [28]. Thus, the system is tuned into the required dynamics involving also the tuning of relevant parameters into state variables. AFOs are extended with an evolution law to enable the adaptation of oscillator's intrinsic frequency to one of

the components of the frequency spectrum of the input. Moreover, the oscillator frequency can be very distinguished from the input signal frequency. The main features of this method are overviewed: (I) external optimization process or discrete learning trials are not required as well as exploration/exploitation phases do not need to be distinguished since the learning process of the pattern is embedded in the dynamics of the network; (II) a stable learned pattern against perturbations can be developed and smooth modulation of the pattern in frequency and amplitude may be achieved; (III) on-line modulation of the control pattern can be implemented by smoothly integrating the sensory feedback in the pattern generator; (IV) the controller can be quite simple as no complicated signal processing techniques and no algorithmic processing is required. The frequency adaptation concept has been extended for a large class of oscillators with emphasis on the adaptive frequency Hopf oscillators for the proving of concept. In each oscillator the frequency is adapted to one of the existing of the frequency spectrum of the master signal as well as the corresponding amplitude is also learned. The network output consists of a weighted sum of oscillators among which the phase relations are learned so that their uncoupling can be avoided. Furthermore, the periodic pattern can maintain its corresponding stable limit cycle after the teaching signal removal [184, 185].

3.3 Hopf AFOs

3.3.1 Attractive properties for locomotion control

In his project, Ruffieux (2007) has reviewed and discussed the main CPG models that he thought to be the most mainly used, namely Matsuoka and Hopf AFOs. In relation to the Hopf AFOs, he concluded that they were much simpler and intuitive than the Matsuoka models, had fewer open parameters favoring an easy model implementation on various types of robots, were more focused on swing and stance phases' control (e.g. swing and stance durations) but had less similitude to the biological concepts of extensor and flexor muscles. In regard to Matsuoka model, he founded it to mimic closely the mechanisms of the extensor and flexor muscles and, consecutively, reflexes and responses could be designed in the same fashion as they act in a real body. However, a huge search space for parameters could be generated as a result of the model complexity, which is considered prejudicial for the model portability to generalized robots [186]. Another interesting property of the Hopf oscillator characterized by the exhibition of a harmonic limit cycle is the possibility of the frequency

spectrum of a specified signal which one wants to learn being naturally reconstructed by a set of oscillators by matching the distribution of their intrinsic frequencies to the frequency spectrum of the input signal [187]. As the biped locomotion may be considered periodic or pseudo-periodic and therefore constituted of periodic or pseudo-periodic signals, the harmonic limit cycle characteristic is useful for decomposing the respective signals to be learned into a sum of sines and cosines [188].

The CPG model adopted in the Dissertation due to its several advantages and interesting properties previously highlighted for the generation of human walking and also for the rehabilitation scenario is the Hopf AFO.

3.3.2 Model description and simulation

3.3.2.1 The Hopf oscillator

The Hopf oscillator dynamics is described by the following differential equations set:

$$\dot{x} = \gamma\left(\mu - r^2\right)x - \omega y \tag{3.1}$$

$$\dot{y} = \gamma\left(\mu - r^2\right)y + \omega x \tag{3.2}$$

The traditional Hopf state variables are identified by (x, y), while the oscillator intrinsic frequency is defined by ω and $r = \sqrt{x^2 + y^2}$. The convergence speed to the limit cycle and the steady-state amplitude of oscillations are determined by γ and $\mu > 0$, respectively. The following simulation consists of a oscillator producing an arbitrary signal, $5 \cdot \cos(4\pi t)$, where its behavior can be observed in figures 3.1-3.4.

In figure 3.1 is depicted the oscillator's state variables promoting an oscillatory harmonic solution represented by constant amplitude oscillations over time (figure 3.2) and a stable fixed point (in this case, $r = 5$) illustrated in figure 3.3. Consecutively, a stable limit cycle is produced characterized by a stable orbit (figure 3.4).

3.3.2.2 The Hopf AFO - basic unit

After analyzing a simple Hopf oscillator, the following is then the description of a modified Hopf oscillator provided with a learning rule which promotes the adaptation of the oscillator's frequency to the periodic or pseudo-periodic input signal's frequency. The AFO basic unit is as follows:

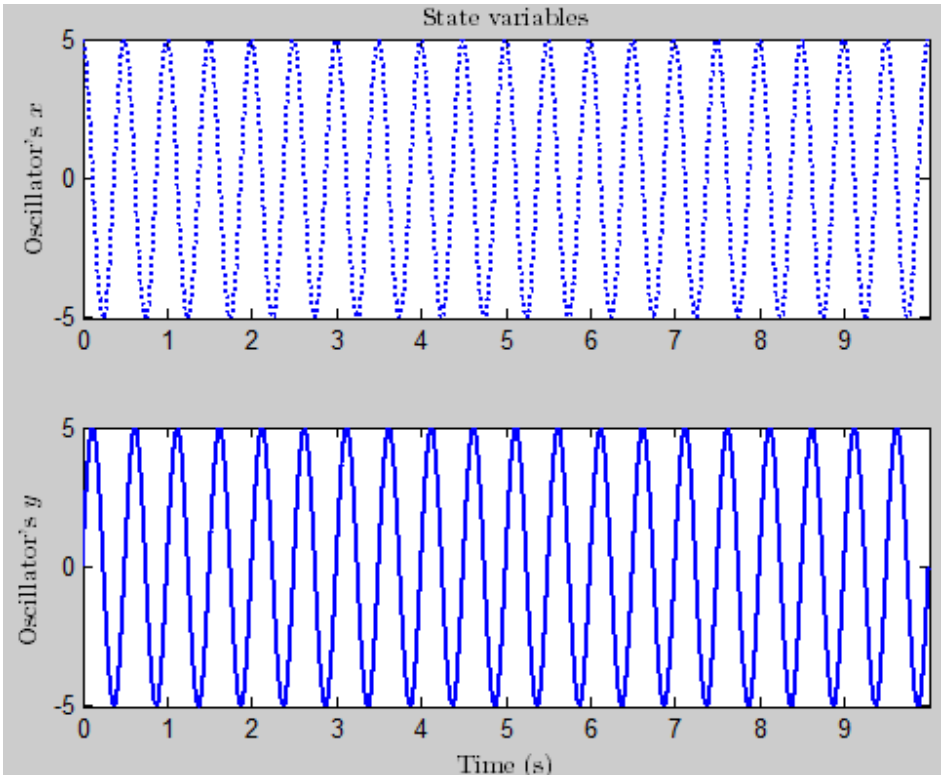

Figure 3.1: Oscillator's state variables x and y.

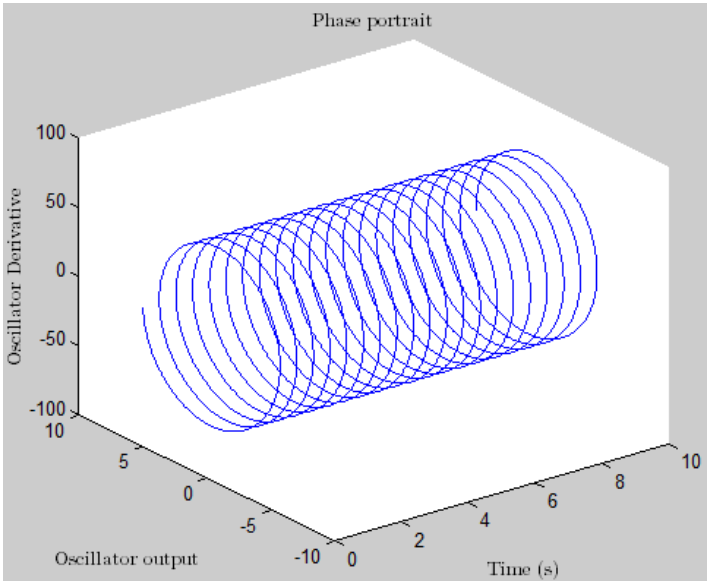

Figure 3.2: Stability of the oscillator over time.

$$\dot{x} = \gamma\left(\mu - r^2\right)x - \omega y + \epsilon F \tag{3.3}$$

$$\dot{y} = \gamma\left(\mu - r^2\right)y + \omega x \tag{3.4}$$

$$\dot{\omega} = -\epsilon F\frac{y}{r} \tag{3.5}$$

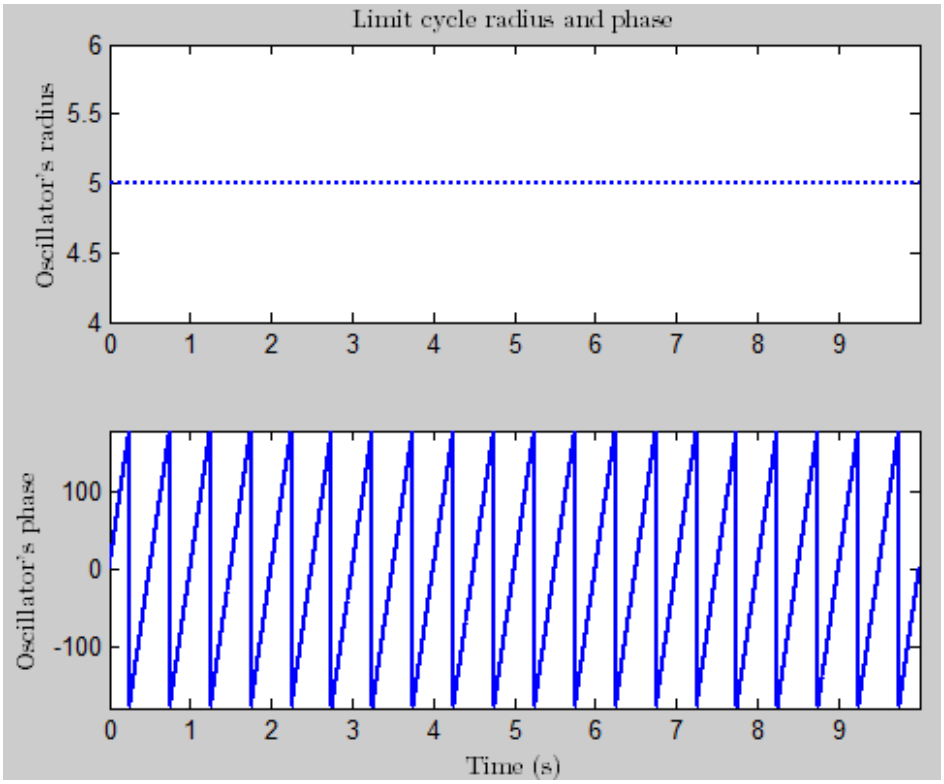

Figure 3.3: Oscillator's radius and phase x and y.

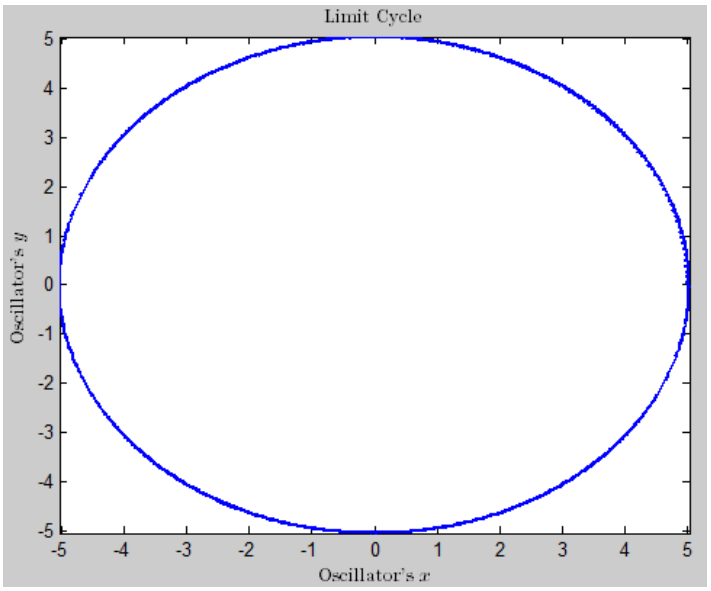

Figure 3.4: Exhibition of a stable harmonic limit cycle.

In the equations above it is indicated the perturbing periodic input signal F. The latter equation introduces the learning rule by which ω will converge and synchronize to the input signal frequency or one of its frequency components, generally to the closest frequency component of the signal. When the coupling constant (also called perturbation gain or learn-

ing rate) ϵ is null, the system is not subject to any perturbations and will thus oscillate at ω $rad \cdot s^{-1}$, otherwise the oscillator will be coupled to F with a determined coupling strength $\epsilon > 0$ and possibly attain the input signal's frequency phase locking or entrainment. In other words, ϵ has such a direct influence on the synchronization phenomenon that its higher value promotes an enhanced entrainment basin and, according to the literature, the higher the learning rate is, the faster the learning [27]. For more details about this dynamical learning approach, please see [188].

Subsequently, the analysis of the learning dynamical system behavior is developed giving thus a simple adaptation example of the oscillator(s) when perturbed by single- and then multi-frequency periodic signals as inputs.

3.3.2.2.1 Single-frequency periodic input learning Here the oscillator is driven by a simple cosine signal $F = cos(2\pi t)$, with $\mu = 1$, $\gamma \approx 83.33$, $\epsilon = 0.9$ and initial conditions $r(0) = 1$ and $\omega(0) = 6\pi$. In figure 3.5 it is demonstrated the learning process when receiving a single-frequency periodic input signal.

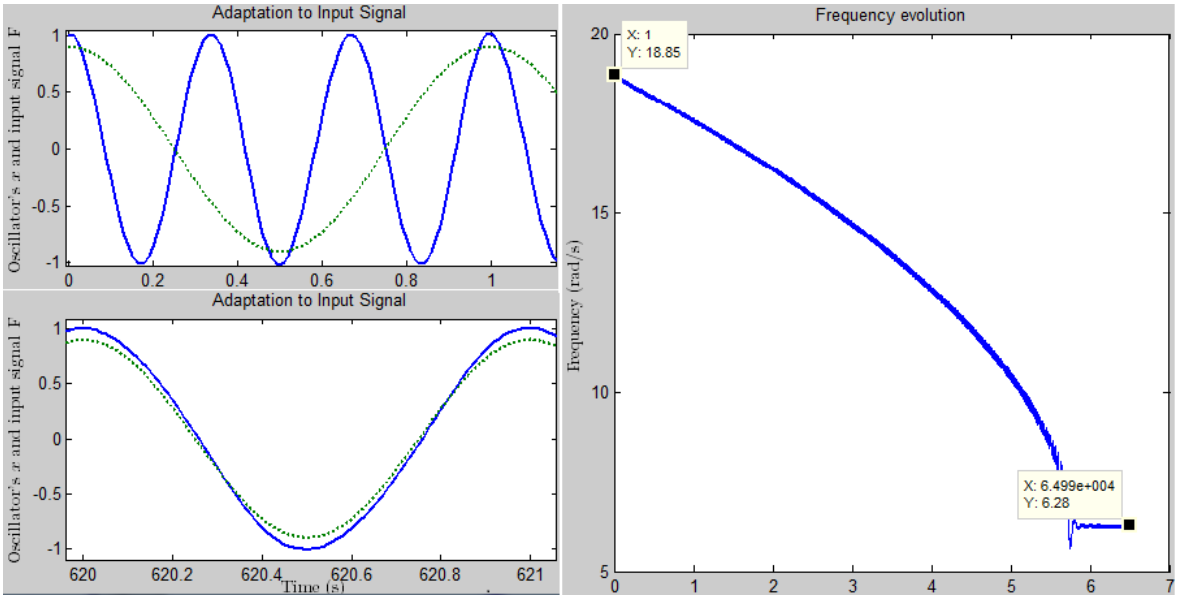

Figure 3.5: Frequency learning in the Hopf AFO. The learning input is a harmonic signal $F = cos(2\pi t)$. The evolution of ω is shown on the right, where one can observe the adaptation to the desired input frequency and its phase-locking. On the left are depicted the oscillations of the Hopf oscillator (blue solid line) corresponding to x-state variable, at the onset of learning (upper graph) and after learning (lower graph), in addition to the plot of the input signal F (green dotted line).

One can also see in the figure above the entrainment of the oscillator to the frequency of the input signal, indicated by the reduction of its frequency, approximately 2π. In figure 3.6 it is illustrated the limit cycle of the oscillator and its oscillations (x and $\dot{x}$) along the

simulation. One can also conclude that ϵ value (= 0.9) is suitable to enable phase-locking of the oscillator considering the distance between the intrinsic frequency of the oscillator and of the periodic input.

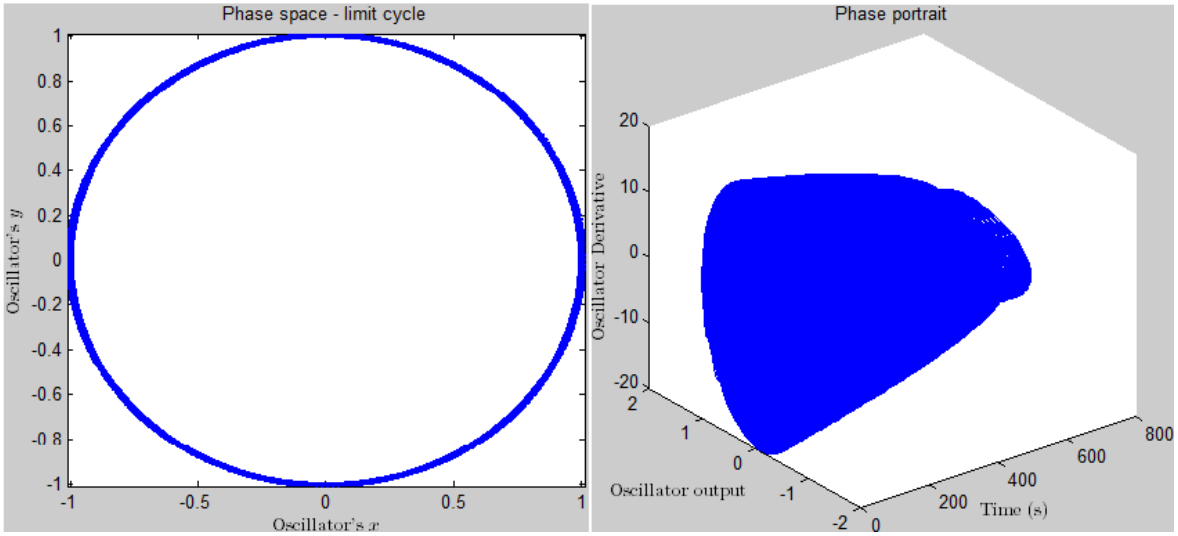

Figure 3.6: Exhibition of a stable harmonic limit cycle and of the stability of the oscillator over time.

Figure 3.6 demonstrates evidence of the limit cycle existence (on the left), although its form and time might have slightly changed. Nonetheless, that change is close to identity ensured by structural stability characteristic of the Hopf oscillator's limit cycle, which prevents alteration of the general behavior of the system due to small perturbations ($\epsilon > 0$) around its limit cycle. After learning, one can also see a very stable steady-state oscillatory regime (on the right).

3.3.2.2.2 Multi-frequency periodic input learning Here a network of coupled Hopf AFOs are presented to learn a multi-frequency signal $F = 0.8sin(15t)+cos(30t)-1.4sin(45t)-0.5cos(60t)$, with $\mu = 1$, $\gamma = 8.0$, $\epsilon = 1.0$ and initial conditions $r(0) = 1$, $\omega_1(0) = 6$, $\omega_2(0) = 27$, $\omega_3(0) = 48$ and $\omega_4(0) = 70$. As the frequency spectrum of the input is limited to four and each oscillator is responsible to code for one frequency component, a set of four oscillators is employed which is able to keep the correct phase relations between the oscillators and whose sum of their outputs should match the learning signal. The initial frequencies of the oscillators are uniformly distributed between 6 and 70, as suggested in [188]. In figures 3.7 and 3.8 the learning process when receiving a multi-frequency periodic input signal is demonstrated.

From figure 3.7 one can observe that the frequencies of each oscillator are adapted to the

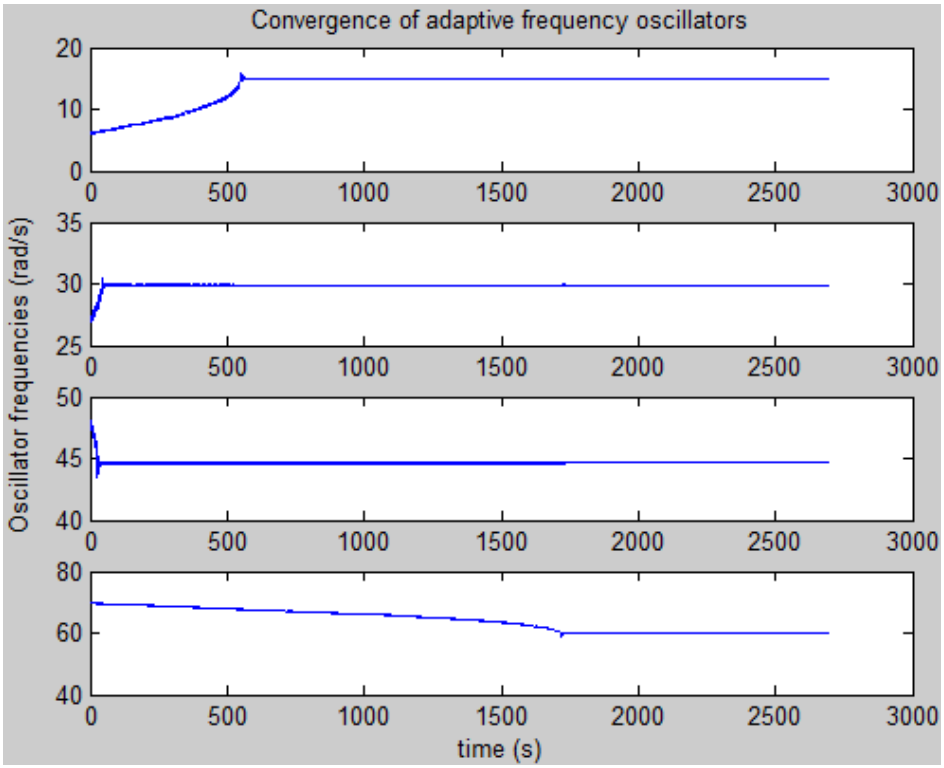

Figure 3.7: The figure illustrates the evolution of four intrinsic frequencies of the four oscillators, (ω_1, ω_2, ω_3, ω_4). Each oscillator can adapt its frequency to one of desired frequencies of the input signal.

desired frequencies of the input signal. Each intrinsic frequency has converged to the closest frequency component of the input as mentioned before. As soon as a intrinsic frequency of some oscillator converge to a desired frequency and stabilize, the correspondent amplitude of the oscillator will also match to the weighted amplitude of the input corresponding to the targeted frequency. Therefore, when all the frequencies of the input signal are learned, the signal is totally learned by the network of oscillators, as one can see in figure 3.8.

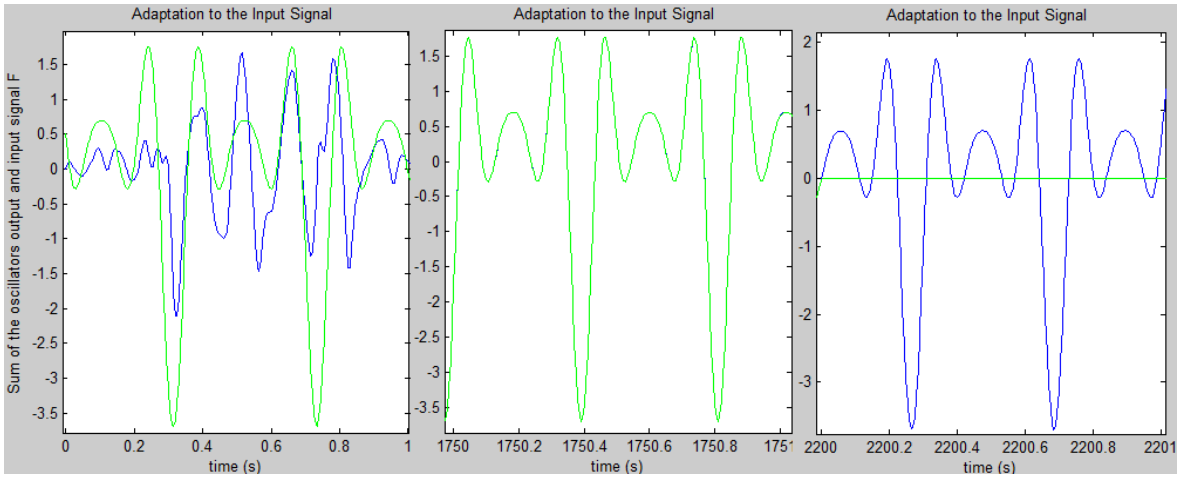

Figure 3.8: Frequency learning in the adaptive Hopf oscillators while receiving the input input, $F = 0.8sin(15t) + cos(30t) - 1.4sin(45t) - 0.5cos(60t)$. In the figure it is shown the sum of the oscillations of the Hopf oscillators corresponding to the x-state variable (solid blue line) in addition to the learning input signal (solid green line): at the onset of learning (left graph), after learning (center graph) and after removing the input signal (right graph).

The graph of figure 3.8 confirms the full learning of the input signal. On the left graph the output of the network of oscillators and the input signal are well differentiated and the adaptation is started. On the central graph the output of the network of the oscillators is already matched with the input. On the right graph the output of the network oscillators is not modified and is continuously stable after the learning signal removal, since the phase relations between the oscillators are kept due to the existing coupling among the oscillators. For that reason there was used a system of coupled oscillators instead of uncoupled oscillators to encode the periodic signal as a stable limit cycle in the system, even when the input signal may disappear. Likewise, the learned signal maintains its stability and is robust against temporary perturbations (as, for instance, considering the disappearing of the learning signal as a possible perturbation).

Chapter 4

Overall system design

Motivated by the growing interest in biologically inspired control of autonomous robots and especially the use of CPGs as a new paradigm to generate coordinated periodic movements, this chapter will highlight the approach introduced in chapter 3 for biped locomotion control. Thereby, generic CPGs encoding the nominal trajectories of a biomechanical system are presented and analyzed, firstly; the referred generic CPG is thereafter applied as a controller capable of integrating sensory feedback for the same biomechanical system from which the learning inputs were learned.

Locomotion behavior can be successfully achieved through the effective reciprocal and dynamic coupling between the brain, body and environment, by means of internal and external feedback pathways [189]. Endorsing this line of thought, the overall system design proposed is thus composed of three main blocks, namely the *High-level control* system (represented by the brainstem or supraspinal sites), the *Low-level control* system (represented by the spinal cord CPGs) and the biomechanical *Biped walker* system. A schematic of their interaction is shown in figure 4.1.

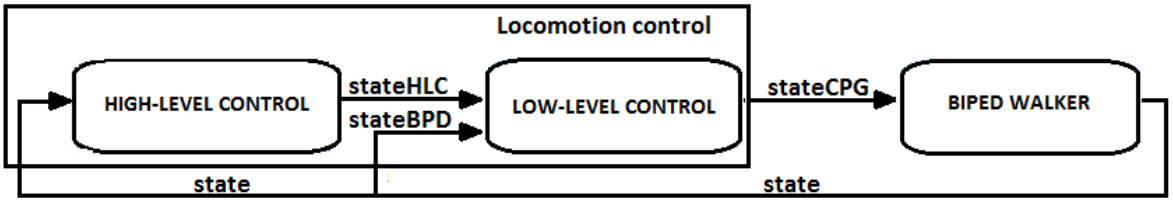

Figure 4.1: Overall architecture control.

In figure 4.1 the interaction among the three modules is represented by arrows of input/output of those modules. The *High-level control* and *Low-level control* systems contribute both for locomotion control, while the *Biped walker* system represents the biped

locomotor adopted in [44].

Emphasis is given to a dual rather than a single system of control, i.e., while the *Low-level control* is responsible for the reproduction of automatic, basic and periodic walking patterns, the *High-level control* system promotes voluntary, complex and non-periodic walking patterns by modulating the CPG system. Moreover, great importance is attributed to sensory feedback in order to enhance the gait stability and thus the range of gait trajectories that can be generated.

In the following, the adopted biped model is overviewed. Subsequently, the design of the control architecture of the CPG controller is presented, and at last, sensory feedback is integrated into the controller to increase the basin of stability of the gait.

4.1 Biped walker system

The *Biped Walker* system gets from the CPGs the generated joint trajectories as desired angles for PD controllers controlling each joint and it provides the real current state produced by the biped model (figure 4.1).

4.1.1 The mechanism structure

The body consists of a two-dimensional, rigid five-link system in the sagittal plane including a torso and two identical legs. Each robot link is characterized by a rigid body with uniformly distributed mass and center of mass (COM) located in its middle.

External forces F are added to the leg tips when reaching the ground, modeling the interaction with the walking surface. The biped gait is controlled by moments M applied to the joints. The controlled joints are namely the torso angle (α), the difference of thigh angles ($\Delta\beta = \beta_{\mathrm{R}} - \beta_{\mathrm{L}}$), the left leg knee angle (γ_{L}) and right leg knee angle (γ_{R}). These variables are explained further below.

The link lengths are denoted as ($\mathrm{l}_0\ \mathrm{l}_1\ \mathrm{l}_2$) and masses as ($\mathrm{m}_0\ \mathrm{m}_1\ \mathrm{m}_2$). The COM of the links are located at distances ($\mathrm{r}_0\ \mathrm{r}_1\ \mathrm{r}_2$) from the corresponding joints. A schematic diagram of the biped is shown in figure 4.2.

From figure 4.2 the coordinate vector assumed by the biped is composed of seven DOFs:

$$q = [x_0\ y_0\ \alpha\ \beta_L\ \beta_R\ \gamma_L\ \gamma_R]^T \tag{4.1}$$

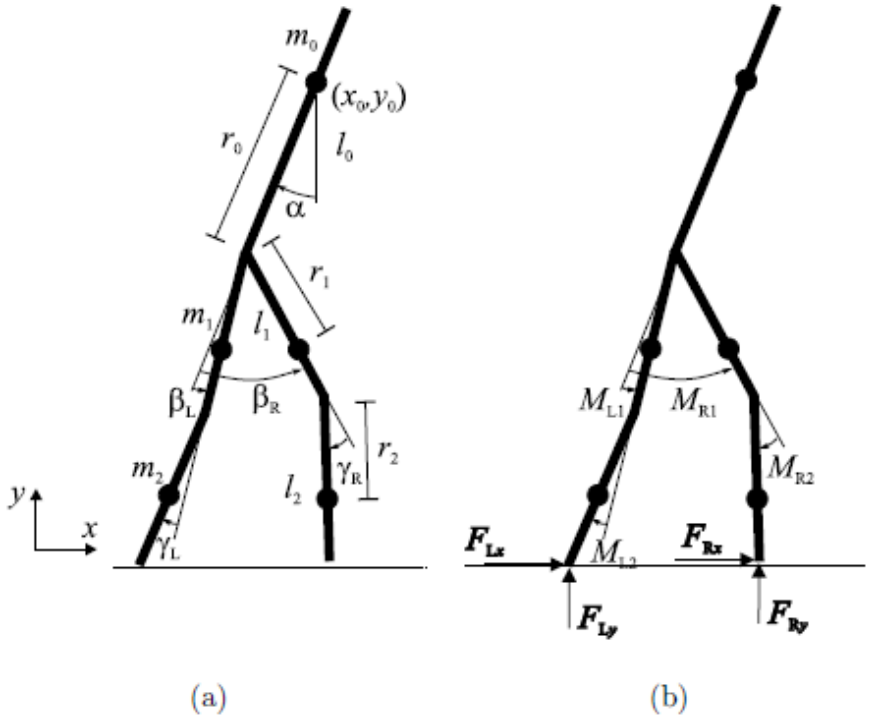

Figure 4.2: Schematic diagram of the biped walker stick man.

The position of torso COM is represented by the coordinates (x_0y_0) and the other coordinates describe the joint angles, namely the torso angle (α), left and right thigh angles (β_L, β_R), left and right knee angles (γ_L, γ_R). The subindices L and R correspond to left and right sides, respectively.

The *Biped walker* system output is a 18-dimensional state vector including the coordinate vector q, the corresponding time derivative $\dot{q}$ and also the touch sensor vector S composed of the binary sensor values of the leg tip s_L and s_R which are equal to 1 as the respective leg reaches the ground and 0 otherwise. Thus,

$$state = [q\ \dot{q}\ S\ COM]^T \tag{4.2}$$

where $S = [s_L\ s_R]$ and $COM = \left[COM_x\ COM_y\right]$.

The moment vector M is given by:

$$M = [M_{L1}\ M_{R1}\ M_{L2}\ M_{R2}]^T \tag{4.3}$$

where the moments M_{L1} and M_{R1} act between the torso and both thighs, while M_{L2} and M_{R2} act at the knee joints (figure 4.2).

The ground contact forces, applied whenever the leg tip touches the ground, are represented by:

$$F = \left[F_{Lx}\ F_{Ly}\ F_{Rx}\ F_{Ry}\right]^T \tag{4.4}$$

where tangential forces are represented by F_{Lx} and F_{Rx} and normal forces by F_{Ly} and F_{Ry} (figure 4.2).

F is closely related to the S, i.e., supposing the left leg tip does not reach the ground ($s_L = 0$; $S = [0\ s_R]$), the ground reaction forces relating the left leg are also null ($F = \left[0\ 0\ F_{Rx}\ F_{Ry}\right]^T$); conversely, supposing that both leg tips are touching the ground ($S = [1\ 1]$), the ground reaction forces relating the both legs are not null.

Through Lagrangian mechanics [41], the system's dynamic equations are obtained:

$$A(q)\,\ddot{q} = b(q,\ \dot{q},\ M,\ F) \tag{4.5}$$

where $A(q) \in \Re^{7x7}$ is the inertia matrix and $b(q,\ \dot{q},\ M,\ F)$ is a vector including the right hand sides of the seven partial differential equations. The A and b closed form formulas can be consulted in [44]. The motion of the body is represented by seven partial differential equations stated as closed form formulas (see Appendix B).

The *Biped walker* system consists of two main blocks, namely the *Biped model* block and the *PD ref controller* block. This section gives an overview of these blocks and their parameters included. Figure 4.3 illustrates a schematic of the blocks within the *Biped walker* system.

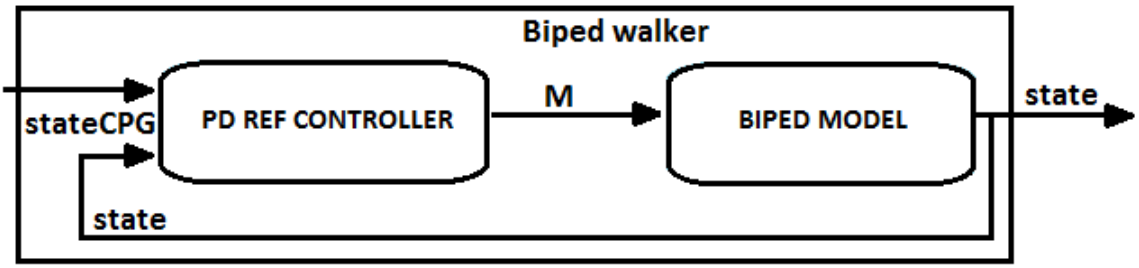

Figure 4.3: Schematic of the *Biped walker* system.

The input signals for the *PD ref controller* block are the state of the biped and the reference state of the CPG-based controller, $state_{CPG}$ (figure 4.1). This variable is composed of four reference signals: the reference torso angle (α_{REF}); the reference difference of thigh angles ($\Delta\beta_{REF}$); the reference left leg knee angle ($\gamma_{L\,REF}$); the reference right leg knee angle

($\gamma_{\text{R REF}}$). M denotes the moment vector given by the *PD ref controller*.

4.1.2 Biped model block

The *Biped model* block simulates the complete walking robot system and it comprises the *Dynamic model*, *Ground contact*, *Knee stopper* and *COM* blocks (figure 4.4). For specifications of robot dimensions, system initial state and properties of the knee limiter and walking surface, please refer to Appendix A.

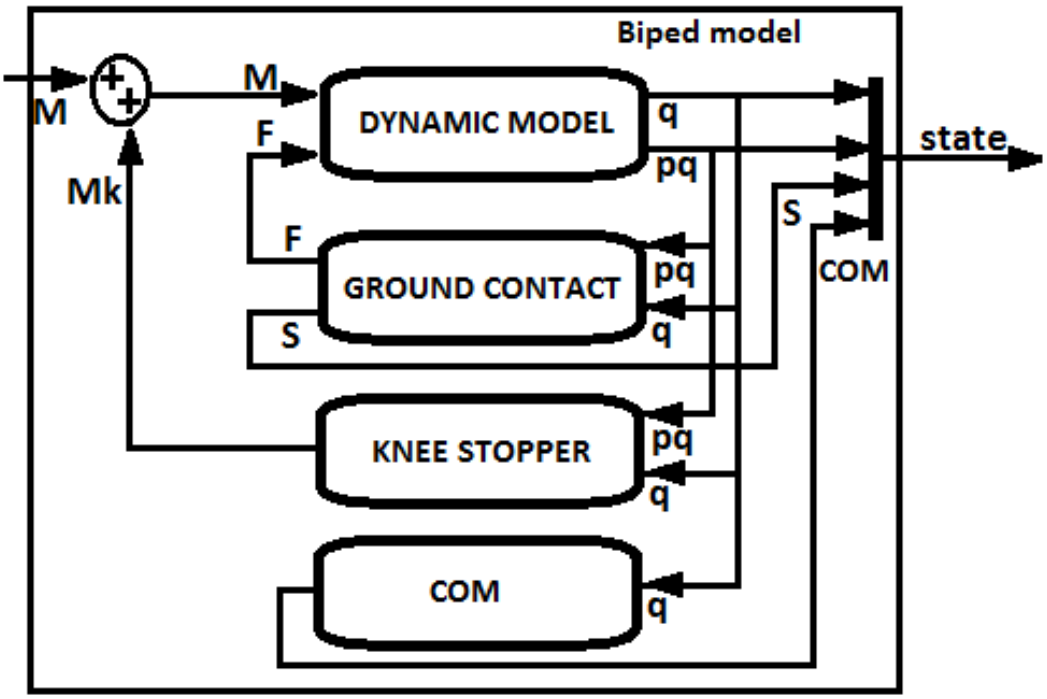

Figure 4.4: The blocks inside the *Biped model* block.

The *Knee stopper* block is useful to restrict knee angles to a user-defined range in order to prevent the joint rotation being outside the limit values, as suggested in [44]. Therefore, a specified knee moment value M_K produced in the *Knee stopper* block is added to the corresponding knee joint moment of the vector M to prevent the joint rotating over (or under) the limit value. For more details, please consult [44]. In relation to other joints, the out-of-range rotation problem does not exist.

The motion of the body is obtained within the *Dynamic model* block, where the biped DOFs are generated and the dynamic equations simulated. The *Ground contact* block determines S and F variables, while the *COM* block calculates the biped COM.

4.1.3 PD ref controller block

In order to get the system producing walking movements, a *PD ref controller* block was developed as depicted in figure 4.3. The input signals of the block are the state of the biped system, state, and the reference signals, $\text{state}_{\text{CPG}}$, from the *Low-level control* system (figure 4.1), while M is the output signal.

A schematic of the blocks within the *PD ref controller* is depicted in figure 4.5.

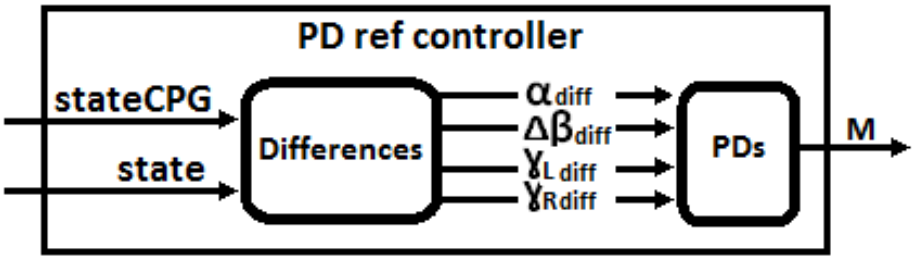

Figure 4.5: Schematic of the blocks with the *PD ref controller* block. This block is inside the *Biped walker* system (figure 4.1)

Two main blocks are detached, namely the *Differences* and the *PDs* blocks. The *Differences* block receives state and $\text{state}_{\text{CPG}}$ as input signals. Strictly related to $state_{CPG}$ is $state_{HLC}$ (figure 4.1), the output signal of the *High-level control* system, also composed of four signals related to controlled trajectories.

The *Differences* block subtracts the input signals and outputs α_{diff}, $\Delta\beta_{\text{diff}}$, $\gamma_{\text{L diff}}$ and $\gamma_{\text{R diff}}$ to the *PDs* block. Then, four independent PD controllers calculate M.

4.1.4 Joint trajectories

Once presented the interaction between the *Biped model* and the *PD ref controller*, it is important to illustrate the walking joint trajectories assumed by the biped system [44] and compare them with the nominal reference trajectories from the $\text{state}_{\text{CPG}}$ vector.

As depicted in figure 4.6, the nominal reference trajectories and those assumed by the biped are quite different. Nonetheless, α trajectory is the case on which their disparities are most significant.

According to Haavisto (2004) [44], the *PD ref controller* parameters were tuned by hand such that they were not perfectly optimized to ensure a better replication of the nominal reference signals. Moreover, they were not tuned in a systematical way, therefore solely working with the specified biped parameters.

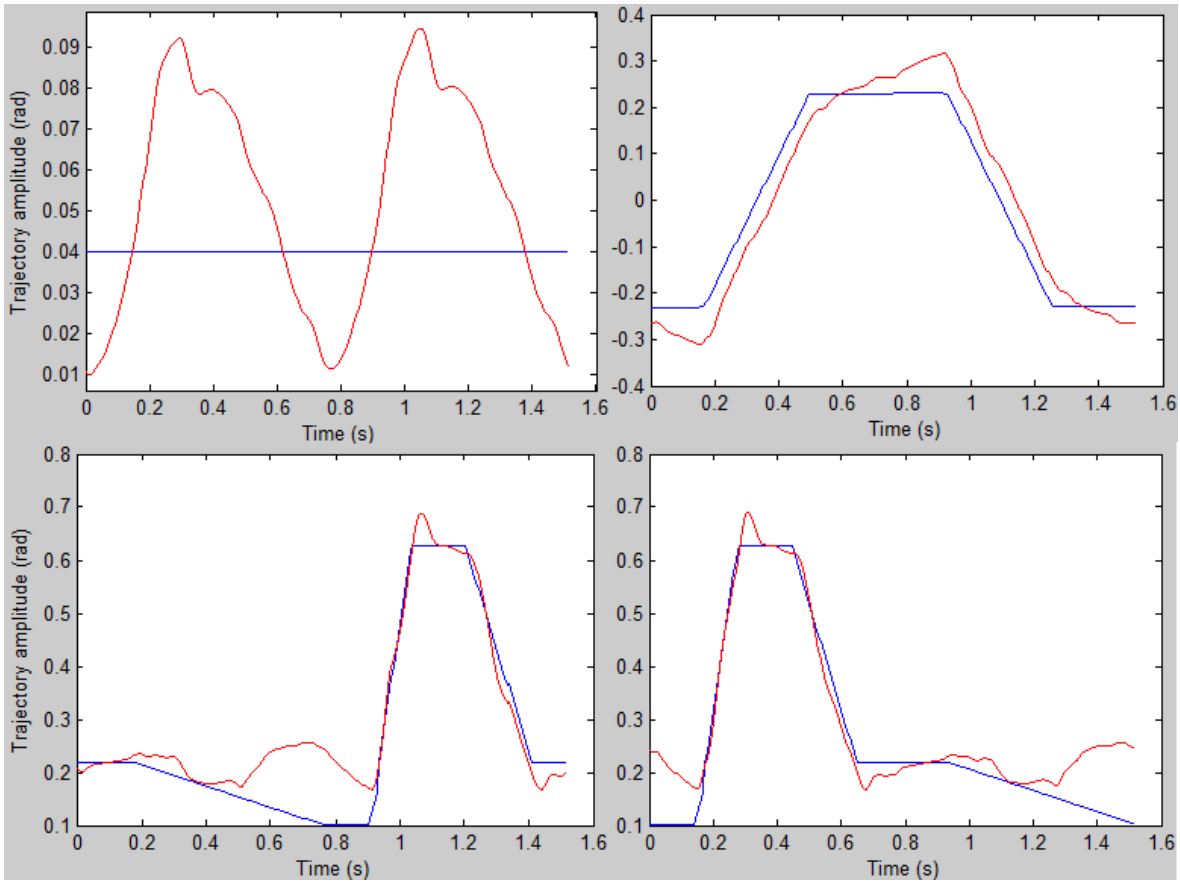

Figure 4.6: Comparison between the nominal reference trajectories from the $\text{state}_{\text{CPG}}$ vector (solid blue line) and the real trajectory signals (solid red line) assumed by the biped system from the simulation model during a single stride period. - Top: trajectories relating the torso angle α (left) and the difference of the thigh angles $\Delta\beta$ (right); - Bottom: trajectories regarding the left (left) and right (right) leg knee angles γ_{L} and γ_{R}.

4.1.5 Graphical user interface

A graphical user interface (GUI) was developed for the simulation of a *Simulink* model including the Biped model block. The GUI enables the biped model simulation and the animating of the system behavior. It is also possible to save the simulation data *Matlab* workspace. In figure 4.7 is illustrated the GUI.

4.2 Locomotion control

The control strategy responsible for the attainment of stable periodic gaits basically comprises the following parts: the learning of biped system reference trajectories and joint coordination through adaptive rules of the dynamical system; the reproduction of these walking patterns with the integration of feedback.

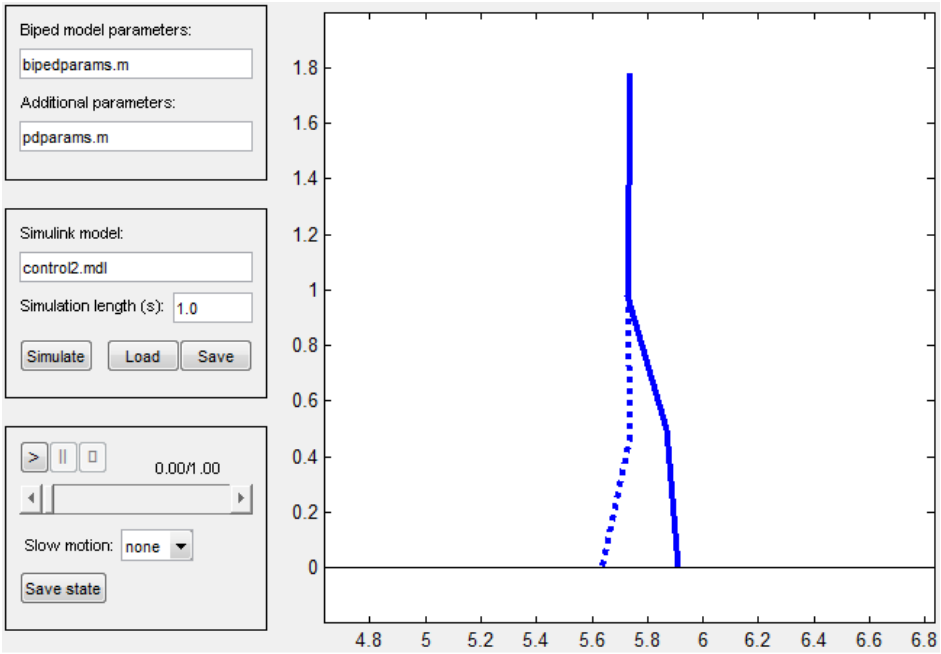

Figure 4.7: The graphical user interface for a controlled biped system simulation.

4.2.1 CPG-based controller design

In chapter 3, a network of AFOs is presented to learn an arbitrary signal through the learning adaptive concept. Here, such a mechanism can be potentially beneficial for adapting the intrinsic frequencies of the oscillators to the frequency components of sensory feedback signals, for instance, from a mechanical system and therefore replicating the sensory signals.

As this work implements a biomechanical system from a simulation model of a biped walker, the relevant applicability of a CPG-based controller for the walking control is then explored .

Once already introduced both the dynamic learning for oscillators and the dynamics of the biped system, the nominal reference trajectories to be learned are firstly presented, then a static analysis of their frequencies is performed and, lastly, a dynamic trajectories learning is described.

Not only the frequency but also the amplitude of the frequency components of the learning signal are learned. As concluded in [188], the coupling between AFOs is required so that the correct phase relationship among them can be developed and preserved in front of temporary perturbations.

4.2.1.1 Reference nominal trajectories

In order to learn the reference nominal trajectories, if the trajectories are not known yet, one should always know the kind of frequency spectrum of the pre-recorded or measured walking trajectories, in order to be able to predict the behavior of the oscillators. Since the nominal trajectories are not explicitly revealed in [44], a static spectral analysis of those signals is performed extracting their spectrum information with the corresponding amplitudes as illustrated in figures 4.8-4.11.

- Difference of the thigh angles ($\Delta\beta$)

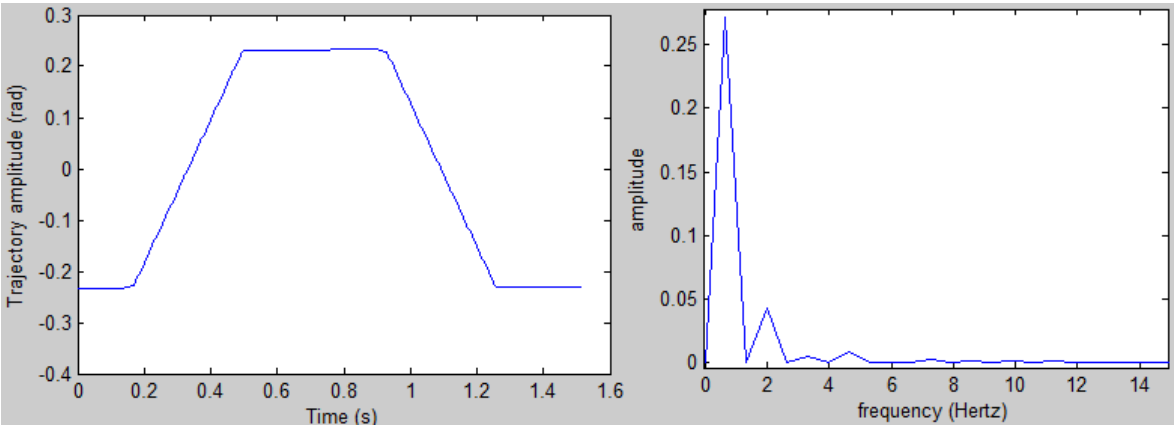

Figure 4.8: Difference of the thigh angles ($\Delta\beta$) and its frequency spectrum.

- Left leg knee angle (γ_{L})

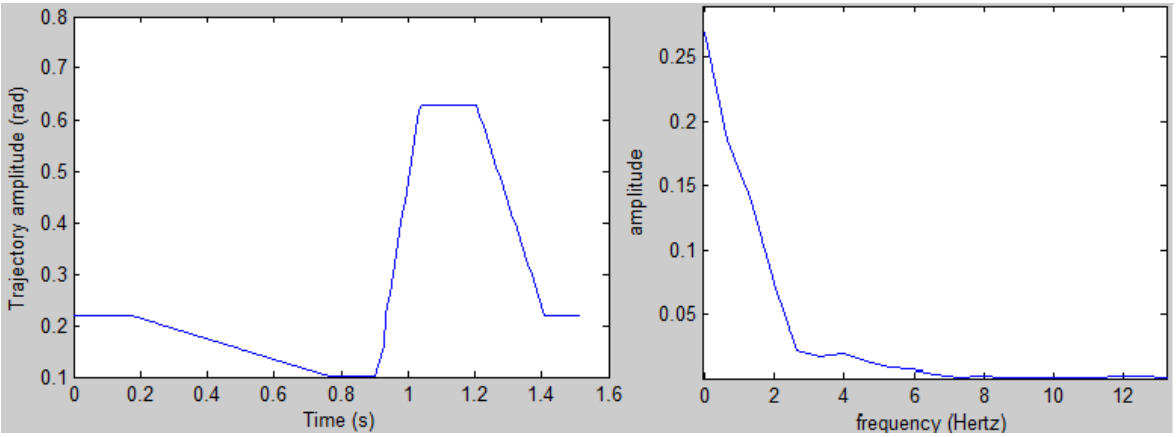

Figure 4.9: Left leg knee angle (γ_L) and its frequency spectrum.

- Right leg knee angle (γ_{R})

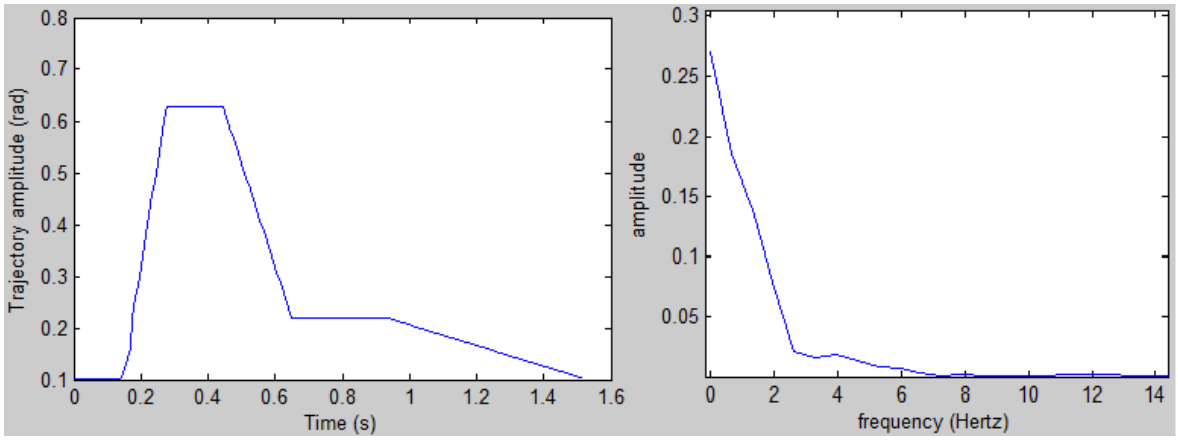

Figure 4.10: Right leg knee angle (γ_R) and its frequency spectrum.

- Torso angle (α)

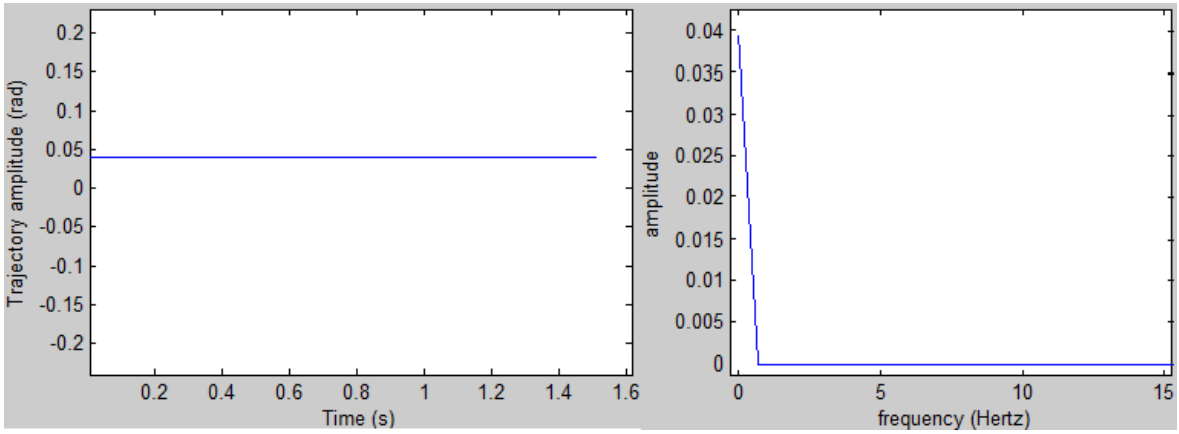

Figure 4.11: Torso angle (α) and its frequency spectrum.

It is recommended a suitable compromise between obtaining a sufficiently good match between the nominal reference signals and the corresponding learned signals and avoiding a highly computational burden due to a broaden number of oscillators. One should verify thus the minimal amount of oscillators necessary to reproduce those signals similar as desirable to the nominal trajectories. This is done by learning the main frequencies of higher power.

The harmonic nature of the Hopf oscillations enables the reproduction of any periodic input signal through an adequate combination of Hopf oscillators. They function as a dynamic Fourier series representation, each frequency component of the input signal being encoded by a single oscillator [28]. Thus, from the spectral analysis previously implemented is possible to manually reproduce a good approximation of the nominal trajectories using a limited range of constituent frequencies.

In figure 4.11 is depicted the generation of the periodic inputs as their complex Fourier series.

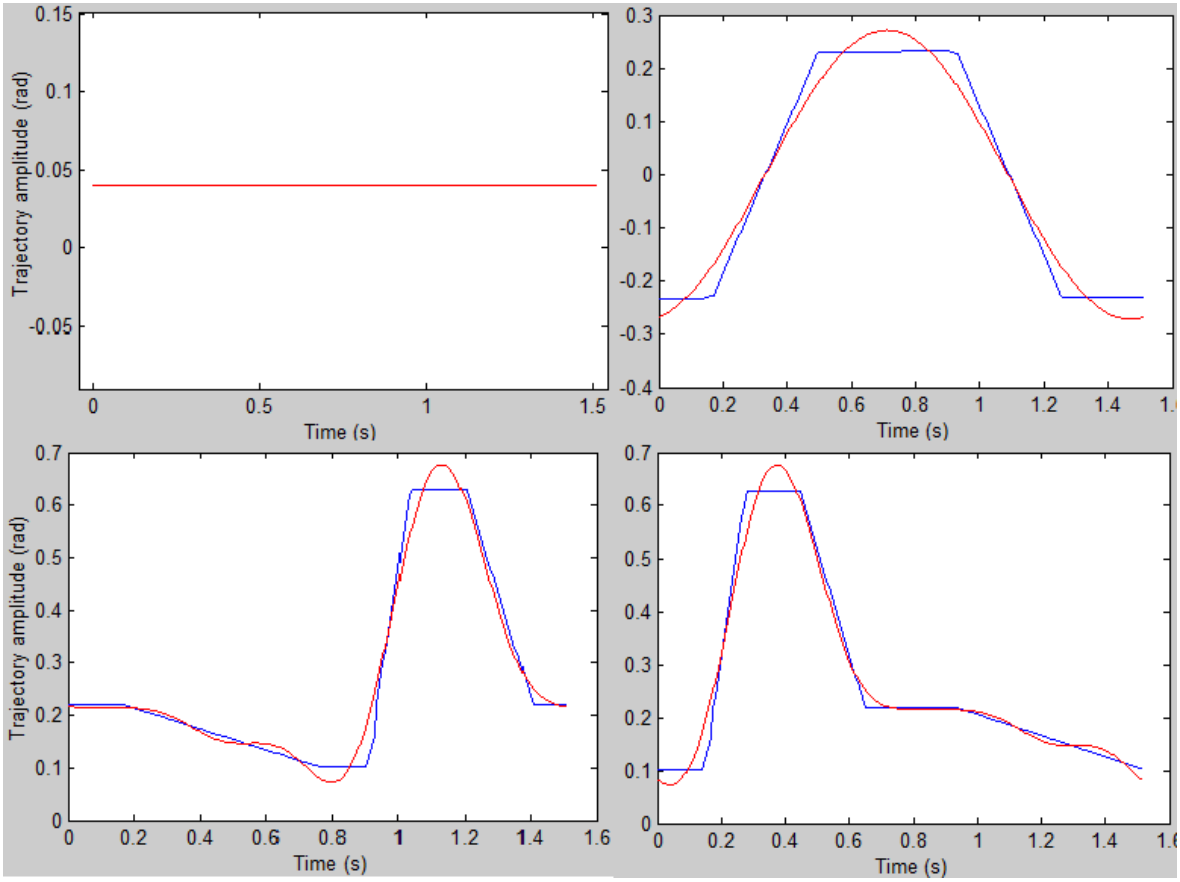

Figure 4.12: Comparison between the nominal reference trajectories from the simulation model (solid blue line) and the manually reproduced signals (solid red line). - Top: trajectories concerning the torso angle α (left) and the difference of the thigh angles $\Delta\beta$ (right); - Bottom: trajectories regarding the left (left) and right (right) leg knee angles γ_L and γ_R.

According to their spectrum, the sum of three sinusoids is considered for the reproduction of $\Delta\beta$ reference signal. Five sinusoids are summed to reproduce γ_L and γ_R reference signals. On the other hand, α reference signal is a constant (0.04 rad), so there is no need to reproduce it by a sum of sinusoids.

As one can observe, the manually reproduced signals can be considered closely similar to the nominal signals without causing any unnatural movement on the trajectories of the joints. It should further be noted that, as indicated by Haavisto (2004) [44], the nominal trajectories were developed through trial and error process and represented merely an example how the biped system could produce a stable and natural gait.

Therefore, these manually reproduced signals can be proposed as valid learning signals to which the network of AFOs should adapt and learn. To this end, it is suggested the use

of three generic CPGs to learn the manually reproduced signals as follows: the thigh CPG composed by three oscillators corresponding to three sinusoids required to reproduce $\Delta\beta$; two knee CPGs composed by five oscillators to learn the frequencies of the five sinusoids necessary to reproduce γ_{L} and γ_{R}.

4.2.1.2 Design of the generic CPGs

Here, the architecture of the CPGs, their properties and results of simulations are analyzed and discussed. Figure 4.13 illustrates an overall schematic of the dynamic learning process. The biped walker generates the learning signals proposed in [44].

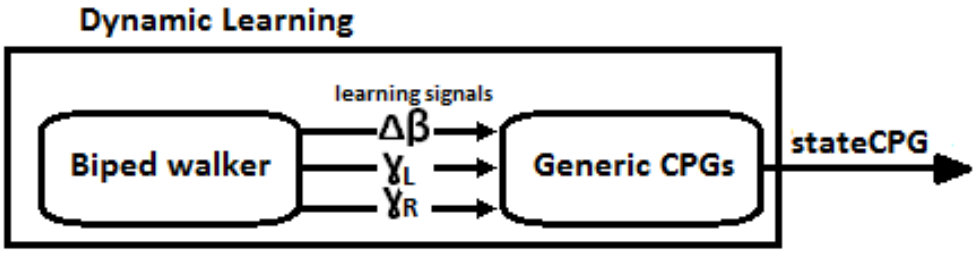

Figure 4.13: Schematic of the dynamic learning of the reference nominal trajectories.

The referred architecture within the *Generic CPGs* block proposed to learn the reference signals is demonstrated in figure 4.14, based on which the *Low-level control* system will generate the reference signals $state_{CPG}$ (figure 4.13) to control the locomotion of the biped system.

Comparing figures 4.13 and 4.14, the learning signals which come from the *Biped walker* system are the input signals of the *Generic CPGs* (figure 4.13), by which each learning signal is learned by each generic CPG. As depicted in figure 4.14, $\Delta\beta$ reference learning signal is provided as input to the thigh CPG composed of three coupled AFOs. The other two learning signals (γ_{L} and γ_{R}) are delivered as inputs to the two knee CPGs both composed of five AFOs.

Each symbol characterized by a tilde ('~') into a circle represents an AFO and the three bigger symbols represent the first oscillator of each generic CPG. Nonetheless, more detailed information about this process and the architecture of a generic CPG is described below.

A generic CPG is constructed by the use of coupled AFOs which are considered the basic building block capable of learning a frequency component of the learning signal. The network of AFOs composing a generic CPG is shown in figure 4.15.

The learned signal learnedS is obtained from the sum of all outputs of the oscillators $\mathrm{x_i}$ weighted by the associated amplitude a_i. This signal is subtracted to *mathrmlearningS*

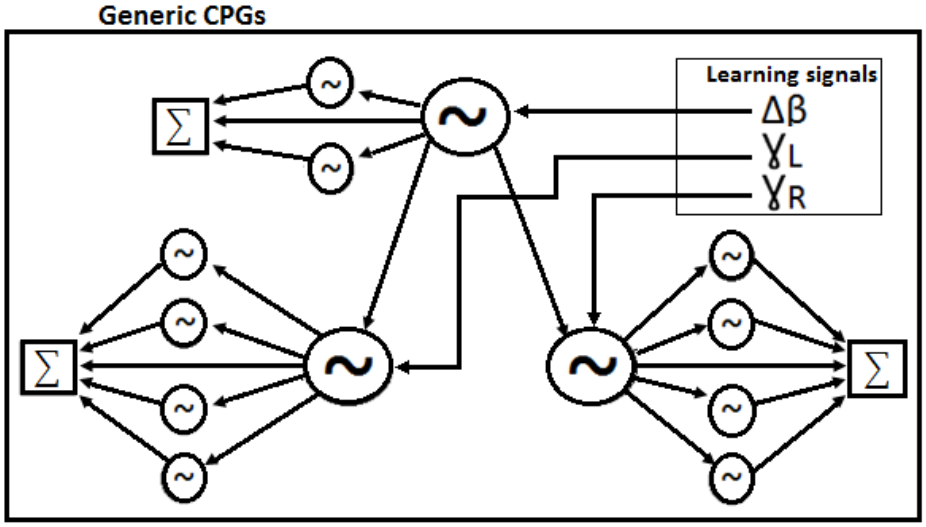

Figure 4.14: Structure of the generic CPGs within the *Generic CPGs* block. A generic CPG is used for each DOF ($\Delta\beta$, γ_L and γ_R). The arrows connecting the first oscillators of each generic CPG represent the phase relationship between the CPGs. Each produced DOF trajectory is the weighted sum of the respective constituent oscillators of the respective CPG.

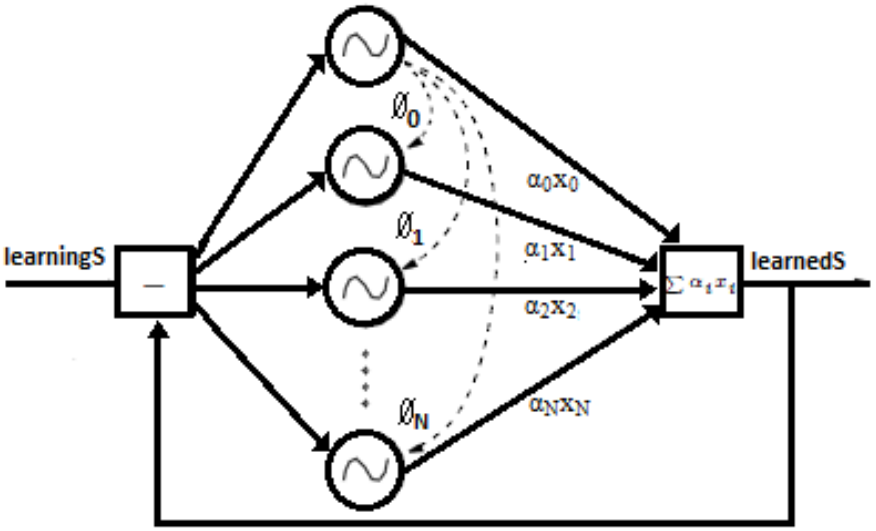

Figure 4.15: Structure of a generic CPG network of Hopf AFOs. The learning signal F(t) = learningS − $\sum a_i x_i$ is delivered to all oscillators, which is the difference between the signal to be learned, learningS, and the signal already learned, learnedS = $\sum a_i x_i$. Unlike the oscillator 0, all the oscillators are given a phase contribution ϕ_i from oscillator 0. For more details, consult [27, 28].

through a negative feedback. The negative feedback loop enables that as soon as an AFO has completely learned a specified frequency component of the input signal, that frequency component may therefore be removed from learningS. The learned frequency stays encoded in the system as a stable limit cycle, though.

Thereby, there remains in learningS only the frequency components still not learned as inputs for the oscillators whose intrinsic frequency has not been converged yet to a stable

frequency. Each AFO is associated to a variable ϕ_i representing the phase difference between an oscillator i and the first oscillator (oscillator 0) of the network. The phase relationship among the oscillators is thus characterized by the transmission of the scaled phase input ϕ_i from oscillator 0.

Confronting figures 4.14 and 4.15, the first oscillator of each CPG from figure 4.14 is stated as the oscillator 0 from figure 4.15. A single generic CPG composed of N oscillators is given by:

$$\dot{x}_i = \gamma\left(\mu - r_i^2\right) x_i - w_i y_i + \epsilon I + \tau sin\left(\theta_i - \phi_i\right) \tag{4.6}$$

$$\dot{y}_i = \gamma\left(\mu - r_i^2\right) y_i + w_i x_i \tag{4.7}$$

$$\dot{\omega}_i = -\epsilon I \frac{y_i}{r_i} \tag{4.8}$$

$$\dot{a}_i = \eta x_i I \tag{4.9}$$

$$\dot{\phi}_i = sin\left(\frac{\omega_i}{\omega_0}\theta_0 - \theta_i - \phi_i\right) \tag{4.10}$$

$$\theta_i = sgn\left(x_i\right) cos^{-1}\left(-\frac{y_i}{r_i}\right) \tag{4.11}$$

$$i \in 0, \ldots, N \tag{4.12}$$

where the i^{th} AFO is described by x_i, y_i and ω_i, already presented in section 3.3.2.2. τ and ϵ are positive coupling constants while η is a learning constant and the three variables contribute for the learning rate control.

The phase difference between oscillator i and 0 is represented by ϕ_i. It converges to the phase difference between the instantaneous phase of oscillator 0, θ_0, scaled at frequency ω_i and the instantaneous phase of oscillator i, θ_i. Each AFO is coupled with oscillator 0 with strength τ in order to keep correct phase relationships among oscillators. Thus, phase synchronization can be achieved [27].

The weighted sum of the outputs of each oscillator constitutes the total output of the system, learnedS, while I represents the remaining of the input signal learningS the generic CPG still has to converge. Each amplitude of an oscillator a_i is closely related to its frequency ω_i. a_i will increase as ω_i is converging to a frequency component of I and will stagnate when the frequency component is disappeared from I due to the negative feedback loop.

It is important to highlight that ϵ controls both the learning rate of the system and the amplitude of oscillations around the targeted frequency. So the faster the learning is, the higher the error of adaptation will be.

On the other hand, one should bear in mind some specifications concerning the learning of such multi-frequency signals. In case of insufficient oscillators to code for all the frequency components of the input signal, the system will only learn the frequency components with more power, such that the learned trajectory will only be a relatively rough approximation [28]. Conversely, if there are excessive oscillators in relation to frequency components available to learn, either some oscillators will not converge to any frequency and their contribution to the learned signal will be null, or else some frequency components will be coded by more than a single oscillator and the sum of the corresponding amplitudes of those oscillators will match the amplitude of the frequency component to which they have synchronized.

Moreover, the less the distance between a frequency component of the input signal and the intrinsic oscillator frequency is and the more its intensity is, the higher the attraction of the frequency component will be to the oscillator. A more detailed discussion about the parameters and initial conditions of AFOs is given in [27, 28, 187].

From figure 4.14, the first oscillator of both knee CPGs are coupled with the first oscillator of the thigh CPG, in order to ensure the correct phase difference among the DOFs. Like the coupling scheme for the establishment of coordinated phase relations among the oscillators of a generic CPG illustrated in figure 4.15, the same principle is applied to keep the reference learning signals of DOFs well coordinated.

Therefore, the equations for the first oscillators are slightly modified to include the aforementioned coupling as follows:

$$\dot{x}_{0,n} = \gamma\left(\mu - r_{0,n}^2\right) x_{0,n} - w_{0,n} y_{0,n} + \epsilon F + \tau sin\left(\theta_{0,n} - \phi_{0,n}\right) \tag{4.13}$$

$$\dot{\phi}_{0,n} = sin\left(\theta_{0,\Delta\beta} - \theta_{0,n} - \phi_{0,n}\right) \tag{4.14}$$

where the first oscillators of n^{th} CPGs are denoted by $(0, n)$ and n = [left knee, right knee].

4.2.1.3 Results of simulations

Here is presented the outcome of the learning process implemented by the proposed CPG architecture illustrated in figure 4.14 when receiving as input the learning signals concerning $\Delta\beta$, γ_R and γ_L reference signals.

Figures 4.16-4.18 show the reproduction of these signals after a transient period. There are illustrated the decline of the error between the reference signal given as learningS and learnedS stated as the CPG output until reaching approximately zero.

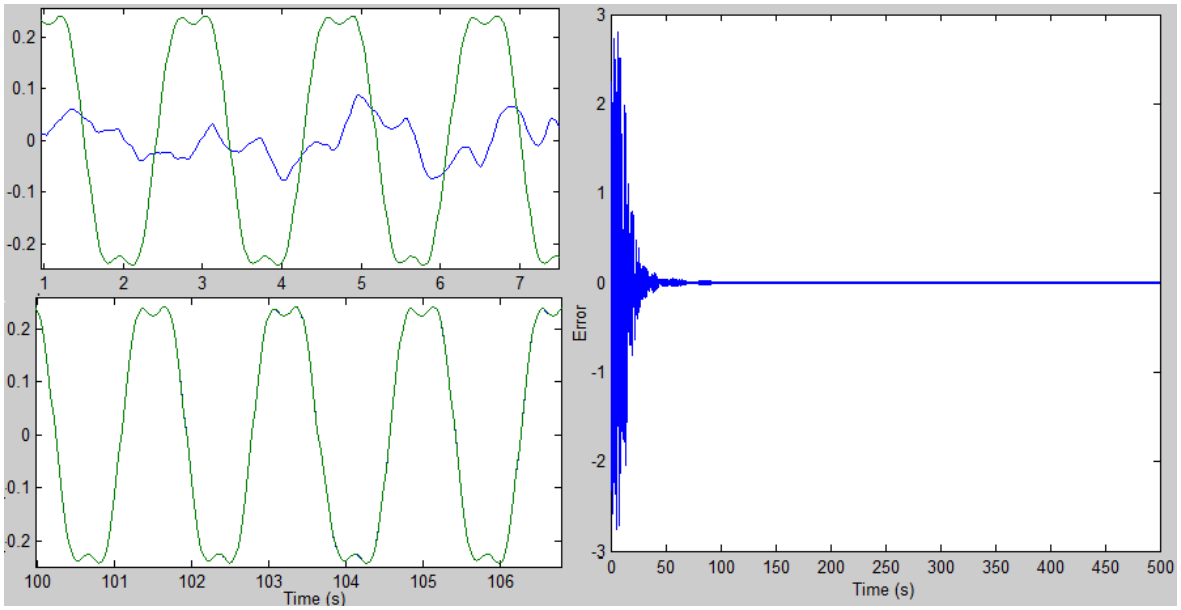

Figure 4.16: Learning of the frequencies and associated amplitudes of the $\Delta\beta$ reference signal in the thigh CPG. The error between the learningS and the learnedS signals is shown on the right, where one can observe its value converging to zero. On the left are depicted the oscillations of the Hopf oscillator (blue solid line) corresponding to x-state variable, at the onset of learning (upper graph) and after learning (lower graph), in addition to the plot of the input signal I (green solid line).

From figure 4.16, *learningS* is a multi-frequency input signal composed of three frequencies, $I = 1.461e-18 + 0.2716sin\,(4.1337t) + 0.0428sin\,(12.4011t) + 0.0049\ sin\,(20.6685t)$. Regarding the parameters of the oscillators: $\mu = 1$; the steady-state amplitude of oscillations $\gamma = 8.0$; the input gains $\epsilon_1 = 0.3$, $\epsilon_2 = 0.9$, $\epsilon_3 = 0.75$; the coupling strengths $\tau_1 = 0.03$, $\tau_2 = 0.005$, $\tau_3 = 0.05$; the learning constants $\eta_1 = 0.5$, $\eta_2 = 0.5$, $\eta_3 = 0.5$; the intrinsic frequencies $\omega_1 = 3.5rad.s^{-1}$, $\omega_2 = 13.0rad.s^{-1}$, $\omega_3 = 21.0rad.s^{-1}$.

From figure 4.17, learningS is a multi-frequency input signal composed of five frequencies, $I = 0.2705 + 0.1854sin\,(4.1337t + 2.8270) + 0.1385sin\,(8.2674t + 4.7124) + 0.0746\ sin\,(12.4011t + 0.1314)+0.0225sin\,(16.5348t + 2.2562)+0.0172sin\,(20.6685t - 0.8672)$. Regarding the parameters of the oscillators: the convergence speed to the limit cycle $\mu = 1$; the steady-state amplitude of oscillations $\gamma = 8.0$; the input gains $\epsilon_1 = 0.3$, $\epsilon_2 = 0.75$, $\epsilon_3 = 0.9$, $\epsilon_4 = 0.9$, $\epsilon_5 = 0.9$; the coupling strengths $\tau_1 = 0.03$, $\tau_2 = 0.03$, $\tau_3 = 0.03$, $\tau_4 = 0.03$, $\tau_5 = 0.03$; the learning constants $\eta_1 = 0.5$, $\eta_2 = 0.5$, $\eta_3 = 0.5$, $\eta_4 = 0.5$, $\eta_5 = 0.5$; the intrinsic frequencies $\omega_1 = 4.0rad.s^{-1}$, $\omega_2 = 11.0rad.s^{-1}$, $\omega_3 = 15.0rad.s^{-1}$, $\omega_4 = 19.0rad.s^{-1}$, $\omega_5 = 23.0rad.s^{-1}$.

From figure 4.18, *learningS* is a multi-frequency input signal composed of five frequencies, $F = 0.2705 + 0.1854sin\,(4.1337t - 0.3146) + 0.1385sin\,(8.2674t + 4.7124) + 0.0746\ sin\,(12.4011t + 3.2730)+0.0225sin\,(16.5348t + 2.2562)+0.0172sin\,(20.6685t - 2.2744)$. Re-

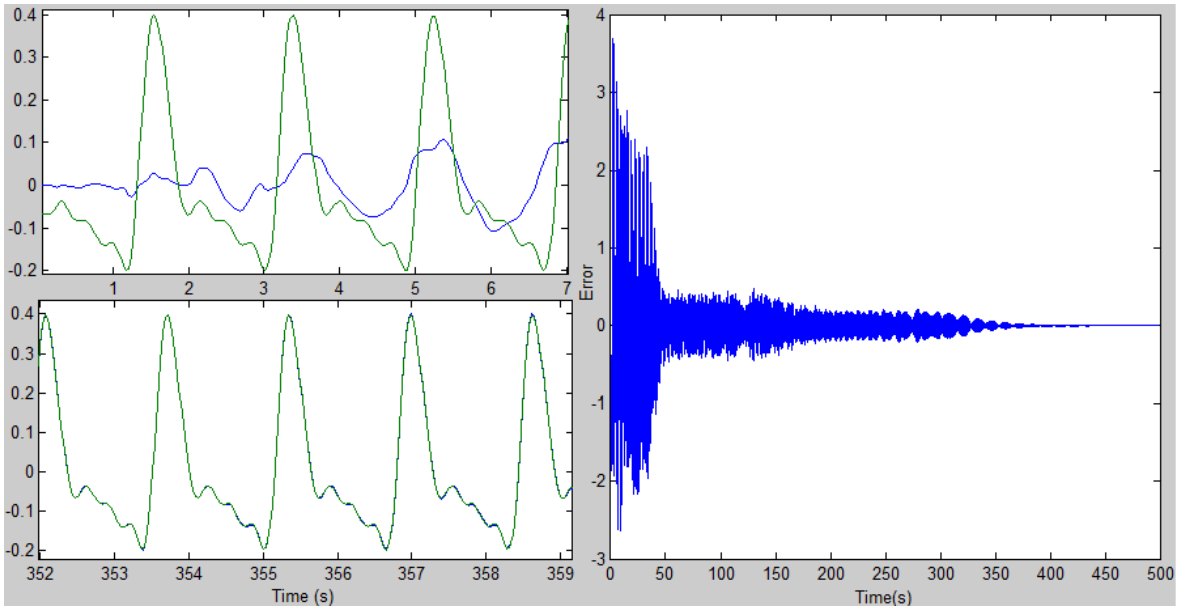

Figure 4.17: Learning of the frequencies and associated amplitudes of the γ_L reference signal in the left knee CPG. The error between the learningS and the learnedS signals is shown on the right, where one can observe the its value converging to zero. On the left are depicted the oscillations of the Hopf oscillator (blue solid line) corresponding to x-state variable, at the onset of learning (upper graph) and after learning (lower graph), in addition to the plot of the input signal I (green solid line).

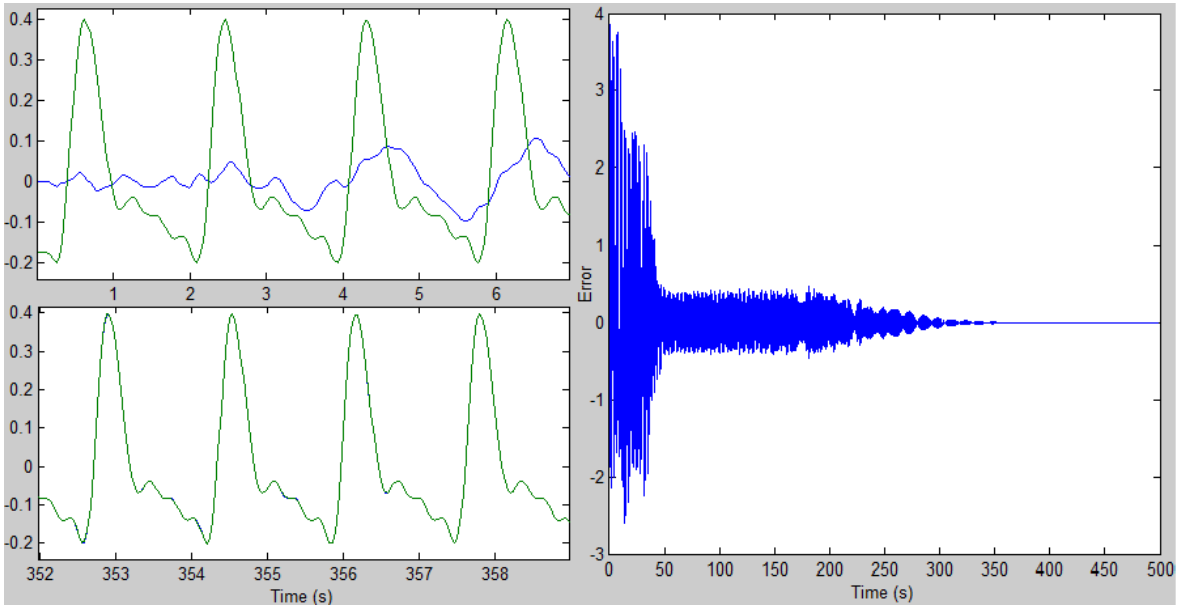

Figure 4.18: Learning of the frequencies and associated amplitudes of the γ_R reference signal in the right knee CPG. The error between the learningS and the learnedS signals is shown on the right, where one can observe the its value converging to zero. On the left are depicted the oscillations of the Hopf oscillator (blue solid line) corresponding to x-state variable, at the onset of learning (upper graph) and after learning (lower graph), in addition to the plot of the input signal I (green solid line).

garding the parameters of the oscillators: the convergence speed to the limit cycle $\mu = 1$; the steady-state amplitude of oscillations $\gamma = 8.0$; the input gains $\epsilon_1 = 0.3$, $\epsilon_2 = 0.75$, $\epsilon_3 = 0.9$,

$\epsilon_4 = 0.9$, $\epsilon_5 = 0.9$; the coupling strengths $\tau_1 = 0.03$, $\tau_2 = 0.03$, $\tau_3 = 0.03$, $\tau_4 = 0.03$, $\tau_5 = 0.03$; the learning constants $\eta_1 = 0.5$, $\eta_2 = 0.5$, $\eta_3 = 0.5$, $\eta_4 = 0.5$, $\eta_5 = 0.5$; the intrinsic frequencies $\omega_1 = 4.0 rad.s^{-1}$, $\omega_2 = 11.0 rad.s^{-1}$, $\omega_3 = 15.0 rad.s^{-1}$, $\omega_4 = 19.0 rad.s^{-1}$, $\omega_5 = 23.0 rad.s^{-1}$.

Comparing the three processes of adaptation evolution from figures 4.16-4.18, the learning speed of $\Delta\beta$ reference signal is naturally higher than those concerning γ_L and γ_R, what seems logic since the generic CPG responsible for $\Delta\beta$ learning is composed of fewer AFOs. All the reference inputs are successfully learned according to the fact that the three generic CPGs have in all cases effectively constructed the desired signals. The dynamical system has shown to be able to learn rhythmic gait patterns of the biped system employed in this work and replay it afterwards.

Comparing the manual reproduction of the reference signals developed in section 4.2.1.1 with the dynamic learning process through the novel system of coupled AFOs simulated in this section, the latter strategy can provide interesting advantages. Specifically, the dynamic learning solves the problem concerning the manual tuning of the oscillators for the learning of specific gait patterns.

In fact, the adaptive rules [27] enable the automatic self-tuning of the intrinsic frequencies, amplitudes and coupling weights of the AFOs to replicate the reference signals in a generalized fashion. In this way, it is possible to implement the proposed dynamical process to simulate the capability of the neural drive of the biped system to generate its own walking gaits, i.e., to learn the motion coordination without pre-specifying the response of the system.

On the other hand, such a dynamical system approach may be interesting and open the way to the online modulation of gaits rather than following fixed trajectories [28]. This may be achieved by learning online different gaits.

4.2.2 Low-level control system

The controller at the spinal level (see figure 4.1) is characterized by employing the novel system of coupled AFOs for the locomotion pattern generation. The global CPG architecture within the *Low-level control* system is thus based on the structure illustrated in figure 4.14 and on the equations 4.6-4.11 indicated in section 4.2 to control the referred DOFs.

However, the equation 4.6 is slightly changed because the CPG controllers are no longer adapting to input signals after complete convergence, so the input signal F of the AFOs

can be set I = 0 accepting no more input learningS nor negative feedback loop learnedS as the learned walking trajectories remain encoded as limit cycles in a network of CPGs. In addition, equation 4.6 and 4.7 are also modified to include the integration of sensory feedback.

Figure 4.19 depicts a schematic of the structure within the *Low-level control* system.

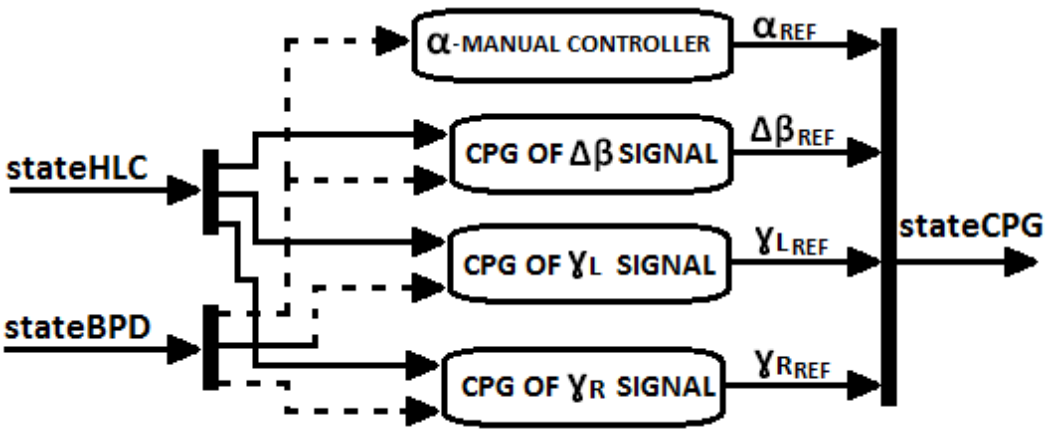

Figure 4.19: Schematic of the reference signals generation by the CPG-based controller within the *Low-level control* system. The internal feedback $\text{state}_{\text{HLC}}$ is represented in solid line, while the external feedback $\text{state}_{\text{BPD}}$ is represented in dashed line.

In figure 4.19 is depicted the generation of the reference state of the CPG-based controller, $\text{state}_{\text{CPG}}$. The CPG-based controller is characterized by three generic CPG controllers for $\Delta\beta_{\text{REF}}$, $\gamma_{\text{L REF}}$ and $\gamma_{\text{R REF}}$ trajectories reproduction, while α_{REF} reference trajectory is manually controlled within the *α-manual controller*.

Although the α_{REF} reference trajectory is initially set to a constant value of 0.04 rad, the signal may be modified when necessary, for instance, to maintain biped posture or balance under the presence of tilted ground. The input signals for the CPG-based controller are the the internal $\text{state}_{\text{HLC}}$ and external $\text{state}_{\text{BPD}}$ feedback from the *High-level control* and *Biped walker* systems, respectively, in order to enhance the CPG controller robustness to unknown environments and unexpected perturbations.

Comparing to figure 4.15, one can see that the input signal learningS and the negative feedback loop learnedS are disregarded since the CPG-based controller within the *Low-level control* system is no longer adapting to any signals, but rather reproducing the reference walking trajectories.

4.2.3 Feedback integration

Supposing the CPG-based controller is not influenced by sensory feedback (open-loop control), the controller can independently generate the nominal reference trajectories to control the biped system in a basic known environment with known conditions in which the modulation of the nominal gait patterns is not required, for instance, when a subject is taking long walks on even ground without being aware he is walking. Nevertheless, human locomotion is characterized by adapting robustly its walking patterns under the presence of more complex environment conditions such as reacting to pushes, circumventing obstacles, walking on uneven ground, climbing stairs, ..., which demand for the modulation of gait patterns (e.g. change on the amplitude, speed or direction of the trajectories). To this effect, taking inspiration from biological animals, the modulation of the gait patterns reproduced by the spinal cord CPGs can be achieved when a higher degree of conscious control like the brainstem give descending commands to enable it. These descending commands are stated as internal feedback $state_{HLC}$ from the *High-level control* system to the CPG-based controller (see figure 4.1). Furthermore, external information characterized by the biomechanical state output and environment conditions can be provided through peripheral sensors (load or position sensors) in the joints in order to ensure the gait stability of the whole system under unexpected environment conditions or perturbations. The referred external information can be stated as external feedback $state_{BPD}$ onto the spinal CPGs. Thus, both internal and external feedback promote the online modulation of trajectories so that the basin of locomotion stability can be enhanced and extended to several environment conditions or unexpected perturbations.

Referring to figures 4.1 and 4.19, it is presented a closed-loop controller characterized by the presence of internal and external feedback for stability enhancement under different environment conditions to which the biped walker should robustly cope with similar to human locomotion. The potential applications of sensory feedback is then below explained where is introduced three sorts of feedback pathways, namely longitudinal stability, phase modulation and postural stability.

4.2.3.1 Longitudinal stability

The longitudinal stability can be potentially questioned in the presence of unexpected perturbations (such as the appearance of obstacles or pushes) or in case of voluntary movements performance for a short period of time. The stability is only measured and evaluated in the longitudinal direction, due to the body of the biped system consisting of a two-dimensional,

rigid five-link system in the sagittal plane. In such conditions, a high degree of conscious control is required, either to create temporary perturbations to simulate voluntary movements or to react to perturbations from the environment. Thus, it is proposed that the brainstem represented by the *High-level control* system (see figure 4.1) should provide descending commands as feedback pathways to the spinal cord CPGs modulating the CPG-controller response and affecting the walking trajectories of the joints involved. These feedback pathways are thought to affect only the amplitude of trajectories ensuring that their phase is preserved, so the feedback signals are projected on the radius of the limit cycle of the oscillators which directly contribute for maintaining longitudinal stability depending on the specific situation. The idea of modulating the amplitude of trajectories rather than their phase was also employed in [28] to guarantee lateral stability. The descending commands are then represented by the $state_{HLC}$ vector composed of three values corresponding to the three controlled joints ($\Delta\beta$, γ_L and γ_R).

On the other hand, Veskos (2005) has implemented the vertical position of the torso as feedback signal for the CPG-controller, thereby obtaining stabler, larger and more constant steady-state amplitude oscillations [190]. Endorsing that line of thought, the vertical position of the torso (y_0) is here stated as external feedback to be projected on the radius of the limit cycle of all the oscillators to affect only the amplitude of the trajectories.

Thus, equations 4.6 and 4.7 are modified to include the feedback terms:

$$\dot{x}_i = \dot{x}_{i(4.6)} + \left(g_i \cdot state_{HLC\ j} + g_e \cdot y_0\right) \frac{x_i}{r_i} \tag{4.15}$$

$$\dot{y}_i = \dot{y}_{i(4.7)} + \left(g_i \cdot state_{HLC\ j} + g_e \cdot y_0\right) \frac{y_i}{r_i} \tag{4.16}$$

where x_i and y_i are the state variables of the ith oscillator, $g_i\,(= 1.0)$ and $g_e\,(= 1.0)$ are the internal (brain - high-level control) and external feedback (biomechanical output) gains, respectively; $state_{HLC\ j}$ is stated as internal feedback coming from the *High-Level control* system onto the j^{th} joint, while y_0 is the vertical position of the torso within the $state_{BPD}$ vector stated as external feedback state given by the *Biped walker* system.

4.2.3.2 Phase modulation

Within the *Biped Walker* system, it is demonstrated in section 4.1.3 that the replication of the nominal reference trajectories by the biped system are far from optimum, due to inadequate PD controller parameters tuned in the *PD ref controller* by the author (see figure 4.7) [44].

Likewise, the values of the real trajectories assumed by the biped from the *state* vector are likely to be somewhat different from those generated by the CPG-based controller in the $state_{CPG}$ vector. Consecutively, the time the legs touch the ground may potentially not be the same for the controller and for the biped system. Furthermore, when some external perturbations are emerged, e.g. tilted surfaces, the controller and biped frequencies at which the legs reach the ground can be considerably different. In such cases, the biped and controller systems become potentially desynchronized which tends to lead to locomotion instability.

Those problems might be addressed by adjusting the phase of the states of the oscillators, so that entrainment of the CPG-based controller with the body dynamics of the biped system can be maintained through tight coupling between the two systems using feedback from the environment. Thus, the detection of the presence/absence of ground reaction forces F extracted from the load sensors can be used to modulate the phases of the oscillators and, consecutively, modify the nominal reference trajectories to effectively control the motion and postural stability of the biped. It should be recalled that the ground reaction forces F are closely related to the touch sensor vector S composed of the binary sensor values of the leg tip s_L and s_R which are equal to 1 as the respective leg reaches the ground and 0 otherwise. The S vector is thus provided as input signal for the CPG-based controller as external feedback within the $state_{BPD}$ vector. To this end, other authors have implemented the so-called *phase resetting* of the oscillators in recent works [28, 55, 66]. They have suggested that the phases of the oscillators should be reset on the swing-to-stance phase transition in case of a specified trajectory may deviate from the nominal trajectory depending on the timing of the touch sensor signals. However, here it is adopted a different approach based on the *phase modulation* of the oscillators applied on biped locomotion and originally implemented in quadrupeds [65]. According to the author [65], there should be included other situations in which the phases of the oscillators should be affected in specific ways, rather than just *resetting* them. The proposed *phase modulation* is thus thought to be more complete and to be more suitable to enhance the locomotion robustness.

The phase modulation of the oscillators presupposes the prior knowledge of the phase values (in polar coordinate) of the oscillators corresponding to the starting and ending phases of both swing and stance periods which are the reference values for which the phases of the oscillators should be adjusted in case of one of four conditions take place as follows:

1. Fast-transition modulation ($\sigma = 1$):

    - swing-to-stance in the unexpected presence of ground reaction forces during the

swing period;

- stance-to-swing in the unexpected absence of ground reaction forces during the stance period;

2. Stop-transition modulation ($ST = 1$):

   - swing-to-stance in case of ground reaction forces continuous absence;
   - stance-to-swing in case of ground reaction forces continuous incidence;

The fast-transition modulations are implemented in all oscillators of the leg where which the event occurs. For instance, at the time the left ground reaction forces are activated (meaning that the left leg tip has suddenly reached the ground, $S = [1\ s_R]$), the phase values of the oscillators should be modified to those established as reference for the beginning of the stance period if they are characteristic of the swing period. Conversely, supposing that left leg is in contact to the ground within the stance period, one should change the phase values of the oscillators to those of the swing period onset as soon as the foot leaves the ground ($S = [0\ s_R]$). Mathematically, it is used a fast-transition variable FT ($FT \in [\pm 400; 0]$), where 400 is pre-determined as a suitable perturbation value to obtain the maximal transition between two maximally distanced points of the $x - y$ state space (figure 4.20). As it will be mentioned in chapter 5, the simulation is run on continuous mode, although the data is collected within a specific sample time. Thus, the fast-transition perturbation factor is continuously added to the derivate states ($\dot{x}$,$\dot{y}$) within the defined sample time range. One can see an example on figure 4.20, where $x-$state is moved from one end of the limit cycle (0.9827) to the other (-0.9974) within the interval of 0.005 s, by continuously applying FT value of -400. In figure 4.21 is depicted the modification of the actual $x-$state value to a established target value of ≈ 0 within the same time period of the previous example. Pursuing this approach, one can attain the target state variable values to which the actual state variables should be modified, controlling the FT value according to the relation between the actual state and the target state established:

- $x_{actual} > x_{target}$: $FT = -400$;
- $x_{actual} < x_{target}$: $FT = +400$;
- $\left|x_{actual} - x_{target}\right| < 5e-4$: $FT = 0$.

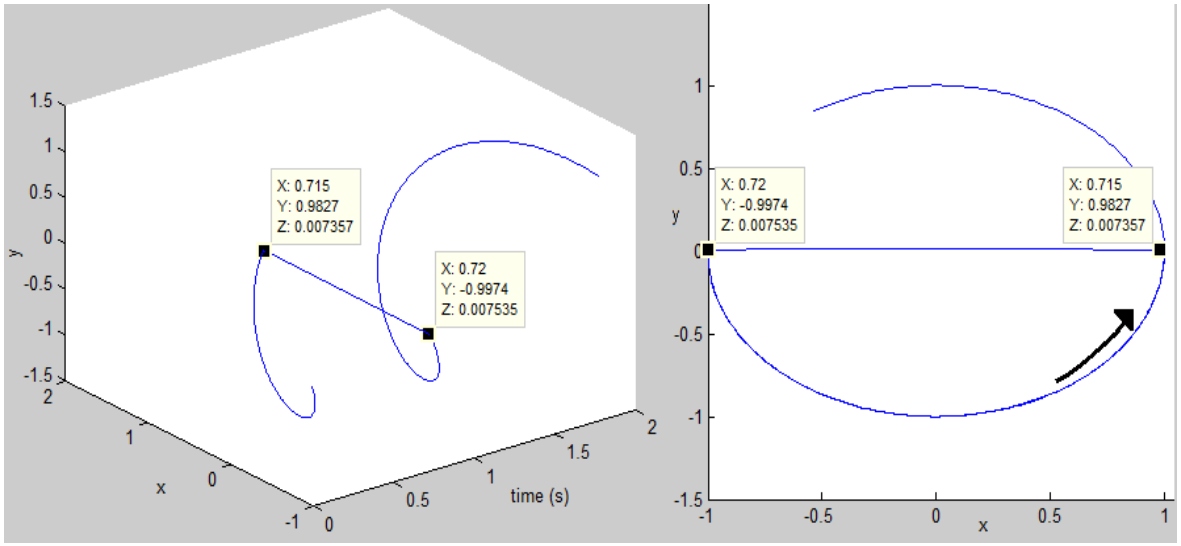

Figure 4.20: Limit cycle of a specific trajectory over time (left panel) and relating to the $x - y$ state space (right panel). A perturbation is applied to $x-$state using a FT value of -400 within $0.715 - 0.72$ s.

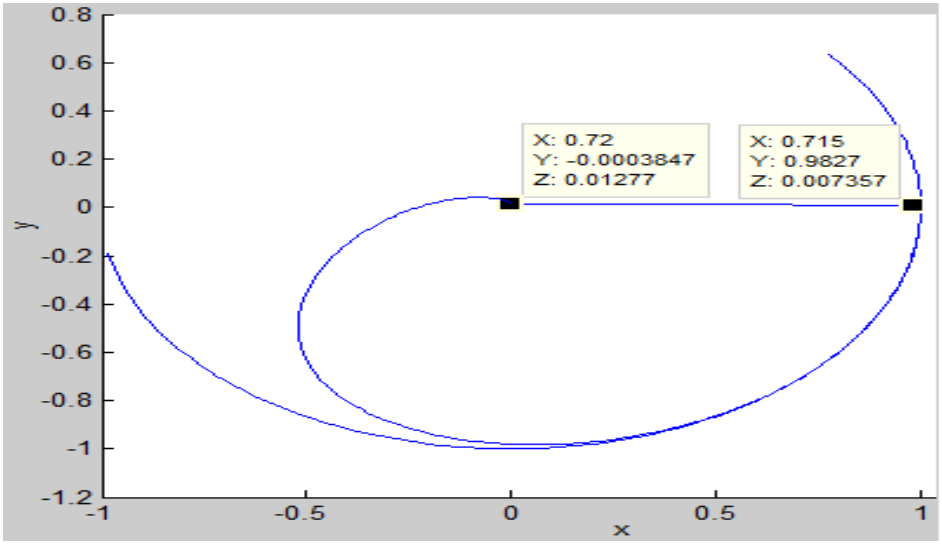

Figure 4.21: Limit cycle of a specific trajectory relating to the $x - y$ state space. A perturbation is applied to $x-$state, deviating its value to ≈ 0 within $0.715 - 0.72$ s.

The stop-transition modulations consist of maintaining the state variables of the oscillators (x, y) constant until the corresponding situation is activated. To this end, the output of the derivate states should be null. For instance, the phases of the oscillators characteristic of the left swing leg will be hindered of entering to the stance period cycle unless the ground reaction forces of the corresponding leg are triggered ($S = [0\ s_R]$). On the other hand, the oscillators are inhibited of entering to the swing period cycle whilst the left leg tip is still in contact to the ground and the ground reaction forces still activated ($S = [1\ s_R]$). It is thus included a stop-transition binary variable ST which assumes the value 1 if the event is

satisfied and 0 otherwise.

In this way, the derivate states of equations 4.14 and 4.15 are slightly modified to include the conditions of phase modulation described.

$$\dot{x}_i = \left(\dot{x}_{i(4.6)} + FT \cdot \sigma\right) \cdot (1 - ST) \tag{4.17}$$

$$\dot{y}_i = \left(\dot{y}_{i(4.7)} + FT \cdot \sigma\right) \cdot (1 - ST) \tag{4.18}$$

where σ is a binary variable which is equal to 1 if the condition is satisfied and 0 otherwise.

4.2.3.3 Postural stability

Besides the phase modulation, the biped COM information feedback is also important for postural stability maintenance during locomotion. A stable locomotion requires that the behavior of biped COM must be compatible, adequate and strictly related to the polygon of support and the feet motion described along the gait cycles. This feedback pathway is inspired by the behavior of the human before a tilted ground. For instance, supposing that a person is walking on a terrain with positive slope, if the tilt of the body is excessively backwards the person cannot have the required balance to take a step forward and, consecutively, falls to the backwards. The postural stability is critically challenged in the presence of tilted ground, so its control is of great importance. The COM of the biped system is thus provided as input signal for the *α-manual controller* block as external feedback within the $state_{BPD}$ vector (see figure 4.19).

Since the torso has superior mass comparing to those of the legs and knees, one may say that the biped COM is quite similar to the torso COM, i.e., the torso COM has a great influence of the biped COM. Therefore, it is proposed to control the α_{REF} trajectory (see figure 4.19) according to the biped COM state which will affect the torso angle trajectory α assumed by the biped system and, consecutively, the torso COM. In relation to the example case of the positive sloped floor aforementioned suggested, assuming the biped COM is excessively backwards (i.e., COM_x is too low) one should then enhance the α_{REF} signal so that the torso COM can also be increased as well as the biped COM.

Chapter 5

Methodology

5.1 Experimental setup

The experiments are performed in the *MatlabR*2009*b*®/*Simulink*® environment, although divided in two parts: firstly, the controller is applied to a mechanical orthosis and then to a biped model simulator.

Regarding the controller-orthosis experiments, a fixed step size of 0.001s is employed, in coherence with the orthosis controller's sampling frequency of 1kHz [191]. *xPC Target* is the real-time software environment employed to test the controller in real time by generating code with *Real-Time Workshop*. Endorsing the capability of the CPGs of generating rhythmic outputs for a multitude of tasks, one has applied the CPG controller to a mechanical orthosis to control a robot swinging task, so that real experiment results can validate the CPG control model.

With respect to the controller-biped model simulations, they are performed in continuous time, using the *ode45 (Dormand-Prince)* variable-step solver, like the solver type used in the biped model [44]. However, the controller and the biped system outputs are discretized using the *Zero-Order Hold* function block with a sample time of 0.005s. The goal is to study and address some locomotion stability challenges, including the scenarios with no feedback pathways (open-loop control), with external feedback only (closed-loop control without internal feedback), with internal feedback only (closed-loop control without external from environment and biomechanical system) and with both external and internal feedback (closed-loop control with voluntary modulation).

5.2 Experimental procedures

5.2.1 CPG-orthosis experiments

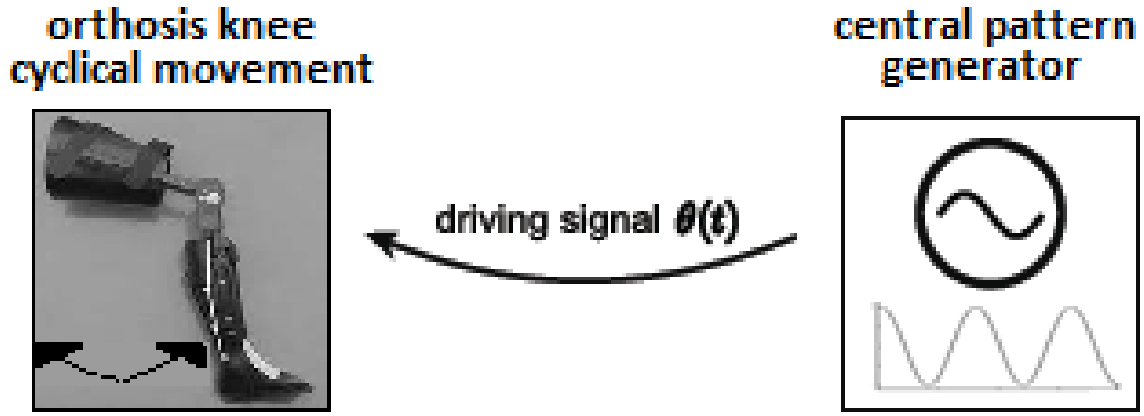

Figure 5.1: Sketch of the swinging task. The CPG generates the rhythmic signal to the controlled joint.

The experiments are elaborated in cooperation with the Bioengineering group from *CSIC* (*Consejo Superior de Investigaciónes Científicas*, Madrid), which has provided the opportunity of working with a recently developed orthosis [191]. The goals are to verify how the reference signal reproduced by the CPG-based controller is replicated as the real angle pattern by the mechanical system, what is the deviation from the reference input, and more importantly, if the stability is reached, i.e., to observe whether the CPG is capable to generate stable swinging motion with the correct frequency and phase when applied to a mechanical system. Moreover, experiments are made either on the orthosis controller based on the position (position controller) or on a controller based on the velocity (velocity controller), in order to test which situation respond in a more suitable fashion to the stimulating signal.

The open-loop CPG controller generates a 0.67Hz periodic signal of normalized amplitude range of 0-60°. This is the desired reference swing motion for the knee trajectory, similar to the knee flexion during the swing phase of healthy humans [192]. These experiments were only done in open-loop.

5.2.2 CPG-biped model in open-loop control

The purpose of this simulation is to implement stable and steady-state walking gaits through the correct design of joint nominal trajectories and interlimb coordination via phase relations among the oscillators. Concerning the problem of how each individual subject generates his

own walking gaits, it is also important to question how the neural drive of the biped system can learn its motion coordination without pre-specifying the response of the system.

To address this challenge, the employment of coupled adaptive frequency oscillators (AFOs) capable of learning arbitrary periodic signals in a supervised learning framework is endorsed [28]. AFOs can learn the walking trajectories characteristic of the biped system and reproduce them after the completion of the learning process. The hypothesis validation of neuromechanical entrainment between the CPG-based controller and the biomechanical systems may form the basis for the possibility of these artificial oscillators being synchronized to the biological oscillators located in the spinal cord of humans on the reproduction of stable walking patterns.

5.2.3 CPG-biped model in closed-loop control

Another theoretical assumption discussed in chapter 1 important for validation is that the spinal (automatic) and brain (voluntary) control are superposed or interact in a fashion way, by verifying the recovery of the system to a stable gait after the introduction of perturbations. To this purpose simulations are implemented in closed-loop, including internal and external feedback pathways. The sensory feedback feedback consists of sensory inputs not only for modulating the CPG trajectories, but also for creating entrainment of the controller with the body dynamics of the robot [55] and increasing postural balance stability [193].

The feasibility of applying the CPG controller is analyzed and the possibility of the CPG successfully implement realistic locomotion through periodic gaits is verified. These validations constitute the framework for a later work concerning the possibility of increasing the basin of stability of gaits and its robustness through the integration of sensory feedback as opposed to implementing an open-loop controller. In the following, the simulations with the different feedback pathways are explained.

The external feedback information such as the biomechanical state output and environment conditions are also crucial to locomotion robustness, since the brainstem can only actuate and give non-periodic descending commands if it receives environmental information. On the other hand, considering that the human CPG activity in the spinal cord can use the feedback from peripheral sensors, it is suggested that the external feedback may improve the gait features in addition to automatically control gait and respond to unexpected perturbations [194, 195].

A simulation concerns the assumption validation of the enhancement of the gait char-

acteristics by implementing external modulation of the CPG-controller through the external feedback delivery. This validation may partially conclude about potential benefits of implementing external feedback in contrast to a open-loop controller without the integration of feedback information [195]. To this effect, it is proposed the delivery of the torso vertical position information as feedback pathway onto the CPG-based controller.

With regards to the robustness and adaptation qualities characteristic of human locomotion, these skills are believed to be derived from the close interaction between the spinal CPGs and the brainstem which may share a hierarchical relationship for controlling and modulating the walking patterns. To this end, volitional commands from the brainstem are provided as internal perturbations to the CPGs to modulate temporarily their response and, after the cessation of the voluntary modulation period, the steady-state walking patterns should be recovered by the automatic control of the CPG-based controller.

Another simulation is performed to introduce internal perturbations for a sustained period of time on the right knee joint to verify the recovery of the system to a stable gait after that period.

The validation of the previous simulation can enable the simulation of more complex behaviors (reaction to perturbations) and the coordination of automated and voluntary control which can ultimately be relevant for therapy and/or assistance in further developments. The following simulations are performed to verify the implementation of voluntary modulation in a complementary manner through the integration of internal feedback to the CPG controller characterizing a voluntary and non-periodic movements: (1) walking on tilted ground; (2) walking on a terrain with obstacles.

5.3 Stability criteria

Taking into consideration that gait is one of the most common daily tasks and a significant proportion of falls occur during gait [196], an assessment of stability should be provided to predict the likelihood of someone falling or stumbling. The stability analysis may be very useful to give directions on finding connecting links between coordination hypothesis from dynamical systems (such as the CPG models) and mechanisms based in biomechanics and motor control. Furthermore, it can lead to novel hypotheses of control.

Gait stability can be static or dynamic. Static stability in human locomotion is considered to be attained whenever the center of mass (COM) of the body falls inside the convex hull of

the foot support area (generally known as support polygon) [197]. While in single-support phase the support polygon is equivalent to the area of the stance foot, in the double-support phase the support polygon is a convex hull delimited by the two feet. According to this concept, whether the COM is located outside the support polygon, the body is statically unstable and will fall [180].

However, in general animals at higher speed, gait is found to decrease the degree of static stability during certain parts of the gait cycle as the COM falls outside the polygon of support [180]. Human locomotion is thus not bound to the *static* concept of stability. At high gait speeds, dynamic stability does not impose the constraint of the COM to pass through the region covered by feet on the ground. During human normal walking, the double phase support constitutes only about 20 % of the cycle and as the walking speed increases, the period of double leg support decreases [198].

Full (2002) defines locomotor stability as the process by which state variables of the system (e.g., velocities, angles, positions) stay within a certain operation range according to which they are able to return to a steady-state, periodic gait after a disturbance [180]. There have been reported several methods of instability detection or prevention [199].

In this work, the *locomotor stability* concept is endorsed. Two methods for gait assessment are adopted, namely the stability based on upper-body motion measures and stability based on measures derived from dynamical systems theory.

5.3.1 Upper-body motion measures

The upper-body motion measures here adopted are the body COM position and the center of pressure (COP) beneath the foot (in this case, the foot of the biped system is merely the leg tip). Focus is given to how the COM position is related to the COP and the support polygon.

COP is considered the point on the support phase where the ground reaction forces total sum acts [200]. As introduced in section 4.1, two types of forces are exerted on a foot which model the walking surface: the normal (F_N) and tangential (F_T) ground reaction forces. Supposing that the foot cannot slide over the walking surface, the F_T forces are anulled remaining the F_N forces. The resultant total normal force (F_{RN}) is given by [200]:

$$F_{RN} = \sum_{i=1}^{n} F_{Ni} \tag{5.1}$$

The position of COP is determined as follows [200]:

$$COP = \frac{\sum_{i=1}^{n} p_{FNi} \cdot F_{Ni}}{F_{RN}} \tag{5.2}$$

where p_{FNi} is the position of the $i^{th} F_N$ force.

Regarding the biped COM, its determination depends on the COM positions of the segments [201]:

$$\begin{aligned} COM_x = [&(COM_{T\,x})(Mass_T) + (COM_{RTh\,x})(Mass_{RTh}) \\ &+ (COM_{LTh\,x})(Mass_{LTh}) + (COM_{RK\,x})(Mass_{RK}) \\ &+ (COM_{LK\,x})(Mass_{LK})]/Mass_{total} \end{aligned} \tag{5.3}$$

$$\begin{aligned} COM_y = [&\left(COM_{T\,y}\right)(Mass_T) + \left(COM_{RTh\,y}\right)(Mass_{RTh}) \\ &+ \left(COM_{LTh\,y}\right)(Mass_{LTh}) + \left(COM_{RK\,y}\right)(Mass_{RK}) \\ &+ \left(COM_{LK\,y}\right)(Mass_{LK})]/Mass_{total} \end{aligned} \tag{5.4}$$

where T is the torso, RTh is the right thigh, LTh is the left thigh, RK is the right knee and LK is the left knee. Let one understand by means of an example shown in figure 5.2 how the behavior described by the COM and COP should be related in a stable gait.

From figure 5.2 a single stride is simulated and there are depicted some upper-body motion measures, the COM_x and COP, in addition to the motion of the leg tips for the sake of clarity. Let one assume at the beginning of the simulation, for instance, that the stance leg tip (identified by the blue line) is from the front left leg and the swing leg tip (identified by green line) refers to the rear right leg. Until the COP (represented by the magenta line) equals the left stance leg tip, this gait period corresponds to the double support phase (DSP) in which both leg tips are in contact to the ground.

As soon as COP reaches the stance leg tip, DSP period is ended and the single support phase (SSP) period begins, in which the rear right leg tip starts to move in order to promote a step forward. Equal values of COP and of the stance leg means that the COP is entirely settle on a single foot in contact to the ground. When the green line has just crossed the blue line (around sample 101), the right swing leg tip, initially the rear leg tip, has now become the front leg because it has longitudinally surpassed the stance leg tip. As soon as the front

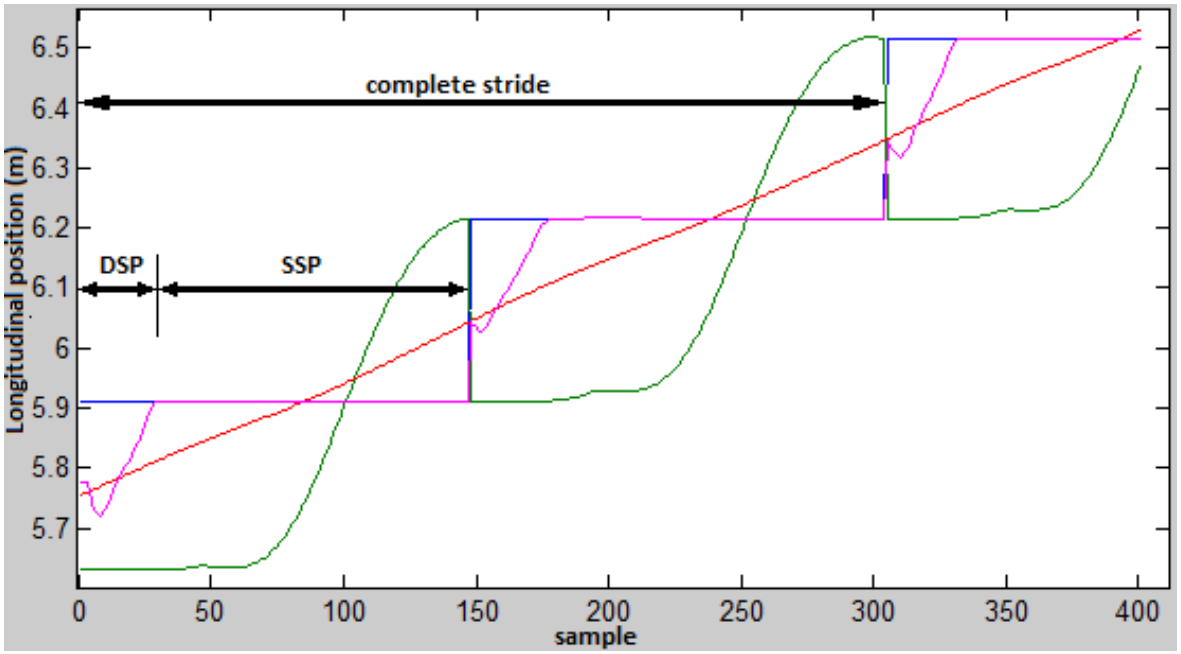

Figure 5.2: Stability analysis through the method of upper-body motion measure of a gait pattern characterized as the normal walking gait on even ground. The behavior of the COP (magenta line), COM_x (red line), stance leg tip (blue line) and swing leg tip (green line) is described. A single stride is simulated including the double support phase (DSP) and the single support phase (SSP).

right swing leg tip reaches the ground (sample 148), the SSP is finished and DSP starts again. In this case the blue line represents now the front right stance leg tip, while the green line represents the rear left swing leg tip. From sample 0 to approximately 305 two steps are performed completing thus a stride or gait cycle.

Concerning the COM_x (represented by the red line), it is during the DSP period falling inside the support polygon delimited by the two stance leg tips, while in the SSP period the support polygon is merely the $x-$position of the stance leg tip and the COM_x is located outside the support polygon, crossing the support polygon in the middle of the SSP (see for instance samples 85 and 239). As one can observe, the behavior of the COM_x is consistent over the 2-3 step periods.

Therefore, in the presence of a sequence of stable strides and in the absence of large perturbations, each stride should be an approximate mapping of the stride described in the figure above.

5.3.2 Measures derived from dynamical system theory

A strategy based on the detection of any type of gait perturbation in limit cycle walkers is from [29, 202]. CPGs can encode rhythmic trajectories as limit cycles of coupled nonlinear

oscillators systems which enable the perturbations being quickly forgotten and the system returning to the limit cycle after a short transient period [187]. The detection whether a biped system is undergoing a perturbation which may lead to a fall or a stumble is dependent on the effective estimation of the system being inside or outside the basin of attraction (i.e., a region in the state space that envelopes the limit cycle).

Therefore, the proposed algorithm for instability detection is characterized by the deviation estimation between the real and the expected biped system state. The algorithm named *The Nearest Neighbor Gait Index* (NNGI) is aimed to find the degree of deviation of the biped system to its limit cycle by observing the real state assumed by the biped and is based on a normal walking pattern called *Reference Limit Cycle* (RLC). It is first determined the state in the RLC that best can match the real state of the biped system and it is subsequently calculated the weighted deviation between the expected and the real states. The weighted deviation can quantify the distance of the biped system with respect to the normal gait.

The NNGI algorithm is thus developed in three stages: the definition of the RLC; the selection of a set of candidate states in the RLC (neighbors); determination of the nearest neighbor (NN). The RLC, considered to describe a normal gait, is defined offline and represented by the stable, steady-state walking trajectories exhibited in closed-loop control (feedback is integrated). RLC is determined taking into account the interaction with the environment. It is obtained as the mean trajectory of the three joint angles and velocities ($\Delta\beta$, $\dot{\Delta\beta}$, γ_L,$\dot{\gamma_L}$, γ_R, $\dot{\gamma_R}$) after the normalization to stride percentage and the mean stride duration determination.

In relation to the set of candidate neighbors, one may argue that in absence of effective perturbations the current real state of the biped system at time t is most likely to be within the interval of states around the expected state in the RLC at time t and is likely to deviate considerably from the referred interval in the presence of a quite large perturbation. According to the author [202], the interval length is manually tuned and an excessively long interval of candidates may not detect perturbations effectively. Nonetheless, by finding the state that best represents the current state of the biped in the selected set of candidates rather than finding in the complete RLC enables the reduction of computational burden.

Concerning the NN determination, the *Nearest Neighbor* method is based on finding the closest candidate state similar to the real state. The closest candidate within the interval or the NN is defined as the least Euclidean distance in the state space.

Once the NNGI algorithm is complete with the NN determination, the deviation from

normal walking is calculated. The deviation measurement is based on the weighted deviation (D-statistic) proposed in [203]. It consists of the squared error between the expected state in the RLC and real state of the biped weighed by the standard deviation at a specified instant and variable which can quantify the variability of a given variable during normal gait. To see the equations involved, please refer to [29]. For the sake of clarity, an example is provided as follows (figure 5.3).

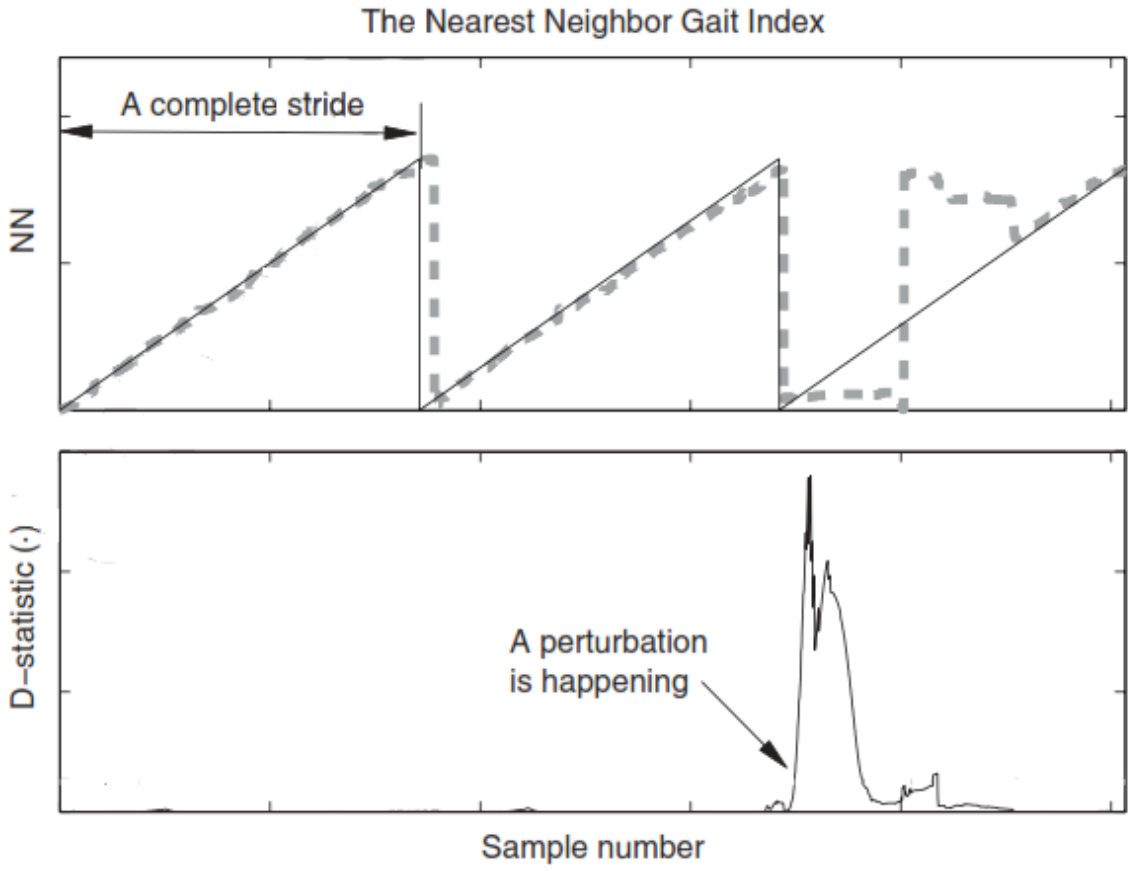

Figure 5.3: The NN and the D-statistic determination [29].

From figure 5.3 it can be observed in the upper panel the NN (gray dashed line) and the RLC (black solid line), while in the lower panel it is indicated the D-statistic. Basically, if the NN can follow in a neighborhood the RLC, one can assume the biped system is performing a stable walking, as illustrated in the first two strides. Conversely, a sufficiently large perturbation undergone in the third stride is the cause of triggering a substantial deviation of the NN from the RLC, suggesting that the biped system is further way from its limit cycle and from the normal gait.

While the former method of stability measure is more suitable to verify the stability of the biped during the total simulation, the latter is more adequate to observe whether the

system will continue walking stably or will become unstable after the detection of a perturbation event. Furthermore, one can inspect how and why the biped may fall by considering the upper-body motion measures, due to the close relationship between the COM and COP behaviors during each stride.

Chapter 6

Results and discussion

Results from hardware tests and numerical simulations are presented and discussed in this section. While the minor part of the work concerns the simulation of the coupling between the CPG controller and a mechanical orthosis, the majority of the simulations relates to the coupling of the referred controller to the biped model described in chapter 4.

6.1 CPG-orthosis in open-loop control experiment

Experiments are made either on a controller based on the position (position controller) or on a controller based on the velocity (velocity controller), in order to test which situation respond in a more suitable fashion to the stimulating signal from the CPG system, an open-loop controller responsible for the generation of a sinusoidal signal of 0.67 Hz with an amplitude range of 0-60 degrees. The main objectives of this experiment are described in section 5.2.1.

In figure 6.1 it is illustrated the generation of the reference trajectory derived from the CPG controller in addition to the real trajectory produced by the orthosis velocity controller.

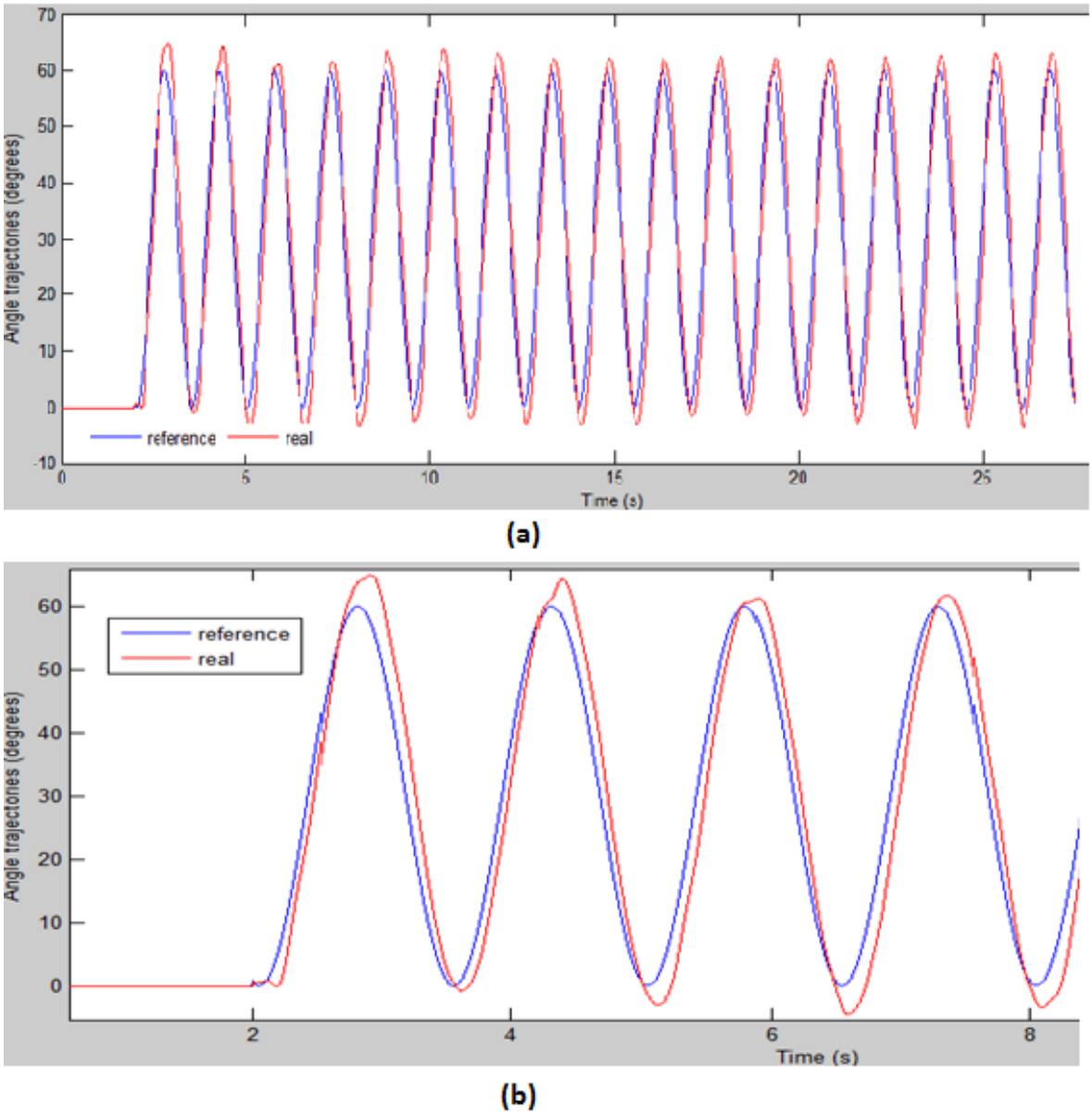

Figure 6.1: The CPG reference input (blue) and the real angle pattern (red) trajectories when using the orthosis velocity controller. (a) total time simulation; (b) focus on the initial stage of the simulation.

As one can see, in general the real angle pattern is characterized by the evidence of a certain instability over time as one assists to permanent oscillations of the real amplitude (figure 6.1 (a)). Furthermore, the real trajectory overshoot in relation to the reference is somewhat notable which can be translated on a quite perceptibly significant percentage error. See, for instance, the overshoot immediately after 2 and 5 s (figure 6.1 (b)). Moreover, one could notice that the response of the orthosis velocity controller illustrated in the previous figure was very probably the best response the controller could provide after several trials. Most of the time was spent on tuning the control gain parameters (Kp, Ki, Kd and Kff)

included in the velocity controller to find a response of adequate velocity and efficiency (for more specifications about the gain parameters and control scheme, refer to [191]). To this contribution, considerable efforts and time consuming were made since the tuning of the control gains in a close-loop velocity controller tended to bring some complexity.

In figure 6.2 it is depicted the generation of the reference trajectory derived from the CPG controller in addition to the real trajectory demonstrated by the orthosis position controller.

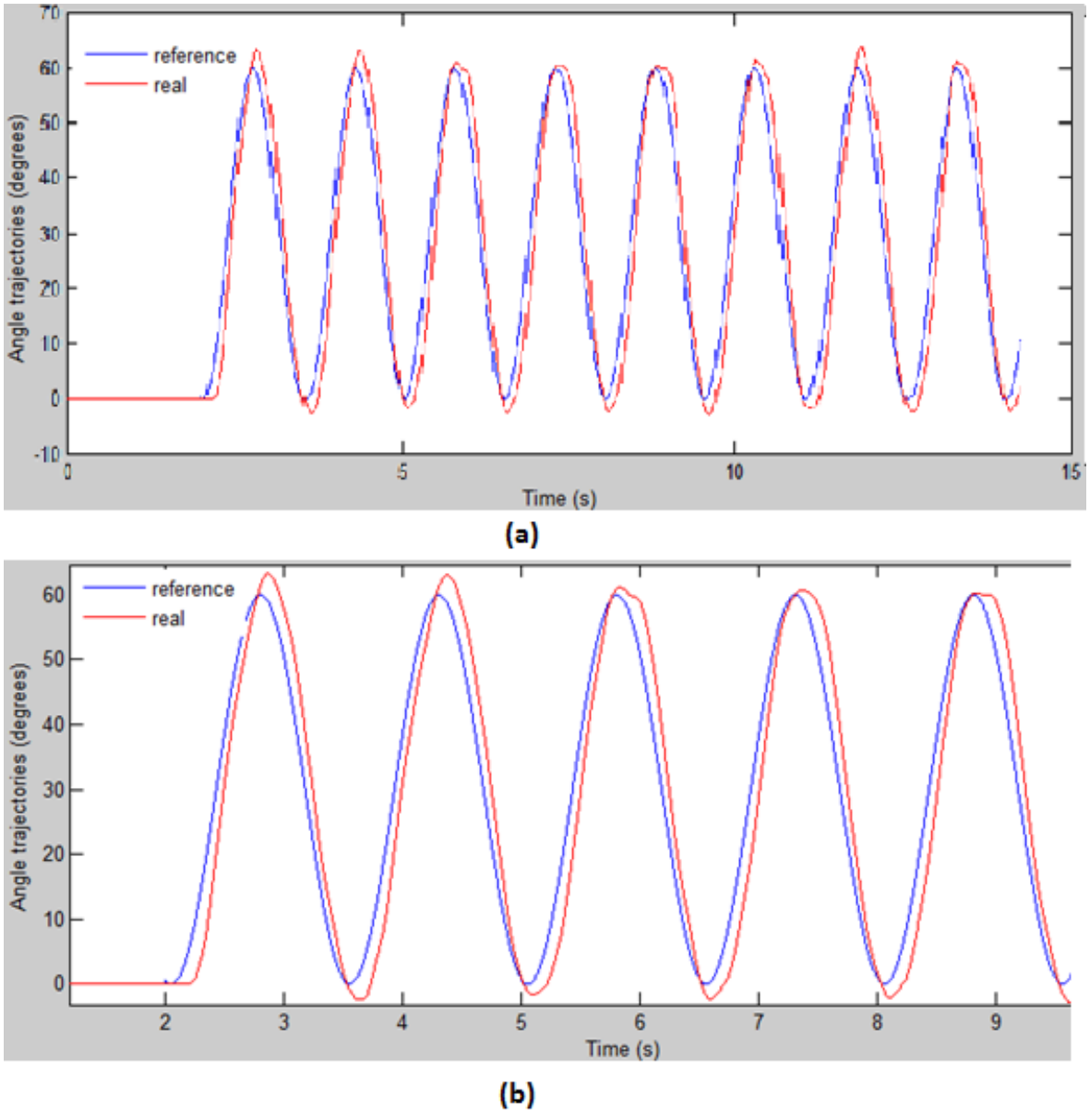

Figure 6.2: The CPG reference input (blue) and the real angle pattern (red) trajectories when using the orthosis position controller. (a) total time simulation; (b) focus on the initial stage of the simulation.

In comparison with the velocity controller, in general the real angle pattern is marked by lower instability over time as one assists to less oscillations of the real amplitude (figure 6.2

(a)). Furthermore, the real trajectory overshoot in relation to the reference is generally inferior confronting to that when using the velocity controller and, consecutively, the percentage error from the reference is also lower. See, for instance, the low upper overshoot closer to 6, 7.5 and 9.0 s (figure 6.2 (b)). Moreover, one could notice that the controller response illustrated in the previous figure was very probably the best response the controller could provide. Unlike the velocity controller, the time spending on tuning the control gain values (Kp, Ki, Kd) to find a response of suitable velocity and efficiency was manifestly lower. To this contribution, less efforts and time consuming were made since the tuning of the control gains in a open-loop position controller tended to be less complex.

Finally, one last experiment was made to both controllers on testing the behavior of the system in front of a specific perturbation which was produced by providing some resistance to the swing motion of the mechanical system with the help of human hands. That action has promoted serious repercussions either on the real angle velocity or on the deviation from the reference input. The reason by which the system detains after the perturbation can possibly be the saturation of the motor controller, according to the developer of the orthosis [191]. Those saturations can be probably related to an excessive amount of torque given to the motor. This situation showed that the integrated system in open-loop is very sensible to perturbations from environment.

Having compared the outcomes of the two approaches, one can argue that the position controller could provide somewhat better response, lower overshoot, better stability and a more feasibility of its parameters tuning. The reason by which the system has not followed exactly the path given by the CPG may be due to not having attained a better adjustment of the PID control and also due to inherent limitations of the entire hardware. Conversely, the ability of the CPG controller to generate synchronously with the mechanical system stable swinging motion with the correct frequency and phase is confirmed.

6.2 CPG-biped model in open-loop control

The feasibility of the CPG controller to generate stable and steady-state joint trajectories when coupled to a biped model and to demonstrate neuromechanical entrainment is here verified. The control is implemented in open-loop, i.e., without the feedback of sensory information integration representing thus the most basic scheme of control. The internal (g_i) and external (g_e) feedback gains are therefore null. Focus is given to observe whether

the controller can independently generate the nominal reference trajectories to control the biped system on a normal even ground without the presence of any perturbations. In order to learn the desired reference trajectories for further reproduction, it was proposed a process wherefore the frequency analysis through a dynamical system was possible by using a system of coupled AFOs, implying a continuous refinement of the CPG tuning parameters for the acquirement and improving of the learning process (see section 4.2.1). To observe the outcomes of the learning process of the reference signals, refer to figures 4.16-4.18.

Figure 6.3 demonstrates the generation of the reference trajectories derived from the CPG controller and the real trajectories reproduced by the biomechanical system.

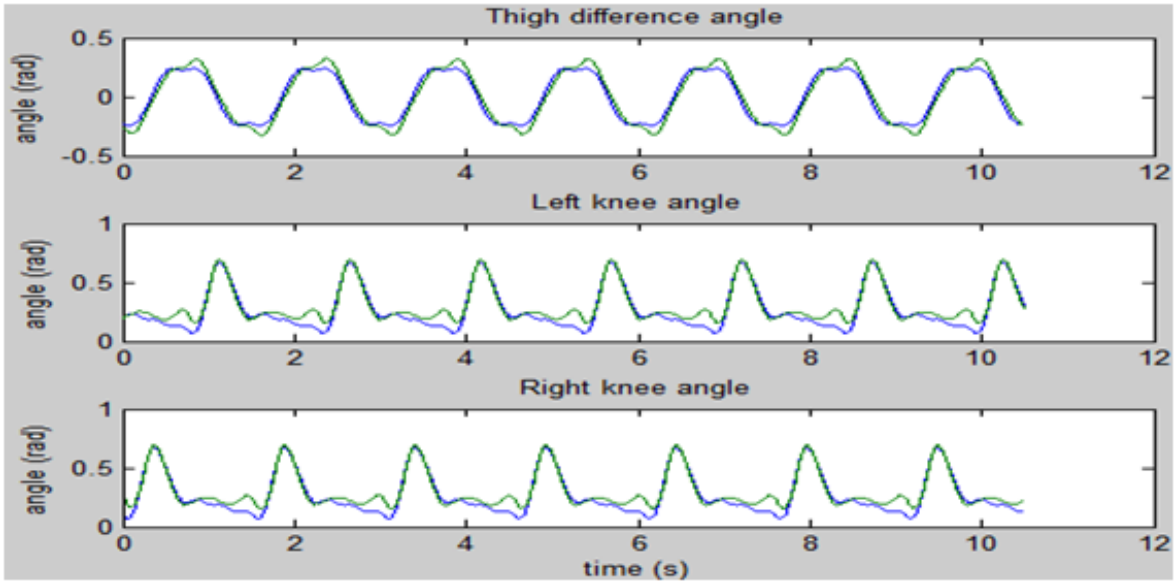

Figure 6.3: Comparison between the CPG reference (blue) and the biped system real (green) trajectories. $\Delta\beta$, γ_L and γ_R signals are plotted at the top, middle, bottom, respectively.

In figure 6.3 it is observed the attainment of stable periodic trajectories, what can be translated on the correct design of the joint nominal trajectories through the phases of the nonlinear oscillators and on the successful interlimb coordination through the phase relation among the oscillators. Likewise, the biomechanical system reproduces also stable real trajectories synchronously with the reference signals, although one can also see that the nominal reference trajectories are not perfectly replicated by the biped system onto real trajectories. This problem is related to the gain parameters hand-tuning in the *PD ref controller* (see section 4.1.3 for more details). A stable periodic gait is then achieved by the biped system, whereby the spinal CPGs can provide the basic control units required to promote automatic locomotion.

6.3 CPG-biped model in closed-loop control

The control scheme in closed-loop includes the integration of feedback pathways, both internal and external, from the brainstem and the spinal cord, respectively. Like in the human behavior, the biped system should produce stable gaits of long distances automatically and efficiently yet adaptable to changes in the environment.

6.3.1 External modulation

The external modulation of the CPG-based controller is characterized by the integration of external sensory feedback, as explained in chapter 5. Other authors have already suggested some improvements on the gait features by including external feedback to modulate the response of the controller [190, 194, 195]. The following simulation consists of the verification of the enhancement of the gait characteristics by providing the information of the vertical position of the torso as external feedback signal onto the CPG controller. Figures 6.4-6.6 illustrate the limit cycle described by the biped COM_y for posture stability analysis and further comparison without and with the feedback signal.

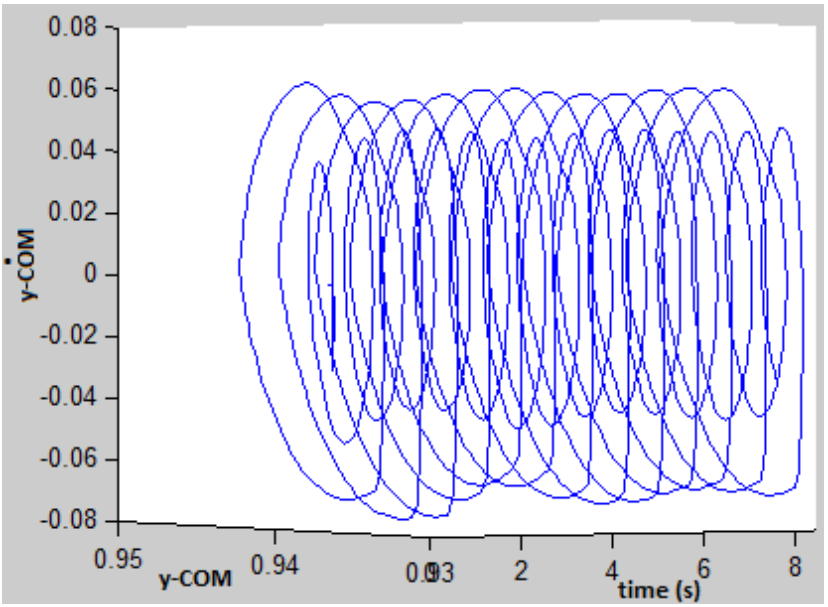

Figure 6.4: Mechanical system amplitude oscillations of the stable oscillatory regime described by the biped COM without the integration of the feedback signal.

From figures 6.4-6.6 there are observed mechanical system oscillations characteristic of a stable limit cycle over time, stated as a *tunnel* in the 3D plot. This graph type enables also the observation of possible mechanical DC drifts, translating an assessment of

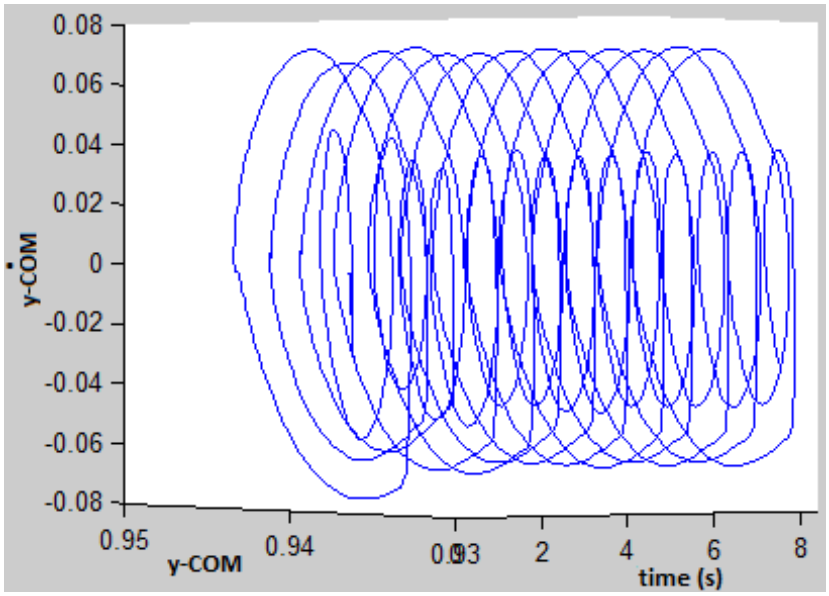

Figure 6.5: Mechanical system amplitude oscillations of the stable oscillatory regime described by the biped COM with the integration of the feedback signal and feedback gain $g_e = 1.0$.

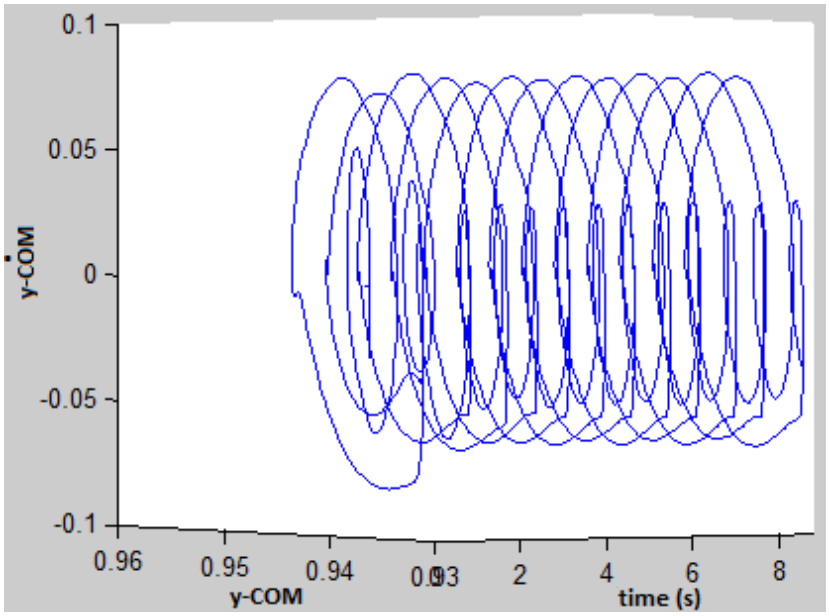

Figure 6.6: Mechanical system amplitude oscillations of the stable oscillatory regime described by the biped COM with the integration of the feedback signal and feedback gain $g_e = 2.0$.

the entrainment *quality* [190]. In this respect, one can see slight DC drifts throughout the mechanical system oscillations in the absence of external feedback suggesting the exhibition of suboptimal entrainment (figure 6.4). Conversely, when the external feedback is available, there are apparently no DC drifts or at least are less pronounced after the fifth (figure 6.5) and third (figure 6.6) oscillation periods. The quality of neuromechanical entrainment is therefore somewhat better in the two latter cases. Furthermore, in both cases of feedback

integration (figures 6.5 and 6.6), a better stable oscillatory regime is found, faster steady-state oscillations are attained (after the fifth and third oscillation periods, respectively) and larger steady-state oscillation amplitudes (without feedback: $y - COM \in [0.9345 - 0.9435]$ $y - \dot{COM} \in [-0.06929 - 0.06125]$; $g_e = 1$: $y - COM \in [0.9340 - 0.9446]$ $y - \dot{COM} \in [-0.06693 - 0.07219]$; $g_e = 2$: $y - COM \in [0.9335 - 0.9455]$ $y - \dot{COM} \in [-0.06608 - 0.08229]$) are observed (refer to Appendix C). These observations demonstrating a better stability nature are in agreement with the arguments favoring the inclusion of sensory feedback highlighted in [190]. By using $g_e = 2.0$ from figure 6.6, the largest oscillation amplitudes are achieved as well as the transient regime to the steady-state is the fastest.

On the other hand, one has achieved higher walking speed and stride length with the integration of external feedback (without feedback - *mean velocity* = 0.384135, *mean stride length* = 0.573323; $g_e = 1.0$ - *mean velocity* = 0.402367, *mean stride length* = 0.599645; $g_e = 2.0$ - *mean velocity* = 0.413062, *mean stride length* = 0.615063) (refer to Appendix C). Inclusively, the highest values are obtained by using $g_e = 2.0$. These results are very interesting, since noticeable increases in walking speed and stride length translate the good neuromechanical entrainment of the oscillators to the feedback signal and to the natural dynamics of the mechanical system. However, the gait asymmetry is also higher when providing $g_e = 2.0$ and lower without the feedback signal (without feedback - *asymmetry error* = $3.22016E-06$; $g_e = 1.0$ - *asymmetry error* = $3.41513E-05$; $g_e = 2.0$ - *asymmetry error* = $2.40959E-03$) (refer to Appendix C). Due to the fact that gait asymmetry compromises the naturalness of movements, one has decided to select $g_e = 1.0$ as the best feedback gain since it can enhance some gait characteristics likewise and the asymmetry error is rather small and may be thus disregarded. These outcomes may partially conclude about potential benefits of implementing external feedback in contrast to a open-loop controller without the integration of feedback information.

Let one observe the periodic gait attained by providing the vertical position of torso feedback to modulate the response of the controller depicted in figure 6.7. From figure 6.7, one may argue that the feasibility of applying the CPG controller as the source of reference input trajectories while being modulated according to the mechanical output state (in this case, vertical position of torso) during locomotion is verified, due to the evidence of longitudinal stability observed throughout the gait. The possibility of the CPG thus successfully implement realistic locomotion through periodic gaits is ensured. The spinal CPGs have proved

to be able to use feedback to automatically control gait. This control scheme simulates, for instance, a human taking long walks on even ground without being aware he is walking. Moreover, improvements on the gait features such as higher mean walking velocity and step length while ensuring the production of natural walking movements is one of the contributions of this work.

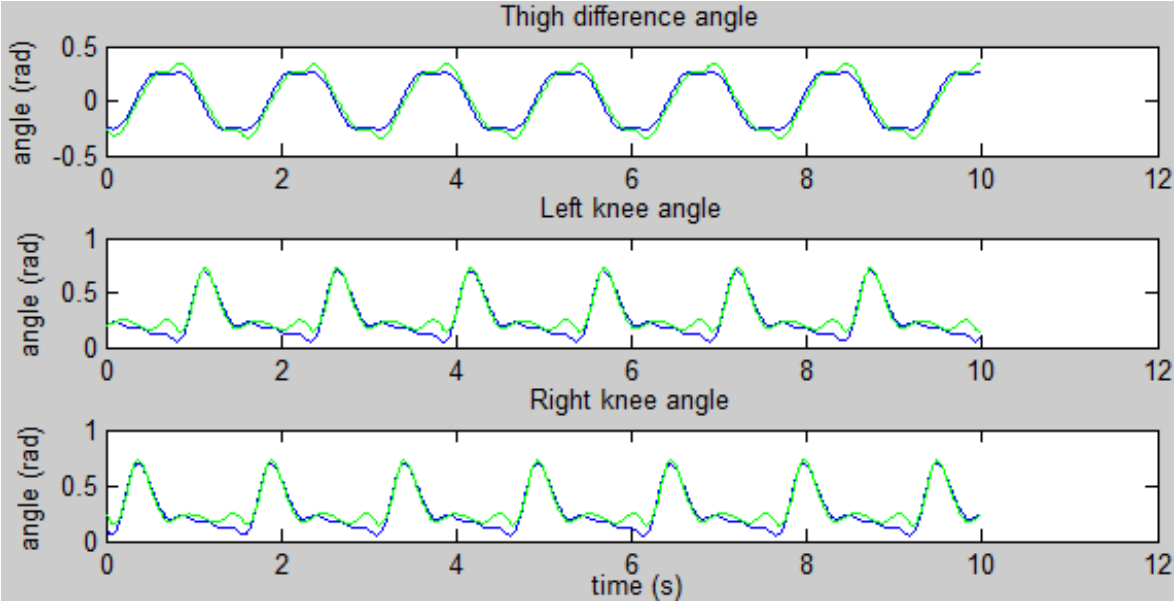

Figure 6.7: Comparison between the CPG reference (blue) and the biped system real (green) trajectories. $\Delta\beta$, γ_L and γ_R signals are plotted at the top, middle, bottom, respectively.

The stability of the locomotion on even ground with the inclusion of sensory feedback presented in the figure above is depicted on the figures 6.8 and 6.9 according to the two adopted stability criteria (see section 5.3 for details).

It is illustrated in the upper panel of figure 6.8 that the NN follows in the neighborhood the RLC throughout the simulation (around six strides), what translates strong evidence of stability. In the lower panel, one can observe that the maximum weighted distance between the expected state in the RLC and real state assumed by the biped does not exceed the value of 200. This deviation can be considered negligible, taking into account the deviation values of about hundred million (10^8) caused by the introduction of internal perturbations to simulate voluntary movements (see for instance figure 6.24). One thought that the normal walking pattern or the RLC should be represented by the walking trajectories produced in close-loop control with external feedback integration rather than be represented by the walking trajectories generated in open-loop control. One believes that the basic human locomotion on even ground at long distances, which implies an automatic control from the spinal cord,

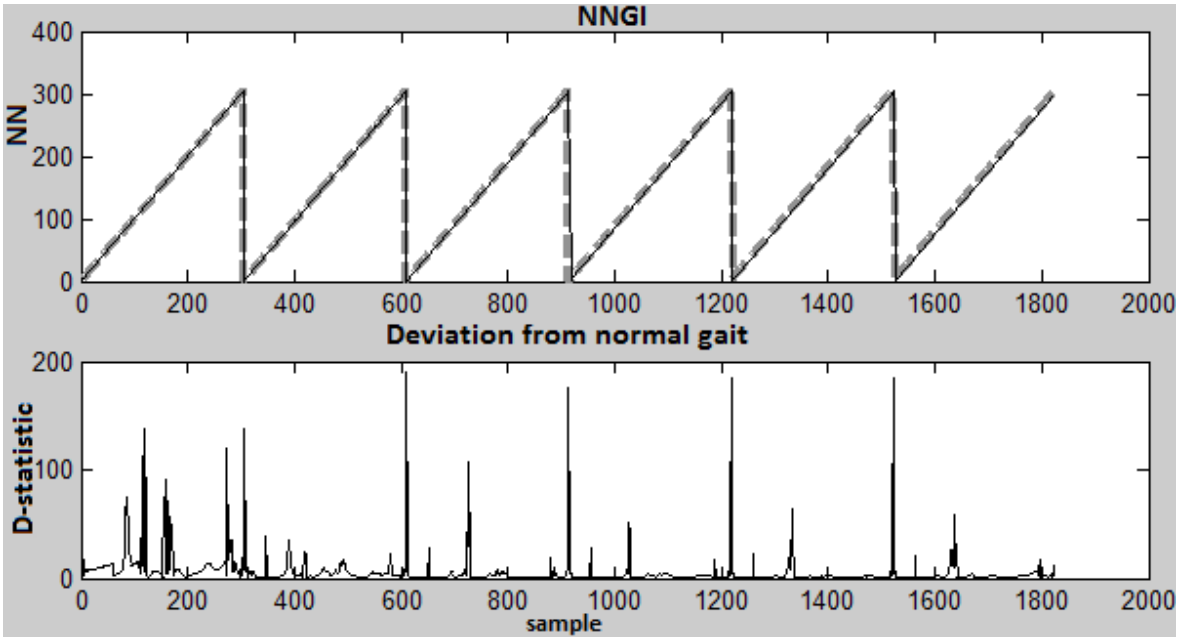

Figure 6.8: Stability analysis through the NNGI method of the locomotion characterized as a normal walking gait on even ground. The NN (gray dashed line) and the RLC (black solid line) are illustrated in the upper panel; the bottom panel shows the D-statistic (solid line).

is composed of a series of stable strides with small disturbances whose intensity is sufficient high to cause variability among strides and low enough to maintain the body stability so that the human collapse is prevented. So, concerning the normal walking in the absence of large perturbations, each stride is almost an exact mapping of the previous one as depicted in the upper panel. Thus, the control scheme of the CPG-base controller should be sensitive to external information by including external feedback, unlike the control scheme of the open-loop controller.

From figure 6.9, COM_x and COP in addition to the motion of the leg tips are depicted for the sake of clarity. On the right panel it is observed within a single stride the motions of the several measures characteristic of a stable stride, according to theory explained in section 5.3.1. Furthermore, on the left panel it is indicated the same behavior over several strides, by which each stride is an approximate mapping of the previous one, demonstrating evidence of stability throughout the simulation.

6.3.2 Internal modulation

The simulation consists of introducing internal perturbations representing the internal descending commands from the brainstem to the spinal CPGs for a sustained period of time around 300-500 ms on the right knee joint on three different moments, namely in the early

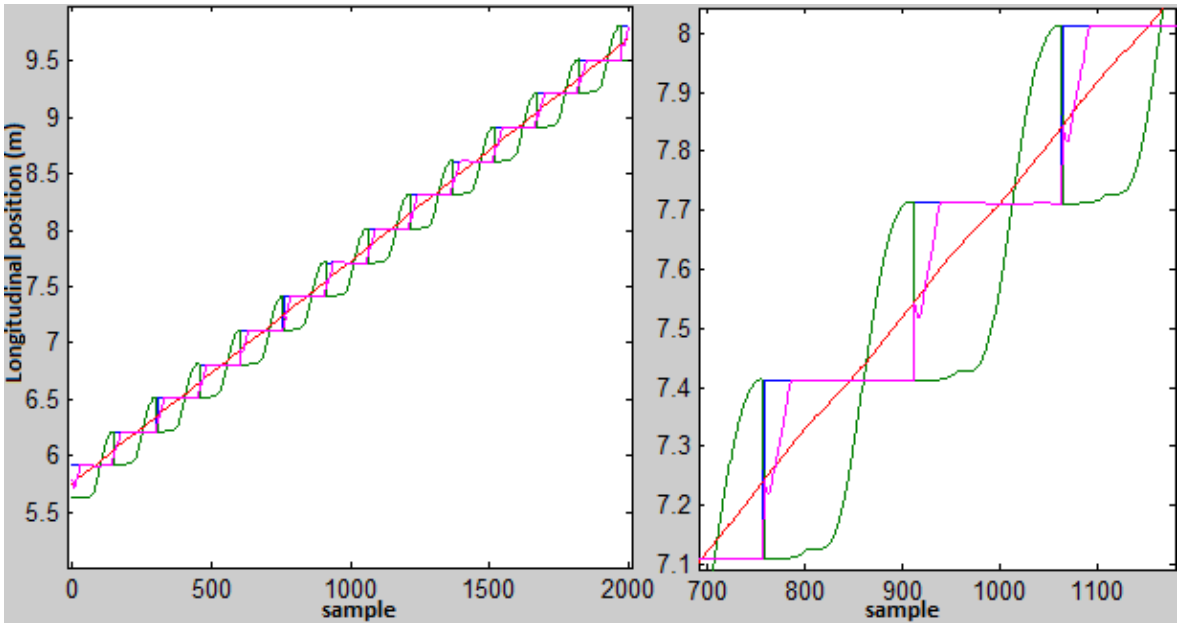

Figure 6.9: Stability analysis through the method of upper-body motion measure of the locomotion characterized as a normal walking gait on even ground. The behavior of the COP (magenta line), COM_x (red line), stance leg tip (blue line) and swing leg tip (green line) is described throughout the total simulation (on the left panel) and during a single stride (on the right panel) for greater clarity and insight.

swing, late swing and stance phases. The evidence of stability after the internal perturbation events under different periods is exhibited in figures 6.10-6.12 in addition to a comparison of how the system has evolved and adapted under those different situations.

Comparing the three cases of internal perturbation employment in the early swing, late swing and in the stance phase (figures 6.10-6.12), one can argue that the total system could reach stability in several ways, presenting different adaptation modes according to the moment when the internal perturbation is applied. From the top panels of (a), one can observe that during the perturbation period a significant deviation of the NN from the RLC has occurred suggesting that the biped system has moved way from its limit cycle and from the normal gait.

Nonetheless, the biped system returns to its limit cycle characteristic of the normal gait after the perturbation period by tracking in the neighborhood the RLC. One can thus assume the performance of a stable gait. From the bottom panels of (a), there are illustrated the occurrence of perturbations translated on substantial error margins between the the expected state in the RLC and real state assumed by the biped and, consequently, on critical deviations from the normal walking. In relation to (b), in all cases the limit cycles have demonstrated stable oscillations by a relatively faster steady-state regime. The situation conferring more evidence of stability with faster steady state achievement is the perturbation in the early

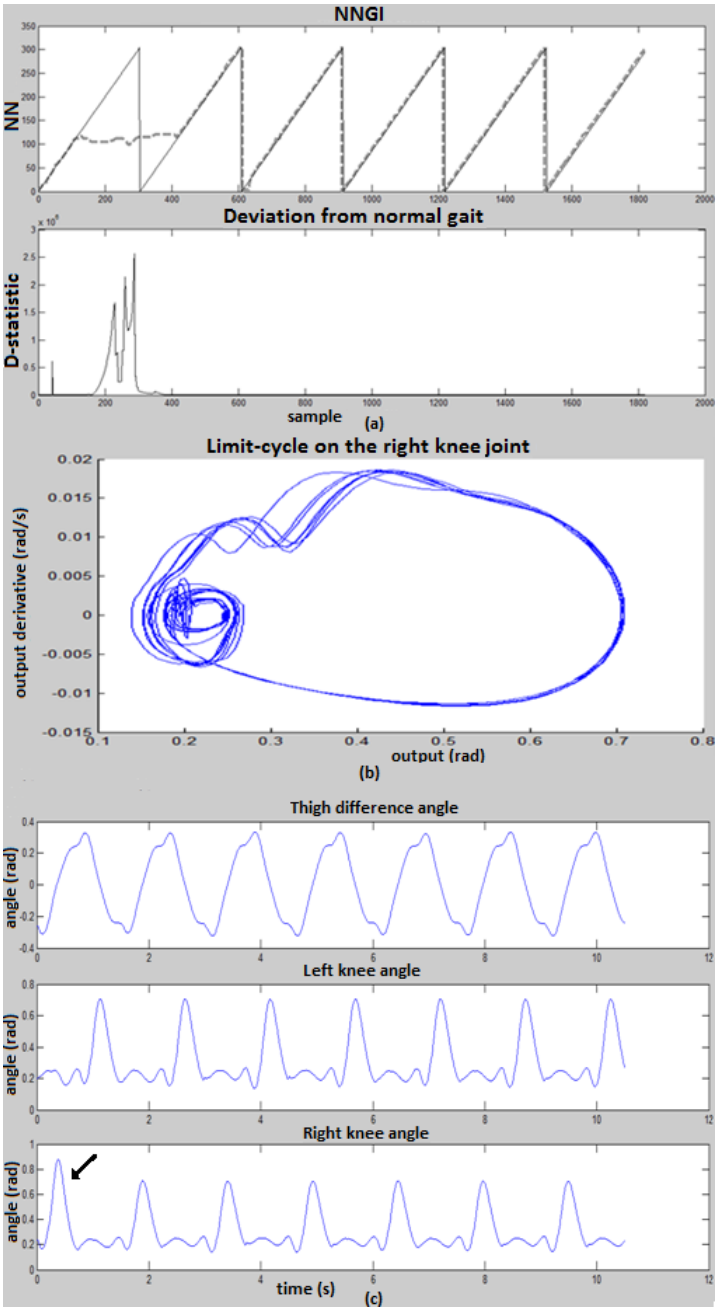

Figure 6.10: Stability analysis of the locomotion under the application of an internal perturbation in the early swing (0.245- 0.745 s). (a) The NN (dashed line) and the RLC (solid line) are illustrated in the upper panel; the bottom panel shows the D-statistic (solid line). (b) The resultant limit cycle of the right knee joint is displayed. (c) The real trajectories assumed by the biped system.

swing. Conversely, the perturbation in the stance phase is the situation causing less evidence of stability with some glitches during the transient phase. Concerning (c), in all figures it is noticeable a slight alteration on the right knee angular trajectory at the time the perturbations are applied.

However, these differences in stability may be disregarded since in all situations strong

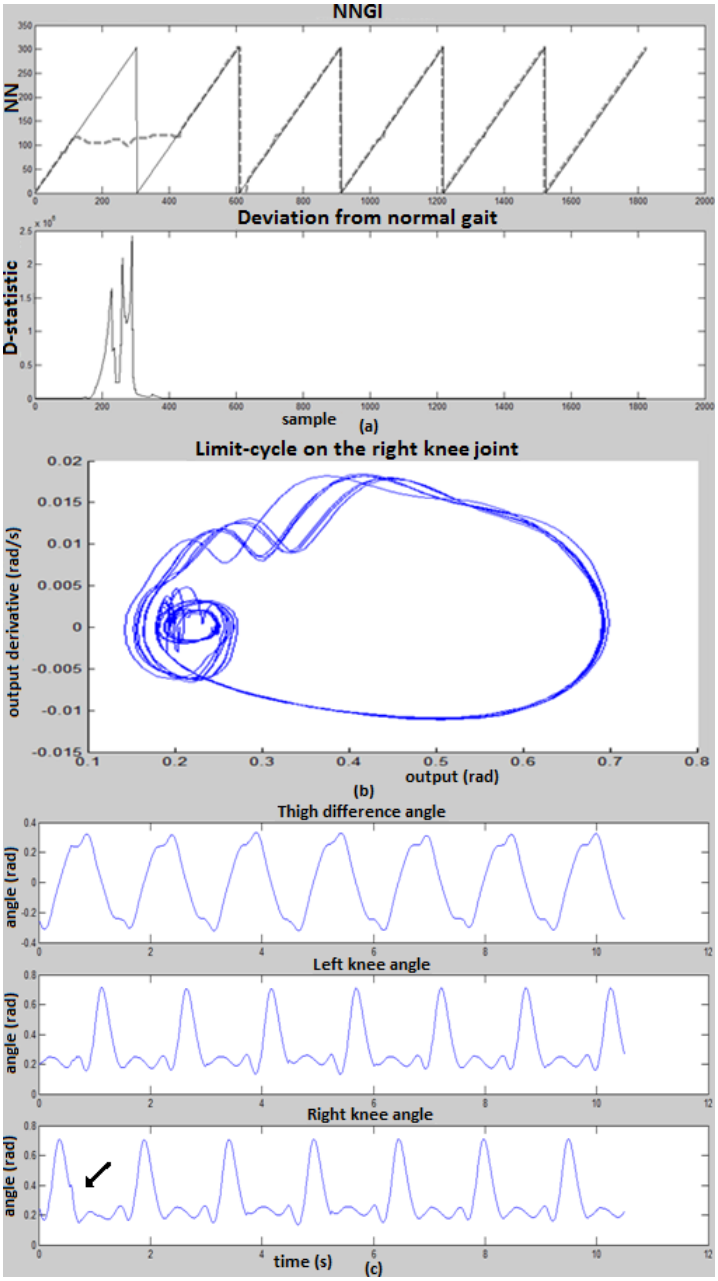

Figure 6.11: Stability analysis of the locomotion under the application of an internal perturbation in the late swing (0.535- 1.035 s). (a) The NN (dashed line) and the RLC (solid line) are illustrated in the upper panel; the bottom panel shows the D-statistic (solid line). (b) The resultant limit cycle of the right knee joint is displayed. (c) The real trajectories assumed by the biped system.

evidence of gait stability is demonstrated. Moreover, the different adaptation modes observed are in agreement to the foundation that the responses of adaptation cannot be stereotyped due to the variation of motor output and biomechanical conditions at different moments of the step cycle [194].

The neural system has manifested to reach neuromechanical entrainment and to be able to sustain stable oscillations moving away from its initial conditions very quickly, to attain

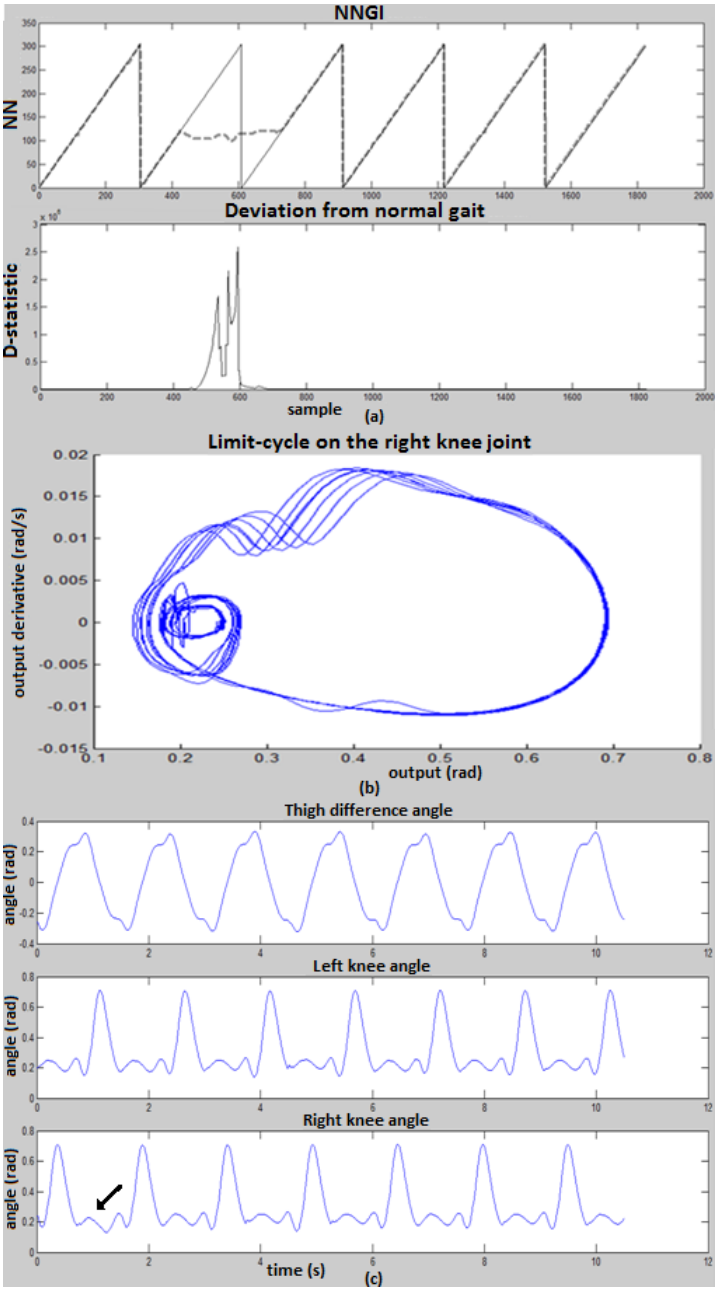

Figure 6.12: Stability analysis of the locomotion under the application of an internal perturbation in the stance phase (0.735- 1.235 s). (a) The NN (dashed line) and the RLC (solid line) are illustrated in the upper panel; the bottom panel shows the D-statistic (solid line). (b) The resultant limit cycle of the right knee joint is displayed. (c) The real trajectories assumed by the biped system.

relatively faster the steady-state, to present negligible glitches in the biped outputs and reduced transient periods. One may hypothesize that the biped with the proposed locomotion control system can achieve robust walking by changing the joint trajectories adaptively according to the moment when the internal perturbation is applied. From this simulation, it was possible to implement in a complementary manner the voluntary modulation through

the implementation of sustained internal perturbations to the CPG controller characterizing voluntary and non-periodic movements and to verify the returning of the system steady-state walking patterns stimulated by the automatic control of the CPG-based controller.

6.3.3 Coordination of voluntary and automated control

The outcomes obtained from the previous simulation endorse the simulation of more complex behaviors (reaction to other perturbations) and the coordination of automated and voluntary control.

The following simulation is a case study aimed at assessing the viability of the biped system being able to walk adaptively on tilted ground and the capability of the controller to provide robust stable gaits on upslope/downslope terrains and to what range of slope angles. In this set of trials, sudden change of slopes is applied, either sudden increases or sudden decreases. Figure 6.10 illustrates the biped collapse without walking robustly on a tilted ground of 1.0° of slope. In this case, the stability analysis by means of upper-body motion measure is preferred over the method of perturbation detection, since unlike the former method, the latter is not able to provide a better insight of the causes of instability (section 5.3.2).

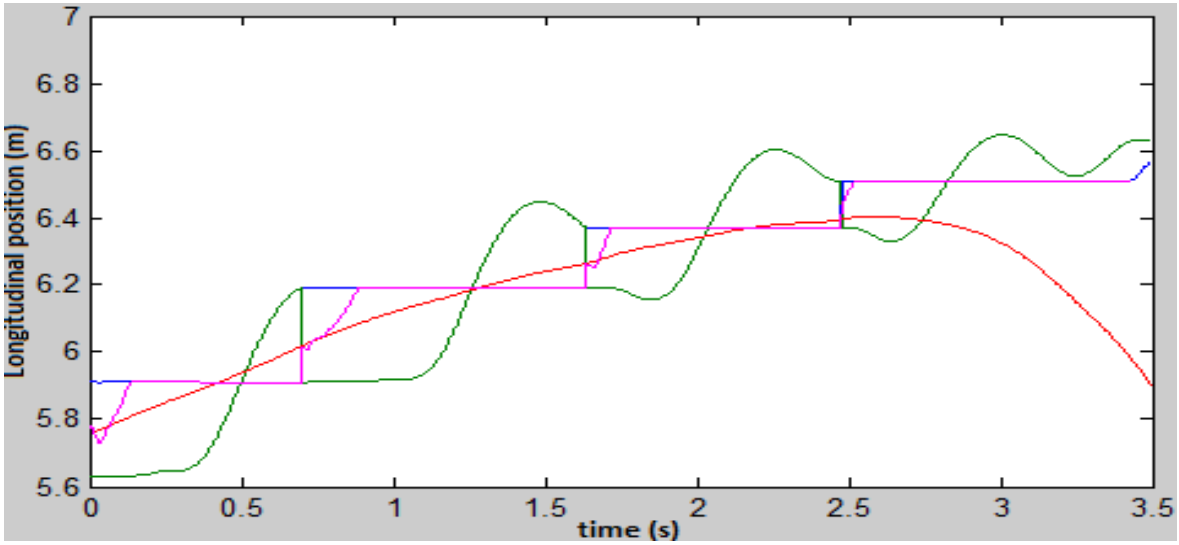

Figure 6.13: Stability analysis through the method of upper-body motion measure of the locomotion on tilted ground of 1.0° of slope. The behavior of the COP (magenta line), COM_x (red line), stance leg tip (blue line) and swing leg tip (green line) is described throughout the total simulation.

Figure 6.13 shows that the biped COM_x diminishes progressively its speed (slope) over each stride inducing non-natural movements of the swing leg tip. The support polygon (equivalent to the distance between the two stance leg tips) at the beginning of double support phase (DSP) period becomes also increasingly small. The progressive backward tilt of

the body caused by the progressive COM_x velocity decreasing reaches a limit value after the third step (around 2.5s), at which the body cannot obtain the required minimum balance to take the step forward and, consecutively, falls to the backwards. This event is expressed by the turning point of COM_x and consecutive declining. Therefore, one may argue that the posture stability is critically challenged in the presence of tilted ground, so its control is of great importance.

One of the reasons for this lack of robustness for locomotion on tilted ground may be the substantial desynchronization existent between the controller and the biomechanical system. This is related to the quite different timings at which the controller and the biped system transit between swing-stance and stance-swing phases. In fact, the upslope surface considerably decreases the period of the swing phase as the foot touches the ground sooner than expected and the controller, which should be expected to switch to the stance phase, is not prepared to react to this change. Conversely, the controller is just able to generate trajectories on flat ground and therefore the biped and controller systems become potentially desynchronized, what leads to locomotion instability. A solution for the aforementioned problem may be to enhance the coupling between the controller and the biomechanical system through the inclusion of sensory feedback so that the controller can independently control the swing and stance duration. This may be achieved through the phase modulation of the oscillators proposed in [65] for quadruped locomotion and here adopted to biped locomotion. In figure 6.14 is depicted the analysis of stability of the locomotion on tilted ground of 1.0° of slope using the phase modulation of the oscillators.

From figure 6.14 one can observe a major improvement on the gait stability. Besides the relatively consistent behavior of COM_x throughout the strides in which its slope is roughly constant, the biped does not collapse as it demonstrates to keep the minimum required postural balance to give the step forward. Nonetheless, one may argue that the postural balance is far from being optimized, due to the noticeable non-natural movements of the swing leg tip (green line) among strides in addition to different step lengths at the beginning of DSP.

In order to neutralize the evident left-right gait asymmetry illustrated in the figure 6.14, it may be important to control, albeit indirectly, the biped COM to enhance the posture stability. This can be achieved by modifying the reference torso angle signal of the controller α_{REF}, nominally set to a value of 0.04rad (section 4.1.3), in order to affect the torso angle trajectory assumed by the biped system. The same simulation is presented, this time including the control of the biped COM (figure 6.15).

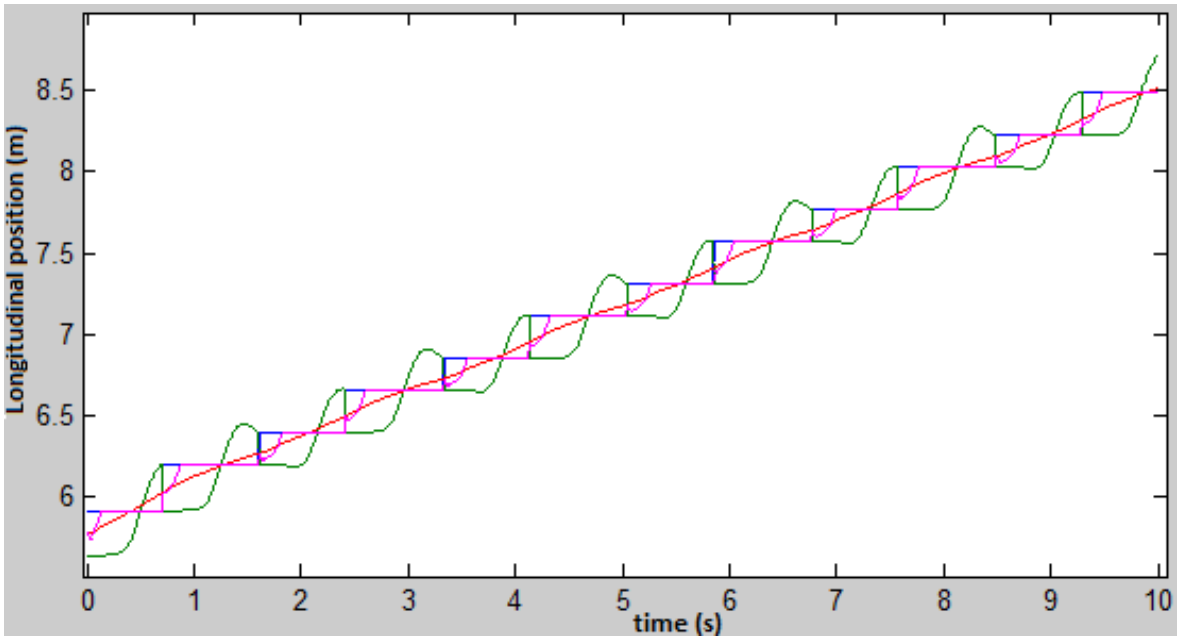

Figure 6.14: Stability analysis through the method of upper-body motion measure of the locomotion on tilted ground of 1.0° of slope. The behavior of the COP (magenta line), COM_x (red line), stance leg tip (blue line) and swing leg tip (green line) is described throughout the total simulation. α_{REF} = 0.04rad.

From the figure 6.15 it is evident a progressive improvement on gait stability and on the gait symmetry whether using α_{REF} = 0.05rad (a) or α_{REF} = 0.07rad (b), since the swing leg tip motions are more natural and the step lengths at the DSP onset among strides are closely identical. Inclusively, using a value of α_{REF} = 0.07rad (on the right panel), better outcomes on this level are achieved. This validation suggests that the more is the slope of the terrain, the higher should be α_{REF} signal. Let one see on figure 6.16 what happens when only α_{REF} is affected without implementing the phase modulation method.

As one can observe in figure 6.16, worse results in terms of gait naturalness and stability were obtained in relation to those provided with the phase modulation inclusion. Both biped COM control and phase modulation are thus essential to provide a combined and reinforced effect on the gait robustness in the presence of tilted ground. It now remains to be analyzed the feasibility of walking on downslope terrains. Figure 6.17 illustrates the biped collapse without walking robustly on a tilted ground of $-0.8°$ of slope.

Figure 6.17 shows that the biped COM_x increases progressively its speed (slope) over each step cycle inducing increasingly lower step length at the DSP onset and contributing therefore for the gait asymmetry. The support polygon at the beginning of DSP period becomes also increasingly small. The progressive forward inclination of the body caused by the progressive COM_x velocity rise reaches a limit value after the second step (around 1.37s),

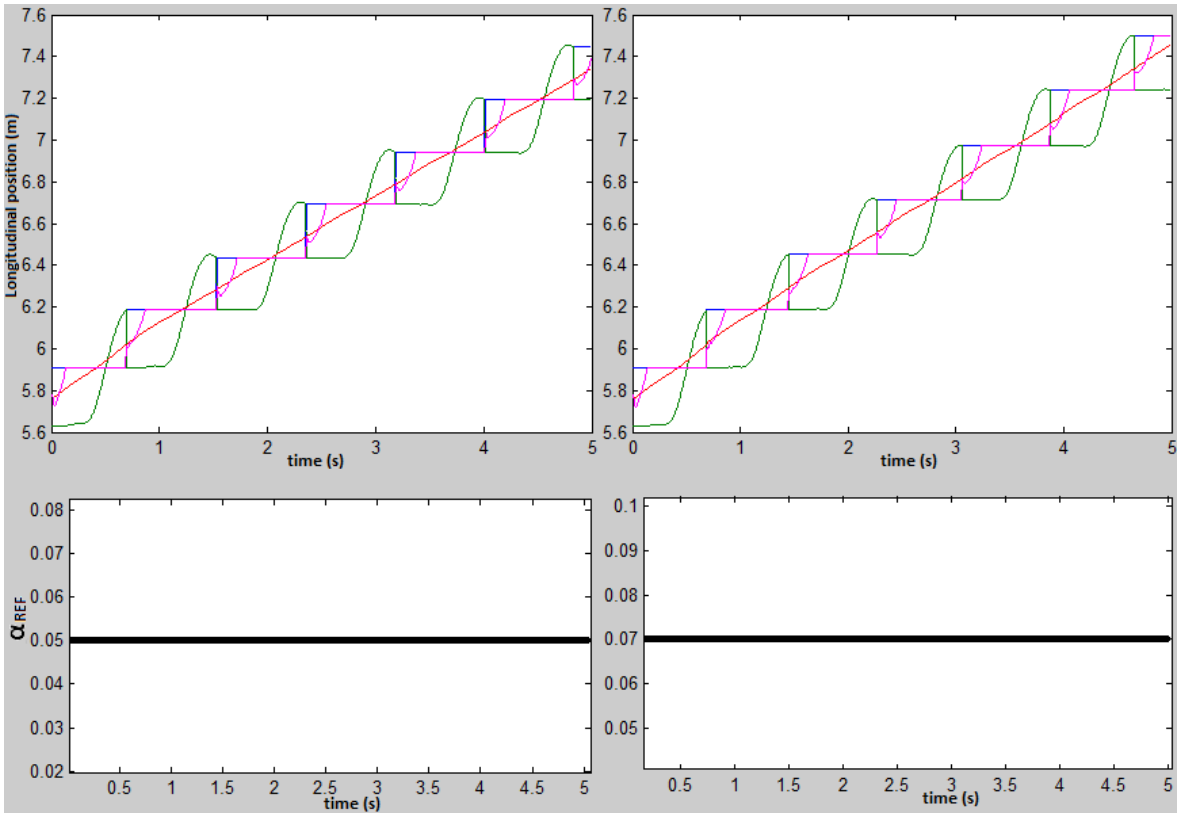

Figure 6.15: Stability analysis through the method of upper-body motion measure of the locomotion on tilted ground of 1.0° of slope. The behavior of the COP (magenta line), COM_x (red line), stance leg tip (blue line) and swing leg tip (green line) is described throughout the total simulation. α_{REF} = 0.05rad on the left panel; α_{REF} = 0.07rad on the right panel.

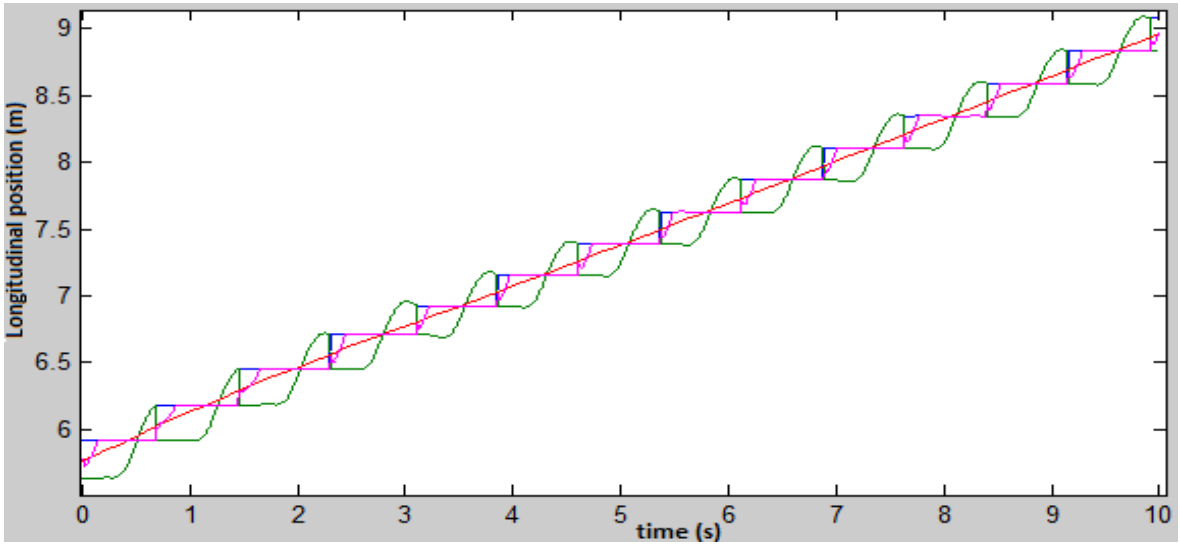

Figure 6.16: Stability analysis through the method of upper-body motion measure of the locomotion on tilted ground of 1.0° of slope. The behavior of the COP (magenta line), COM_x (red line), stance leg tip (blue line) and swing leg tip (green line) is described throughout the total simulation. α_{REF} = 0.07rad.

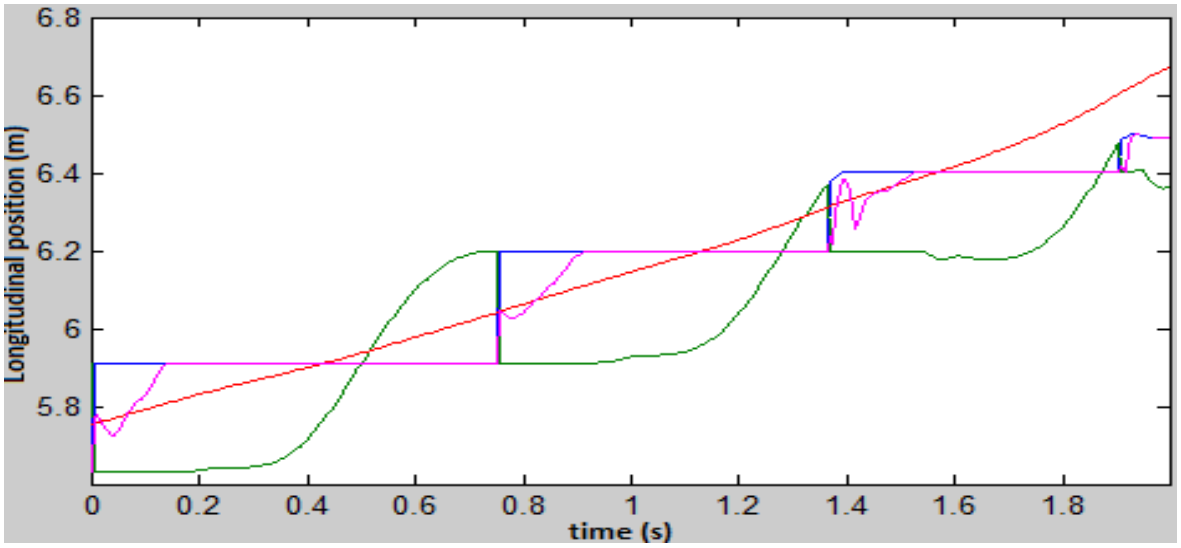

Figure 6.17: Stability analysis through the method of upper-body motion measure of the locomotion on tilted ground of −0.8° of slope. The behavior of the COP (magenta line), COM_x (red line), stance leg tip (blue line) and swing leg tip (green line) is described throughout the total simulation. α_{REF} = 0.04rad.

at which the body consecutively falls forwards. This event is expressed by the far too high COM_x value at the SSP onset after the second step. One may interpret these outcomes as a consequence of the excessive α_{REF} value delivered by the controller in relation to downslope terrains. Figure 6.18 presents the stability analysis of the gait provided by the application of lower α_{REF} values than that nominally established (0.04rad).

On the left panel of figure 6.18 it is observed a slight improvement on gait stability and on the gait symmetry by using α_{REF} = 0.015rad comparing to the case of figure 6.17, due to the COM_x velocity not rising so fast. Furthermore, the third step length (around 2.1s) is higher than that of the previous case. Considering the right panel, significant improvement on gait stability and on the gait symmetry is found, in which more natural and consistent swing leg tip motions and step lengths at the DSP onset among strides are observed. One may infer that α_{REF} = 0.005rad is suitable for the biped system walking on descending terrain with −0.8° of slope. This validation suggests that the more negative is the slope of the terrain, the lower should be α_{REF} signal.

Another contribution of this work is to verify the feasibility of CPG-based controller to broad the locomotion robustness facing more complex terrains with positive, zero and negative slopes within the same simulation. This validation is innovative in relation to recent studies [28, 55, 62–64] in which only a type of slope is performed in each simulation, rather than using upslope and downslope angles in the same simulation. Figures 6.19 and 6.20 illustrate two case studies of such robust adaptation provided by the CPG-based controller.

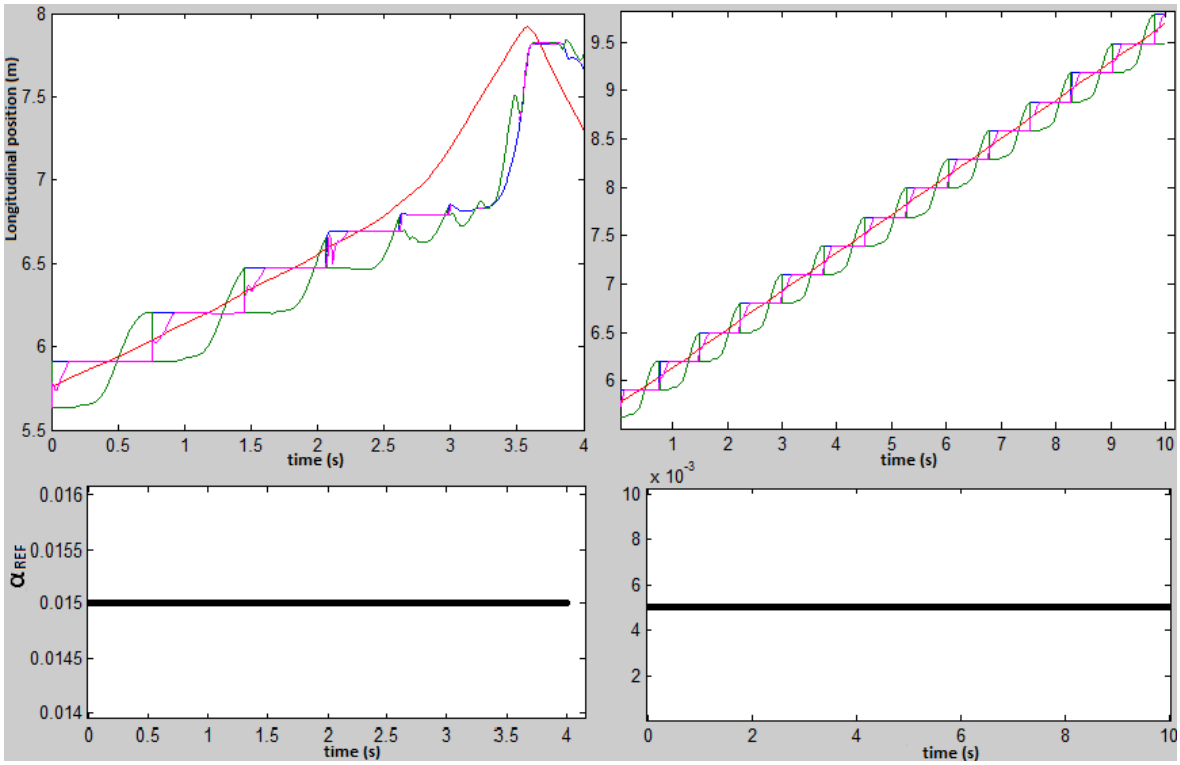

Figure 6.18: Stability analysis through the method of upper-body motion measure of the locomotion on tilted ground of $-0.8°$ of slope. The behavior of the COP (magenta line), COM_x (red line), stance leg tip (blue line) and swing leg tip (green line) is described throughout the total simulation. α_{REF} = 0.015rad on the left panel; (b) α_{REF} = 0.005rad on the right panel.

The slope angles are chosen arbitrarily.

One can see from the figures 6.19 and 6.20 that the controller is effective on controlling biped locomotion on more complex terrains with different slopes by adjusting the α_{REF} trajectory. The controller has proved to modify the nominal reference trajectories according to specific environment disturbances, promoting thus adaptive and stable walking. To that effect, phase modulation of the oscillators and the postural balance control are the major contributors to stability maintenance as well as the integration of sensory feedback is fundamental to the response against unexpected perturbations such as tilted ground. Figures 6.21 and 6.22 illustrate the stick figures of the stable gaits corresponding to those of figures 6.19 and 6.20.

Figure 6.21 shows that the biped system walks on the flat surface at the beginning of the simulation. Then, it walks on the upslope surface of $\approx +1.56°$ after 7.2m long. The biped system walks again on the level surface after 8.6m long. At approximately 17s the biped system starts going down the surface continuously with a downslope angle of $\approx -0.81°$ till the end of the simulation. The simulation outcomes from figures 6.19 and 6.21 demonstrating

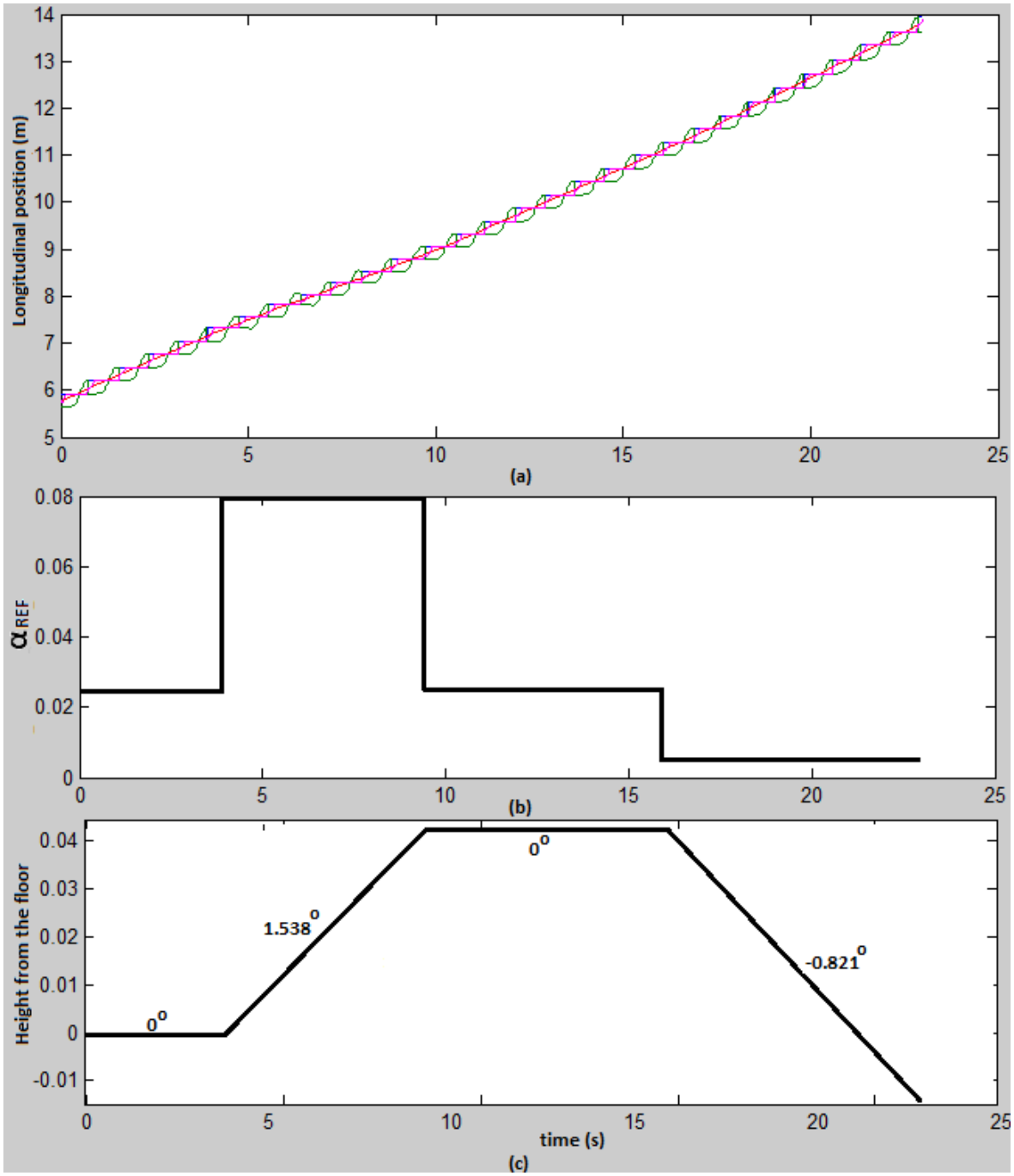

Figure 6.19: Simulation of the biped locomotion on a complex terrain with positive, zero and negative slopes, respectively. (a) Stability analysis through the method of upper-body motion measure; the behavior of the COP (magenta line), COM_x (red line), stance leg tip (blue line) and swing leg tip (green line) is described throughout the total simulation; (b) Adaptation of α_{REF} according to the floor slope; (c) Height from the floor with the respective slopes.

gait stability on transient slope surfaces, namely $flat - upslope - flat - downslope$, verify that the robot with the proposed locomotion control system can walk adaptively to these environmental variations.

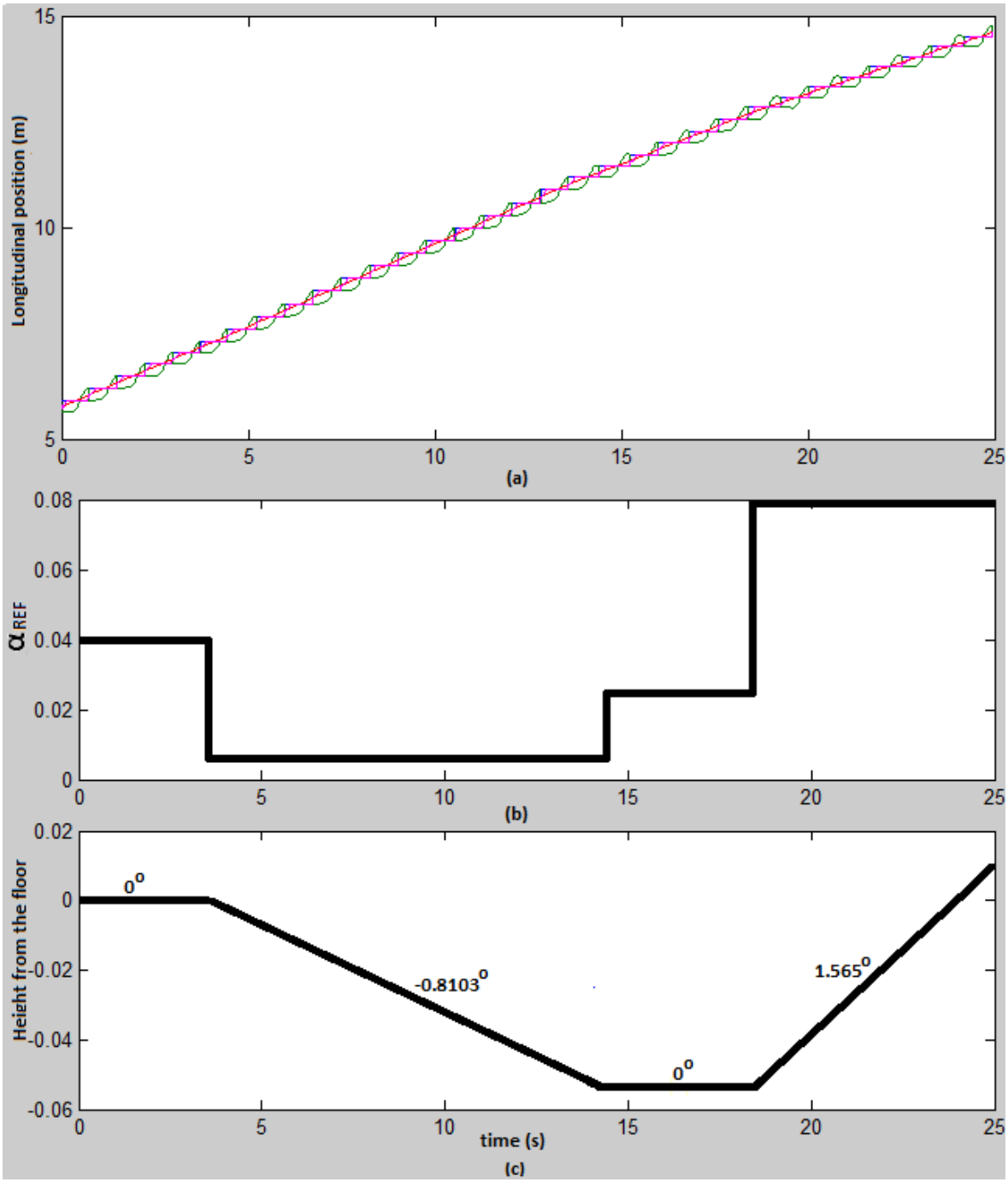

Figure 6.20: Simulation of the biped locomotion on a complex terrain with negative, zero and positive slopes, respectively. (a) Stability analysis through the method of upper-body motion measure; the behavior of the COP (magenta line), COM_x (red line), stance leg tip (blue line) and swing leg tip (green line) is described throughout the total simulation; (b) Adaptation of α_{REF} according to the floor slope; (c) Height from the floor with the respective slopes.

The simulation from figure 6.22 is very similar to that from 6.21, except for the display order of the tilted ground. It is shown that the biped system walks on the flat surface at the beginning of the simulation. Then, it walks on the downslope surface of $\approx -0.81°$ after 7.2m

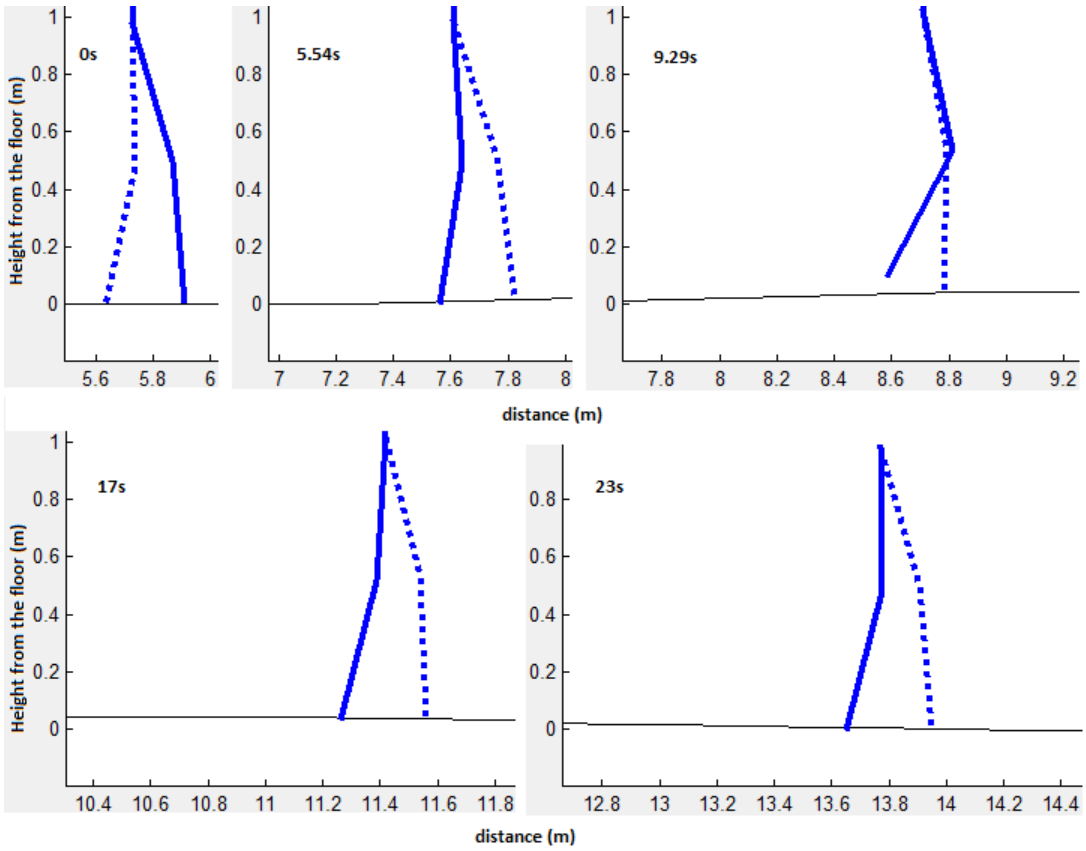

Figure 6.21: Different slopes in simulation. Upslope and downslope are shown, respectively, separated by flat surface. The upslope and downslope angles are respectively $\approx +1.56°$ and $\approx -0.81°$.

long. The biped system walks again on the level surface after 10.8m long. At approximately 18.6s the biped system starts going up the surface continuously with an upslope angle of $\approx +1.56°$ till the end of the simulation. The simulation outcomes from figures 6.20 and 6.22 demonstrating gait stability on transient slope surfaces, namely $flat - downslope - flat - upslope$, verify that the robot with the proposed locomotion control system can walk adaptively to these environmental variations.

Another contribution of this work is the study of the slope range in which the biped system can demonstrate stable gaits. Changes on some walking gait features in the presence of non-zero slope values are assessed. Moreover, the feasibility of walking downhill and uphill is analyzed and compared. Figures 6.23 and 6.24 show the profiles of the mean step length and gait velocity, respectively, according the slope angle of the floor.

Figures 6.23 and 6.24 demonstrate the performance of the system on the generation of stable gaits for a slope range of $[-2.5° : +3.0°]$. One can argue that the biped system decreases its mean step length and gait velocity as the upslope terrain becomes steeper and increases it along a higher downhill slope. This assumption is in line with the conclusions

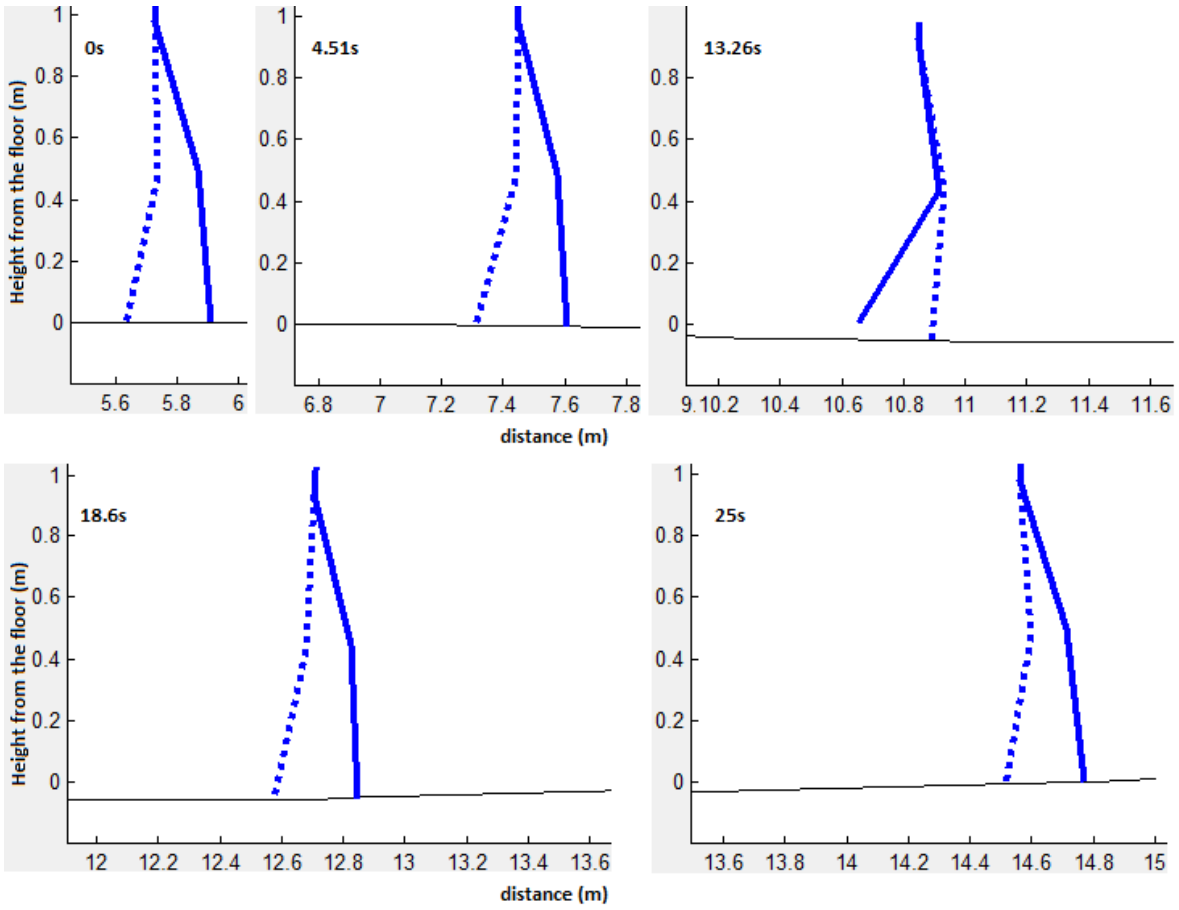

Figure 6.22: Different slopes in simulation. Downslope and upslope are shown, respectively, separated by flat surface. The upslope and downslope angles are respectively $\approx -0.81°$ and $\approx +1.56°$.

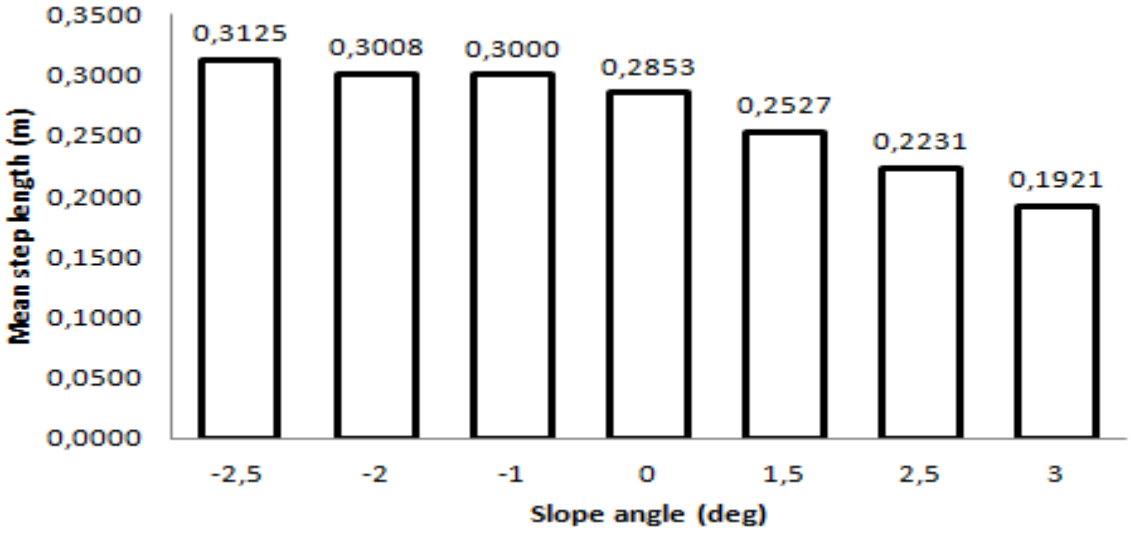

Figure 6.23: Actual mean step length versus the slope angle of the floor. The biped system can walk stably in this range of floor slope angles.

drawn in other works [55, 62, 63] and suggest that the controller can robustly produce stable

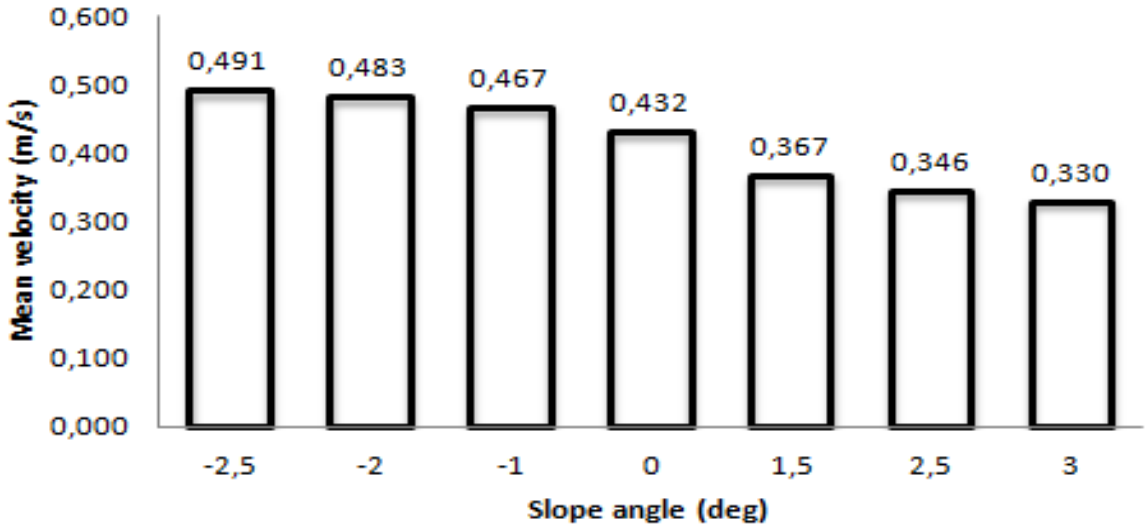

Figure 6.24: Actual mean gait velocity versus the slope angle of the floor. The biped system can walk stably in this range of floor slope angles.

gaits by modulating independently and adaptively the swing and stance duration depending on the slope angle. This fact endorses the *phase modulation* method proposed for robustness locomotion enhancement under non-flat environment [65].

On the other hand, the range of slopes shown above does not represent the slope limits beyond which the biped system becomes unstable and consecutively collapses. The fact is that this range of slopes is achieved by means of the manual tuning of the reference torso angle (α_{REF}) through a process of trial and error. This is due to the lack of knowledge about the full relationship among the several state variables that ensures gait stability. Thus, in spite of knowing that the α_{REF} should increase with the slope angle of the floor and vice-versa, one cannot neither automatically predict the precise moment to alter α_{REF} nor to which value, except through the trial and error process. Conversely, one strongly believes that the biped system is able of walking stably on a higher range of slopes, once the dynamics of the biped system is fully understand, being thus possible to modulate the α_{REF} automatically depending on the biped states.

Nonetheless, the range of slopes here presented, $[-2.5^\circ : +3.0^\circ]$, is higher than those proposed in recent studies: in [62] the gaits were stable for slopes between -0.9° and $+0.7^\circ$; the biped system could achieve stable gait with a sudden slope maximum increase of $+1.4^\circ$ and with a sudden slope maximum decrease of -1.4° in [204]; in [55] stable gaits are simulated changing the slope angle of the floor from 0° to $+6^\circ$, although the simulation is not performed for downslope terrain and undesired gait asymmetry is introduced by disparate step cycle values beyond $+4.5^\circ$ of slope angle; a stable gait is produced on uphill terrain

with a slope angle of $\approx +0.23°$ in [64]. Therefore, one may say that this work introduces innovation in the broad range of slope angles.

Below, in figures 6.25 and 6.26 are depicted the stick figures of stable gait on tilted ground of $+3.0°$ and $-2.5°$, respectively, in addition to the stability analysis and α_{REF} evolution.

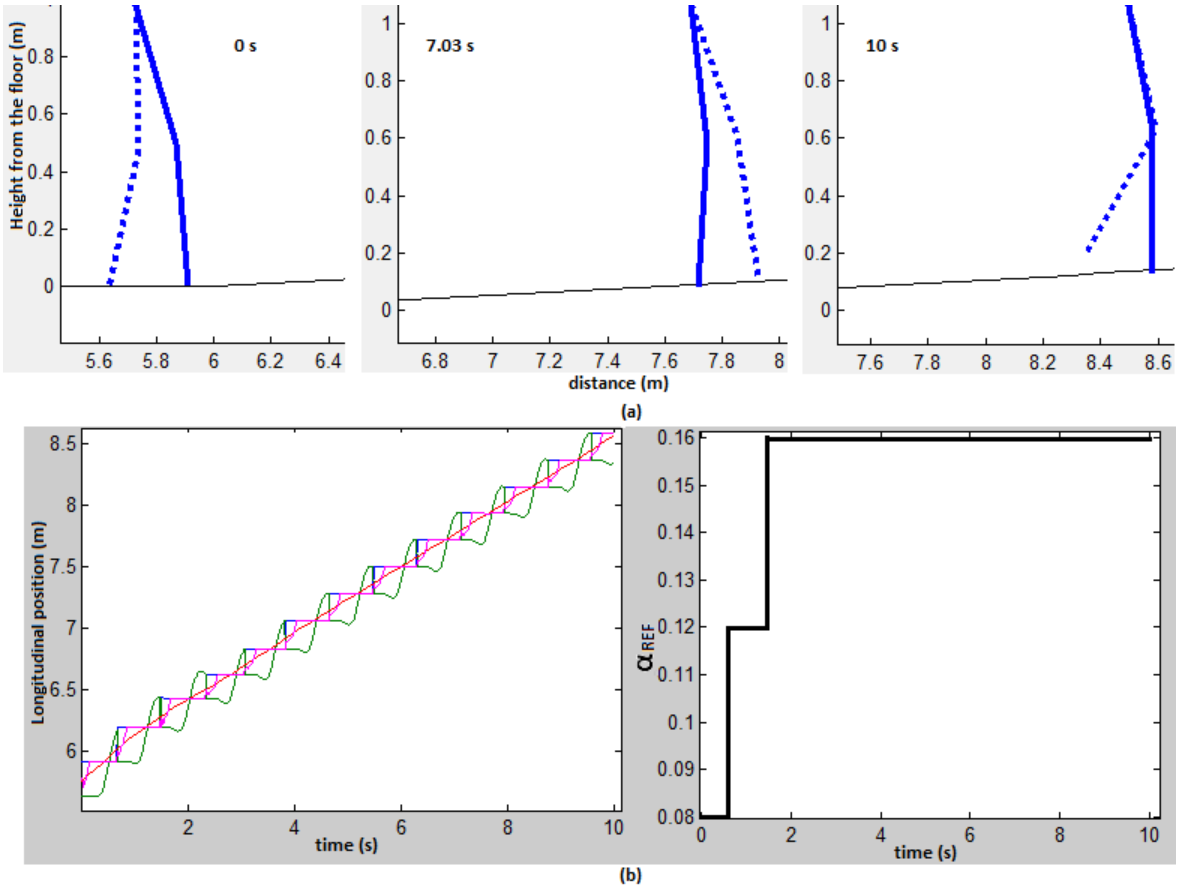

Figure 6.25: Slope angle of $+3.0°$ in simulation. (a) Stick figure of the biped system traced at 0s, 7.03s and 10.0s; (b) on the left panel is illustrated the stability analysis through the method of upper-body motion measure, while on the right panel is depicted the modulation of α_{REF}.

Figure 6.25 (a) shows the biped system placed on a flat surface at the beginning of the simulation, waling subsequently uphill (from 5.9s). On the left panel of (b) is demonstrated the production of stable and uniform strides. The successive increments on the α_{REF} are required to adjust the biped COM forward, due to the biped system being excessively bended backward.

Figure 6.26 (a) shows the biped system walking downhill after around 5.9s). On the left panel of (b) is demonstrated the production of stable and uniform strides. The decrements on the α_{REF} imply that the biped system is excessively bended forward, while the increment on the α_{REF} suggests the excessive backward lean of the body.

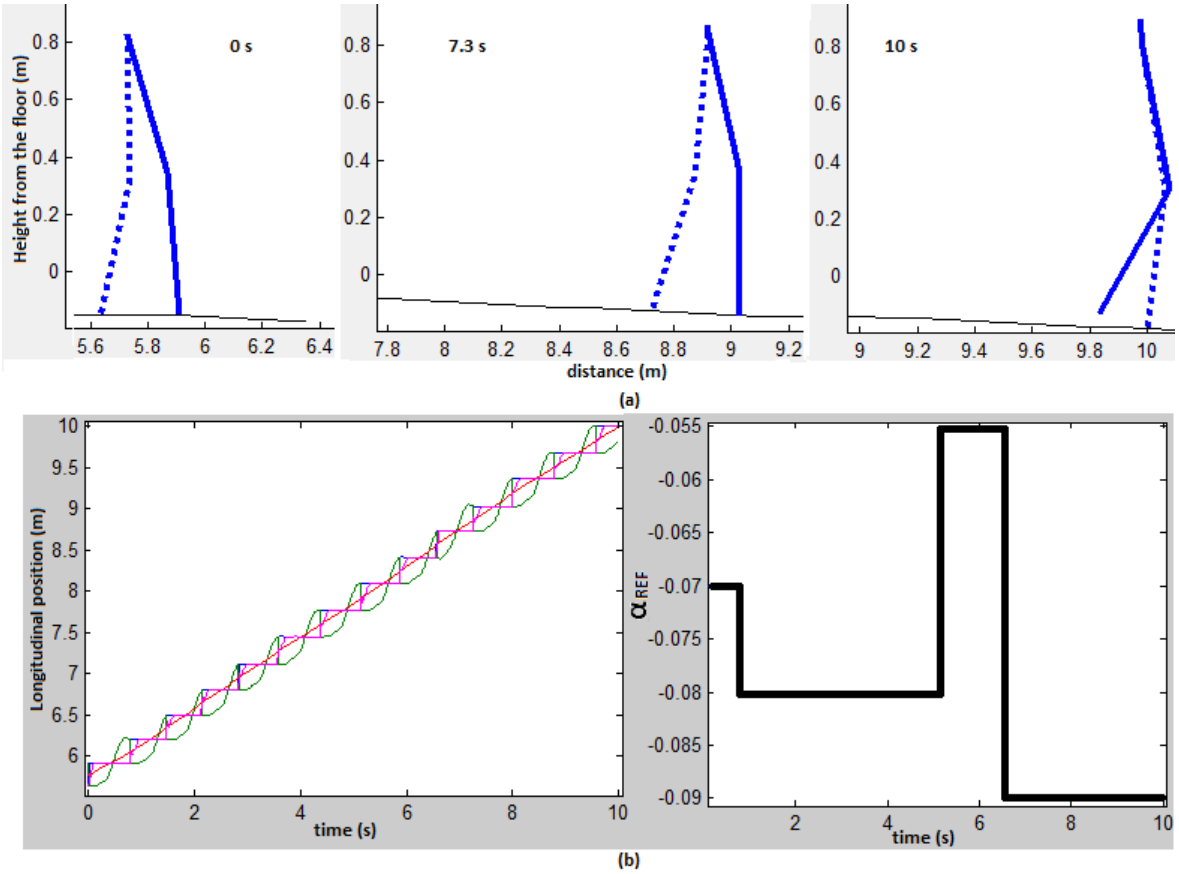

Figure 6.26: Slope angle of $-2.5°$ in simulation. (a) Stick figure of the biped system traced at 0s, 7.3s and 10.0s; (b) on the left panel is illustrated the stability analysis through the method of upper-body motion measure, while on the right panel is depicted the modulation of α_{REF}

.

Stable gaits are achieved not only on flat ground but also on a higher set of floor slopes, apart from that stable gaits are attained switching between zero, positive and negative ground slopes within the same simulation.

The following simulation is another case study to analyze the adaptation viability of the biped locomotion on an obstacle overtaking. In this example, not only the integration of internal sensory feedback to develop voluntary movements can play a key role on the locomotion robustness but also the coordination of automated and voluntary control may be important for gait stability: when the obstacle is still to be overcome, the CPG-controller should be modulated by the internal sensory feedback stated as temporary internal perturbations to voluntarily circumvent the obstacle; once the obstacle is overcome, the CPG-based controller should return to its automated control and provide normal walking patterns. In figures 6.27 and 6.28 are depicted the gait analysis produced by the biped system, firstly without the adaptation strategy, and subsequently, with the integration of internal feedback.

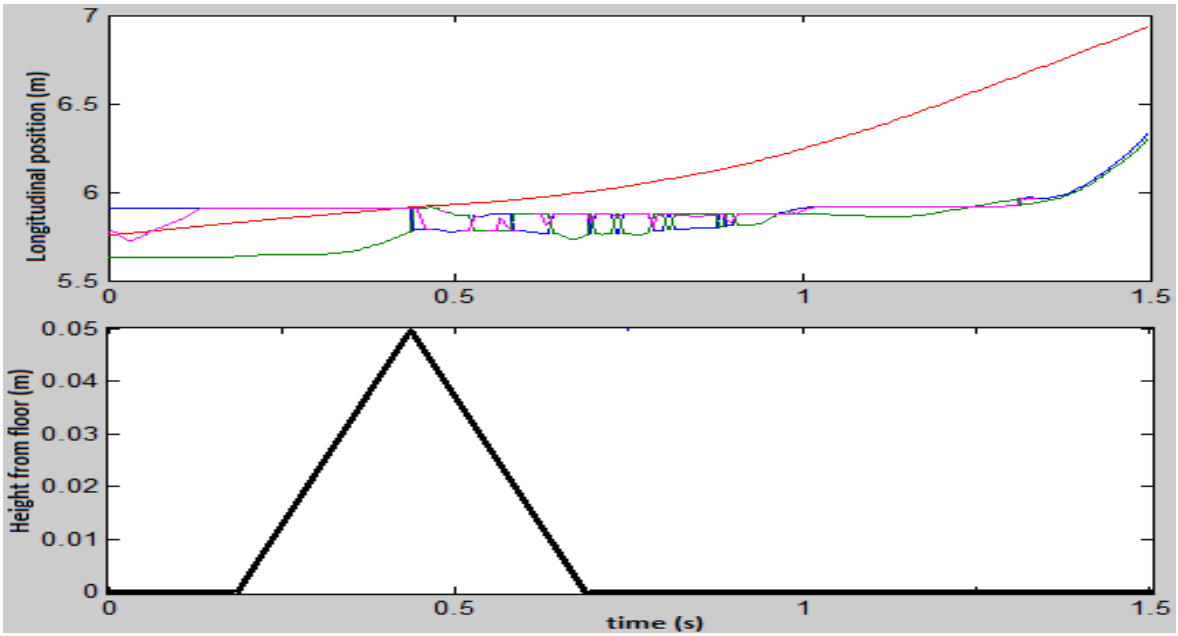

Figure 6.27: On the upper panel is the stability analysis through the method of upper-body motion measure of the locomotion on uneven ground with an obstacle of 0.05m high; the behavior of the COP (magenta line), COM_x (red line), stance leg tip (blue line) and swing leg tip (green line) is described throughout the total simulation. On the lower panel is depicted the presence of an obstacle.

From figure 6.27 it is possible to see that the biped system cannot circumvent the obstacle, and consecutively, the leg tip touches the ground sooner as expected (around 0.44s). Consequently, the biped stumbles, its COM moves excessively forwards and finally collapses. With the integration of internal modulation in figure 6.28, the biped can generate several strides throughout having overtaken the obstacle (a), while the obstacle has induced slight deviation of the biped system from the normal walking behavior (upper panel of (b)). The controller has effectively coped with the presence of a disturbance such as an obstacle demonstrating thus robustness.

Let one enhance the robustness challenge by introducing two obstacles. Figure 6.29 shows that the biped system can circumvent the obstacles, in spite of falling further ahead due to an ineffective coordination of automated and voluntary control.

As one may observe from figure 6.29, the biped system can successfully circumvent the two followed obstacles both of 0.05m. After passing the obstacles no more voluntary movements are required such that internal modulation is deactivated and the automated control from the CPGs is reactivated to generate periodic and automatic gait patterns. Nonetheless, the coordination of such modulations is not effective, since the biped falls by the excessive forward inclination of the body (suggested by the high biped COM value (b)).

As α_{REF} signal is that nominally established, 0.04rad, a lower signal should compen-

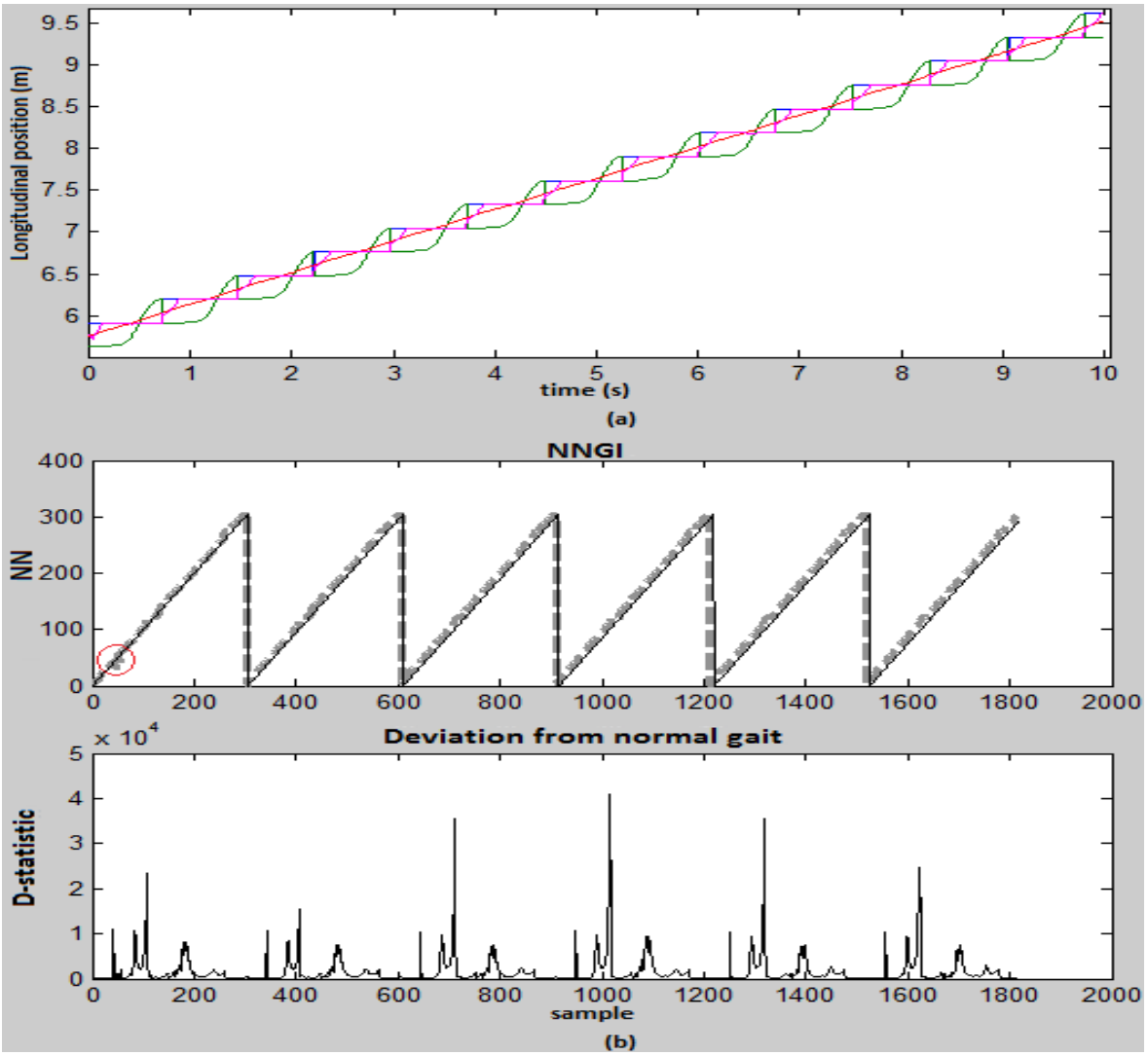

Figure 6.28: Stability analysis. (a) Method of upper-body motion measure of the locomotion on uneven ground with an obstacle of 0.05m high; the behavior of the COP (magenta line), COM_x (red line), stance leg tip (blue line) and swing leg tip (green line) is described throughout the total simulation. (b) Method of perturbation detection under the presence of an obstacle; the NN (dashed line) and the RLC (solid line) are illustrated in the upper panel; the bottom panel shows the D-statistic (solid line)

sate and address the problem of the high body inclination. The outcomes derived from the proposed solution are shown in the following figures. Figure 6.30 illustrates the stability analysis of the locomotion and the evolution of α_{REF}. In figure 6.31 is shown the related stick figure.

Through the correct adjustment of the α_{REF} signal (shown on the lower panel of figure 6.30), the biped system does not collapse, unlike the previous case. However, like in the case of the adaptation of α_{REF} signal on tilted ground, its tuning is not automatic, rather manual through trial and error process. Locomotion robustness is thus increased with the effective coordination of voluntary and automated movements (figure 6.31).

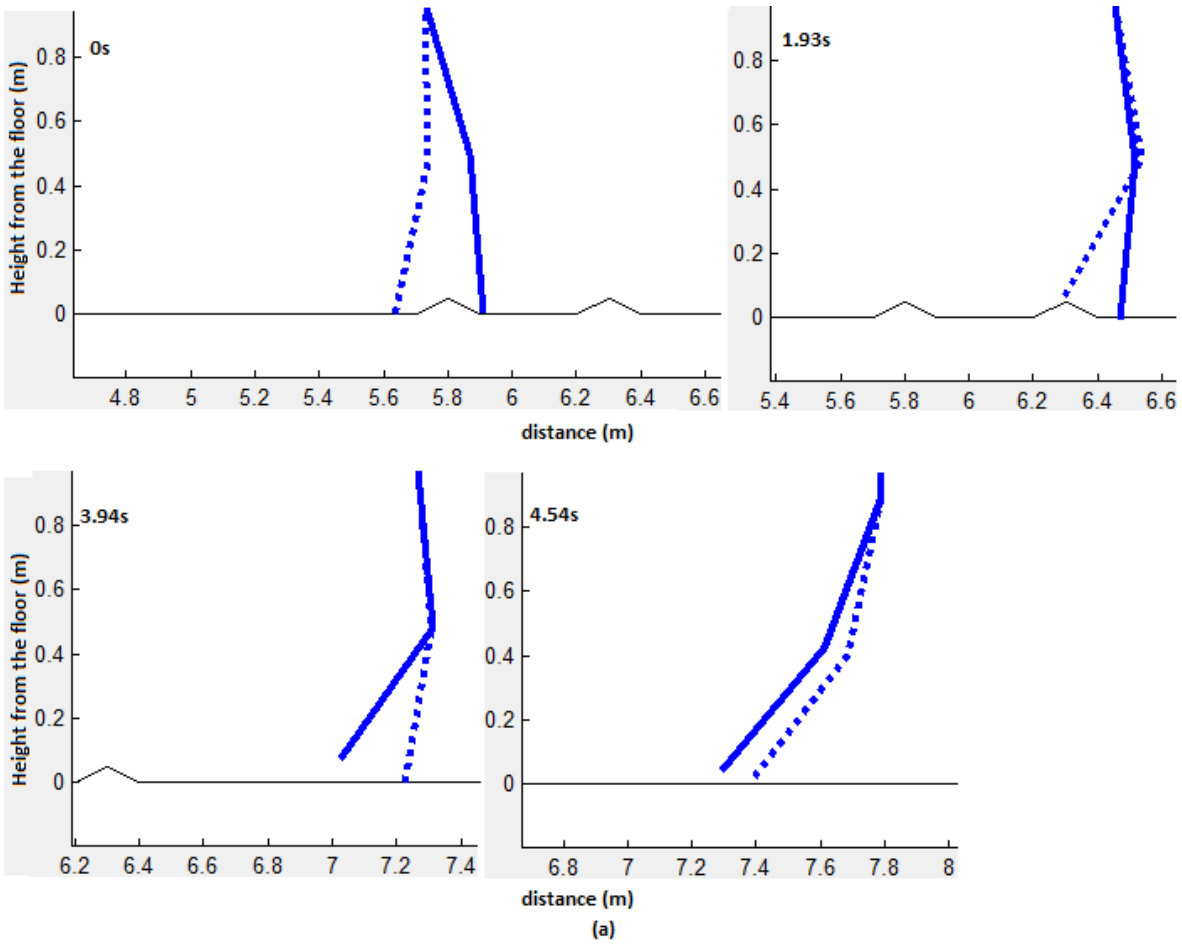

Figure 6.29: (a) It is illustrated the stick figure on uneven ground with two obstacles; after overcoming the obstacles the biped system ends up collapsing. (b) Stability analysis through the method of upper-body motion measure.

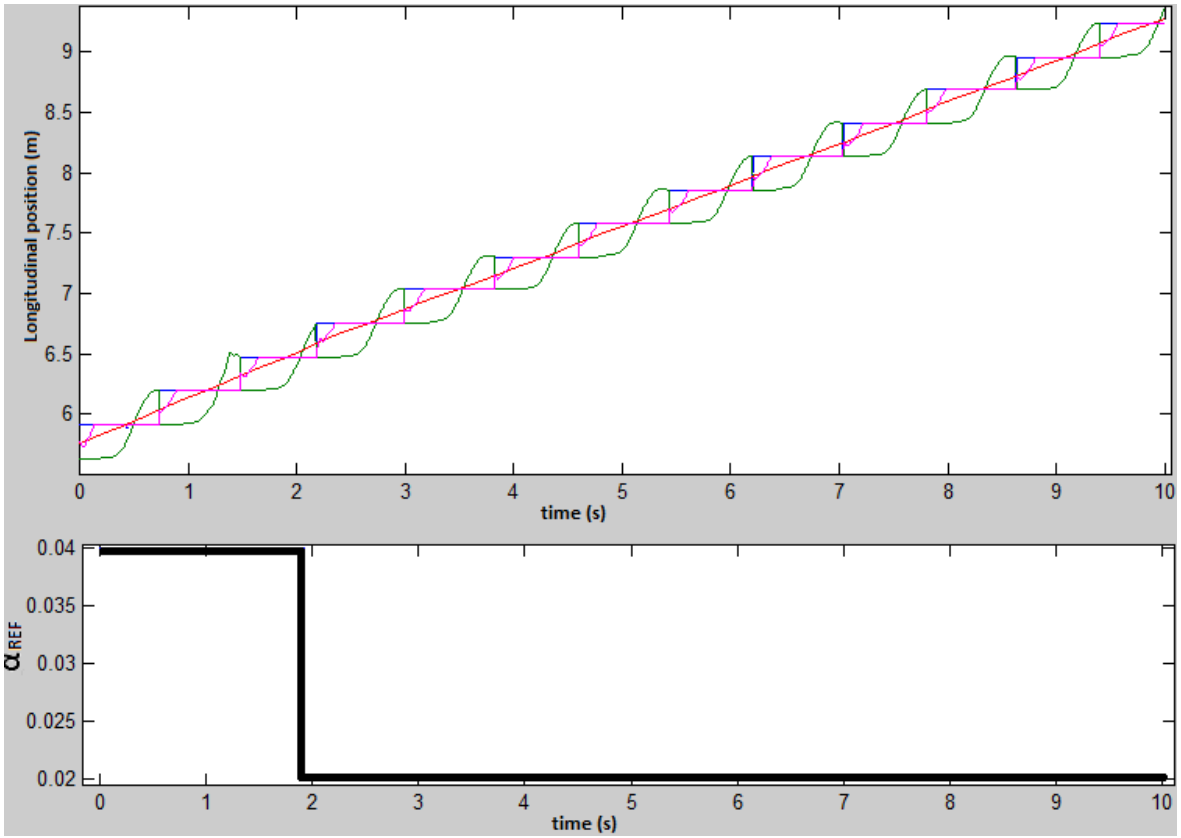

Figure 6.30: On the top panel is indicated the stability analysis through the method of upper-body motion measure of the locomotion on uneven ground with obstacles. The evolution of α_{REF} is described on the lower panel.

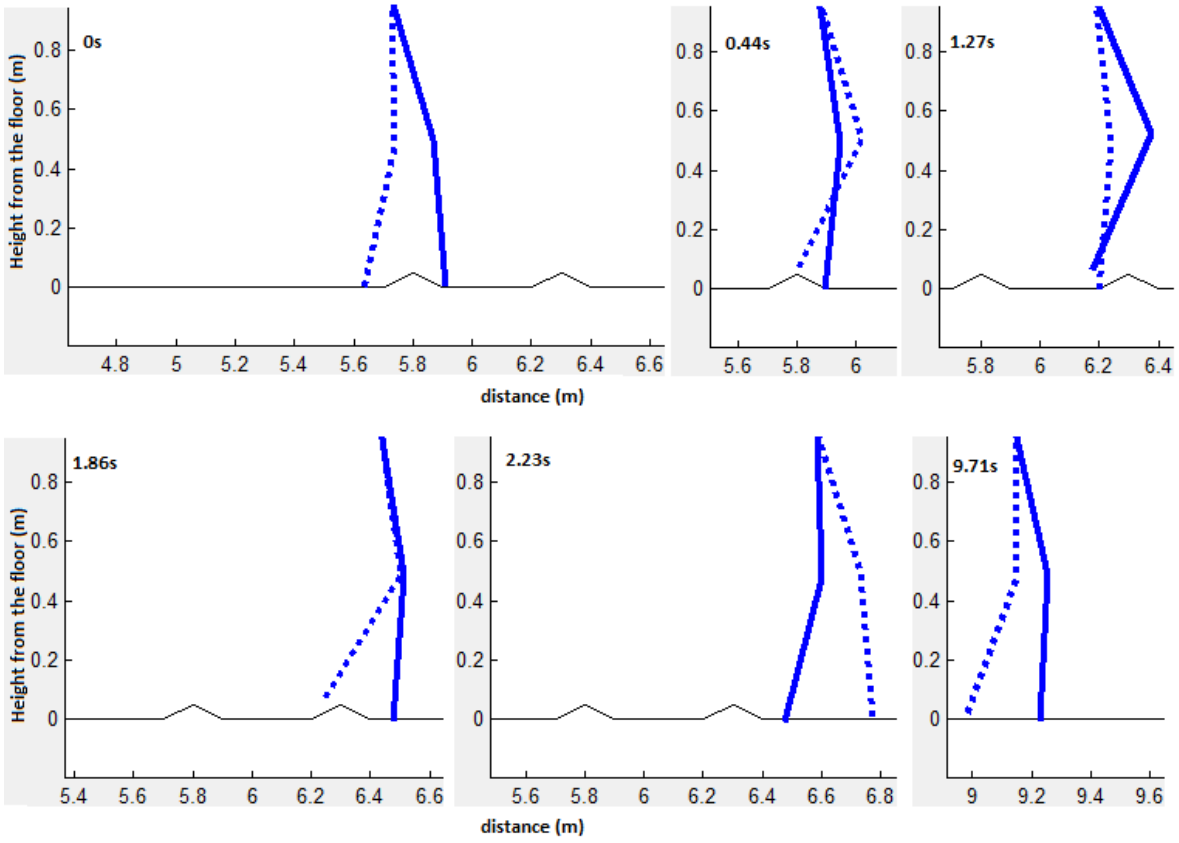

Figure 6.31: Obstacles in simulation. Stick figure on uneven ground with two obstacles; after overcoming the obstacles the biped system continues to walk stably.

Chapter 7

Conclusions and future developments

In the present work, a bio-inspired closed-loop controller based on a CPG model constituted of Hopf AFOs is proposed to produce stable mechanical oscillations when coupled to the mechanical orthosis and to generate stable gaits when coupled to the biped model.

Regarding the mechanical orthosis experiments, the controller has proved to be effective on the generation of a stable swinging task with the desired frequency in open-loop control while being synchronized with the natural dynamics of the mechanical system. The position controller of the orthosis has provided better response to the stimulating signal from the CPG system, lower overshoot and better stability features and more feasibility of its parameters tuning. Nonetheless, by applying a perturbation on the mechanical orthosis, serious repercussions either on the real angle velocity or on the deviation from the reference input were promoted, by which one may conclude that the integrated system in open-loop can be very sensible to perturbations from environment. A closed-loop CPG controller should be thus developed to be able to adapt to unexpected disturbances.

Concerning the biped model simulations in open-loop control, the purpose is to mimic some systems of the human body, more specifically, the human CPGs, responsible for the generation of rhythmic gait movements. The CPG-based controller has demonstrated effectiveness in the learning of the correct design of joint nominal trajectories and in the attainment of interlimb coordination via phase relations among the oscillators. The dynamic rules inherent to the adaptive oscillators enable the automatic self-tuning of the intrinsic frequencies, amplitudes and coupling weights in order to replicate the reference signals in a generalized fashion. In this way, it is possible to implement the proposed dynamical process to simulate the capability of the neural drive of the biped system to generate its own walking gaits, i.e., to learn the motion coordination without pre-specifying the response of the system.

On the other hand, such a dynamical system approach is interesting due to not restricting the controller to fixed pre-recorded gait patterns. Inclusively, the reproduction of stable and steady-state walking patterns on the biped system has been achieved. Both experiment with the orthosis and simulation with the biped model in open-loop control have validated therefore the hypothesis of entrainment achievement between the CPG-based controller and the (bio)mechanical systems. This evidence may open up the possibility of these artificial oscillators being synchronized to the biological oscillators located in the spinal cord of humans on the reproduction of stable walking patterns in futurre work. From the two-dimension biped model here studied, oscillators have proved to successfully simulate the behavior of the thighs and knee angles. The CPG modelling using nonlinear oscillators may thus replicate patterns similar to human CPG, becoming possible the human gait simulation. On the other hand, this finding can be very useful for robot-assisted therapy to help patients with movement disorders. The synchronization between the artificial and biological oscillators can enable the delivery of assistance depending on the effort of the patient, according to the concept of *assistance-as-needed*, so that the desired motion is derived from the combined effort of the patient and the necessary amount of assistance from the device. The ultimate goal should be therefore the assistance/rehabilitation of gait locomotory tasks.

Concerning the biped model simulations in closed-loop control, the goal is to understand and increase the knowledge of the underlying neural control principles of human locomotion, nowadays still under-exploited, that can be useful for human assistance and therapy thereafter. Considering that the control system of the human locomotion is a hierarchical interaction between the brainstem, spinal cord and the biomechanics, the closed-loop CPG-based controller is sensitive to sensorial information about the conditions of the environment or unexpected perturbations or disturbance supplied as external feedback of the system as well as descending commands from the brainstem stated as internal feedback which can influence the way the lower level CPG controllers are responding and interacting.

The inclusion of the vertical position of torso as external feedback onto the CPGs not only has shown to enable the implementation of realistic locomotion through periodic gaits on flat ground, but also could improve some gait characteristics such as broad margins of stability in addition to higher mean velocity and step length translating a better neuromechanical entrainment of the oscillators to the feedback signal and to the natural dynamics of the mechanical system. The spinal CPGs have proved to be able to use feedback to automatically control gait. This control scheme simulates, for instance, a human taking long walks

on even ground without being aware he is walking.These achievements may partially conclude about potential benefits of implementing external feedback in contrast to a open-loop controller without the integration of feedback information.

On the other hand, it is especially important to learn about some of the features which make human walking into such an efficient, automated yet highly adaptable type of behavior to unexpected perturbations. In this line of thought, simulations including both internal and external feedback were implemented to evaluate their interactional potential on providing locomotion robustness in the presence of environment changes such as tilted ground and terrain with obstacles. In relation to the viability of the biped system being able to walk adaptively on tilted ground and the capability of the controller to provide robust stable gaits on upslope/downslope terrains, the biped system is able to walk uphill as well as downhill. Moreover, stable gaits can be attained for slopes between -2.5° and $+3.0^{\circ}$, even though there is a strong believe that the biped system is able of walking stably on a higher range of slopes, once the dynamics of the biped system is more fully understand, being thus possible to modulate the α_{REF} automatically, rather than using a manual tuning through the trial and error process. Furthermore, simulations were implemented with transient slope surfaces, specifically *flat - upslope - flat - downslope* and *flat - downslope - flat - upslope* terrains, in which the biped system with the proposed locomotion control system is able to walk adaptively to these environmental variations depending on the slope angle. With regard to the adaptation feasibility of the biped locomotion on obstacles overtaking, the controller has effectively coped with the presence of such unexpected disturbances, by overcoming the obstacles and by the ability of recovery to stable walking after the introduction of perturbations. In both case studies of tilted ground and ground with obstacles, one could validate the theoretical assumption that the spinal (automatic) and brain (voluntary) control are superposed or interact in a fashion way to achieve robust locomotion. Not only the integration of internal sensory feedback to develop voluntary movements has played a key role on the locomotion robustness but also the coordination of automated and voluntary movements was effective on the gait stability. To that effect, phase modulation of the oscillators and the postural balance control were the major contributors to stability maintenance against the environmental variations.

The endorsement of this principles can enable the simulation of more complex behaviors such as reaction to other perturbations (stumbling reaction, push recovery) and other environment changes (like stair climbing, failures, ...) which can be relevant for therapy

and/or assistance, for instance, assisted gait movements which require great overstrain of the physiotherapists in intensity and variety and other walking movements performed in daily life which cannot be performed inside the clinical rehabilitations. Therefore, the biologically inspired control based on the CPG model can enable the design of intelligent assistive training devices for the enhancement of the restoration of motor function for patients with impairments of the CNS, like stroke, SCI,TBI, ..., and for the improvement of people's quality of life and community integration. With a more insight of the neural control principles with the simulation of more complex and detailed behaviors of the human locomotion CPG and its interaction with the brainstem through optimized control algorithms of the CPG model, automated motor rehabilitation can maximize the therapeutic/assistive outcomes and offer a large variety of new fascinating aspects in treatment, diagnosis, and interdisciplinary cooperation to the benefit of the patients.

In contrast to other recent works that have implemented a control excluding any longitudinal sensory feedback from the biomechanical system [28, 55, 62], improvements on stability and gait features such as higher mean walking velocity, step length were attained with the integration of the vertical position of torso feedback. Moreover, stable gaits are produced on flat ground as well as on a higher set of floor slopes compared to that achieved in [55, 62–64, 204], and also on transient slope surface, alternating between upslope, leveled slope and downslope surfaces within the same simulation offering more locomotion robustness than the compared works. In response to the *phase resetting* method to provide strong coupling of the controller with the mechanical system for the maintenance of the postural balance and stability against environmental variations proposed in [28, 55, 66], the *phase modulation* of the oscillators applied in quadrupeds locomotion is rather adopted here and implemented in human locomotion, which one thinks to be more suitable to enhance the coupling of the controller with the biomechanical system and to improve the locomotion robustness. Up until now, only a very few studies have implemented simulations of biped locomotion on uneven ground with obstacles through CPG model using nonlinear oscillators [205–207], so implementing obstacle avoidance is another contribution of this work.

Future developments include the automatic strategies for the control of the postural balance in the presence of unexpected perturbations or environmental changes. Specifically, the automatic tuning of the reference torso angle (α_{REF}) depending on the floor slope angle and on the characteristics of the obstacles is then crucial. Furthermore, in order to increasingly mimic the highly adaptable human locomotion, more simulations recreating the reaction to

other perturbations (stumbling reaction, push recovery) and other environment changes (like stair climbing, failures, ...) should be performed. On the other hand, reflex circuits onto the CPGs should be integrated since the reflex modulation during gait can be used to infer the activity of the CPGs, due to the phase- and task-dependency of reflexes. Later work studying the possibility of increasing the basin of stability through the integration of sensory feedback is encouraged.

This study has thus great application in the project of autonomous robots and in the rehabilitation technology for present and future research, not only in the project of smaller, intelligent and cost-effective prosthesis and orthosis for continuous therapy training in a home or work environment rather than only in clinical facilities, but also in the searching of better procedures for motor functions recovery/assistance of human beings.

Bibliography

[1] Central CPO. Hand-made medical device products., 2009.

[2] J. Kahle and et al. Orthotics overview., 2012.

[3] H. Herr. Exoskeletons and orthoses: classification, design challenges and future directions. *Journal of Neuroengineering and Rehabilitation*, 6, 2009.

[4] C. Fleischer. Embedded control system for a powered leg exoskeleton. *Computer Engineering*, pages 1–9, 2006.

[5] G. Belforte, G. Eula, S. Sirolli, and S. Appendino. Design and testing of two mechatronics systems for robotized neurorehabilitation. *The Romanian Review Precision Mechanics, Optics & Mechatronics*, 39, 2011.

[6] Ekso bionics, April 2012.

[7] Rex - the robotic exoskeleton, April 2012.

[8] H. A. Quintero, R. J. Farris, and M. Goldfarb. Control and implementation of a powered lower limb orthosis to aid walking in paraplegic individuals. *Interface*, pages 953–958, 2011.

[9] G. Belforte, L. Gastaldi, and M. Sorli. Pneumatic active gait orthosis. *Mechatronics*, 11(3):301–323, 2001.

[10] A.M. Dollar and H. Herr. Lower extremity exoskeletons and active orthoses: Challenges and state-of-the-art. *Robotics, IEEE Transactions on*, 24(1):144 –158, feb. 2008.

[11] A. Agrawal, S. K. Banala, S. K. Agrawal, and S. A. Binder-Macleod. Design of a two degree-of-freedom ankle-foot orthosis for robotic rehabilitation. *9th International Conference on Rehabilitation Robotics 2005 ICORR 2005*, pages 41–44, 2005.

[12] D. P. Ferris, K. E. Gordon, G. S. Sawicki, and A. Peethambaran. An improved powered ankle-foot orthosis using proportional myoelectric control. *Gait & Posture*, 23(4):425–428, 2006.

[13] J. A. Ward, S. Balasubramanian, and J. He. Robotic gait trainer reliability and stroke patient case study. *Organization*, 00(c):554–561, 2007.

[14] S. Hwang, J. Kim, J. Yi, K. Tae, K. Ryu, and Y. Kim. Development of an active ankle foot orthosis for the prevention of foot drop and toe drag. In *Biomedical and Pharmaceutical Engineering, 2006. ICBPE 2006. International Conference on*, pages 418 –423, dec. 2006.

[15] A. Roy, H. I. Krebs, S. L. Patterson, T. N. Judkins, I. Khanna, L. W. Forrester, R. M. Macko, and N. Hogan. Measurement of human ankle stiffness using the anklebot. *2007 IEEE 10th International Conference on Rehabilitation Robotics*, 00(c):356–363, 2007.

[16] K. A. Shorter, G. F. Kogler, E. Loth, W. K. Durfee, and E. T. Hsiao-Wecksler. A portable powered ankle-foot orthosis for rehabilitation. *Journal Of Rehabilitation Research And Development*, 48(4):459–472, 2011.

[17] J. M. Font-Llagunes, G. Arroyo, G. Serrancolí, and F. Romero. A powered lower limb orthosis for gait assistance in incomplete spinal cord injured subjects. In *Proceedings of the 4th International Symposium on Applied Sciences in Biomedical and Communication Technologies*, ISABEL '11, pages 109:1–109:4, New York, NY, USA, 2011. ACM.

[18] Y. Park, B. Chen, D. Young, L. Stirling, R. J. Wood, E. Goldfield, and R. Nagpal. Bio-inspired active soft orthotic device for ankle foot pathologies, 2011.

[19] R. Kobetic, C. S. To, J. R. Schnellenberger, M. L. Audu, T. C. Bulea, R. Gaudio, G. Pinault, S. Tashman, and R. J. Triolo. Development of hybrid orthosis for standing, walking, and stair climbing after spinal cord injury. *East*, 46(3):447–462, 2009.

[20] M. Goldfarb and W. K. Durfee. Design of a controlled-brake orthosis for fes-aided gait. *IEEE transactions on rehabilitation engineering a publication of the IEEE Engineering in Medicine and Biology Society*, 4(1):13–24, 1996.

[21] S. Gharooni, M. O. Tokhi, and B. Heller. *The Use of Elastic Element in a Hybrid Orthosis for Swing Phase Generation in Orthotic Gait*, pages 1–4. 5th annual conference of the international functional electrical stimulation society, 2000.

[22] R. J. Farris, H. A. Quintero, T. J. Withrow, and M. Goldfarb. Design of a joint-coupled orthosis for fes-aided gait. *2009 IEEE International Conference on Rehabilitation Robotics*, pages 246–252, 2009.

[23] W. K. Durfee and A. Rivard. Design and simulation of a pneumatic, stored-energy, hybrid orthosis for gait restoration. *Journal of Biomechanical Engineering*, 127(6):1014–1019, 2005.

[24] G. Obinata, S. Fukada, T. Matsunaga, T. Iwami, Y. Shimada, K. Miyawaki, K. Hase, and A. Nakayama. Hybrid control of powered orthosis and functional neuromuscular stimulation for restoring gait. *Conference Proceedings of the International Conference of IEEE Engineering in Medicine and Biology Society*, pages 4879–4882, 2007.

[25] Y. Stauffer, Y. Allemand, M. Bouri, J. Fournier, R. Clavel, P. Metrailler, R. Brodard, and F. Reynard. The walktrainer–a new generation of walking reeducation device combining orthoses and muscle stimulation. *IEEE Transactions on Neural and Rehabilitation Systems Engineering*, 17(1):38–45, 2009.

[26] I. DÃ■az, J. J. Gil, and E. SÃąnchez. Lower-limb robotic rehabilitation: Literature review and challenges. *Journal of Robotics*, pages 1–11, 2011.

[27] L. Righetti, J. Buchli, and A. J. Ijspeert. Dynamic hebbian learning in adaptive frequency oscillators. *Phys. D.*, 216:269–281, 2006.

[28] L. Righetti and A. J. Ijspeert. Programmable central pattern generators: an application to biped locomotion control. In *Proc. 2006 IEEE ICRA*, pages 1585–1590, 2006.

[29] J. A. Gallego, A. Forner-Cordero, and et al. Detection of gait perturbations based on proprioceptive information. application to limit cycle walkers. *Applied Bionics and Biomechanics*, 9:205–220, 2012.

[30] R. S. Kirby, M. S. Wingate, K. Van Naarden Braun, and et al. Prevalence and functioning of children with cerebral palsy in four areas of the united states in 2006: a report from the autism and developmental disabilities monitoring network. *Research in Developmental Disabilities*, 32(2):462–469, 2011.

[31] D. C. Burke and T. S. Tiong. Stability of the cervical spine after conservative treatment. *Paraplegia*, 13(3):191–202, 1975.

[32] National Spinal Cord Injury Statistical Center. Spinal cord injury facts and figures at a glance. *The journal of spinal cord medicine*, 35(1):68–9, 2008.

[33] Y. Zhang, A. M. Chapman, and et al. The incidence, prevalence, and mortality of stroke in france, germany, italy, spain, the uk, and the us: A literature review. *Stroke Research and Treatment*, 2012:1–11, 2012.

[34] C. Chevallereau and Y. Aoustin. Optimal reference trajectories for walking and running of a biped robot. *Robotica*, 19(5):557–569, August 2001.

[35] C. K. Chow and D. H. Jacobson. Studies of human locomotion via optimal programming. *Mathematical Biosciences*, 10(3-4):239–306, 1971.

[36] J. W. Grizzle, G. Abba, and F. Plestan. Asymptotically stable walking for biped robots: analysis via systems with impulse effects, 2001.

[37] M. Hardt, K. Kreutz-Delgado, and J. W. Helton. Optimal biped walking with a complete dynamical model. *Proceedings of the 38th IEEE Conference on Decision and Control Cat No99CH36304*, 3(December):2999–3004, 1999.

[38] S. Kajita and K. Tani. Experimental study of biped dynamic walking. *Control Systems Magazine IEEE*, 16(1):13–19, 1996.

[39] Q. H. Q. Huang, K. Yokoi, and et al. Planning walking patterns for a biped robot, 2001.

[40] K. H. Nishiwaki, T. Sugihara, and et al. Online mixture and connection of basic motions for humanoid walking control by footprint specification. *Proceedings 2001 ICRA IEEE International Conference on Robotics and Automation Cat No01CH37164*, 4:4110–4115, 2001.

[41] O. Haavisto and H. Hyotyniemi. *Clustered Regression Control of a Biped Robot Model, Humanoid Robots: New Developments*. InTech, 2007.

[42] Y. Hurmuzlu, F. GÃl'not, and B. Brogliato. Modeling , stability and control of biped robots a general framework. *Framework*, 40(10):1647–1664, 2001.

[43] A. J. Ijspeert. Central pattern generators for locomotion control in animals and robots: a review. *Neural Networks*, 21(4):642–653, 2008.

[44] A.O. Haavisto and B.H. HyÃűtyniemi. Simulation tool of a biped walking robot model. Technical report, Helsinki Universit. Technol. Control Eng. Lab., 2004.

[45] C. Chevallereau, G. Abba, and et al. Rabbit: a testbed for advanced control theory. *Control Systems Magazine, IEEE*, 23(5):57–79, 2003.

[46] V. Dietz. Spinal cord pattern generators for locomotion. *Clinical Neurophysiology*, 114:1379–1389, 2003.

[47] M. MacKay-Lyons. Central pattern generation of locomotion: a review of the evidence. *Physical Therapy*, 82(1):69–83, 2002.

[48] F. M. Silva and J. A. T. Machado. *Kinematic aspects of robotic biped locomotion systems*, volume 1, pages 266–272. Ieee, 1997.

[49] J. Ayers, J. L. Davis, and A. Rudolph. *Neurotechnology for Biomimetic Robots*, volume 1714. The MIT Press Cambridge, MA, USA, 2002.

[50] Hiroshi Kimura, Kazuo Tsuchiya, Akio Ishiguro, and Hartmut Witte. Adaptive motion of animals and machines. *New York*, 21(2):141–154, 2006.

[51] R. Ronsse, N. Vitiello, and et al. Adaptive oscillators with human-in-the-loop : Proof of concept for assistance and rehabilitation. *Robotics*, pages 668–674, 2010.

[52] V. Dietz. *Rehabilitation of Locomotor Function After a Central Motor Lesion*. 2012.

[53] M. D. Rinderknecht, F. A. Delaloye, A. Crespi, R. Ronsse, and A. J. Ijspeert. Assistance using adaptive oscillators: Sensitivity analysis on the resonance frequency. In *in Proc. International Conference on Rehabilitation Robotics, Zurich, Switzerland*, 2011.

[54] Mike Domenik Rinderknecht, Fabien Andre Delaloye, Alessandro Crespi, Renaud Ronsse, and Auke Jan Ijspeert. Assistance using adaptive oscillators: Robustness to errors in the identification of the limb parameters.

[55] S. Aoi and K. Tsuchiya. Locomotion control of a biped robot using nonlinear oscillators. *Autonomous Robots*, 19(3):219–232, 2005.

[56] Y. Ikemoto and W. Yu. The roles of cpg phase modulation and reflexive muscular patterns in balance recovery reflexive responses to perturbation during walking - a simulation study. *Conference Proceedings of the International Conference of IEEE Engineering in Medicine and Biology Society*, 2007:2389–2392, 2007.

[57] G. Cheron, M. Duvinage, and et al. From spinal central pattern generators to cortical network: Integrated BCI for walking rehabilitation. *Neural Plasticity*, 2012:1–13, 2012.

[58] G. C. Nandi, A. Ijspeert, and A. Nandi. Biologically inspired cpg based above knee active prosthesis. *2008 IEEERSJ International Conference on Intelligent Robots and Systems*, pages 2368–2373, 2008.

[59] X. Guo, L. Chen, and et al. A study on control mechanism of above knee robotic prosthesis based on cpg model, 2010.

[60] M. Duvinage, T. Castermans, and et al. Modeling human walk by pcpg for lower limb neuroprosthesis control, 2011.

[61] M. Duvinage, R. Jimenez-Fabian, T. Castermans, O. Verlinden, and T. Dutoit. An active foot lifter orthosis based on a pcpg algorithm. *IEEE International Conference on Rehabilitation Robotics Rehab Week Zurich*, 2011:1–7, 2011.

[62] J. Spitz, Y. Or, and M. Zacksenhouse. Towards a biologically inspired open loop controller for dynamic biped locomotion. In *Robotics and Biomimetics (ROBIO), 2011 IEEE International Conference on*, pages 503 –508, dec. 2011.

[63] K. Tsuchiya, S. Aoi, and K. Tsujita. Locomotion control of a biped locomotion robot using nonlinear oscillators. In *Intelligent Robots and Systems, 2003. (IROS 2003). Proceedings. 2003 IEEE/RSJ International Conference on*, volume 2, pages 1745 – 1750 vol.2, oct. 2003.

[64] M.K. Habib, L. L. Guang, and et al. Bipedal locomotion control via cpgs with coupled nonlinear oscillators. In *Mechatronics, ICM2007 4th IEEE International Conference on*, pages 1 –6, may 2007.

[65] L. Righetti and A. J. Ijspeert. Pattern generators with sensory feedback for the control of quadruped locomotion, 2008.

[66] J. Nakanishi, J. Morimoto, and et al. Learning from demonstration and adaptation of biped locomotion with dynamical movement primitives. *Learning*, 47(2-3):79–91, 2004.

[67] H. van Hedel and V. Dietz. Rehabilitation of locomotion after spinal cord injury. *Restorative Neurology and Neuroscience*, 28:123–134, 2010.

[68] D. Hevroni, A. Rattner, and et al. Hippocampal plasticity involves extensive gene induction and multiple cellular mechanisms. *Journal of molecular neuroscience MN*, 10(2):75–98, 1998.

[69] A. Curt, H. J. Van Hedel, and et al. Recovery from a spinal cord injury: significance of compensation, neural plasticity, and repair. *Journal of Neurotrauma*, 25(5):677–85, 2008.

[70] R. J. Nudo. Postinfarct cortical plasticity and behavioral recovery. *Stroke*, 38(2):840–845, 2007.

[71] S. C. Cramer and J. D. Riley. Neuroplasticity and brain repair after stroke. *Current Opinion in Neurology*, 21:76–82, 2008.

[72] T. A. Dodds, D. P. Martin, W. C. Stolov, and R. A. Deyo. A validation of the functional independence measurement and its performance among rehabilitation inpatients. *Archives of Physical Medicine and Rehabilitation*, 74(5):531–536, 1993.

[73] R. W. Ashworth. Preliminary trial of carisprodal in multiple sclerosis. *Practitioner*, 192:540–542, 1964.

[74] A. D. Pandyan, G. R. Johnson, C. I. Price, R. H. Curless, M. P. Barnes, and H. Rodgers. A review of the properties and limitations of the ashworth and modified ashworth scales as measures of spasticity. *Clinical Rehabilitation*, 13(5):373–383, 1999.

[75] J. Hidler, D. Nichols, M. Pelliccio, and K. Brady. Advances in the understanding and treatment of stroke impairment using robotic devices. *Topics in Stroke Rehabilitation*, 12(2):22–35, 2005.

[76] C. L. Richards, F. Malouin, and C. Dean. Gait in stroke: assessment and rehabilitation. *Clinics in Geriatric Medicine*, 15(4):833–855, 1999.

[77] A. S. Ryan, C. L. Dobrovolny, K. H. Silver, G. V. Smith, and R. F. Macko. Cardiovascular fitness after stroke: Role of muscle mass and gait deficit severity. *Journal of Stroke and Cerebrovascular Diseases*, 9(4):185–191, 2000.

[78] K. L. Kilgore, M. Scherer, R. Bobblitt, J. Dettloff, D. M. Dombrowski, N. Godbold, J. W. Jatich, R. Morris, J. S. Penko, E. S. Schremp, and et al. Neuroprosthesis consumersÊij forum: consumer priorities for research directions. *Journal Of Rehabilitation Research And Development*, 38(6):655–660, 2001.

[79] K. D. Anderson. Targeting recovery: priorities of the spinal cord-injured population. *Journal Of Neurotrauma*, 21(10):1371–83, 2004.

[80] K. M. Michael, J. K. Allen, and R. F. Macko. Reduced ambulatory activity after stroke: the role of balance, gait, and cardiovascular fitness. *Archives of Physical Medicine and Rehabilitation*, 86(8):1552–1556, 2005.

[81] P. L. Ditunno, M. Patrick, M. Stineman, and J. F. Ditunno. Who wants to walk? preferences for recovery after sci: a longitudinal and cross-sectional study. *Spinal cord the official journal of the International Medical Society of Paraplegia*, 47(3):500–506, 2008.

[82] J. C. Moreno, A. J. Del Ama, A. De Los Reyes-GuzmÃąn, A. Gil-Agudo, R. Ceres, and J. L. Pons. Neurorobotic and hybrid management of lower limb motor disorders: a review. *Medical & Biological Engineering & Computing*, pages 1119–1130, 2011.

[83] S. Kim, S. Banala, and et al. Robot-assisted modifications of gait in healthy individuals. *Experimental Brain Research*, 202:809–824, 2010. 10.1007/s00221-010-2187-5.

[84] J.L. Merritt and M.K. Yoshida. Knee-ankle-foot orthoses: Indications and practical applications of long leg braces. *Phys Med Rehabil*, 14:395–420, 2000.

[85] R.L. Waters and B. R. Lunsford. Energy cost of paraplegic locomotion. *The Journal of Bone and Joint Surgery*, 67(8):1245–1250, 1985.

[86] D. A. Yngve, R. Douglas, and J. M. Roberts. The reciprocating gait orthosis in myelomeningocele. *Journal Of Pediatric Orthopedics*, 4(3):304–310, 1984.

[87] P. Jaspers, L. Peeraer, W. V. Petegem, and G. V. Perre. The use of an advanced reciprocating gait orthosis by paraplegic individuals: a follow-up study. *Spinal Cord*, 35:585–589, 1997.

[88] G.K. Rose. The principles and practice of hip guidance articulations. *Prosthet Orthot Int*, 3(1):37–43, 1979.

[89] J. H. Patrick and M. R. McClelland. Low energy cost reciprocal walking for the adult paraplegic. *Paraplegia*, 23:113–117, 1985.

[90] C. Kirtley. Principles and practice of paraplegic locomotion: experience with the walkabout walking system. *Aust Orthot Prosthet Mag*, 7(2):4–8, 1992.

[91] S. Lotta, A. Fiocchi, R. Giovannini, R. Silvestrin, L. Tesio, A. Raschi, L. Macchia, V. Chiapatti, M. Zambelli, and C. Tosi. Restoration of gait with orthoses in thoracic paraplegia: a multicentric investigation. *Paraplegia*, 32(9):608–15, 1994.

[92] M. Franceschini, S. Baratta, M. Zampolini, D. Loria, and S. Lotta. Reciprocating gait orthoses: a multicenter study of their use by spinal cord injured patients. *Arch Phys Med Rehabil*, 78(6):582–6, 1997.

[93] S. Fatone. A review of the literature pertaining to kafos and hkafos for ambulation. *Jpo Journal of Prosthetics and Orthotics*, 18:137–168, 2006.

[94] M. Vukobratovic, D. Hristic, and Z. Stojiljkovic. Development of active anthropomorphic exoskeletons. *Medical and Biological Engineering*, 12(1):66–80, 1975.

[95] J E Pratt, B T Krupp, C J Morse, and S H Collins. The roboknee: an exoskeleton for enhancing strength and endurance during walking. *IEEE International Conference on Robotics and Automation 2004 Proceedings ICRA 04 2004*, 3(April):2430–2435 Vol.3, 2004.

[96] J. A. Blaya and H. Herr. Adaptive control of a variable-impedance ankle-foot orthosis to assist drop-foot gait, 2004.

[97] C. Fleischer and G. Hommel. A human–exoskeleton interface utilizing electromyography, 2008.

[98] K. Bharadwaj and T.G. Sugar. Kinematics of a robotic gait trainer for stroke rehabilitation. In *Robotics and Automation, 2006. ICRA 2006. Proceedings 2006 IEEE International Conference on*, pages 3492 –3497, may 2006.

[99] J. Kim, S. Hwang, and Y. Kim. *Development of an active ankle-foot orthosis for hemiplegic patients*, page 110. ACM Press, 2007.

[100] I. Khanna, A. Roy, M. M. Rodgers, H. I. Krebs, R. M. Macko, and L. W. Forrester. Effects of unilateral robotic limb loading on gait characteristics in subjects with chronic stroke. *Journal of NeuroEngineering and Rehabilitation*, 7:23, 2010.

[101] K. A. Shorter, Y. Li, E. A. Morris, G. F. Kogler, and E. T. Hsiao-Wecksler. Experimental evaluation of a portable powered ankle-foot orthosis.

[102] K. Suzuki, Y. Kawamura, T. Hayashi, T. Sakurai, Y. Hasegawa, and Y. Sankai. Intention-based walking support for paraplegia patient. *2005 IEEE International Conference on Systems Man and Cybernetics*, 3(12):2707–2713, 2007.

[103] H. Kawamoto, T. Hayashi, T. Sakurai, K. Eguchi, and Y. Sankai. Development of single leg version of hal for hemiplegia. *Conference Proceedings of the International Conference of IEEE Engineering in Medicine and Biology Society*, pages 5038–5043, 2009.

[104] A. Tsukahara, R. Kawanishi, and et al. Sit-to-stand and stand-to-sit transfer support for complete paraplegic patients with robot suit hal. *Advanced Robotics*, 24(11):1615–1638, 2010.

[105] Strausser K. A., T. A. Swift, and et al. Prototype medical exoskeleton for paraplegic mobility: First experimental results. *ASME Conference Proceedings*, 2010(44175):453–458, 2010.

[106] G. Belforte, G. Eula, S. Appendino, and S. Sirolli. Pneumatic interactive gait rehabilitation orthosis: design and preliminary testing. *Proceedings of the Institution of Mechanical Engineers Part H Journal of engineering in medicine*, 225(2):158–169, 2011.

[107] E. Moore. Hal-5: The exoskeleton robot 'to suit you', 03 2011. CNET-news-Health Tech.

[108] K. H. Low. Robot-assisted gait rehabilitation: From exoskeletons to gait systems. In *Defense Science Research Conference and Expo (DSR), 2011*, pages 1 –10, aug. 2011.

[109] Y. Nakamura. The development of actuators with backdrivability., 2009.

[110] R. J. Farris, H. A. Quintero, and M. Goldfarb. Preliminary evaluation of a powered lower limb orthosis to aid walking in paraplegic individuals. *IEEE Transactions on Neural and Rehabilitation Systems Engineering*, 19(6):652–9, 2011.

[111] A. Agrawal, V. Sangwan, S. K. Banala, S. K. Agrawal, and S. A. Binder-Macleod. Design of a novel two degree-of-freedom ankle-foot orthosis. *Journal of Mechanical Design*, 129(11):1137, 2007.

[112] G. S. Sawicki and D. P. Ferris. A pneumatically powered knee-ankle-foot orthosis (kafo) with myoelectric activation and inhibition. *Journal of NeuroEngineering and Rehabilitation*, 6(1):23, 2009.

[113] F. Casolo, S. Cinquemani, and M. Politecnico di Milano Dipartimento di Meccanica Cocetta. On active lower limb exoskeletons actuators. *Proceeding ofthe 5th International Symposium on Mechatronics and its Applications (ISMA08)*, pages 25–30, 2008.

[114] D. Ferris, J. M. Czerniecki, and B. Hannaford. An ankle-foot orthosis powered by artificial pneumatic muscles. *Appl Biomech*, 21(2):189–197, 2005.

[115] J. F. Veneman, R. Kruidhof, E. E. G. Hekman, R. Ekkelenkamp, E. H. F. Van Asseldonk, and H. Van Der Kooij. Design and evaluation of the lopes exoskeleton robot for interactive gait rehabilitation. *IEEE Transactions on Neural and Rehabilitation Systems Engineering*, 15(3):379–386, 2007.

[116] S. Mohammed and Y. Amirat. Towards intelligent lower limb wearable robots: Challenges and perspectives - state of the art. In *Robotics and Biomimetics, 2008. ROBIO 2008. IEEE International Conference on*, pages 312 –317, feb. 2009.

[117] V. Dietz, G. Colombo, L. Jensen, and L. Baumgartner. Locomotor capacity of spinal cord in paraplegic patients. *Annals of Neurology*, 37(5):574–582, 1995.

[118] M.R. Popovic, T. Keller, I. Pappas, V. Dietz, and M. Morari. Surface-stimulation technology for grasping and walking neuroprostheses. *IEEE Engineering in Medicine and Biology Magazine*, 20(1):82–93, January 2001.

[119] A. Kantrowitz. *A report of the Maimonides Hospital.* New York, Brooklyn, 1960, 1960.

[120] W. T. Liberson, H. J. Holmquest, D. Scot, and M. Dow. Functional electrotherapy: Stimulation of the peroneal nerve synchronized with the swing phase of the gait of hemiplegic patients. *Arch. Phys. Med. Rehabil.*, 42:101–105, 1961.

[121] D. Graupe and K. H. Kohn. Transcutaneous functional neuromuscular stimulation of certain traumatic complete thoracic paraplegics for independent short-distance ambulation. *Neurol Res*, 19(3):323–33, 1997.

[122] E. B. Marsolais and R. Kobetic. Functional electrical stimulation for walking in paraplegia. *The Journal of Bone and Joint Surgery*, 69(5):728–733, 1987.

[123] R. Kobetic, R. J. Triolo, and E. B. Marsolais. Muscle selection and walking performance of multichannel fes systems for ambulation in paraplegia. *IEEE Transactions on Rehabilitation Engineering*, 5(1):23–29, March 1997.

[124] S. Dosen and D. Popovic. Functional electrical stimulation for walking: rule based controller using accelerometers. In *Student Paper, 2008 Annual IEEE Conference*, pages 1 –5, feb. 2008.

[125] L. Yang, D. N. Condie, M. H. Granat, J. P. Paul, and D. I. Rowley. Effects of joint motion constraints on the gait of normal subjects and their implications on the further development of hybrid fes orthosis for paraplegic persons. *J Biomech*, 29(2):217–26, 1996.

[126] K. Fujita, Y. Handa, N. Hoshimiya, and M. Ichie. Stimulus adjustment protocol for fes-induced standing in paraplegia using percutaneous intramuscular electrodes. *Rehabilitation Engineering, IEEE Transactions on*, 3(4):360 –366, dec 1995.

[127] J. A. Hoffer, M. Baru, S. Bedard, E. Calderon, G. Desmoulin, P. Dhawan, G. Jenne, J. Kerr, M. Whittaker, and T. J. Zwimpfer. Initial results with fully implanted neurostep fes system for foot drop. *10th Annual Conference of the International Functional Electrical Stimulation Society*, 78(3):53–55, 2005.

[128] P. N. Taylor, J. H. Burridge, A. L. Dunkerley, D. E. Wood, J. A. Norton, C. Singleton, and I. D. Swain. Clinical use of the odstock dropped foot stimulator: its effect on the speed and effort of walking. *Archives of Physical Medicine and Rehabilitation*, 80(12):1577–1583, 1999.

[129] T. A. Thrasher and M. R. Popovic. Functional electrical stimulation of walking: function, exercise and rehabilitation. *Annales de rÃl'adaptation et de mÃl'decine physique revue scientifique de la SociÃl'tÃl' franÃğaise de rÃl'Ãl'ducation fonctionnelle de rÃl'adaptation et de mÃl'decine physique*, 51(6):452–60, 2008.

[130] C. L. Lyons, J. B. Robb, J. J. Irrgang, and G. K. Fitzgerald. Differences in quadriceps femoris muscle torque when using a clinical electrical stimulator versus a portable electrical stimulator. *Physical Therapy*, 72(10):723–730, 2005.

[131] T. Lam, D. L. Wolfe, J.J. Eng, and A. Domingo. *Lower Limb Rehabilitation Following Spinal Cord Injury*. Spinal Cord Injury Rehabilitation Evidence, 2010.

[132] A. Thrasher, Feng Wang, and B. Andrews. Self adaptive neuro-fuzzy control of neural prostheses using reinforcement learning. In *Engineering in Medicine and Biology Society, 1996. Bridging Disciplines for Biomedicine. Proceedings of the 18th Annual International Conference of the IEEE*, volume 1, pages 451 –452 vol.1, oct-3 nov 1996.

[133] R. Spadone, G. Merati, E. Bertocchi, E. Mevio, A. Veicsteinas, A. Pedotti, and M. Ferrarin. Energy consumption of locomotion with orthosis versus parastep-assisted gait: a single case study. *Spinal cord the official journal of the International Medical Society of Paraplegia*, 41(2):97–104, 2003.

[134] E. C. Field-Fote. Combined use of body weight support, functional electric stimulation, and treadmill training to improve walking ability in individuals with chronic incomplete spinal cord injury. *Archives of Physical Medicine and Rehabilitation*, 82(6):818–824, 2001.

[135] G. H. Creasey, C. H. Ho, R. J. Triolo, D. R. Gater, A. F. DiMarco, K. M. Bogie, and M. W. Keith. Clinical applications of electrical stimulation after spinal cord injury. *The journal of spinal cord medicine*, 27(4):365–375, 2004.

[136] M. Chan, R. Tong, and K. Chung. Bilateral upper limb training with functional electric stimulation in patients with chronic stroke. *Neurorehabilitation and Neural Repair*, 23(4):357–365, 2009.

[137] S. Mangold, C. Schuster, T. Keller, A. Zimmermann-Schlatter, and T. Ettlin. Motor training of upper extremity with functional electrical stimulation in early stroke rehabilitation. *Neurorehabilitation and Neural Repair*, 23(2):184–190, 2009.

[138] K.A. Ferguson, G. Polando, R. Kobetic, R.J. Triolo, and E.B. Marsolais. Walking with a hybrid orthosis system. *Spinal Cord*, 37(11):800–4, 1999.

[139] L. Sykes, E. R. Ross, E. S. Powell, and J. Edwards. Objective measurement of use of the reciprocating gait orthosis (rgo) and the electrically augmented rgo in adult patients with spinal cord lesions. *Prosthetics and orthotics international*, 20(3):182–190, 1996.

[140] A.V. Nene and J.H. Patrick. Energy cost of paraplegic locomotion using the parawalker–electrical stimulation "hybrid" orthosis. *Arch Phys Med Rehabil*, 71(2):116–20, 1990.

[141] G. Merati, P. Sarchi, M. Ferrarin, A. Pedotti, and A. Veicsteinas. Paraplegic adaptation to assisted-walking: energy expenditure during wheelchair versus orthosis use. *Spinal cord the official journal of the International Medical Society of Paraplegia*, 38(1):37–44, 2000.

[142] Nightingale E. J., J. Raymond, and J. W. Middleton. Benefits of fes gait in a spinal cord injured population. *Spinal Cord*, 45:646–657, 2007.

[143] D. Graupe, H. Cerrel-Bazo, H. Kern, and U. Carraro. Walking performance, medical outcomes and patient training in fes of innervated muscles for ambulation by thoracic-level complete paraplegics. *Neurological Research*, 30(2):123–130, 2008.

[144] R. Kobetic, E. B. Marsolais, R. J. Triolo, D. T. Davy, R. Gaudio, and S. Tashman. Development of a hybrid gait orthosis: a case report. *Journal of Spinal Cord Medicin*, 26(3):254–258, 2003.

[145] D. Popovic, R. Tomovic, and L. Schwirtlich. Hybrid assistive system - the motor neuroprosthesis. *IEEE Transactions on Biomedical Engineering*, 36(7):729–737, 1989.

[146] C. S. To, R. Kobetic, J. R. Schnellenberger, M. L. Audu, and R. J. Triolo. Design of a variable constraint hip mechanism for a hybrid neuroprosthesis to restore gait after spinal cord injury. *IEEEASME Transactions on Mechatronics*, 13(2):197–205, 2008.

[147] T Ohashi, G Obinata, Y Shimada, and K Ebata. *Control of hybrid FES system for restoration of paraplegic locomotion*, pages 96–101. IEEE, 1993.

[148] M. Ferrarin, F. Palazzo, R. Riener, and J. Quintern. Model-based control of fes-induced single joint movements. *IEEE Transactions on Neural Systems and Rehabilitation Engineering*, 9(3):245–257, 2001.

[149] W. K. Durfee and J. M. Hausdorff. Regulating knee joint position by combining electrical stimulation with a controllable friction brake. *Annals of Biomedical Engineering*, 18(6):575–596, 1990.

[150] U. Stanic and A. Trnkoczy. Closed-loop positioning of hemiplegic patient?s joint by means of functional electrical stimulation. *IEEE Transactions on Biomedical Engineering*, 21(5):365–370, 1974.

[151] H. Vallery and M. Buss. Towards a hybrid motor neural prosthesis for gait rehabilitation : A project description. *Control*, 15:19âĂŞ22, 2005.

[152] W. B. Johnson, S. Fatone, and S. A. Gard. Walking mechanics of persons who use reciprocating gait orthoses. *J Rehabil Res Dev*, 46:435–46, 2009.

[153] C. S. To, R. Kobetic, and R. J. Triolo. Hybrid orthosis system with a variable hip coupling mechanism. In *Engineering in Medicine and Biology Society, 2006. EMBS '06. 28th Annual International Conference of the IEEE*, pages 2928 –2931, 30 2006-sept. 3 2006.

[154] S. E. Irby, K. R. Kaufman, R. W. Wirta, and D. H. Sutherland. Optimization and application of a wrap-spring clutch to a dynamic knee-ankle-foot orthosis. *Rehabilitation Engineering, IEEE Transactions on*, 7(2):130 –134, jun 1999.

[155] M. L. Audu, C. S. To, R. Kobetic, and R. J. Triolo. Gait evaluation of a novel hip constraint orthosis with implication for walking in paraplegia. *Neural Systems and Rehabilitation Engineering, IEEE Transactions on*, 18(6):610 –618, dec. 2010.

[156] W. K. Durfee and M. Goldfarb. Design of a controlled-brake orthosis for regulating fes-aided gait. In *Engineering in Medicine and Biology Society, 1992 14th Annual International Conference of the IEEE*, volume 4, pages 1337 –1338, 29 1992-nov. 1 1992.

[157] M. H. Granat, D. J. Nicol, R. H. Baxendale, and B. J. Andrews. Dishabituation of the flexion reflex in spinal cord-injured man and its application in the restoration of gait. *Brain Research*, 559(2):344–346, 1991.

[158] M. Goldfarb, K. Korkowski, B. Harrold, and W. Durfee. Preliminary evaluation of a controlled-brake orthosis for fes-aided gait., 2003.

[159] M. Solomonow, E. Reisin, E. Aguilar, R. V. Baratta, R. Best, and R. DÊijAmbrosia. Reciprocating gait orthosis powered with electrical muscle stimulation (rgo ii). part ii: Medical evaluation of 70 paraplegic patients. *Orthopedics*, 20(5):411–418, 1997.

[160] S. Gharooni, B. Heller, and M. O. Tokhi. A new hybrid spring brake orthosis for controlling hip and knee flexion in the swing phase, 2001.

[161] R. J. Farris, H. A. Quintero, T. J. Withrow, and M. Goldfarb. Design and simulation of a joint-coupled orthosis for regulating fes-aided gait. *Proceedings of the IEEE International Conference on Robotics and Automation (2009)*, pages 1916–1922, 2009.

[162] A. Kangude, B. Burgstahler, J. Kakastys, and W. Durfee. Single channel hybrid fes gait system using an energy storing orthosis: preliminary design. *Conference Proceedings of the International Conference of IEEE Engineering in Medicine and Biology Society*, pages 6798–6801, 2009.

[163] R. Tomovic. Hybrid actuators for orthotic systems: Hybrid assistive systems. *IV Advances in External Contrl of Human Extremities ECHE Yugoslav Comittee for ETAN Beogard*, pages 1–15, 1978.

[164] G. Colombo, M. Jorg, and V. Dietz. Driven gait orthosis to do locomotor training of paraplegic patients. *Proceedings of the 22nd Annual International Conference of the IEEE Engineering in Medicine and Biology Society Cat No00CH37143*, 4(6):3159–3163, 2000.

[165] Rewalk restoration device, April 2012.

[166] G. Zeilig, H. Weingarden, M. Zwecker, I. Dudkiewicz, A. Bloch, and A. Esquenazi. Safety and tolerance of the rewalk (âĎć) exoskeleton suit for ambulation by people with complete spinal cord injury: A pilot study. *J Spinal Cord Med*, 35:96–101, 2012.

[167] N. J. Postans, J. P. Hasler, M. H. Granat, and D. J. Maxwell. Functional electric stimulation to augment partial weight-bearing supported treadmill training for patients with acute incomplete spinal cord injury: A pilot study. *Archives of Physical Medicine and Rehabilitation*, 82(1):20–25, 2004.

[168] S. Hesse, C. Werner, and A. Bardeleben. Electromechanical gait training with functional electrical stimulation: case studies in spinal cord injury. *Spinal cord the official journal of the International Medical Society of Paraplegia*, 42(6):346–352, 2004.

[169] C. F. Nooijen, N. Ter Hoeve, and E. C. Field-Fote. Gait quality is improved by locomotor training in individuals with sci regardless of training approach. *Journal of NeuroEngineering and Rehabilitation*, 6(6):36, 2009.

[170] I. Schwartz, A. Sajin, I. Fisher, M. Neeb, M. Shochina, M. Katz-Leurer, and Z. Meiner. The effectiveness of locomotor therapy using robotic-assisted gait training in subacute stroke patients: a randomized controlled trial. *PM R the journal of injury function and rehabilitation*, 1(6):516–523, 2009.

[171] T. G. Hornby, D. D. Campbell, J. H. Kahn, T. Demott, J. L. Moore, and H. R. Roth. Enhanced gait-related improvements after therapist- versus robotic-assisted locomotor training in subjects with chronic stroke: a randomized controlled study. *Stroke: A Journal of Cerebral Circulation*, 39(6):1786–1792, 2008.

[172] E. Swinnen, S. Duerinck, J. Baeyens, R. Meeusen, and E. Kerckhofs. Effectiveness of robot-assisted gait training in persons with spinal cord injury: a systematic review. *Journal of rehabilitation medicine official journal of the UEMS European Board of Physical and Rehabilitation Medicine*, 42(6):520–526, 2010.

[173] J. L. Emken and D. J. Reinkensmeyer. Robot-enhanced motor learning: accelerating internal model formation during locomotion by transient dynamic amplification, 2005.

[174] D. S. Reisman, R. Wityk, K. Silver, and A. J. Bastian. Locomotor adaptation on a split-belt treadmill can improve walking symmetry post-stroke. *Brain: A journal of neurology*, 130(Pt 7):1861–1872, 2007.

[175] L. Marchal-Crespo and D. Reinkensmeyer. Review of control strategies for robotic movement training after neurologic injury. *Journal of NeuroEngineering and Rehabilitation*, 6(1):20, 2009.

[176] T. Hayashi, H. Kawamoto, and Y. Sankai. Control method of robot suit hal working as operatorÊijs muscle using biological and dynamical information. *2005 IEEERSJ International Conference on Intelligent Robots and Systems*, 2(1):3063–3068, 2005.

[177] R. Riener, L. Lunenburger, S. Jezernik, M. Anderschitz, G. Colombo, and V. Dietz. Patient-cooperative strategies for robot-aided treadmill training: first experimental results, 2005.

[178] T. Luksch and K. Berns. Control of bipedal walking exploiting postural reflexes and passive dynamics. *Environment*, pages 1–7, 2010.

[179] M. F. Eilenberg, H. Geyer, and H. Herr. Control of a powered ankle-foot prosthesis based on a neuromuscular model. *IEEE Transactions on Neural and Rehabilitation Systems Engineering*, 18(2):164–173, 2010.

[180] R. J. Full, T. Kubow, and et al. Quantifying dynamic stability and maneuverability in legged locomotion. *Integrative and comparative biology*, 42:149–157, 2002.

[181] P. Arena, L. Fortuna, and et al. An adaptive, self-organizing dynamical system for hierarchical control of bio-inspired locomotion. *IEEE transactions on systems man and cybernetics Part B Cybernetics a publication of the IEEE Systems Man and Cybernetics Society*, 34(4):1823–1837, 2004.

[182] J. Buchli, L. Righetti, and et al. Engineering entrainment and adaptation in limit cycle systems. *Biological Cybernetics*, 95(6):645–664, 2006.

[183] S. Schaal, J. Peters, and et al. Learning movement primitives. *Motor Control*, 15(1):1–10, 2004.

[184] L. Righetti, J. Buchli, and et al. Adaptive frequency oscillators applied to dynamic walking i . programmable central pattern generators. *Physica*, pages 2006–2006, 2006.

[185] J. Buchli, L. Righetti, and et al. Adaptive frequency oscillators applied to dynamic walking ii . adapting to resonant body dynamics. *Proceedings of Dynamic Walking*, 2006, 2006.

[186] S. Ruffieux and L. Righetti. Adaptive locomotion controller for a quadruped robot. Technical report, ÃL'cole Polytechnique FÃl'dÃl'rale de Lausanne (EPDL), 2007.

[187] J. Buchli, L. Righetti, and et al. Frequency analysis with coupled nonlinear oscillators. *Physica D: Nonlinear Phenomena*, 237(13):1705–1718, 2008.

[188] L. Righetti, J. Buchli, and A.J. Ijspeert. From dynamic hebbian learning for oscillators to adaptive central pattern generators. In *Proceedings of 3rd International Symposium on Adaptive Motion in Animals and Machines – AMAM 2005*. Verlag ISLE, Ilmenau, 2005. Full paper on CD.

[189] M. Lungarella, G. Metta, R. Pfeifer, and G. Sandini. Developmental robotics: a survey. *Connect. Sci.*, 15(4):151–190, 2003.

[190] P. Veskos and Y. Demiris. Developmental acquisition of entrainment skills in robot swinging using van der pol oscillators. *Biological Cybernetics*, 2:87–93, 2005.

[191] A. Espinosa. Desarrollo de una plataforma robotica cooperativa para la compensacin de la marcha. Master's thesis, Universidad Carlos III de Madrid, 2011.

[192] D. S. Jevsevar, P. O. Riley, and et al. Knee kinematics and kinetics during locomotor activities of daily living in subjects with knee arthroplasty and in healthy control subjects. *Physical Therapy*, 73(4):229–239; discussion 240–242, 1993.

[193] B. Hass. *Motor control.*, chapter 4. Elsevier, 2006.

[194] J. Duysens and et al. A walking robot called human: lessons to be learned from neural control of locomotion. *Journal of Biomechanics*, 35(4):447–453, 2002.

[195] M. D. Lewek, J. Feasel, and et al. Use of visual and proprioceptive feedback to improve gait speed and spatiotemporal symmetry following chronic stroke: A case series. *Physical Therapy*, 92(5):748–56, 2012.

[196] D. A. Winter. Human balance and posture control during standing and walking. *Gait Posture*, 3(4):193–214, 1995.

[197] J. Mrozowski, J. Awrejcewicz, and et al. Analysis of stability of human gait. *Journal of Theoretical. and Applied Mechanics*, 45:91–98, 2007.

[198] D. C. Kar. Gaits and energetics in terrestrial legged locomotion. *Mechanism and Machine Theory*, 38(4):355–366, 2003.

[199] A. Biswas, E. D. Lemaire, and et al. Dynamic gait stability index based on plantar pressures and fuzzy logic. *Journal of biomechanics*, 41(7):1574–1581, 2008.

[200] M. H. P. Dekker. Zero-moment point for stable biped walking. Technical report, Eindhoven, University of Technology, 2009.

[201] D.L. Wight and University of Waterloo. Dept. of Systems Design Engineering. *A Foot Placement Strategy for Robust Bipedal Gait Control*. Canadian theses. University of Waterloo, 2008.

[202] J. A. Gallego, A. Forner-Cordero, and et al. Continuous assessment of gait stability in limit cycle walkers. Biomedical Robotics and Biomechatronics BioRob 2010 3rd IEEE RAS and EMBS International Conference on, 2010.

[203] J. G. D. Karssen and M. Wisse. Fall detection of two-legged walking robots using multi-way principal components analysis. *Robotica*, 27(01):249–257, 2009.

[204] J. M. Guijarro. Simulation of biped walking: Implementing taga's model in pyode. Technical report, The Autonomous Systems Laboratory, Universidad PolitÃl'cnica de Madrid, 2008.

[205] M. Murray Clark and G.T. Anderson. *A Nonlinear Oscillator-based Technique for Implementing Obstacle Avoidance in an Autonomous Mobile Robot*, chapter 4, pages 29–35. 1998.

[206] G. Taga. A model of the neuro-musculo-skeletal system for anticipatory adjustment of human locomotion during obstacle avoidance. *Biological Cybernetics*, 78(1):9–17, 1998.

[207] G. Taga. Nonlinear dynamics of human locomotion: from real-time adaptation to development. In Hiroshi Kimura, Kazuo Tsuchiya, Akio Ishiguro, and Hartmut Witte, editors, *Adaptive Motion of Animals and Machines*, pages 189–204. Springer Tokyo, 2006.

Appendix A

Biped model specifications

field	description	units
Robot dimensions:		
`l`	robot link lengths $[l_0, l_1, l_2]$	m
`r`	center of mass distances $[r_0, r_1, r_2]$	m
`m`	link masses $[m_0, m_1, m_2]$	kg
Robot initial state:		
`coordinates`	$[x_0, y_0, \alpha, \beta_L, \beta_R, \gamma_L, \gamma_R]$	m, (rad)
`speeds`	$[\dot{x_0}, \dot{y_0}, \dot{\alpha}, \dot{\beta_L}, \dot{\beta_R}, \dot{\gamma_L}, \dot{\gamma_R}]$	m/s, (rad)/s
`gcstate`	$[x'_{0L}, sliding_L, x'_{0R}, sliding_R]$	m
Knee angle limiter parameters:		
`kk`	elastic constant	Nm/(rad)
`bk`	damping ratio	Nms/(rad)
`min`	minimum angle for γ_L and γ_R	(rad)
`max`	maximum angle for γ_L and γ_R	(rad)
Ground properties:		
`ground`	surface points $\begin{bmatrix} x_1, x_2, \dots \\ y_1, y_2, \dots \end{bmatrix}$	m
`ky`	normal elastic constant	kg/s^2
`by`	normal damping ratio	kg/s
`kx`	tangential elastic constant	kg/s^2
`bx`	tangential damping ratio	kg/s
`mus`	static friction coefficient μ_s	
`muk`	kinetic friction coefficient μ_k	
Additional parameters:		
	acceleration of gravity	m/s^2
	sample time	s

Figure A.1: Biped model block parameter definitions

Appendix B

Dynamic model formulas

The dynamic model form of the biped is:

$$A(q)\,\ddot{q} = b(q, \dot{q}, M, F) \tag{B.1}$$

The vector q contains the generalized coordinates, F the ground support forces and M the joint moments. As the system has seven degrees of freedom, there exists also seven partial differential equations. in the following, the exact formulas of the inertia matrix $A(q)$ and the right hand side vector $b(q, \dot{q}, F, M)$ are presented.

$A(q)$:

$$A_{11} = m_0 + 2m_1 + 2m_2$$

$$A_{12} = 0$$

$$A_{13} = (-2m_1r_0 - 2m_2r_0)\,cos\,(\alpha) + (-l_1m_2 - m_1r_1)\,cos\,(\alpha - \beta_L) - l_1m_2cos\,(\alpha - \beta_R)$$
$$- m_1r_1cos\,(\alpha - \beta_R) - m_2r_2cos\,(\alpha - \beta_L + \gamma_L) - m_2r_2cos\,(\alpha - \beta_R + \gamma_R)$$

$$A_{14} = (l_1m_2 + m_1r_1)\,cos\,(\alpha - \beta_L) + m_2r_2cos\,(\alpha - \beta_L + \gamma_L)$$

$$A_{15} = (l_1m_2 + m_1r_1)\,cos\,(\alpha - \beta_R) + m_2r_2cos\,(\alpha - \beta_R + \gamma_R)$$

$$A_{16} = -m_2r_2cos\,(\alpha - \beta_L + \gamma_L)$$

$$A_{17} = -m_2r_2cos\,(\alpha - \beta_R + \gamma_R)$$

$$A_{21} = 0$$

$$A_{22} = m_0 + 2m_1 + 2m_2$$

$$A_{23} = (2m_1r_0 + 2m_2r_0)\,sin\,(\alpha) + (l_1m_2 + m_1r_1)\,sin\,(\alpha - \beta_L) + l_1m_2sin\,(\alpha - \beta_R)$$
$$+ m_1r_1sin\,(\alpha - \beta_R) + m_2r_2sin\,(\alpha - \beta_L + \gamma_L) + m_2r_2sin\,(\alpha - \beta_R + \gamma_R)$$

$$A_{24} = (-l_1m_2 - m_1r_1)\,sin\,(\alpha - \beta_L) - m_2r_2sin\,(\alpha - \beta_L + \gamma_L)$$

$$A_{25} = (-l_1m_2 - m_1r_1)\,sin\,(\alpha - \beta_R) - m_2r_2sin\,(\alpha - \beta_R + \gamma_R)$$

$$A_{26} = m_2r_2sin\,(\alpha - \beta_L + \gamma_L)$$

$$A_{27} = m_2r_2sin\,(\alpha - \beta_R + \gamma_R)$$

$$A_{31} = (-2m_1r_0 - 2m_2r_0)\,cos\,(\alpha) + (-l_1m_2 - m_1r_1)\,cos\,(\alpha - \beta_L) - l_1m_2cos\,(\alpha - \beta_R)$$
$$- m_1r_1cos\,(\alpha - \beta_R) - m_2r_2cos\,(\alpha - \beta_L + \gamma_L) - m_2r_2cos\,(\alpha - \beta_R + \gamma_R)$$

$$A_{32} = (2m_1r_0 + 2m_2r_0)\,sin\,(\alpha) + (l_1m_2 + m_1r_1)\,sin\,(\alpha - \beta_L) + l_1m_2sin\,(\alpha - \beta_R)$$
$$+ m_1r_1cos\,(\alpha - \beta_R) - m_2r_2cos\,(\alpha - \beta_L + \gamma_L) - m_2r_2cos\,(\alpha - \beta_R + \gamma_R)$$

$$A_{33} = 2l_1^2m_2 + 2m_1r_0^2 + 2m_2r_0^2 + 2m_1r_1^2 + 2m_2r_2^2 + (2l_1m_2r_0 + 2m_1r_0r_1)\,cos\,(\beta_L)$$
$$+ (2l_1m_2r_0 + 2m_1r_0r_1)\,cos\,(\beta_R) + 2m_2r_0r_2cos\,(\beta_L - \gamma_L) + 2l_1m_2r_2cos\,(\gamma_L)$$
$$+ 2m_2r_0r_2cos\,(\beta_R - \gamma_R) + 2l_1m_2r_2cos\,(\gamma_R)$$

$$A_{34} = -l_1^2m_2 - m_1r_1^2 - m_2r_2^2 + (-l_1m_2r_0 - m_1r_0r_1)\,cos\,(\beta_L) - m_2r_0r_2cos\,(\beta_L - \gamma_L)$$
$$- 2l_1m_2r_2cos\,(\gamma_L)$$

$$A_{35} = -l_1^2m_2 - m_1r_1^2 - m_2r_2^2 + (-l_1m_2r_0 - m_1r_0r_1)\,cos\,(\beta_R) - m_2r_0r_2cos\,(\beta_R - \gamma_R)$$
$$- 2l_1m_2r_2cos\,(\gamma_R)$$

$$A_{36} = m_2 r_2 \left(r_2 + r_0 cos\left(\beta_L - \gamma_L\right) + l_1 cos\left(\gamma_L\right)\right)$$

$$A_{37} = m_2 r_2 \left(r_2 + r_0 cos\left(\beta_R - \gamma_R\right) + l_1 cos\left(\gamma_R\right)\right)$$

$$A_{41} = \left(l_1 m_2 + m_1 r_1\right) cos\left(\alpha - \beta_L\right) + m_2 r_2 cos\left(\alpha - \beta_L + \gamma_L\right)$$

$$A_{42} = \left(-l_1 m_2 - m_1 r_1\right) sin\left(\alpha - \beta_L\right) - m_2 r_2 sin\left(\alpha - \beta_L + \gamma_L\right)$$

$$A_{43} = -l_1^2 m_2 - m_1 r_1^2 - m_2 r_2^2 + r_0 \left(-l_1 m_2 - m_1 r_1\right) cos\left(\beta_L\right) - m_2 r_0 r_2 cos\left(\beta_L - \gamma_L\right) - 2 l_1 m_2 r_2 cos\left(\gamma_L\right)$$

$$A_{44} = l_1^2 m_2 + m_1 r_1^2 + m_2 r_2^2 + 2 l_1 m_2 r_2 cos\left(\gamma_L\right)$$

$$A_{45} = 0$$

$$A_{46} = m_2 r_2 \left(-r_2 - l_1 cos\left(\gamma_L\right)\right)$$

$$A_{47} = 0$$

$$A_{51} = \left(l_1 m_2 + m_1 r_1\right) cos\left(\alpha - \beta_R\right) + m_2 r_2 cos\left(\alpha - \beta_R + \gamma_r\right)$$

$$A_{52} = \left(-l_1 m_2 - m_1 r_1\right) sin\left(\alpha - \beta_R\right) - m_2 r_2 sin\left(\alpha - \beta_R + \gamma_R\right)$$

$$A_{53} = -l_1^2 m_2 - m_1 r_1^2 - m_2 r_2^2 + r_0 \left(-l_1 m_2 - m_1 r_1\right) cos\left(\beta_R\right) - m_2 r_0 r_2 cos\left(\beta_R - \gamma_R\right) - 2 l_1 m_2 r_2 cos\left(\gamma_r\right)$$

$$A_{54} = 0$$

$$A_{55} = l_1^2 m_2 + m_1 r_1^2 + m_2 r_2^2 + 2 l_1 m_2 r_2 cos\left(\gamma_R\right)$$

$$A_{56} = 0$$

$$A_{57} = m_2 r_2 \left(-r_2 - l_1 cos\left(\gamma_R\right)\right)$$

$$A_{61} = -m_2 r_2 cos\left(\alpha - \beta_L + \gamma_L\right)$$

$$A_{62} = m_2 r_2 sin\left(\alpha - \beta_L + \gamma_L\right)$$

$$A_{63} = m_2 r_2 \left(r_2 + r_0 cos\left(\beta_L - \gamma_L\right) + l_1 cos\left(\gamma_L\right)\right)$$

$$A_{64} = m_2 r_2 \left(-r_2 - l_1 cos\left(\gamma_L\right)\right)$$

$$A_{65} = 0$$

$$A_{66} = m_2 r_2^2$$

$$A_{67} = 0$$

$$A_{71} = -m_2 r_2 cos\left(\alpha - \beta_R + \gamma_R\right)$$

$$A_{72} = m_2 r_2 sin\left(\alpha - \beta_R + \gamma_R\right)$$

$$A_{73} = m_2 r_2 \left(r_2 + r_0 cos\left(\beta_R - \gamma_R\right) + l_1 cos\left(\gamma_R\right)\right)$$

$$A_{74} = 0$$

$$A_{75} = m_2 r_2 \left(-r_2 - l_1 cos\left(\gamma_R\right)\right)$$

$$A_{76} = 0$$

$$A_{77} = m_2 r_2^2$$

$b\left(q, \dot{q}, F, M\right)$:

$$\begin{aligned}
b_1 = & -2\dot{\alpha}^2 m_1 r_0 sin\left(\alpha\right) + F_{Rx} - \dot{\beta}_R^2 m_1 r_1 sin\left(\alpha - \beta_R\right) - \dot{\alpha}^2 l_1 m_2 sin\left(\alpha - \beta_L\right) + F_{Lx} - \dot{\gamma}_L^2 m_2 r_2 sin\left(\alpha - \beta_L + \gamma_L\right) \\
& - \dot{\alpha}^2 m_1 r_1 sin\left(\alpha - \beta_R\right) - \dot{\beta}_R^2 l_1 m_2 sin\left(\alpha - \beta_R\right) - \dot{\alpha}^2 l_1 m_2 sin\left(\alpha - \beta_R\right) - \dot{\gamma}_R^2 m_2 r_2 sin\left(\alpha - \beta_R + \gamma_R\right) \\
& - \dot{\beta}_L^2 m_2 r_2 sin\left(\alpha - \beta_L + \gamma_L\right) - \dot{\beta}_L^2 m_1 r_1 sin\left(\alpha - \beta_L\right) - \dot{\beta}_R^2 m_2 r_2 sin\left(\alpha - \beta_R + \gamma_R\right) - \dot{\alpha}^2 m_1 r_1 sin\left(\alpha - \beta_L\right) \\
& - \dot{\beta}_L^2 l_1 m_2 sin\left(\alpha - \beta_L\right) - \dot{\alpha}^2 m_2 r_2 sin\left(\alpha - \beta_R + \gamma_R\right) - \dot{\alpha}^2 m_2 r_2 sin\left(\alpha - \beta_L + \gamma_L\right) + 2\dot{\alpha}\dot{\beta}_R l_1 m_2 sin\left(\alpha - \beta_R\right) \\
& + 2\dot{\beta}_R \dot{\gamma}_R m_2 r_2 sin\left(\alpha - \beta_R + \gamma_R\right) - 2\dot{\alpha}\dot{\gamma}_R m_2 r_2 sin\left(\alpha - \beta_R + \gamma_R\right) + 2\dot{\alpha}\dot{\beta}_L m_2 r_2 sin\left(\alpha - \beta_L + \gamma_L\right) \\
& + 2\dot{\alpha}\dot{\beta}_L m_1 r_1 sin\left(\alpha - \beta_L\right) + 2\dot{\alpha}\dot{\beta}_R m_2 r_2 sin\left(\alpha - \beta_R + \gamma_R\right) + 2\dot{\alpha}\dot{\beta}_L l_1 m_2 sin\left(\alpha - \beta_L\right) \\
& - 2\dot{\alpha}^2 m_2 r_0 sin\left(\alpha\right) + 2\dot{\alpha}\dot{\beta}_R m_1 r_1 sin\left(\alpha - \beta_R\right) + 2\dot{\beta}_L \dot{\gamma}_L m_2 r_2 sin\left(\alpha - \beta_L + \gamma_L\right) - 2\dot{\alpha}\dot{\gamma}_L m_2 r_2 sin\left(\alpha - \beta_L + \gamma_L\right) \\
b_2 = & -\dot{\beta}_L^2 m_2 r_2 cos\left(\alpha - \beta_L + \gamma_L\right) + F_{Ry} - 2gm_2 - \dot{\gamma}_R^2 m_2 r_2 cos\left(\alpha - \beta_R + \gamma_R\right) - \dot{\beta}_R^2 m_2 r_2 cos\left(\alpha - \beta_R + \gamma_R\right) \\
& - \dot{\alpha}^2 m_2 r_2 cos\left(\alpha - \beta_R + \gamma_R\right) - \dot{\gamma}_L^2 m_2 r_2 cos\left(\alpha - \beta_L + \gamma_L\right) - \dot{\alpha}^2 m_1 r_1 cos\left(\alpha - \beta_R\right) - \dot{\beta}_R^2 m_1 r_1 cos\left(\alpha - \beta_R\right) \\
& - \dot{\alpha}^2 \left(2m_1 + 2m_2\right) r_0 cos\left(\alpha\right) - \dot{\alpha}^2 l_1 m_2 cos\left(\alpha - \beta_R\right) - \dot{\beta}_R^2 l_1 m_2 cos\left(\alpha - \beta_R\right) + F_{Ly} - \dot{\alpha}^2 m_2 r_2 cos\left(\alpha - \beta_L + \gamma_L\right) \\
& - 2gm_1 + 2\dot{\alpha}\dot{\beta}_R l_1 m_2 cos\left(\alpha - \beta_R\right) + 2\dot{\beta}_R \dot{\gamma}_R m_2 r_2 cos\left(\alpha - \beta_R + \gamma_R\right) - 2\dot{\alpha}\dot{\gamma}_R m_2 r_2 cos\left(\alpha - \beta_R + \gamma_R\right) \\
& + 2\dot{\alpha}\dot{\beta}_R m_2 r_2 cos\left(\alpha - \beta_R + \gamma_R\right) - 2\dot{\alpha}\dot{\gamma}_L m_2 r_2 cos\left(\alpha - \beta_L + \gamma_L\right) + 2\dot{\beta}_L \dot{\gamma}_L m_2 r_2 cos\left(\alpha - \beta_L + \gamma_L\right) \\
& + 2\dot{\alpha}\dot{\beta}_L m_2 r_2 cos\left(\alpha - \beta_L + \gamma_L\right) + 2\dot{\alpha}\dot{\beta}_R m_1 r_1 cos\left(\alpha - \beta_R\right) - cos\left(\alpha - \beta_L\right) \\
& \left(\dot{\alpha}\dot{\beta}_L \left(-2l_1 m_2 - 2m_1 r_1\right) + \dot{\alpha}^2 \left(l_1 m_2 + m_1 r_1\right) + \dot{\beta}_L^2 \left(l_1 m_2 + m_1 r_1\right)\right) - gm_0 \\
b_3 = & \dot{\gamma}_R^2 l_1 m_2 r_2 sin\left(\gamma_R\right) + F_{Ry} l_2 sin\left(\alpha - \beta_R + \gamma_R\right) - F_{Lx} l_1 cos\left(\alpha - \beta_L\right) - F_{Rx} l_1 cos\left(\alpha - \beta_R\right) \\
& - F_{Lx} l_2 cos\left(\alpha - \beta_L + \gamma_L\right) + F_{Ly} r_0 sin\left(\alpha\right) + F_{Ry} r_0 sin\left(\alpha\right) + F_{Ly} l_1 sin\left(\alpha - \beta_L\right) + F_{Ly} l_2 sin\left(\alpha - \beta_L + \gamma_L\right) \\
& - gm_2 r_2 sin\left(\alpha - \beta_R + \gamma_R\right) - \dot{\gamma}_R^2 m_2 r_0 r_2 sin\left(\beta_R - \gamma_R\right) - \dot{\beta}_R^2 m_2 r_0 r_2 sin\left(\beta_R - \gamma_R\right) - gm_2 r_2 sin\left(\alpha - \beta_L + \gamma_L\right) \\
& + \dot{\gamma}_L^2 l_1 m_2 r_2 sin\left(\gamma_L\right) - \dot{\gamma}_L^2 m_2 r_0 r_2 sin\left(\beta_L - \gamma_L\right) - \dot{\beta}_R^2 m_1 r_0 r_1 sin\left(\beta_R\right) - \dot{\beta}_L^2 m_2 r_0 r_2 sin\left(\beta_L - \gamma_L\right)
\end{aligned}$$

$$
\begin{aligned}
&- \dot{\beta}_R^2 l_1 m_2 r_0 sin(\beta_R) - \dot{\beta}_L^2 m_1 r_0 r_1 sin(\beta_L) - g l_1 m_2 sin(\alpha - \beta_R) + F_{Ry} l_1 sin(\alpha - \beta_R) - g m_1 r_1 sin(\alpha - \beta_R) \\
&- g l_1 m_2 sin(\alpha - \beta_L) - g m_1 r_1 sin(\alpha - \beta_L) - \dot{\beta}_L^2 l_1 m_2 r_0 sin(\beta_L) - (F_{Lx} r_0 + F_{Rx} r_0) cos(\alpha) \\
&- 2\dot{\alpha}\dot{\gamma}_L m_2 r_0 r_2 sin(\beta_L - \gamma_L) + 2\dot{\beta}_L \dot{\gamma}_L m_2 r_0 r_2 sin(\beta_L - \gamma_L) + 2\dot{\alpha}\dot{\beta}_L m_2 r_0 r_2 sin(\beta_L - \gamma_L) + 2\dot{\alpha}\dot{\beta}_R m_1 r_0 r_1 sin(\beta_R) \\
&- 2g m_2 r_0 sin(\alpha) + 2\dot{\alpha}\dot{\gamma}_R l_1 m_2 r_2 sin(\gamma_R) + 2\dot{\alpha}\dot{\beta}_R m_2 r_0 r_2 sin(\beta_R - \gamma_R) - 2\dot{\alpha}\dot{\gamma}_R m_2 r_0 r_2 sin(\beta_R - \gamma_R) \\
&+ 2\dot{\alpha}\dot{\gamma}_L l_1 m_2 r_2 sin(\gamma_L) - 2\dot{\beta}_L \dot{\gamma}_L l_1 m_2 r_2 sin(\gamma_L) - 2g m_1 r_0 sin(\alpha) + 2\dot{\alpha}\dot{\beta}_R l_1 m_2 r_0 sin(\beta_R) \\
&+ 2\dot{\alpha}\dot{\beta}_L l_1 m_2 r_0 sin(\beta_L) + 2\dot{\alpha}\dot{\beta}_L m_1 r_0 r_1 sin(\beta_L) - 2\dot{\beta}_R \dot{\gamma}_R l_1 m_2 r_2 sin(\gamma_R) \\
&+ 2\dot{\beta}_R \dot{\gamma}_R m_2 r_0 r_2 sin(\beta_R - \gamma_R) - F_{Rx} l_2 cos(\alpha - \beta_R + \gamma_R)
\end{aligned}
$$

$$
\begin{aligned}
b_4 = {} & M_{L1} + F_{Lx} l_1 cos(\alpha - \beta_L) + F_{Lx} l_2 cos(\alpha - \beta_L + \gamma_L) - F_{Ly} l_1 sin(\alpha - \beta_L) + g l_1 m_2 sin(\alpha - \beta_L) \\
&+ g m_1 r_1 sin(\alpha - \beta_L) - \dot{\alpha}^2 l_1 m_2 r_0 sin(\beta_L) - \dot{\alpha}^2 m_1 r_0 r_1 sin(\beta_L) - \dot{\alpha}^2 m_2 r_0 r_2 sin(\beta_L - \gamma_L) \\
&- 2\dot{\alpha}\dot{\gamma}_L l_1 m_2 r_2 sin(\gamma_L) + 2\dot{\beta}_L \dot{\gamma}_L l_1 m_2 r_2 sin(\gamma_L) - \dot{\gamma}_L^2 l_1 m_2 r_2 sin(\gamma_L) \\
&- F_{Ly} l_2 sin(\alpha - \beta_L + \gamma_L) + g m_2 r_2 sin(\alpha - \beta_L + \gamma_L)
\end{aligned}
$$

$$
\begin{aligned}
b_5 = {} & M_{R1} + F_{Rx} l_1 cos(\alpha - \beta_R) + F_{Rx} l_2 cos(\alpha - \beta_R + \gamma_R) - F_{Ry} l_1 sin(\alpha - \beta_R) + g l_1 m_2 sin(\alpha - \beta_R) \\
&+ g m_1 r_1 sin(\alpha - \beta_R) - \dot{\alpha}^2 l_1 m_2 r_0 sin(\beta_R) - \dot{\alpha}^2 m_1 r_0 r_1 sin(\beta_R) - \dot{\alpha}^2 m_2 r_0 r_2 sin(\beta_R - \gamma_R) \\
&- 2\dot{\alpha}\dot{\gamma}_R l_1 m_2 r_2 sin(\gamma_R) + 2\dot{\beta}_R \dot{\gamma}_R l_1 m_2 r_2 sin(\gamma_R) - \dot{\gamma}_R^2 l_1 m_2 r_2 sin(\gamma_R) - F_{Ry} l_2 sin(\alpha - \beta_R + \gamma_R) \\
&+ g m_2 r_2 sin(\alpha - \beta_R + \gamma_R)
\end{aligned}
$$

$$
\begin{aligned}
b_6 = {} & M_{L2} - F_{Lx} l_2 cos(\alpha - \beta_L + \gamma_L) + \dot{\alpha}^2 m_2 r_0 r_2 sin(\beta_L - \gamma_L) - \dot{\alpha}^2 l_1 m_2 r_2 sin(\gamma_L) + 2\dot{\alpha}\dot{\beta}_L l_1 m_2 r_2 sin(\gamma_L) \\
&- \dot{\beta}_L^2 l_1 m_2 r_2 sin(\gamma_L) + F_{Ly} l_2 sin(\alpha - \beta_L + \gamma_L) - g m_2 r_2 sin(\alpha - \beta_L + \gamma_L)
\end{aligned}
$$

$$
\begin{aligned}
b_7 = {} & M_{R2} - F_{Rx} l_2 cos(\alpha - \beta_R + \gamma_R) + \dot{\alpha}^2 m_2 r_0 r_2 sin(\beta_R - \gamma_R) - \dot{\alpha}^2 l_1 m_2 r_2 sin(\gamma_R) + 2\dot{\alpha}\dot{\beta}_R l_1 m_2 r_2 sin(\gamma_R) \\
&- \dot{\beta}_R^2 l_1 m_2 r_2 sin(\gamma_R) + F_{Ry} l_2 sin(\alpha - \beta_R + \gamma_R) - g m_2 r_2 sin(\alpha - \beta_R + \gamma_R)
\end{aligned}
$$

Appendix C

Measurement of the gait characteristics

The following tables indicate the measurement of some gait features in the absence and presence of external feedback.

- Mean velocity

Table C.1: Without external feedback.

	Time	**x-Position**	**Mean velocity**
initial	0.14	5.911284	
final	9.84	9.637401	
			0.384135

Table C.2: With external feedback and feedback gain $g_e = 1.0$.

	Time	**x-Position**	**Mean velocity**
initial	0.14	5.911313	
final	9.84	9.814273	
			0.402367

Table C.3: With external feedback and feedback gain $g_e = 2.0$.

	Time	**x-Position**	**Mean velocity**
initial	0.14	5.911340	
final	9.84	9.918046	
			0.413062

- Mean stride length

Table C.4: Without external feedback.

Leg	stride	step number i	step number f	x-Position i	x-Position f	length (Δ)
Right	1	146	447	6.197447	6.771165	0.573718
	2	447	755	6.771165	7.344561	0.573395
	3	755	1057	7.344561	7.917173	0.572611
	4	1057	1360	7.917173	8.491067	0.573894
	5	1360	1666	8.491067	9.064279	0.573211
	6	1666	1969	9.064279	9.637400	0.573121
	Mean					**0.573325**
Left	1	295	601	6.484137	7.058410	0.574273
	2	601	907	7.058410	7.630514	0.572103
	3	907	1208	7.630514	8.204024	0.573509
	4	1208	1513	8.204024	8.777791	0.573767
	5	1513	1817	8.777791	9.350748	0.572956
	Mean					**0.573322**

Table C.5: With external feedback and feedback gain $g_e = 1.0$.

Leg	stride	step number i	step number f	x-Position i	x-Position f	length (Δ)
Right	1	148	458	6.216165	6.810276	0.594111
	2	458	759	6.810276	7.412786	0.602509
	3	759	1064	7.412786	8.011894	0.599107
	4	1064	1367	8.011894	8.612968	0.601074
	5	1367	1671	8.612968	9.213365	0.600396
	6	1671	1975	9.213365	9.814138	0.600773
	Mean					**0.599662**
Left	1	305	607	6.514902	7.110726	0.595823
	2	607	912	7.110726	7.712278	0.601552
	3	912	1215	7.712278	8.311889	0.599611
	4	1215	1519	8.311889	8.912655	0.600765
	5	1519	1823	8.912655	9.513042	0.600387
	Mean					**0.599628**

Table C.6: With external feedback and feedback gain $g_e = 2.0$.

Leg	stride	step number i	step number f	x-Position i	x-Position f	length (Δ)
Right	1	149	460	6.231230	6.829259	0.598028
	2	460	763	6.829259	7.447518	0.618259
	3	763	1067	7.447518	8.063921	0.616402
	4	1067	1371	8.063921	8.680335	0.616414
	5	1371	1675	8.680335	9.297015	0.616680
	6	1675	1978	9.297015	9.914384	0.617368
	Mean					**0.613858**
Left	1	312	610	6.522956	7.139811	0.616854
	2	610	915	7.139811	7.754996	0.615185
	3	915	1219	7.754996	8.371493	0.616497
	4	1219	1523	8.371493	8.987877	0.616383
	5	1523	1826	8.987877	9.604299	0.616422
	Mean					**0.616268**

- Stride left-right asymmetry

Table C.7: Comparison of the mean stride left-right asymmetry in the absence and in the presence of external feedback.

Case	leg	mean stride length	error
Without feedback	right	0.573325	3.22016E-06
	left	0.573322	
Feedback gain $g_e = 1.0$	right	0.599662	3.41513E-05
	left	0.599628	
Feedback gain $g_e = 2.0$	right	0.613858	2.40959E-03
	left	0.616268	